Journal of Immunology Research

# Extracellular Vesicles (EVs) And Pathogens

Lead Guest Editor: Ana Claudia Torrecilhas
Guest Editors: Alicia Rojas, Patrícia Xander, and Wagner Batista

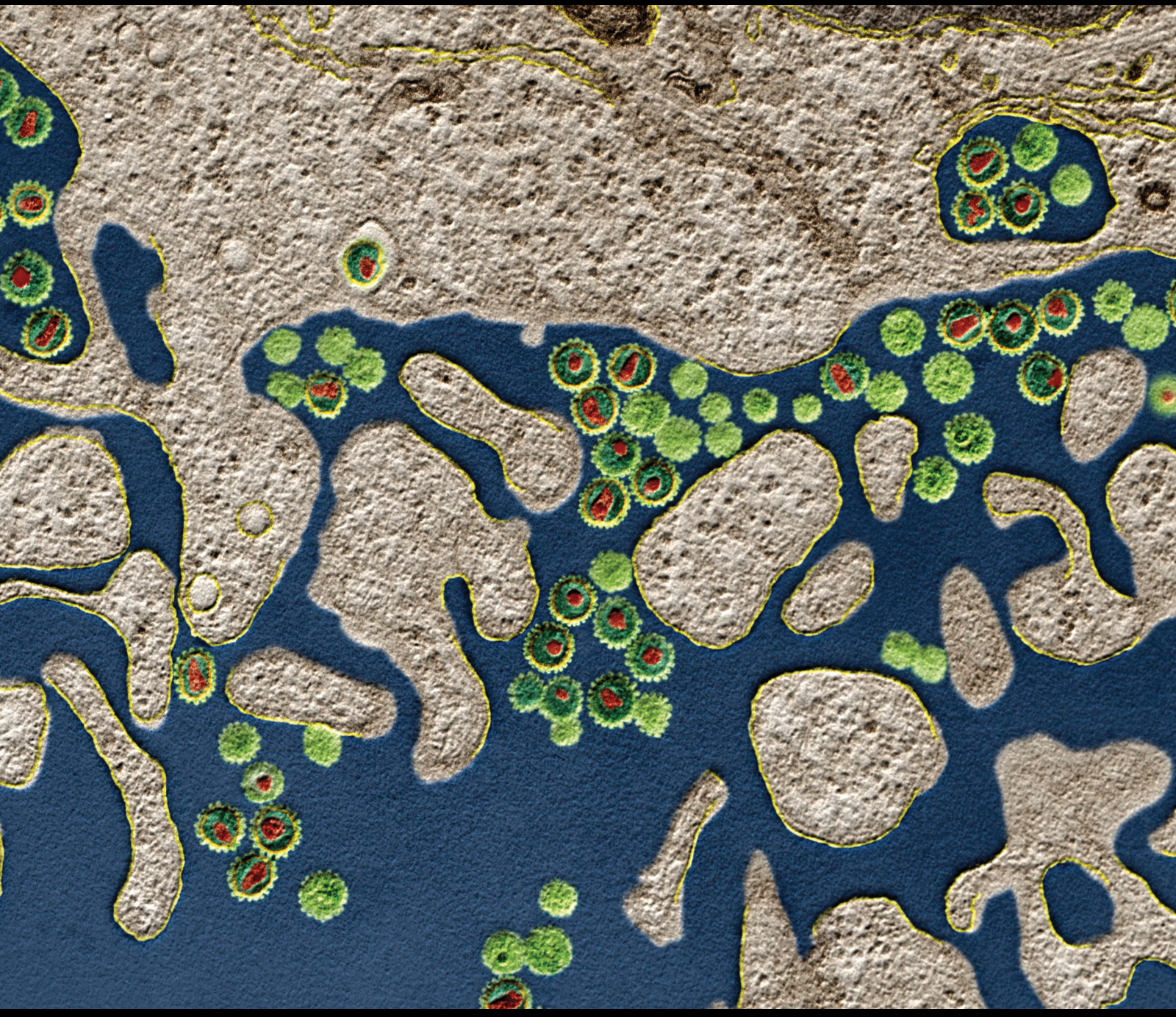

# Extracellular Vesicles (EVs) And Pathogens

Journal of Immunology Research

# Extracellular Vesicles (EVs) And Pathogens

Lead Guest Editor: Ana Claudia Torrecilhas
Guest Editors: Alicia Rojas, Patrícia Xander, and Wagner Batista

# Contents

Hindawi
Journal of Immunology Research
Volume 2022, Article ID 5230603, 11 pages
https://doi.org/10.1155/2022/5230603

*Review Article*

# Extracellular Vesicles in *Trypanosoma cruzi* Infection: Immunomodulatory Effects and Future Perspectives as Potential Control Tools against Chagas Disease

**Nuria Cortes-Serra**,[1,2] **Melisa Gualdron-Lopez**,[1,2] **Maria-Jesus Pinazo**,[1,3] **Ana Claudia Torrecilhas**,[4] **and Carmen Fernandez-Becerra**[1,2,3]

[1]*ISGlobal, Barcelona Institute for Global Health, Hospital Clínic-Universitat de Barcelona, Carrer Rosselló 149-153, CEK Building. E-08036 Barcelona, Spain*
[2]*IGTP Institut d'Investigació Germans Trias i Pujol, Badalona, Spain, Ctra. de Can Ruti. Camí de les Escoles, S/n, 08916 Badalona (Barcelona), Spain*
[3]*CIBERINFEC, ISCIII-CIBER de Enfermedades Infecciosas, Instituto de Salud Carlos III, Spain*
[4]*Laboratório de Imunologia Celular e Bioquímica de Fungos e Protozoários, Departamento de Ciências Farmacêuticas, Universidade Federal de São Paulo (UNIFESP), Rua São Nicolau, 210 Diadema, CEP, 09913-030 SP, Brazil*

Correspondence should be addressed to Ana Claudia Torrecilhas; ana.torrecilhas@unifesp.br and Carmen Fernandez-Becerra; carmen.fernandez@isglobal.org

Received 10 April 2022; Revised 2 July 2022; Accepted 19 July 2022; Published 17 August 2022

Academic Editor: Daniele Maria-Ferreira



Chagas disease, caused by the protozoa parasite *Trypanosoma cruzi*, is a neglected tropical disease and a major public health problem affecting more than 6 million people worldwide. Many challenges remain in the quest to control Chagas disease: the diagnosis presents several limitations and the two available treatments cause several side effects, presenting limited efficacy during the chronic phase of the disease. In addition, there are no preventive vaccines or biomarkers of therapeutic response or disease outcome. Trypomastigote form and *T. cruzi*-infected cells release extracellular vesicles (EVs), which are involved in cell-to-cell communication and can modulate the host immune response. Importantly, EVs have been described as promising tools for the development of new therapeutic strategies, such as vaccines, and for the discovery of new biomarkers. Here, we review and discuss the role of EVs secreted during *T. cruzi* infection and their immunomodulatory properties. Finally, we briefly describe their potential for biomarker discovery and future perspectives as vaccine development tools for Chagas Disease.

## 1. Chagas Disease

Chagas disease (CD) or American trypanosomiasis is a neglected tropical disease (NTD) caused by the protozoan intracellular parasite *Trypanosoma cruzi*. The disease is widely distributed across Latin America, with an estimated 6 to 7 million individuals infected, affects vulnerable populations, and has an important impact on the health, social and economic well-being of infected individuals (WHO, 2022, accessed March 14, 2022, https://www.who.int/news-room/fact-sheets/detail/chagas-disease-american-trypanosomiasis). In the last decades, CD has become an emerging infectious disease in nonendemic regions such as Europe, North America, Japan, and Australia, with the immigration of infected people from endemic countries contributing to the spread of the infection [1–3]. Importantly, many challenges remain to control CD effectively in nonendemic areas, such as access to diagnosis (with up to 90% of cases being undiagnosed), access to treatment, and screening of pregnant women and blood banks [1, 4–6].

The transmission of the parasite occurs through contact with the infected feces/urine of blood-sucking triatomine bugs (bug vector), congenital transmission, blood transfusion, and oral ingestion of contaminated food [7]. The

disease consists of two stages: the acute phase, occurring up to one week after infection and being mostly asymptomatic, and the chronic phase, with 30-40% of chronic patients manifesting cardiac and digestive symptoms [7, 8].

CD control presents multiple challenges: the parasite-host interactions are not yet completely understood; the diagnosis has several limitations; the two available treatments present several side effects and limited efficacy during the chronic phase of the disease; and there are no preventive vaccines for human or veterinary use. Additionally, there are no prognosis markers or biomarkers of therapeutic response [4, 9, 10]. In this scenario, the development of new therapeutic tools is urgently needed.

## 2. Extracellular Vesicles

Extracellular vesicles (EVs) are small particles formed by a lipid bilayer secreted by all cell types into the extracellular microenvironment and present in all body fluids [11]. Particles are divided into several subtypes, such as exosomes, microvesicles, and apoptotic bodies, according to their origin, size, and molecular composition [11–13]. Their content, which reflects the cell of origin, includes cytosolic and cell-surface proteins, nucleic acids, lipids, and metabolites. EVs mediate intercellular communication in a great variety of biological processes during homeostasis and in pathological conditions, where they act as messenger entities that deliver specific cargo to recipient cells, thereby altering their physiological status. The molecular signatures and functional properties of EVs, together with their remarkable stability in biofluids and systemic distribution, endow them with great potential to be used as biomarkers for the diagnosis and prognosis of diseases, as therapeutic vehicles for drug and gene therapy, and for developing new vaccine platforms against infectious diseases [14–18].

EVs have been described and are currently being studied in several protozoan parasites and helminths, such as *T. cruzi, Leishmania* spp., *T. brucei*, *Toxoplasma gondii*, *Plasmodium* spp., *Giardia intestinalis*, *Schistosoma mansoni*, and *Fasciola hepatica* [19–29]. In the context of the parasitic diseases that these organisms cause, EVs are known to play a major role in intercellular communication between the parasite and the host. Importantly, EVs can modulate the host immune response, increase parasite invasion, and alter the integrity and function of cells and tissues, resulting in different disease outcomes [20, 28, 30–34]. Moreover, the EV's capacity to mediate immune evasion through a broad type of mechanisms contributes to the exacerbation of infection [15]. On the other hand, EVs can also trigger protective responses by activating an immune cell effector mechanism that benefits the host, controlling parasite replication, and promoting host survival [17, 18, 23, 35, 36]. EVs released by parasites induce an immune modulatory effect and, together with their proven capacity for direct and indirect antigen presentation in the adaptive immune response [16], make them promising tools for vaccine or immunotherapy development [17, 18, 37].

Although EVs have not yet been tested as vaccines in clinical trials for parasitic diseases, several studies have demonstrated their potential. In Toxoplasmosis, EVs derived from dendritic cells incubated with *T. gondii* antigens induce a systemic immune response in mouse models. The vaccinated animals demonstrated increased survival and lower cerebral parasite burden after parasite challenge [38–40]. Another group has shown that EVs released by cells infected with *T. gondii* alter cell proliferation, causing changes in neighboring cells, which is the most likely mechanism for modulating the host's immune system [41]. In addition, using *P. yoelii* as a murine model of malaria, it has been shown that EVs generated from infected reticulocytes when administered in the presence of CpG as adjuvant elicited a potent host humoral immune response, decreased parasitemia, and protected mice against a challenge with a lethal strain of *P. yoelii* [23, 42].

EVs released in parasitic diseases contain parasite and host proteins, nucleic acids, and glycoconjugates or lipids from the parasite membrane [33, 43–46]. This characteristic, together with the fact that EVs are found in all biological fluids and present a specific molecular signature, dependent on the cell of origin, makes them interesting tools for biomarker discovery [47–49]. In *P. falciparum* and *P. vivax*, high circulating levels of EVs have been associated with the clinical symptoms and severity of the disease, showing that EV concentrations may have applications as biomarkers of malaria severity [50, 51]. In schistosomiasis, schistosomal miRNAs were detected in EVs isolated from patients before treatment. These levels decreased after treatment, indicating that EVs could be used as new diagnostic tools for patients presenting low parasitic burden, and as new biomarkers for therapeutic response [52].

## 3. Molecular Composition and Virulent Factors Associated with the Shedding of EVs by *T. cruzi* Parasite

The shedding of EVs by *T. cruzi* was first described in epimastigote form in 1979 [53]. Later, Gonçalves's group demonstrated that infective trypomastigote form from four different *T. cruzi* strains (Y, YuYu, CA1, and RA) released surface antigens bound to the particles by a spontaneous process [54]. However, it was not until 2013 that the first proteomic analysis of the *T. cruzi* secretome was performed [55]. In this study, EVs released by noninfective epimastigotes and infective metacyclic trypomastigote forms were isolated by ultracentrifugation, and two EV subtypes (larger and smaller), as well as vesicle-free fractions, were analyzed by mass spectrometry. The results showed a rich collection of proteins involved in metabolism, host-parasite interaction, signaling, nucleic acid binding, parasite survival, and virulence [55]. From then on, other proteomic studies emerged to characterize the exoproteome of trypomastigote forms [56] and to detect antigens associated with vesicles secreted by *T. cruzi* trypomastigotes [57]. Later on, another proteomic analysis of trypomastigote EVs was performed using two different strains (Y and YuYu), known to modulate the host immune responses differentially [45]. The analysis confirmed previous protein identification and showed

quantitative and qualitative differences in the EV cargo of the two strains, which correlated with differences in their infection profile [45]. Recently, another study characterized the proteome and the nanomechanical properties of EVs released from trypomastigotes and epimastigotes, finding marked differences in the EV cargo between both stages [58]. The first proteomic characterization of plasma-derived EVs purified directly from a heart transplant patient with chronic Chagas disease (CCD) was performed recently, identifying both human and parasite proteins in circulating EVs [46, 59].

The molecular cargo released in EVs by the different stages of *T. cruzi* parasites cultured *in vitro* is summarized in Figure 1. Among the proteins identified in EVs released to the conditioned medium by different *T. cruzi* stages, the presence of virulent factors is worth highlighting, as their expression in the parasite is fundamental for disease establishment and progression of infection. This is the case for trans-sialidases (TS), mucin, mucin-associated surface protein (MASP), cruzipain, and phosphatases, among others [19] (Table 1). These molecules, whose functions have been studied for years in the context of infection and the parasite, are involved in attachment and invasion of the host cells, protecting the parasite from complement-mediated lysis system, and may act as proinflammatory agents [60–65]. However, the function of these molecules in EVs is not yet well known and requires further investigation.

## 4. Immunomodulatory Role of EVs Derived from Trypomastigote Forms and *T. cruzi*-Infected Cells

The early events of *T. cruzi* infection are crucial for the establishment of the disease. The parasites contain molecules that induce the host innate immune response [62]. As macrophages and other mononuclear cells are among the host's first line of defense, several research groups have focused on the study of these cells and their interaction with EVs secreted by the parasite. EVs are among the mechanisms used by the parasite to escape the immune system. It has been shown that microvesicles released by THP-1 cells, after interacting with trypomastigotes in the early stages of infection, are able to inhibit the C3 convertase, protecting the parasite against the complement system and increasing its chances of survival [66]. These authors also demonstrated that a subpopulation of microvesicles carrying transforming growth factor beta (TGF-$\beta$), after incubation with Vero cells, increased *T. cruzi* invasion [66] (Figure 2(a)). Previous studies have also shown that *T. cruzi* infection requires the activation of the TGF-$\beta$ signaling pathway to increase parasite invasion in epithelial and cardiac cells and that TGF-$\beta$ is also involved in the development of CCD cardiomyopathy, being crucial for the formation of cardiac fibrosis [67, 68].

It has been observed that EVs released by several *T. cruzi* strains (Y, Colombiana, CL-14, and YuYu) modulate the inflammatory response of macrophages via the TLR2-dependent pathway, involving the signaling pathways of mitogen-activated protein kinases (MAPK), and trigger an inflammatory response mediated by proinflammatory TNF-$\alpha$ and IL-12, IL-6, and NO [69] (Figure 2(b)). In the same line, other studies exploring the EV's contribution to the proinflammatory response of THP1 macrophages showed that vesicles isolated from the plasma of CCD patients and experimentally infected mice also triggered the synthesis of proinflammatory cytokines and oxidative and nitrosative products [70]. Interestingly, the expression levels of proinflammatory genes observed in this study depended on the patient's disease stage, being higher in CCD patients presenting symptoms than in individuals suffering the indeterminate form of the disease [70] (Figure 2(b)). Notably, an unbalanced immune response favoring a proinflammatory environment is one of the main features responsible for disease progression. In this scenario, therapies capable of preventing tissue damage or reprogramming macrophages to increase microbicide and effector functions could be a useful tool for CD treatment. More recently, Vasconcelos and collaborators showed that the viability and/or integrity of the parasite are necessary factors for the release of EVs, which trigger a proinflammatory response in the host cell *in vitro*, and may be a strategy developed by the parasite that is aimed at creating a more favorable environment for establishing infection in the host [71]. However, other studies have shown that bone marrow-derived macrophages treated with *T. cruzi*-derived EVs (strain Y) induced lipid body and prostaglandin E2 (PGE2) formation prior to infection. Twenty-four hours after *T. cruzi* infection, these EV-treated macrophages decreased the production of PGE2, TNF-$\alpha$, and IL-6, decreasing the production of proinflammatory cytokines and oxidative and nitrosative products, which favored parasite infection and persistence (Figure 2(c)) [72].

The therapeutic potential of EVs is variable in different models and needs to be addressed carefully. Infected macrophages can also modulate the activation of other human THP-1 cells, promoting an inflammatory response [69]. Using a NF-$\kappa$B activation reporter CHO cell line, the authors showed that EVs secreted from infected cells induced the translocation of NF-$\kappa$B after interacting with TLR2 in this model. Moreover, both EVs from trypomastigotes forms and from infected macrophages altered the gene expression of proinflammatory cytokines, such as TNF-$\alpha$, IL-6, and IL-1$\beta$, and signal transducer molecules, such us STAT-1 and STAT-3 in THP1 macrophages (Figure 2(b)) [69]. In another report, the mechanism of NF-$\kappa$B-mediated proinflammatory cytokine response was studied further and identified two proteins involved in sensing DNA damage, cGAS, and PARP1 (a DNA repair enzyme), as factors responsible for the proinflammatory phenotype induced by the parasite and infected cell-derived EVs. Oxidized DNA was detected in EVs secreted by infected macrophages and in EVs from the plasma of chronically infected mice. Interestingly, the inhibition of PARP1 decreased the overall proinflammatory response and heart inflammation of chronically infected mice, suggesting that chemical inhibitors of this enzyme could become potential therapeutic targets for CD [73]. Notably, in some of the described *in vitro* models, *T. cruzi*-infected cells released higher levels of EVs compared to

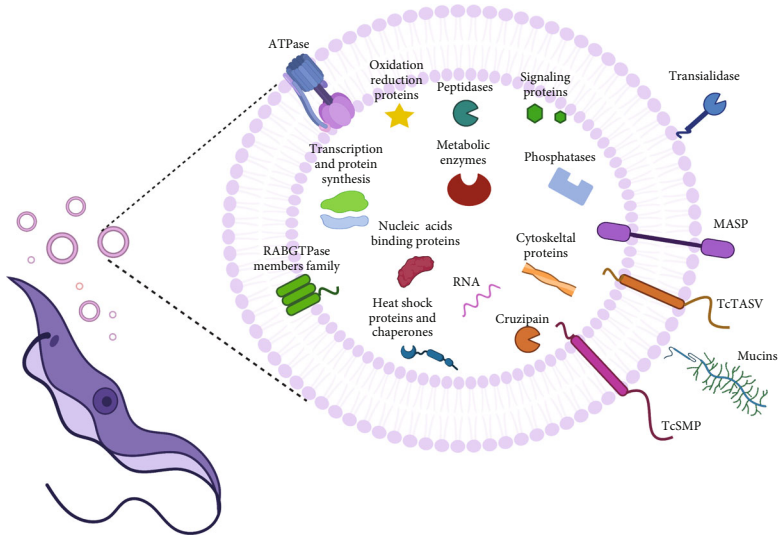


Figure 1: Schematic illustration summarizing the molecules identified in extracellular vesicles secreted by *T. cruzi* trypomastigotes. Several proteomic studies have identified *T. cruzi* virulence factors in EVs isolated from *T. cruzi* trypomastigotes, such as *trans*-sialidases, mucins, MASP proteins, the protease cruzipain, phosphatases, TcSMP, and TcTASV. Other molecules that can be found in trypomastigote EVs are signaling proteins, peptidases, oxidation/reduction proteins, ATPases, transcription and protein synthesis proteins, metabolic enzymes, cytoskeletal proteins, nucleic acid-binding proteins, heat shock proteins and chaperones, members of the RAB GTPase family and RNA, among others (created with http://BioRender.com).

Table 1: Main virulence factors associated to EVs shedding by *T. cruzi* parasites.

| *T. cruzi* virulence factors | Description | EV source | References |
|---|---|---|---|
| *trans*-sialidase (TS) | *T. cruzi* is unable to synthesize sialic acid (SA) *de novo*, TS transfers $\alpha$2-3-linked SA from host glycoproteins and glycolipids to acceptors containing terminal $\beta$-galactosyl residues present on the parasite surface. Avoiding lysis by serum factors and increasing invasion in the mammalian host (parasite sialylation) | T | 55–58 |
| Mucins (mucin-like glycoproteins: tGPI-mucins, eGPI or mtGPI-mucin) | Trypomastigotes (T)<br>(i) Mucins are the main acceptors of SA in the parasite's surface<br>(ii) Activation of the host innate immune system<br>(iii) Induce the production of TNF-$\alpha$, IL-12, and NO<br>Epimastigotes (E)<br>(i) Similar cell surface glycoprotein complex, called GP24, GP31, and GP37<br>(ii) Molecules maybe affect parasite migration in the vector<br>Metacyclic trypomastigotes (MT)<br>(i) Reported originally as the 35/50-kDa antigens<br>(ii) Mucins from MT increased infectivity and the ability of the parasite to shed the mucins upon invasion of the host cell | T<br>E<br>MT | 28, 55,57,76 |
| Mucin-associated surface proteins (MASP) | MASPs proteins, considered one of the most antigenic *T. cruzi* proteins, are a very diverse protein family, with members involved in host-cell invasion and survival and multiplication of intracellular amastigotes (A) | E<br>T<br>A | 55-58 |
| Phosphatases | In *T. cruzi*, phosphatases present multiple roles, such as providing a source of inorganic phosphate, facilitating epimastigotes differentiation, and promoting infection | E<br>MT<br>T | 55-58 |
| TcSMP family | TcSMP induce calcium signaling and lysosome mobilization, facilitating the formation of the parasitophorous vacuole and parasite invasion | E<br>MT | 55 |
| TcTASV family | Still unknown function, this family has been suggested as a potential target for intervention against *T. cruzi,* mainly due to the observation that some host-molecules trigger TcTASV-C expression *in vivo* during the infection. | T<br>A | 60 |
| Cruzipain | The major cysteine peptidase involved in host immune evasion, cell invasion, and intracellular development | E<br>T | 28, 55, 57, 76 |

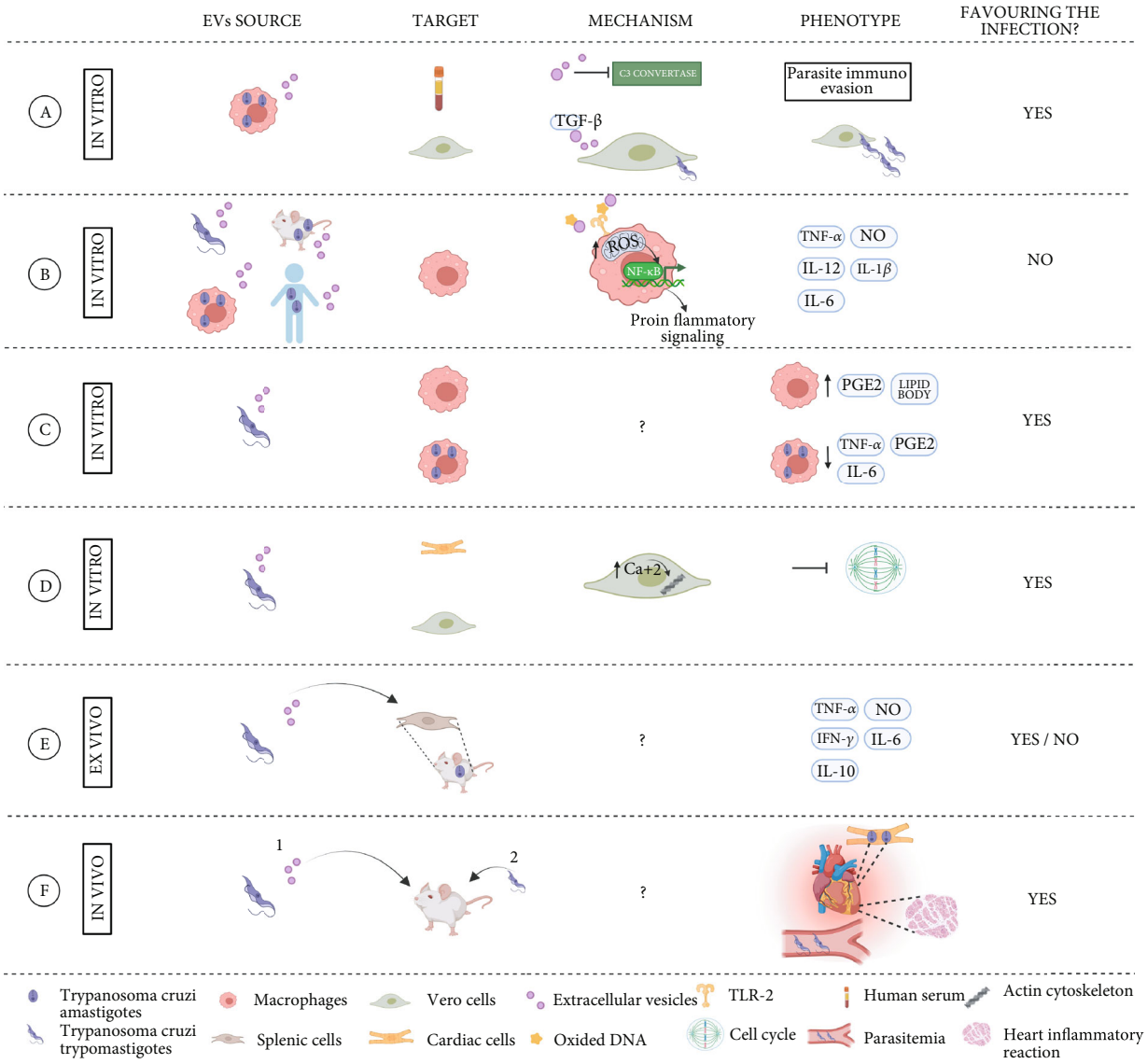


Figure 2: Immunomodulatory role of extracellular vesicles derived from *T. cruzi* and *T. cruzi*-infected cells. Summary of the main studies targeting the immunomodulatory effect of EVs in *T. cruzi* infection: EV source, target cell or body fluid, mechanism of action (if known), phenotype, and final effect on the infection process. (a) EVs secreted by infected macrophages can inhibit the C3 convertase, protecting the parasite against the complement system and increasing its chances of survival, and promote rapid cell invasion. (b) EVs from *T. cruzi* trypomastigotes, infected cells, infected individuals, and infected mice are recognized by uninfected macrophages via TLR2, inducing the translocation of NF-$\kappa$B and modulating the synthesis of proinflammatory cytokines. (c) *T. cruzi* EVs induce the formation of lipid body and PGE2 in noninfected macrophages and downregulate the synthesis of TNF-$\alpha$, PGE2, and IL-6 in infected macrophages. (d) EVs secreted by the parasite alter cell permeability and intracellular levels of calcium in nonimmune host cells, modifying the dynamics of the cytoskeleton and arresting the cell cycle. (e) EVs secreted by trypomastigotes induce an ex vivo production of pro and anti-inflammatory cytokines in splenic cells from chronically-infected mice. (f) *In vivo* studies in mice, injected with trypomastigotes-derived EVs prior to *T. cruzi* infection, have shown an increase of circulating EVs in plasma and parasitemia, cardiac tropism, and inflammation (created with http://BioRender.com).

noninfected cells, and these differ largely in their protein cargo [69, 74].

Little is known about the mechanisms by which *T. cruzi* EVs alter nonimmune host cells. A recent *in vitro* study showed that epithelial cells (Vero) and cardiac muscle cells (HL-1), incubated with parasite EVs, altered cell permeability and intracellular levels of calcium, which modified the dynamics of the actin cytoskeleton and arrested the cell cycle (Figure 2(d)). All together, these changes could explain the increased host-cell invasion observed in this study [75].

The role of EVs in the immune response of the chronic stage of *T. cruzi* infection has been studied less. Nogueira and collaborators studied the *ex vivo* effect of EVs secreted by different *T. cruzi* strains (Y, Colombiana, CL-14, and

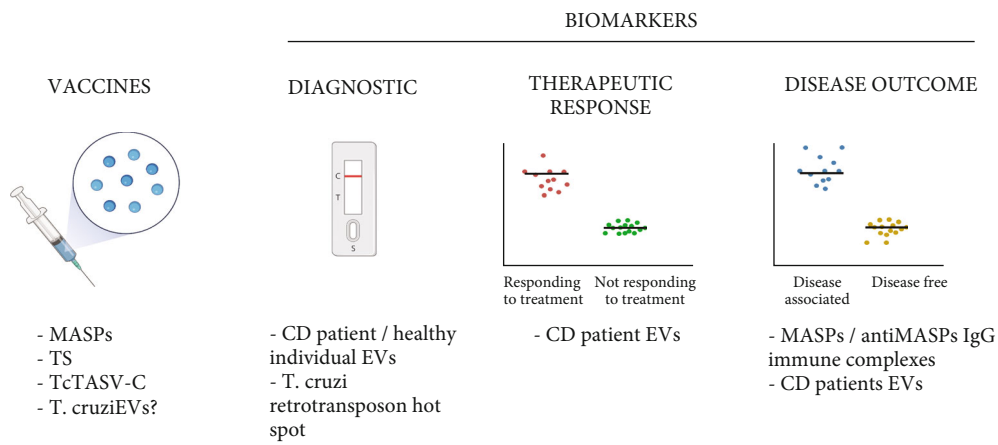


Figure 3: Potential role of EVs as new tools for CD prevention and control. EVs from *T. cruzi* or parasite proteins found in the EVs have been tested as vaccine antigens for Chagas disease. EVs isolated from CD patients, the retrotransposon hot spot *T. cruzi* protein, and the immunocomplexes found in CD patients are also being studied for their potential as biomarkers for diagnosis, therapeutic response, and disease outcome (created with http://BioRender.com).

YuYu) when used to stimulate splenocytes from chronically infected mice. Interestingly, the immunomodulatory responses caused by the EV stimulus depended on the parasite strain. As previously reported, in other cell types, splenic cells also produced NO, TNF-$\alpha$, IL-6, and IFN-$\gamma$ upon stimulation with parasite EVs. However, an increase in the production of anti-inflammatory cytokine IL-10 by T and B cells was also observed, which is in contrast with the proinflammatory profile found in other studies, and reinforces the importance of IL-10 in modulating the balance between inflammatory and anti-inflammatory responses, avoiding tissue damage (Figure 2(e)) [76]. Several *in vivo* studies addressing the EV effect on the pathological features of CD have also been performed, all of which used well-established mouse models. Some of these studies have shown that animals treated with parasite-derived EVs prior to *T. cruzi* infection are distinguished by increased circulating EVs in plasma, parasitemia, cardiac tropism, and inflammation (Figure 2(f)) [28, 66, 72] . Moreover, some studies found a reduction of NO and TNF-$\alpha$ levels in plasma and a decreased production of TNF-$\alpha$ and IL-6 in spleen cells from infected animals [72]. However, some discrepancies have been observed in the mortality rates linked to EV immunization, with some studies reporting increased mortality [28] while no differences were found in others [72].

There is growing evidence that the immunomodulatory properties of EVs depend on the *T. cruzi* strain and the parasite stage [74, 76, 77]. *T. cruzi*-derived EVs from different strains present different protein cargos, which correlates with differences in the sensitivity to complement-mediated lysis, parasite invasion, infectivity, virulence, and immunomodulatory responses [45, 76]. In relation to the effect of the EVs released by host cells after interacting with different parasite developmental stages, it has been found that all *T. cruzi* stages are able to induce the release of EVs by host cells, with mammalian infective forms causing the highest release [74].

## 5. EVs as a Potential Source of New Biomarkers in Chagas Disease

The use of EVs as a new platform to identify biomarkers has been described in the last few years for different pathologies, including parasitic diseases [78]. Taking into consideration that one of the biggest challenges for CD is the lack of validated biomarkers to indicate therapeutic response and disease outcomes [59], EVs could become a promising source for developing new biomarkers in infectious diseases.

As previously mentioned, the MASP multigene family is one of the major virulence factors of *T. cruzi*. It plays a fundamental role in cell invasion and has an associated humoral immune response in CD patients. Interestingly, this response is different depending on the clinical stage of the individuals, being lower in the sera of patients presenting cardiac affection compared to sera from those suffering from the gastrointestinal form of the disease [65]. Further research showed that the EVs released by the parasite containing MASP proteins are targeted by the immune system, triggering the formation of circulating immune complexes containing anti-MASP Immunoglobulin Gs (IgGs). The EVs forming immune complexes inhibit the complement system. Interestingly, the highest percentage of inhibition appeared in the digestive group, compared to the asymptomatic and cardiac patients. Taking advantage of this particularity, these immune complexes could be used as biomarkers for the differential diagnosis or prognosis of CD, in particular in patients with digestive manifestations [61]. In the same line, microvesicles also have potential as differential diagnosis or prognosis biomarkers during CD infection. The antibodies contained in the sera from CD patients detected antigens from EVs released by host cells after interacting with the infective forms of the parasite. Interestingly, these molecules were recognized differently by patients presenting the cardiac or indeterminate phase of the disease, indicating the existence of specific markers

associated with a differential diagnosis depending on the organ involved [74].

EV concentration in the body fluids of healthy individuals and patients presenting several forms of the disease has also been studied as a potential biomarker for differential diagnosis, with no clear results. While some studies did not find any statistical differences in the number of vesicles in CD patients compared to healthy controls [74], others did find differences in terms of concentration, showing that treated patients presented lower concentrations of circulating EVs than healthy donors [48]. In this study, human THP-1 cells were incubated with circulating EVs, followed by ELISA to measure cytokines and determine whether the concentration of circulating EVs was associated with differential activation of the immune system. IFN-$\gamma$ and IL-17 showed a differential profile when compared to chronic Chagas patients and healthy controls, finding that patient samples induced a higher production of IFN-$\gamma$, and lower production of IL-17, a profile that could contribute to parasite persistence and tissue damage due to continuous inflammatory signaling [48] .

Two of the features of CD are chronic inflammation and oxidative stress, which are specially exacerbated in individuals suffering the cardiac form of the disease. It has been shown that microparticles generated during *T. cruzi* infection carry the host's signature for oxidative, nitrosative, and inflammatory states. Thus, EVs provide information about the disease's progression and could be useful for evaluating disease severity [70].

In a different study, a group of human and parasite proteins were identified in plasma-derived EVs from a heart transplant patient with chronic CD, while being absent in EVs from the plasma of healthy individuals. Interestingly, several human proteins and one parasite protein (pyruvate phosphate dikinase) were found to be present or upregulated before treatment and were absent or downregulated after treatment. Although these results should be interpreted with caution, as they represent a single clinical case and need to be validated in a larger cohort, they represent a proof-of-principle of the potential of this approach to discover new biomarkers of therapeutic response [46].

Finally, EVs from *T. cruzi* are also attractive candidates for use in the serological diagnosis of CD. In an attempt to identify antigens, present in trypomastigote excreted-secreted EVs, Bautista-López and collaborators incubated trypomastigote-excreted antigens associated with EVs with affinity columns containing IgG antibodies from healthy donors, or Chagas patients with clinical symptoms. Chagasic IgG affinity resin was highly enriched in *trans*-sialidases and showed a significant enrichment in mitochondrial proteins, retrotransposon hot spot (RHS) proteins, paraflagellar rod proteins, proteases, and multiple uncharacterized proteins [57]. RHS and *T. cruzi* paraflagellar rod-3 protein were further explored for their potential as serological antigens for the diagnosis of *T. cruzi* infection, showing robust cross-reactivity with sera from patients presenting all clinical forms of CD. Interestingly, no cross-reactivity with RHS was detected when using sera from patients with other parasitic diseases, which could be relevant for the development of a new diagnostic test with high specificity [57]. The potential control strategies that could be associated with EVs secreted by *T. cruzi* or *T. cruzi*-infected cells, such as biomarker discovery and/or vaccine development, are summarized in Figure 3.

## 6. Chagas Disease Prevention: Future Perspectives of EVs as New Vaccine Antigens against *T. cruzi* Infection

Even though vaccines could be a very useful cost-effective tool for the prevention and control of *T. cruzi* infection and transmission, we are still a long way from having a beneficial vaccine for CD [79]. The lack of financial support and interest from governments and the pharmaceutical industry, together with the genetic complexity of the parasite, have contributed to the slow progress in its development [80]. Multiple attempts have been made to develop safe and effective vaccines for CD. Currently, there are two main target product profiles for developing vaccines for CD. The first one, which could be used alone or in combination with drug therapy, aims to prevent, or at least delay, the progression of cardiac and digestive manifestations in patients presenting the indeterminate form of the disease [80]. The second one is aimed at developing a preventive vaccine [81]. Unfortunately, although some of the candidates were able to induce a partial protective response, none of them showed complete protective immunity [81]. In this scenario, new approaches and ideas are needed to develop a protective vaccine for *T. cruzi* infection. Immunization with molecules delivered into EVs is an interesting possibility for exploring *T. cruzi* infection.

Interestingly, one of the protein families present in *T. cruzi*-derived EVs, which has been tested as a potential vaccine antigen, is the MASP family. Taking into consideration that MASPs play a major role in host-cell invasion, that they are one of the most important *T. cruzi* virulence factors, and that several MASP family members have predicted MHC-I and MHC-II epitopes, a synthetic MASP-derived peptide was tested as a vaccine candidate in a murine model of CD [65, 82, 83]. Mice immunized with the synthetic MASP peptide conjugated to keyhole limpet hemocyanin showed an 86% survival rate after being infected with trypomastigotes and had a much lower parasite load in the heart, liver, and spleen compared to untreated animals. Moreover, vaccinated animals produced neutralizing antibodies and developed a protective cytokine response against parasite infection. Interestingly, the vaccine engaged both humoral and cellular responses, indicating that MASP proteins are promising targets for the development of a CD vaccine [83].

Another well-known *T. cruzi* virulence factor, which is essential for the invasion process and present in EVs, is the TS family. Several investigators have tested immunization with multiple gene-encoding members of the TS family, in different vaccine platforms (bacterial and viral vectors, or as a recombinant protein) and formulations (alone, together with other *T. cruzi* glycoconjugates, and associated with adjuvants) [81, 84]. Although the results obtained showed

some limitations, some vaccine formulations induced immunity in mouse models challenged with *T. cruzi*, producing antibodies, preventing the development of tissue damage, and having an impact on the mortality of infected animals [84]. In that context, TS antigens conjugated to EVs could be a different approach to developing vaccines for CD.

Another *T. cruzi* protein family secreted in EVs that has been considered for immunization is the *T. cruzi* trypomastigote alanine, valine, and serine (TcTASV-C). To evaluate the performance of TcTASV-C as a vaccine antigen, mice were vaccinated following a DNA-prime protein-boost schedule of immunization. However, when animals were challenged with a highly virulent *T. cruzi* strain two weeks after the final dose, the results obtained were not very promising. Although TcTASV-C-vaccinated mice showed a strong humoral response, there was a delay in the appearance of circulating trypomastigotes, and they presented lower parasitemia, exhibiting only a 30% higher survival rate than controls [60].

Finally, preliminary results have shown that mice immunization with 3 doses of EVs derived from trypomastigote forms of *T. cruzi* (Y strain), administered in the presence of $Al(OH)_3$ as adjuvant, could induce some level of protection against experimental CD. Preliminary results showed that vaccinated mice presented lower parasitemia than non-vaccinated animals. However, no significant changes were observed in the survival of all animal groups. Further investigation needs to be carried out to understand which molecules are responsible for this potential protection. Moreover, experimental assays using EVs isolated from trypomastigote forms from different DTUs are needed to verify the influence of virulence factors in vaccination against experimental CD (Torrecilhas. A. C., unpublished data).

The use of different experimental models, cell types, adjuvants, doses, and vaccination regimens may also determine the development of the protective response. The key questions remaining for the development of new vaccine tools for CD are as follows: further characterization of the immune responses, development of highly efficient antigen delivery systems, animal models mimicking the chronic phase of the disease, assessment of parasite diversity and antigenic variation, study of coinfections, and use of adjuvants and new vaccination regimens together with more studies focusing on parasite tissue distribution [79].

## 7. Conclusions

In the last decade, research on the biology, function, and potential applications of EVs has grown exponentially. Even though the number of studies regarding *T. cruzi* infection and EVs is increasing every year, there is still a long way to go. Many questions remain in relation to the role of EVs in the pathogenesis of the disease and its mechanisms in pathogen-host interaction. Do the virulent factors maintain their virulent function when associated with EVs? Even though the function of these molecules has been perfectly described on the parasite surface, their specific function in vesicles is still not well known. Do the EVs secreted by the parasite or infected cells protect the host, or otherwise favor the infection? The EVs secreted by trypomastigotes favor host cell invasion and promote parasite immune evasion, increasing its survival in *in vitro* and *in vivo* studies. However, EVs secreted by the parasite, infected cells, infected individuals, and infected mice are also able to modulate macrophages, triggering a proinflammatory response against the parasite. Importantly, this inflammatory response, if unbalanced, is one of the main features responsible for disease progression in Chagas disease. Finally, it is urgent that we continue to explore the potential of EVs for antigen discovery, vaccine development, therapeutic strategies, and biomarkers, as these are among the most important challenges that we face in our efforts to control CD.

## Conflicts of Interest

No potential conflicts of interest were reported by the authors.

## Authors' Contributions

NC-S, MG-L, ACT, and CF-B wrote the manuscript. NC-S, MG-L, MJP, ACT, and CF-B contributed to the final manuscript editing. Figures have been idealized and were done by NC-S and CF-B. All authors reviewed the manuscript and approved the submitted version.

## Acknowledgments

Research in the ACT Lab is supported by Fundação de Amparo à Pesquisa do Estado de São Paulo (FAPESP) grant 2019/15909-0 and FAPESP grant 2020/07870-4, Conselho Nacional de Desenvolvimento Científico e Tecnológico (CNPq) grant 408186/2018-6 and CNPq 302104/2019-4, and CAPES. Research in the CF-B Lab is funded by Fundació La Marató de TV3 (reference 566/U/2018) and CIBER-Consorcio Centro de Investigación Biomédica en Red (CB 2021), Instituto de Salud Carlos III, Ministerio de Ciencia e Innovación, and Unión Europea–NextGenerationEU. Barcelona Institute for Global Health (ISGlobal) receives support from the Spanish Ministry of Science, Innovation and Universities through the Centro de Excelencia Severo Ochoa 2019–2023 Program (CEX2018-000806-S). ISGlobal and Institut d'Investigació en Ciències de la Salut Germans Trias i Pujol (IGTP) are members of the Centres de Recerca de Catalunya (CERCA Program), Generalitat de Catalunya.

## References

[1] S. Antinori, L. Galimberti, R. Bianco, R. Grande, M. Galli, and M. Corbellino, "Chagas disease in Europe: a review for the internist in the globalized world," *European Journal of Internal Medicine*, vol. 43, pp. 6–15, 2017.

[2] J. C. Dias, A. C. Silveira, and C. J. Schofield, "The impact of Chagas disease control in Latin America: a review," *Memórias do Instituto Oswaldo Cruz*, vol. 97, no. 5, pp. 603–612, 2002.

[3] J. Gascon, C. Bern, and M. J. Pinazo, "Chagas disease in Spain, the United States and other non-endemic countries," *Acta Tropica*, vol. 115, no. 1-2, pp. 22–27, 2010.

[4] J. A. Perez-Molina, A. M. Perez, F. F. Norman, B. Monge-Maillo, and R. Lopez-Velez, "Old and new challenges in Chagas disease," *The Lancet Infectious Diseases*, vol. 15, no. 11, pp. 1347–1356, 2015.

[5] J. R. Coura and P. A. Viñas, "Chagas disease: a new worldwide challenge," *Nature*, vol. 465, no. S7301, pp. S6–S7, 2010.

[6] M. J. Pinazo and J. Gascon, "The importance of the multidisciplinary approach to deal with the new epidemiological scenario of Chagas disease (global health)," *Acta Tropica*, vol. 151, pp. 16–20, 2015.

[7] C. Bern, "Chagas' disease," *The New England Journal of Medicine*, vol. 373, no. 5, pp. 456–466, 2015.

[8] R. M. Saraiva, M. F. F. Mediano, F. S. Mendes et al., "Chagas heart disease: an overview of diagnosis, manifestations, treatment, and care," *World Journal of Cardiology*, vol. 13, no. 12, pp. 654–675, 2021.

[9] J. Alonso-Padilla, N. Cortes-Serra, M. J. Pinazo et al., "Strategies to enhance access to diagnosis and treatment for Chagas disease patients in Latin America," *Expert Review of Anti-Infective Therapy*, vol. 17, no. 3, pp. 145–157, 2019.

[10] J. A. Perez-Molina and I. Molina, "Chagas disease cardiomyopathy treatment remains a challenge - authors' reply," *Lancet*, vol. 391, no. 10136, pp. 2209-2210, 2018.

[11] M. Yáñez-Mó, P. R. M. Siljander, Z. Andreu et al., "Biological properties of extracellular vesicles and their physiological functions," *Journal of extracellular vesicles*, vol. 4, no. 1, article 27066, 2015.

[12] C. Théry, K. W. Witwer, E. Aikawa et al., "Minimal information for studies of extracellular vesicles 2018 (MISEV2018): a position statement of the International Society for Extracellular Vesicles and update of the MISEV2014 guidelines," *Journal of Extracellular Vesicles*, vol. 7, no. 1, article 1535750, 2018.

[13] M. Colombo, G. Raposo, and C. Thery, "Biogenesis, secretion, and intercellular interactions of exosomes and other extracellular vesicles," *Annual Review of Cell and Developmental Biology*, vol. 30, no. 1, pp. 255–289, 2014.

[14] Y. Zhang, Y. Liu, H. Liu, and W. H. Tang, "Exosomes: biogenesis, biologic function and clinical potential," *Cell & Bioscience*, vol. 9, no. 1, p. 19, 2019.

[15] A. Marcilla, L. Martin-Jaular, M. Trelis et al., "Extracellular vesicles in parasitic diseases," *Journal of Extracellular Vesicles*, vol. 3, no. 1, p. 25040, 2014.

[16] G. Coakley, R. M. Maizels, and A. H. Buck, "Exosomes and other extracellular vesicles: the new communicators in parasite infections," *Trends in Parasitology*, vol. 31, no. 10, pp. 477–489, 2015.

[17] J. H. Campos, R. P. Soares, K. Ribeiro, A. C. Andrade, W. L. Batista, and A. C. Torrecilhas, "Extracellular vesicles: role in inflammatory responses and potential uses in vaccination in cancer and infectious diseases," *Journal of Immunology Research*, vol. 2015, Article ID 832057, 14 pages, 2015.

[18] G. G. Mekonnen, M. Pearson, A. Loukas, and J. Sotillo, "Extracellular vesicles from parasitic helminths and their potential utility as vaccines," *Expert Review of Vaccines*, vol. 17, no. 3, pp. 197–205, 2018.

[19] A. C. Torrecilhas, R. P. Soares, S. Schenkman, C. Fernández-Prada, and M. Olivier, "Extracellular vesicles in trypanosomatids: host cell communication," *Frontiers in Cellular and Infection Microbiology*, vol. 10, article 602502, 2020.

[20] A. J. Szempruch, S. E. Sykes, R. Kieft et al., "Extracellular vesicles from *Trypanosoma brucei* mediate virulence factor transfer and cause host anemia," *Cell*, vol. 164, no. 1-2, pp. 246–257, 2016.

[21] M. Olivier and C. Fernandez-Prada, "Leishmania and its exosomal pathway: a novel direction for vaccine development," *Future Microbiology*, vol. 14, no. 7, pp. 559–561, 2019.

[22] S. M. Pope and C. Lasser, "Toxoplasma gondii infection of fibroblasts causes the production of exosome-like vesicles containing a unique array of mRNA and miRNA transcripts compared to serum starvation," *Journal of Extracellular Vesicles*, vol. 2, no. 1, 2013.

[23] L. Martin-Jaular, E. S. Nakayasu, M. Ferrer, I. C. Almeida, and H. A. Del Portillo, "Exosomes from Plasmodium yoelii-infected reticulocytes protect mice from lethal infections," *PLoS One*, vol. 6, no. 10, article e26588, 2011.

[24] P. Y. Mantel and M. Marti, "The role of extracellular vesicles in Plasmodium and other protozoan parasites," *Cellular Microbiology*, vol. 16, no. 3, pp. 344–354, 2014.

[25] I. Evans-Osses, A. Mojoli, M. Monguio-Tortajada et al., "Microvesicles released from Giardia intestinalis disturb host-pathogen response in vitro," *European Journal of Cell Biology*, vol. 96, no. 2, pp. 131–142, 2017.

[26] A. Marcilla, M. Trelis, A. Cortes et al., "Extracellular vesicles from parasitic helminths contain specific excretory/secretory proteins and are internalized in intestinal host cells," *PLoS One*, vol. 7, no. 9, article e45974, 2012.

[27] F. C. Nowacki, M. T. Swain, O. I. Klychnikov et al., "Protein and small non-coding RNA-enriched extracellular vesicles are released by the pathogenic blood fluke Schistosoma mansoni," *Journal of Extracellular Vesicles*, vol. 4, no. 1, article 28665, 2015.

[28] A. C. Trocoli Torrecilhas, R. R. Tonelli, W. R. Pavanelli et al., "Trypanosoma cruzi:parasite shed vesicles increase heart parasitism and generate an intense inflammatory response," *Microbes and Infection*, vol. 11, no. 1, pp. 29–39, 2009.

[29] M. M. Maia, A. B. da Cruz, I. S. Pereira, N. N. Taniwaki, G. M. Namiyama, and V. L. Pereira-Chioccola, "Characterization of murine extracellular vesicles and Toxoplasma gondii infection," *Parasite Immunology*, vol. 43, no. 9, article e12869, 2021.

[30] P. Y. Mantel, A. N. Hoang, I. Goldowitz et al., "Malaria-infected erythrocyte-derived microvesicles mediate cellular communication within the parasite population and with the host immune system," *Cell Host & Microbe*, vol. 13, no. 5, pp. 521–534, 2013.

[31] N. Regev-Rudzki, D. W. Wilson, T. G. Carvalho et al., "Cell-cell communication between malaria-infected red blood cells via exosome- like vesicles," *Cell*, vol. 153, no. 5, pp. 1120–1133, 2013.

[32] A. C. Torrecilhas, R. I. Schumacher, M. J. Alves, and W. Colli, "Vesicles as carriers of virulence factors in parasitic protozoan diseases," *Microbes and Infection*, vol. 14, no. 15, pp. 1465–1474, 2012.

[33] H. Toda, M. Diaz-Varela, J. Segui-Barber et al., "Plasma-derived extracellular vesicles from *Plasmodium vivax* patients signal spleen fibroblasts via NF-kB facilitating parasite cytoadherence," *Nature Communications*, vol. 11, no. 1, p. 2761, 2020.

[34] E. Dekel, D. Yaffe, I. Rosenhek-Goldian et al., "20S proteasomes secreted by the malaria parasite promote its growth," *Nature Communications*, vol. 12, no. 1, p. 1172, 2021.

[35] X. Zhou, F. Xie, L. Wang et al., "The function and clinical application of extracellular vesicles in innate immune

regulation," *Cellular & Molecular Immunology*, vol. 17, no. 4, pp. 323–334, 2020.

[36] G. Dong, V. Wagner, A. Minguez-Menendez, C. Fernandez-Prada, and M. Olivier, "Extracellular vesicles and leishmaniasis: current knowledge and promising avenues for future development," *Molecular Immunology*, vol. 135, pp. 73–83, 2021.

[37] M. Khosravi, E. S. Mirsamadi, H. Mirjalali, and M. R. Zali, "Isolation and functions of extracellular vesicles derived from parasites: the promise of a new era in immunotherapy, vaccination, and diagnosis," *International Journal of Nanomedicine*, vol. 15, pp. 2957–2969, 2020.

[38] F. Aline, D. Bout, S. Amigorena, P. Roingeard, and I. Dimier-Poisson, "Toxoplasma gondii antigen-pulsed-dendritic cell-derived exosomes induce a protective immune response against T. gondii infection," *Infection and Immunity*, vol. 72, no. 7, pp. 4127–4137, 2004.

[39] C. Beauvillain, M. O. Juste, S. Dion, J. Pierre, and I. Dimier-Poisson, "Exosomes are an effective vaccine against congenital toxoplasmosis in mice," *Vaccine*, vol. 27, no. 11, pp. 1750–1757, 2009.

[40] C. Beauvillain, S. Ruiz, R. Guiton, D. Bout, and I. Dimier-Poisson, "A vaccine based on exosomes secreted by a dendritic cell line confers protection against T. gondii infection in syngeneic and allogeneic mice," *Microbes and Infection*, vol. 9, no. 14-15, pp. 1614–1622, 2007.

[41] M. J. Kim, B. K. Jung, J. Cho et al., "Exosomes secreted by Toxoplasma gondii-infected L6 cells: their effects on host cell proliferation and cell cycle changes," *The Korean Journal of Parasitology*, vol. 54, no. 2, pp. 147–154, 2016.

[42] L. Martin-Jaular, A. de Menezes-Neto, M. Monguio-Tortajada et al., "Spleen-dependent immune protection elicited by CpG adjuvanted reticulocyte-derived exosomes from malaria infection is associated with changes in T cell subsets' distribution," *Frontiers in Cell and Development Biology*, vol. 4, p. 131, 2016.

[43] K. A. Babatunde, S. Mbagwu, M. A. Hernandez-Castaneda et al., "Malaria infected red blood cells release small regulatory RNAs through extracellular vesicles," *Scientific Reports*, vol. 8, no. 1, p. 884, 2018.

[44] I. Aparici-Herraiz, M. Gualdron-Lopez, C. J. Castro-Cavadia et al., "Antigen discovery in circulating extracellular vesicles from Plasmodium vivax patients," *Frontiers in Cellular and Infection Microbiology*, vol. 11, article 811390, 2022.

[45] K. S. Ribeiro, C. I. Vasconcellos, R. P. Soares et al., "Proteomic analysis reveals different composition of extracellular vesicles released by two Trypanosoma cruzis trains associated with their distinct interaction with host cells," *Journal of Extracellular Vesicles*, vol. 7, no. 1, article 1463779, 2018.

[46] N. Cortes-Serra, M. T. Mendes, C. Mazagatos et al., "Plasma-derived extracellular vesicles as potential biomarkers in heart transplant patient with chronic Chagas disease," *Emerging Infectious Diseases*, vol. 26, no. 8, pp. 1846–1851, 2020.

[47] F. Properzi, M. Logozzi, and S. Fais, "Exosomes: the future of biomarkers in medicine," *Biomarkers in Medicine*, vol. 7, no. 5, pp. 769–778, 2013.

[48] R. P. Madeira, L. M. Dal'Mas Romera, B. P. de Cássia, C. Mady, B. M. Ianni, and A. C. Torrecilhas, "New biomarker in Chagas disease: extracellular vesicles isolated from peripheral blood in chronic Chagas disease patients modulate the human immune response," *Journal of Immunology Research*, vol. 2021, Article ID 6650670, 14 pages, 2021.

[49] M. Gualdron-Lopez, E. L. Flannery, N. Kangwanrangsan et al., "Characterization of Plasmodium vivax proteins in plasma-derived exosomes from malaria-infected liver-chimeric humanized mice," *Frontiers in Microbiology*, vol. 9, p. 1271, 2018.

[50] F. M. Campos, B. S. Franklin, A. Teixeira-Carvalho et al., "Augmented plasma microparticles during acute Plasmodium vivax infection," *Malaria Journal*, vol. 9, no. 1, p. 327, 2010.

[51] U. Sahu, P. K. Sahoo, S. K. Kar, B. N. Mohapatra, and M. Ranjit, "Association of TNF level with production of circulating cellular microparticles during clinical manifestation of human cerebral malaria," *Human Immunology*, vol. 74, no. 6, pp. 713–721, 2013.

[52] T. Meningher, G. Lerman, N. Regev-Rudzki et al., "Schistosomal microRNAs isolated from extracellular vesicles in sera of infected patients: a new tool for diagnosis and follow-up of human schistosomiasis," *The Journal of Infectious Diseases*, vol. 215, no. 3, pp. 378–386, 2017.

[53] J. F. da Silveira, P. A. Abrahamsohn, and W. Colli, "Plasma membrane vesicles isolated from epimastigote forms of *Trypanosoma cruzi*," *Biochimica et Biophysica Acta*, vol. 550, no. 2, pp. 222–232, 1979.

[54] M. F. Gonçalves, E. S. Umezawa, A. M. Katzin et al., "*Trypanosoma cruzi*: shedding of surface antigens as membrane vesicles," *Experimental Parasitology*, vol. 72, no. 1, pp. 43–53, 1991.

[55] E. Bayer-Santos, C. Aguilar-Bonavides, S. P. Rodrigues et al., "Proteomic analysis of Trypanosoma cruzi secretome: characterization of two populations of extracellular vesicles and soluble proteins," *Journal of Proteome Research*, vol. 12, no. 2, pp. 883–897, 2013.

[56] R. M. Queiroz, C. A. Ricart, M. O. Machado et al., "Insight into the exoproteome of the tissue-derived trypomastigote form of Trypanosoma cruzi," *Frontiers in Chemistry*, vol. 4, p. 42, 2016.

[57] N. L. Bautista-Lopez, M. Ndao, F. V. Camargo et al., "Characterization and diagnostic application of Trypanosoma cruzi trypomastigote excreted-secreted antigens shed in extracellular vesicles released from infected mammalian cells," *Journal of Clinical Microbiology*, vol. 55, no. 3, pp. 744–758, 2017.

[58] L. Retana Moreira, A. Prescilla-Ledezma, A. Cornet-Gomez et al., "Biophysical and biochemical comparison of extracellular vesicles produced by infective and non-infective stages of Trypanosoma cruzi," *International Journal of Molecular Sciences*, vol. 22, no. 10, p. 5183, 2021.

[59] N. Cortes-Serra, I. Losada-Galvan, M. J. Pinazo, C. Fernandez-Becerra, J. Gascon, and J. Alonso-Padilla, "State-of-the-art in host-derived biomarkers of Chagas disease prognosis and early evaluation of anti Trypanosoma cruzi treatment response," *Biochimica et Biophysica Acta - Molecular Basis of Disease*, vol. 2020, no. 7, article 165758, 2020.

[60] L. D. Caeiro, C. D. Alba-Soto, M. Rizzi et al., "The protein family TcTASV-C is a novel Trypanosoma cruzi virulence factor secreted in extracellular vesicles by trypomastigotes and highly expressed in bloodstream forms," *PLoS Neglected Tropical Diseases*, vol. 12, no. 5, article e0006475, 2018.

[61] I. M. Díaz Lozano, L. M. De Pablos, S. A. Longhi, M. P. Zago, A. G. Schijman, and A. Osuna, "Immune complexes in chronic Chagas disease patients are formed by exovesicles from Trypanosoma cruzi carrying the conserved MASP N-terminal region," *Scientific Reports*, vol. 7, no. 1, article 44451, 2017.

[62] L. M. da Fonseca, K. M. da Costa, V. S. Chaves et al., "Theft and reception of host cell's sialic acid: dynamics of

Trypanosoma cruzi trans-sialidases and mucin-like molecules on Chagas' disease immunomodulation," *Frontiers in Immunology*, vol. 10, p. 164, 2019.

[63] N. O. Martins, R. T. Souza, E. M. Cordero et al., "Molecular characterization of a novel family of Trypanosoma cruzi surface membrane proteins (TcSMP) involved in mammalian host cell invasion," *PLoS Neglected Tropical Diseases*, vol. 9, no. 11, article e0004216, 2015.

[64] R. F. Neves, A. C. Fernandes, J. R. Meyer-Fernandes, and T. Souto-Padron, "Trypanosoma cruzi-secreted vesicles have acid and alkaline phosphatase activities capable of increasing parasite adhesion and infection," *Parasitology Research*, vol. 113, no. 8, pp. 2961–2972, 2014.

[65] L. M. De Pablos, I. M. Díaz Lozano, M. I. Jercic et al., "The C-terminal region of Trypanosoma cruzi MASPs is antigenic and secreted via exovesicles," *Scientific Reports*, vol. 6, no. 1, article 27293, 2016.

[66] I. Cestari, E. Ansa-Addo, P. Deolindo, J. M. Inal, and M. I. Ramirez, "Trypanosoma cruzi immune evasion mediated by host cell-derived microvesicles," *Journal of Immunology*, vol. 188, no. 4, pp. 1942–1952, 2012.

[67] M. Ming, M. E. Ewen, and M. E. Pereira, "Trypanosome invasion of mammalian cells requires activation of the TGF$\beta$ signaling pathway," *Cell*, vol. 82, no. 2, pp. 287–296, 1995.

[68] R. R. Ferreira, R. D. S. Abreu, G. Vilar-Pereira et al., "TGF-$\beta$ inhibitor therapy decreases fibrosis and stimulates cardiac improvement in a pre-clinical study of chronic Chagas' heart disease," *PLoS Neglected Tropical Diseases*, vol. 13, no. 7, article e0007602, 2019.

[69] A. Cronemberger-Andrade, P. Xander, R. P. Soares et al., "Trypanosoma cruzi-Infected human macrophages shed proinflammatory extracellular vesicles that enhance host-cell invasion via toll-like receptor 2," *Frontiers in Cellular and Infection Microbiology*, vol. 10, p. 99, 2020.

[70] I. H. Chowdhury, S. J. Koo, S. Gupta et al., "Gene expression profiling and functional characterization of macrophages in response to circulatory microparticles produced during Trypanosoma cruzi infection and Chagas disease," *Journal of Innate Immunity*, vol. 9, no. 2, pp. 203–216, 2017.

[71] C. I. Vasconcelos, A. Cronemberger-Andrade, N. Souza-Melo et al., "Stress induces release of extracellular vesicles by Trypanosoma cruzi trypomastigotes," *Journal of Immunology Research*, vol. 2021, Article ID 2939693, 12 pages, 2021.

[72] M. I. Lovo-Martins, A. D. Malvezi, N. G. Zanluqui et al., "Extracellular vesicles shed by Trypanosoma cruzi potentiate infection and elicit lipid body formation and PGE2 production in murine macrophages," *Frontiers in Immunology*, vol. 9, p. 896, 2018.

[73] S. Choudhuri and N. J. Garg, "PARP1-cGAS-NF-$\kappa$B pathway of proinflammatory macrophage activation by extracellular vesicles released during Trypanosoma cruzi infection and Chagas disease," *PLoS Pathogens*, vol. 16, no. 4, article e1008474, 2020.

[74] M. I. Ramirez, P. Deolindo, I. J. de Messias-Reason et al., "Dynamic flux of microvesicles modulate parasite-host cell interaction of Trypanosoma cruzi in eukaryotic cells," *Cell Microbiol*, vol. 19, no. 4, article e12672, 2017.

[75] L. Retana Moreira, F. Rodríguez Serrano, and A. Osuna, "Extracellular vesicles of Trypanosoma cruzi tissue-culture cell-derived trypomastigotes: induction of physiological changes in non-parasitized culture cells," *PLoS Neglected Tropical Diseases*, vol. 13, no. 2, article e0007163, 2019.

[76] P. M. Nogueira, K. Ribeiro, A. C. Silveira et al., "Vesicles from different Trypanosoma cruzi strains trigger differential innate and chronic immune responses," *Journal of Extracellular Vesicles*, vol. 4, no. 1, article 28734, 2015.

[77] M. P. Wyllie and M. I. Ramirez, "Microvesicles released during the interaction between Trypanosoma cruzi TcI and TcII strains and host blood cells inhibit complement system and increase the infectivity of metacyclic forms of host cells in a strain-independent process," *Pathogens and Disease*, vol. 75, no. 7, 2017.

[78] I. Evans-Osses, L. H. Reichembach, and M. I. Ramirez, "Exosomes or microvesicles? Two kinds of extracellular vesicles with different routes to modify protozoan-host cell interaction," *Parasitology Research*, vol. 114, no. 10, pp. 3567–3575, 2015.

[79] J. C. Vazquez-Chagoyan, S. Gupta, and N. J. Garg, "Vaccine development against *Trypanosoma cruzi* and Chagas disease," *Advances in Parasitology*, vol. 75, pp. 121–146, 2011.

[80] O. Rodriguez-Morales, V. Monteon-Padilla, S. C. Carrillo-Sanchez et al., "Experimental vaccines against Chagas disease: a journey through history," *Journal of Immunology Research*, vol. 2015, Article ID 489758, 8 pages, 2015.

[81] E. Dumonteil and C. Herrera, "The case for the development of a Chagas disease vaccine: why? How? When?," *Tropical Medicine and Infectious Disease*, vol. 6, no. 1, p. 16, 2021.

[82] E. S. Nakayasu, T. J. Sobreira, R. Torres Jr. et al., "Improved proteomic approach for the discovery of potential vaccine targets in Trypanosoma cruzi," *Journal of Proteome Research*, vol. 11, no. 1, pp. 237–246, 2012.

[83] C. Serna, J. A. Lara, S. P. Rodrigues, A. F. Marques, I. C. Almeida, and R. A. Maldonado, "A synthetic peptide from *Trypanosoma cruzi* mucin-like associated surface protein as candidate for a vaccine against Chagas disease," *Vaccine*, vol. 32, no. 28, pp. 3525–3532, 2014.

[84] K. M. da Costa, L. Marques da Fonseca, J. S. dos Reis et al., "Trypanosoma cruzi trans-sialidase as a potential vaccine target against Chagas disease," *Front Cell Infect Microbiol*, vol. 11, article 768450, 2021.

Hindawi
Journal of Immunology Research
Volume 2022, Article ID 5187166, 15 pages
https://doi.org/10.1155/2022/5187166

*Research Article*

# Proteomic Profiling and Functional Analysis of B Cell-Derived Exosomes upon *Pneumocystis* Infection

**Dan Ma, Qian-Yu Zhang, Heng-Mo Rong, Kan Zhai, and Zhao-Hui Tong**

*Department of Respiratory and Critical Care Medicine, Beijing Institute of Respiratory Medicine and Beijing Chao-Yang Hospital, Capital Medical University, Beijing 100020, China*

Correspondence should be addressed to Zhao-Hui Tong; tongzhaohuicy@sina.com

Received 18 January 2022; Accepted 30 March 2022; Published 14 April 2022

Academic Editor: Patricia Xander



*Pneumocystis* is a life-threatening fungal pathogen that frequently causes fatal pneumonia (PCP) in immunocompromised individuals. Recently, B cells have been reported to play a crucial role in the pathogenesis of PCP through producing antibodies and activating $CD4^+$ T cell response. Exosomes are nanoscale small extracellular vesicles abundant with protein cargo and can mediate immune response during infectious disease. In this study, using tandem mass tag-based quantitative proteomics coupled with bioinformatic analysis, we attempted to characterize exosomes derived from B lymphocytes in response to PCP. Several proteins were verified by parallel reaction monitoring (PRM) analysis. Also, the effects of B cell exosomes on $CD4^+$ T cell response and phagocytic function of macrophages were clarified. Briefly, 1701 proteins were identified from B cell exosomes, and the majority of them were reported in Vesiclepedia. A total of 51 differentially expressed proteins of B cell exosomes were found in response to PCP. They were mainly associated with immune response and transcription regulation. PRM analysis confirmed the significantly changed levels of histone H1.3, vimentin, and tyrosine-protein phosphatase nonreceptor type 6 (PTPN6). Moreover, a functional study revealed the proinflammatory profile of B cell exosomes on $CD4^+$ T cell response in PCP. Taken together, our results suggest the involvement of exosomes derived from B cells in cell-to-cell communication, providing new information on the function of B cells in response to PCP.

## 1. Introduction

*Pneumocystis jirovecii* is an opportunistic fungal pathogen that causes life-threatening pneumonia in immunocompromised patients [1]. With the widespread use of highly active antiretroviral therapy in human immunodeficiency virus (HIV)-positive patients, the incidence of *Pneumocystis* pneumonia (PCP) in this population has decreased. At present, PCP is more common in HIV-negative patients [2, 3]. Importantly, HIV-negative patients often present with more severe symptoms requiring mechanical ventilation, and the mortality of these patients is higher (27%–50%) than that of patients with non-HIV PCP (4%–15%) [4, 5].

Vital roles of $CD4^+$ T cells and macrophages in host defense against *Pneumocystis* have been well documented, considering that depletion of both cell populations results in the inability to control *Pneumocystis* infection [6, 7]. There is accumulating evidence indicating that B lymphocytes also participate in the immune response during PCP. Patients receiving anti-CD20 monoclonal antibody rituximab are at a high risk of developing PCP [8, 9]. Murine models of PCP have demonstrated that apart from generating *Pneumocystis*-specific antibodies, B cells could also prime $CD4^+$ T cells through antigen presentation [10, 11]. Furthermore, IL-10-producing B regulatory cells exhibit an immunomodulatory function by regulating T helper (Th)1/Th17 cell responses during *Pneumocystis* infection [12]. However, the precise mechanism of the interaction between B cells and other immune cells in PCP remains to be fully elucidated.

Exosomes are small extracellular vesicles (EVs) (40–160 nm in diameter) that originate from multivesicular bodies and are released into extracellular space upon fusion with the plasma membrane. Exosomes carry biomolecules (including proteins, nucleic acids, lipids, and metabolites) and, thus, they can mediate intercellular communication

under physiological and pathological conditions [13]. It is now well established that antigen-presenting cells (macrophages, dendritic cells, and B cells) can release exosomes to modulate the immune response in various types of infection [14, 15].

Previous studies have shown that B cells are capable of secreting antigen-presenting exosomes containing major histocompatibility complex (MHC) class I (MHC-I), class II (MHC-II), and costimulatory molecules, which could induce antigen-specific $CD4^+$ T cell response or cytotoxic $CD8^+$ T cell response [16–19]. Yet, there is also evidence that B cell-derived exosomes are immunosuppressive. For example, the Fas ligand expressed on B cell-derived exosomes could induce apoptosis in $CD4^+$ T cells; therefore, it may be applied to restrain T cell-mediated responses in transplant recipients [20]. Another study has reported that $CD39^+$ $CD73^+$ EVs from B cells inhibit chemotherapeutic antitumor $CD8^+$ T cell response [21]. Thus, the protein composition of B cell exosomes suggests their immune properties and their crucial role in mediating different immune responses. Here, we sought to purify exosomes released from lung B cells of mice and perform high-throughput tandem mass tag (TMT)-labeled quantitative proteomics [22] to characterize the exosomal protein components during PCP. Parallel reaction monitoring (PRM) targeted proteomics was carried out for validation. In addition, the effects of B cell exosomes on $CD4^+$ T cell response and macrophage function were analyzed.

## 2. Materials and Methods

*2.1. Animals.* Healthy 6–8-week-old female C57BL/6 N mice and severe combined immunodeficient (SCID) mice were obtained from Vital River Lab Animal Co., Ltd (Beijing, China). The mice were housed in pathogen-free conditions and fed with autoclaved chow and water. All of the animal experiments were performed under deep anesthesia with 0.5% sodium pentobarbital (intraperitoneal injection, 50 mg/kg). All efforts were made to ameliorate animals' suffering. The animal procedures were approved by the Capital Medical University Animal Care and Use Committee.

*2.2. Lung Infection with Pneumocystis. Pneumocystis murina* (ATCC PRA-111™) was purchased from American Type Culture Collection (Manassas, VA, USA) and maintained in SCID mice as previously described [12]. Then, $1 \times 10^6$ *Pneumocystis* cysts diluted in 100 $\mu$L phosphate buffered saline (PBS) were injected into C57BL/6 N mice trachea to generate the PCP model. Uninfected C57BL/6 N mice were inoculated with 100 $\mu$L PBS.

*2.3. Isolation of Lung B Cells.* The mice were killed by exsanguination at 14 days after infection. After perfusion with 3 mL sterilized PBS through the right ventricle, lungs were extracted and minced into small pieces. Lung tissues were then digested in Roswell Park Memorial Institute (RPMI)-1640 media (Solarbio, Beijing, China) containing 10% fetal bovine serum (FBS, Hyclone, Logan, UT, USA), 50 U/mL DNase I (Sigma-Aldrich, St. Louis, MO, USA), and 1 mg/mL collagenase IV (Solarbio) for 60 min at 37°C. The digestions were filtered through 40-$\mu$m cell strainer and further separated using Lymphocyte Separation Media (MP Biomedicals, Santa Ana, CA, USA) to obtain mononuclear cells. B cells from *Pneumocystis*-infected mice and uninfected control mice were isolated using CD19 MicroBeads (Miltenyi Biotec, Bergisch Gladbach, Germany) following the manufacturer's instructions. Flow cytometric analysis showed that the purity was more than 90%. In addition, as we used primary cells, the apoptosis of B cells was determined using Annexin V Apoptosis Detection Kit FITC (Invitrogen, Carlsbad, CA, USA).

*2.4. Exosome Isolation and Characterization.* Exosome-depleted FBS was prepared by ultracentrifugation at 120,000 × g for 16 h at 4°C, and the supernatant was passed through a 0.22 $\mu$m polythersulfone syringe filter (Millipore, Billerica, MA, USA). Purified B cells of each group were cultured in RPMI-1640 medium supplemented with 10% exosome-depleted FBS at a density of $1.5 \times 10^6$/mL. After 48 h, the cell culture supernatants were collected and centrifuged at 400 × g for 6 min to remove cells and further at 2000 × g for 30 min to remove cell debris. The supernatants were mixed with Ribo™ Exosome Isolation Reagent (RiboBio, Guangzhou, China) and incubated overnight at 4°C. The mixtures were centrifuged at 1500 × g for 30 min at 4°C, and the supernatants were aspirated. Eventually, the exosome-containing pellets were resuspended in PBS for the following experiments.

*2.4.1. Western Blot.* Exosomal proteins were extracted with a radioimmunoprecipitation assay buffer (Solarbio) supplemented with 1 mM phenylmethylsulfonyl fluoride (Solarbio) and incubated on ice for 20 min. Protein concentration was determined using the BCA Protein Assay Kit (Pierce, Rockford, IL, USA). The protein lysates (30 $\mu$g) were subjected to 10% SDS-PAGE gel for separation and transferred to polyvinylidene fluoride membranes (Millipore). The membranes were blocked with 5% nonfat powdered milk in 1 × Tris -buffered saline tween (TBST) buffer for 1 h at room temperature and then incubated with primary antibodies against ALG-2-interacting protein X (ALIX) (Proteintech, Rosemont, IL, USA, 12422-1-AP, 1 : 1000), CD9 (Abcam, Cambridge, UK, ab92726, 1 : 2000), and heat shock protein 90 (HSP90) (Cell Signaling Technology, Danvers, MA, USA, #4877, 1 : 1000) overnight at 4°C. After washing with 1 × TBST, the membranes were incubated with horseradish peroxidase-conjugated anti-rabbit antibody (Cell Signaling Technology, #7074S) for 1 h at room temperature. Bands were visualized using enhanced chemiluminescence reagent (Millipore) and detected by ChemiDoc system (Bio-Rad, Hercules, CA, USA).

*2.4.2. Transmission Electron Microscopy.* A total of 20 $\mu$L of isolated exosomes were loaded onto copper grids (Ted Pella Inc., Redding, CA, USA) and allowed to absorb for 2 min. The samples were further fixed with 2% phosphotungstic acid (Solarbio) for 10 min. After air drying at room

temperature, the samples were observed under a JEM1230 transmission electron microscope (JEOL, Tokyo, Japan).

*2.4.3. Nanoparticle Tracking Analysis.* Size distribution of exosomes was measured by ZetaView PMX 110 (Particle Metrix, Meerbusch, Germany) and its corresponding software ZetaView 8.04.02. The samples were appropriately diluted using 1 × PBS buffer (Solarbio). Brownian motion of particles was tracked and recorded by the NTA instrument at 11 different positions. Each sample was analyzed three times.

### *2.5. TMT-Based Quantitative Proteomic Analysis*

*2.5.1. Sample Preparation.* Three biological replicates of B cell exosomes isolated from *Pneumocystis*-infected and uninfected control mice were prepared. Each biological replicate was pooled from 10 mice. Quantitative proteomics was conducted by Applied Protein Technology (Shanghai, China). To extract protein, exosome samples were lysed with SDT buffer (4% (*w*/*v*) SDS, 100 mM Tris-HCl, and 0.1 M DTT, pH 7.6). The amount of protein was analyzed with the BCA method, as mentioned above. Protein digestion by trypsin was performed by employing the filter-aided sample preparation (FASP) procedure described by Wisniewski et al. [23]. The digested peptides of each sample were desalted on C18 Cartridges (Empore™ SPE Cartridges C18 (standard density), bed I.D. 7 mm, volume 3 mL, Sigma), concentrated by vacuum centrifugation, and further reconstituted in 40 $\mu$L of 0.1% (*v*/*v*) formic acid.

*2.5.2. TMT Labeling and Peptide Fractionation.* The peptide mixture (100 $\mu$g) of each sample was labeled with TMT 6-Plex Isobaric Mass Tagging Kit (Thermo Scientific, Rockford, IL, USA) and then fractionated using High pH Reversed-Phase Peptide Fractionation Kit (Thermo Scientific) in accordance with the manufacturer's instructions.

*2.5.3. Liquid Chromatography and Tandem Mass Spectrometry (LC-MS/MS).* Each peptide fraction was subjected to Easy nLC, an HPLC liquid phase system (Proxeon Biosystems, now Thermo Fisher Scientific, Waltham, MA, USA). Eluent A was 0.1% formic acid, and eluent B was 84% acetonitrile supplemented with 0.1% formic acid. The chromatographic column was equilibrated with 95% eluent A. Then, the peptides were loaded onto a reverse phase trap column (Thermo Scientific Acclaim PepMap100, 100 $\mu$m × 2 cm, nanoViper C18) and separated by the C18-reversed phase analytical column (Thermo Scientific Easy Column, 10 cm long, 75 $\mu$m inner diameter, 3 $\mu$m resin) at a flow rate of 300 nL/min controlled by IntelliFlow technology. The MS data were obtained using a Q Exactive mass spectrometer (Thermo Scientific) operated in the positive ion mode. The parameters were set as follows: the survey scan of precursor ions, 300–1,800 *m*/*z*; automatic gain control target, 1*e*6; maximum inject time, 50 ms; dynamic exclusion duration, 60.0 s; full scans acquired at a resolution of 70,000 at 200 *m*/*z*; resolution for MS/MS scans, 17,500 at 200 *m*/*z*; MS/MS activation type, high-energy collisional dissociation (HCD) fragmentation; isolation width, 2 *m*/*z*; normalized collision energy, 30 eV; the underfill ratio, 0.1%; the instrument was run with peptide recognition mode enabled.

*2.5.4. Protein Identification and Quantification.* MS/MS raw data were searched by Proteome Discoverer 1.4 (Thermo Fisher Scientific) against the SwissProt database of *Mus musculus* (number of sequences: 76417, updated to January 6, 2021) using the algorithms of the MASCOT engine (Matrix Science, London, UK; version 2.2). The criteria for protein identification were as follows. Trypsin was selected as the digestive enzyme; two missed cleavages were allowed; peptide mass tolerances were set at 20 ppm for all MS spectra acquired; fragment mass tolerances were set at 0.1 Da for all MS/MS spectra acquired; fixed modifications were set as carbamidomethylation (C), TMT 6-plex (N-terminal), and TMT 6-plex (lysine, K); oxidation (methionine, M) and TMT 6-plex (tyrosine, Y) were defined as variable modifications; the peptide and protein false discovery rate (FDR) was set at ≤0.01. Proteins were quantified on the basis of the median of only unique peptides of each protein. To control experimental bias, the median protein ratio was normalized to 1. Differentially expressed proteins (DEPs) were defined as those with fold change > 1.2 (up- or downregulation) and $p$ value < 0.05. The mass spectrometry proteomics data have been deposited in the ProteomeXchange Consortium via the PRIDE partner repository with the dataset identifier PXD030103.

*2.6. Bioinformatic Analysis.* Gene ontology (GO) annotation of the identified proteins and DEPs was performed using the Database for Annotation, Visualization and Integrated Discovery (DAVID, Version 6.8) [24, 25]. Protein Analysis Through Evolutionary Relationships (PANTHER) classification system was used to categorize the proteins [26]. Kyoto Encyclopedia of Genes and Genomes (KEGG) pathway enrichment analysis was conducted by Metascape [27]. All of the identified proteins were compared with the total and top 100 murine proteins recorded in Vesiclepedia (http://www.microvesicles.org, version 4.1, release date: August 15, 2018) [28, 29]. To further explore the properties of B cell exosomal proteins, the web-based tools SignalP 5.0 [30] and SecretomeP 2.0 [31] were used to predict classically and nonclassically secreted proteins, respectively.

*2.7. PRM Analysis.* To verify the results of TMT-labeled proteomics, 21 peptides of eight proteins were further quantified by LC-PRM/MS analysis. Sample preparation was the same as that for the TMT protocol. Tryptic peptides were separated using Easy nLC 1200 system (Thermo Scientific). Then, Q-Exactive HF mass spectrometry (Thermo Scientific) was applied for 60 min. Detection mode was set at positive ion mode. MS2 activation type was HCD. Peptide was quantified based on the ratio to the heavy isotope-labeled peptide DIPVPKPK. The raw data were analyzed by Skyline 3.5.0 (MacCoss Lab, University of Washington) [32].

*2.8. $CD4^+$ T Cell Proliferation Assay.* $CD4^+$ T cells were isolated from the spleens of two uninfected mice by CD4 (L3T4) MicroBeads (Miltenyi Biotec) in accordance with the manufacturer's instructions and then labeled with 1 $\mu$M

carboxyfluorescein diacetate succinimidyl ester (CFSE, BD Biosciences, San Jose, CA, USA) for 10 min at 37°C. After washing with PBS, the CFSE-labeled T cells and unlabeled control T cells were cultured in a 96-well plate at a density of $2 \times 10^6$/mL and stimulated with plate-coated anti-CD3 monoclonal antibody (mAb) (5 $\mu$g/mL, eBioscience, San Diego, CA, USA) and anti-CD28 mAb (2 $\mu$g/mL, eBioscience). To evaluate the effect of exosomes on T cell proliferation, exosomes derived from uninfected and PCP B cells of equal quantity were added. After 72 h of culture, the cells were collected and the proliferation rate was determined by flow cytometry (FACSCanto II, BD Biosciences). The obtained data were analyzed with FlowJo software (TreeStar, Ashland, OR, USA).

*2.9. In Vitro Differentiation of Th1 Cells.* Naive $CD4^+$ $CD62L^+$ T cells from the spleens of two uninfected mice were purified with $CD4^+$ $CD62L^+$ T Cell Isolation Kit (Miltenyi Biotec). The isolated cells were cultured in a 96-well plate at a density of $2 \times 10^6$/mL and stimulated with plate-coated anti-CD3 mAb and anti-CD28 mAb, as described above. Cytokines and mAb used for Th1 cell differentiation were IL-2 (10 ng/mL), IL-12 (10 ng/mL), and anti-IL-4 mAb (10 $\mu$g/mL). Medium condition was defined as adding mere IL-2 (10 ng/mL). Coculture experiment was conducted to investigate the impact of B cell exosomes on Th1 cell differentiation rate. Naive $CD4^+$ T cells were treated with exosomes released from uninfected and PCP B cells of equal quantity. The cells were cultured for 48 h and then restimulated for 4 h at 37°C with phorbol myristate acetate (PMA, 50 ng/mL, Sigma-Aldrich) and ionomycin (1 $\mu$g/mL, Sigma-Aldrich) in the presence of brefeldin A (10 $\mu$g/mL, Enzo Life Science, Farmingdale, NY, USA). After permeabilization, the cells were stained with anti-mouse IFN-$\gamma$ antibody (eBioscience) and analyzed with FACSCanto II. The detailed methods are described in our previous publication [12].

*2.10. Phagocytosis Assay.* Bronchoalveolar lavage fluid (BALF) cells were collected from five uninfected mice by lavaging the lungs three times with sterile PBS using a polyethylene 18 G catheter. After centrifugation at $400 \times g$ for 6 min, $2 \times 10^5$ macrophages were treated with CON and PCP B cell exosomes (both from $1 \times 10^6$ B cells) or left untreated for 2 h and then washed gently with PBS to remove nonadherent cells. Zymosan is a yeast extract, and its major component is $\beta$-glucan, which is the major component of the *Pneumocystis* cell wall. It can bind to several pattern recognition receptors present on macrophages and therefore can be used as a substitution for *Pneumocystis* to test the phagocytosis of this fungus. The isolated alveolar macrophages (AMs) from different groups were then incubated with pHrodo Red Zymosan A BioParticles Conjugate (Life Technologies, Carlsbad, CA, USA) for 1.5 h at 37°C, 5% $CO_2$ (0.1 mg/mL, 200 $\mu$L, and 20 $\mu$g per well). The treated AMs were washed to remove noninternalized particles. For negative control, only AMs were added. The phagocytic function of AMs was assessed by analyzing the fluorescence intensity with flow cytometry.

*2.11. Statistical Analysis.* Statistical analyses were conducted using GraphPad Prism 7.0 (GraphPad Software, La Jolla, CA, USA). Data are presented as mean ± standard deviation. Two-tailed Student's *t* test was used for comparison between two groups. One-way ANOVA with Bonferroni post hoc test was applied for multiple comparisons. *p* values lower than 0.05 were considered statistically significant.

## 3. Results

*3.1. Characterization of B Cell-Derived Exosomes.* To confirm the presence of B cell-derived exosomes, we isolated B cells from the lungs of uninfected control and *Pneumocystis*-infected mice, which were referred to as the CON group and the PCP group, respectively. The mice were killed at 2 weeks after infection, given that the histopathology exhibited the most severe inflammatory response during this period based on our previous study [12]. Interestingly, using Annexin V/Propidium Iodide (PI) staining method, we observed that pulmonary B cells from PCP mice showed increased apoptosis (late stage) (Figure 1), which might be the immunological impact of *Pneumocystis* infection.

Exosomes were then extracted using a polyethylene glycol-based commercial reagent. The morphology of the isolated vesicles was visualized using electron microscopy and showed typical cup-shaped membrane structures with a size of approximately 100 nm (Figure 2(a)). The exosomal markers CD9, ALIX, and HSP90 were detected by western blot (Figure 2(b)). We then measured the size distribution of B cell exosomes. The diameter of the particles analyzed was slightly above 100 nm, consistent with the size range of exosomes (Figure 2(c)). These results indicated that B cells extracted from the lung tissue could generate exosomes *in vitro*.

*3.2. Proteomic Analysis of B Cell Exosomes from Uninfected and Pneumocystis-Infected Mice.* To unveil the protein contents of B cell exosomes comprehensively, we performed high-throughput TMT-labeled quantitative proteomics of exosomes derived from B cells of CON and PCP mice. Three independent biological replicates of each group were analyzed. The detailed information of each biological replicate is presented in Supplementary Table 1. In total, 1701 proteins were identified in B cell-derived exosomes (Supplementary Table 2). Next, we compared our mass spectrometry data with the previously published murine exosomal proteins deposited in Vesiclepedia (August 2018). The Venn diagram shows that 1312 proteins had been reported, and 84 of them were present in the top 100 ranked proteins (Figure 3(a)).

The protein secretion pathway of each identified protein was evaluated with two web-based tools SignalP and SecretomeP. SignalP analysis revealed that 309 proteins contained signal peptides needed for classical, endoplasmic reticulum-(ER-) Golgi secretion pathway (Figure 3(b), Supplementary Table 3). Meanwhile, SecretomeP analysis detected 495 proteins with neural network score (NN-score) above 0.5 and without prediction of signal peptides, which were considered as nonclassically secreted proteins (Figure 3(b),

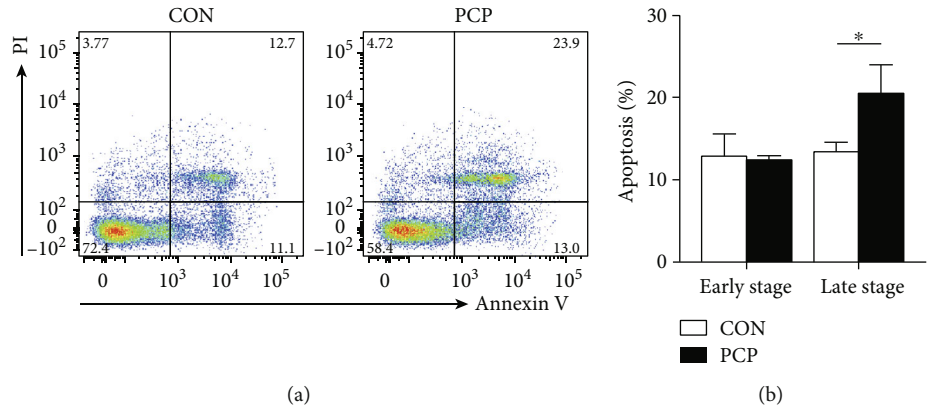


Figure 1: Apoptosis rate of primary B cells. B cells were extracted from the lung tissues of uninfected and *Pneumocystis*-infected mice (8–10 mice per group) using anti-CD19 MicroBeads. B cells were stained with Annexin V and PI. The proportion of apoptosis was assessed via flow cytometry. (a) Representative flow cytometric graph of B cell apoptosis. Annexin $V^+PI^-$ staining represents early apoptosis, while Annexin $V^+PI^+$ staining represents late apoptosis. (b) The comparison of early and late apoptotic percentage of B cells isolated from CON and PCP mice ($n = 3$). $^*p < 0.05$ compared with the CON group by Student's $t$ test. CON: uninfected control mice; PCP: *Pneumocystis* pneumonia mice.

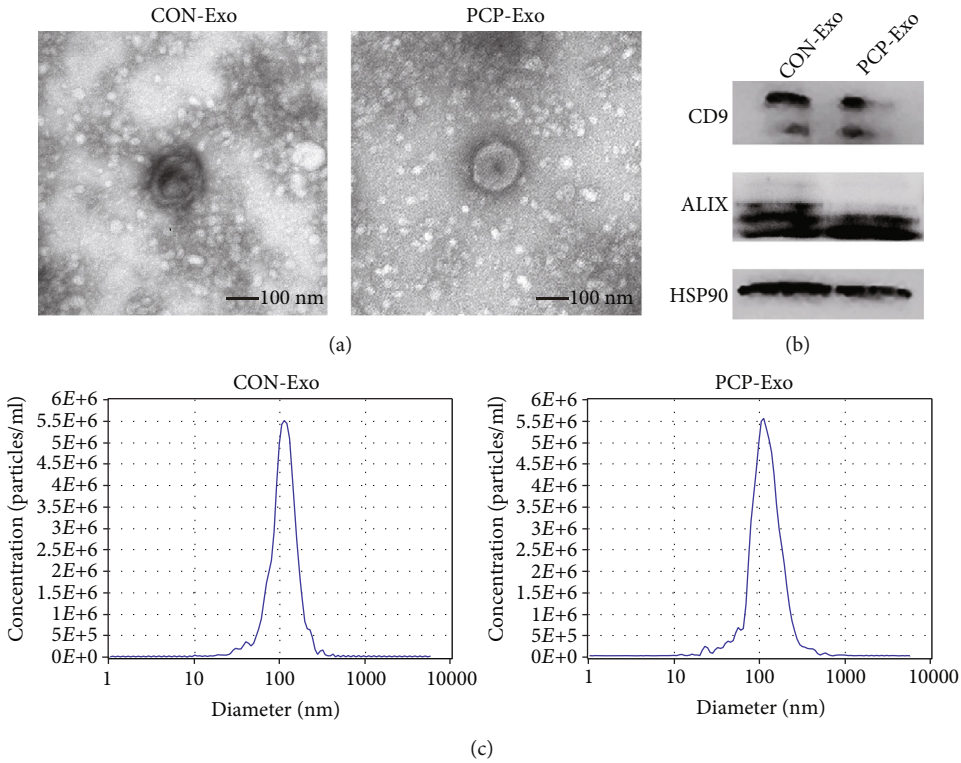


Figure 2: Exosome isolation and characterization. Exosomes were isolated from the culture medium of lung B cells from uninfected and *Pneumocystis*-infected mice (8–10 mice per group). (a) Electron microscopy images of exosomes. Scale bar represents 100 nm. (b) Immunoblot analysis of B cell exosomes for exosomal markers CD9, ALIX, and HSP90. (c) Size distribution of particles analyzed by nanoparticle tracking analysis. CON: uninfected control mice; PCP: *Pneumocystis* pneumonia mice; Exo: exosomes.

Supplementary Table 3). Notably, the remaining 897 (53%) exosomal proteins were predicted to be nonsecretory.

To gain further insights into the functional profile of exosomes derived from B cells, we performed bioinformatic analysis of all of the identified proteins. GO classification based on cellular component showed that approximately 61% of the proteins were annotated with cytoplasm (cystol), followed by extracellular exosome (49%), membrane (44%), and nucleus (43%) (Figure 4(a)). When using molecular function ontology, the majority of the proteins possess protein binding activity (37%), while other functions include nucleotide binding (21%), poly (A) RNA binding (20%), hydrolase activity (14%), and ATP binding (14%) (Figure 4(b)). In terms of biological process, most proteins

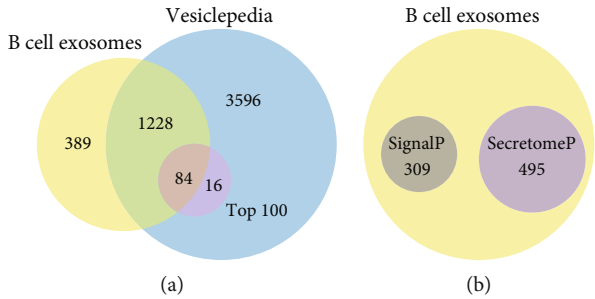


Figure 3: Venn diagrams of proteins identified in B cell exosomes. (a) Comparison of proteins identified in B cell-derived exosomes versus entire and top 100 murine proteins recorded in the Vesiclepedia database. (b) Identified proteins with prediction of classically (SignalP) and nonclassically secreted proteins (SecretomeP).

were involved in transport (11%), protein transport (7%), cell adhesion (6%), translation (6%), proteolysis (6%), and oxidation-reduction process (5%) (Figure 4(c)). PANTHER analysis was employed to classify the exosomal proteins. As shown in Figure 4(d), the exosomes of B cells carried different types of proteins, such as metabolic enzyme, translational protein, cytoskeletal protein, protein-binding activity modulator, and membrane traffic protein.

KEGG pathway enrichment analysis revealed that protein synthesis-related pathways were significantly enriched, including spliceosome, proteasome, ribosome, and protein processing in the ER. Immunological processes such as phagosome, endocytosis, leukocyte transendothelial migration, and complement and coagulation cascades were also overrepresented (Figure 4(e)). After retrieving the mass spectrometry data thoroughly, we found that B cell-specific markers and immunity-related molecules were abundant in exosomes (Table 1). Together, these data implied that exosomes derived from pulmonary B cells of both CON and PCP mice carried protein components suggestive of their formation and cellular origin, which probably exert functions on other immune cells.

*3.3. Pneumocystis Infection Alters the Protein Composition of B Cell Exosomes.* Using TMT-labeling quantitative proteomics, 51 proteins showed differential TMT signal intensity in PCP B cell exosomes with respect to the CON group. More specifically, 46 proteins were upregulated, while five proteins were downregulated, as listed in Table 2 (>1.2 for upregulated proteins and <0.83 for downregulated proteins). Based on the GO annotation, these DEPs are mainly associated with immune response, transcription regulation, and signal transduction (Supplementary Table 4). Of note, most upregulated proteins in B cell exosomes were classified as histones, which could function as damage-associated molecular pattern (DAMP) molecules in inflammatory response. Other DAMPs identified in the proteomics included protein S100-A8 and protein S100-A9, which were slightly increased in B cell exosomes after *Pneumocystis* infection, although not significantly (Table 1, Supplementary Table 2). Collectively, these data suggested that *Pneumocystis* infection stimulates pulmonary B cells to release exosomes abundant with DAMPs and other immune-relevant molecules, further impacting the communication between immune cells.

To validate the mass spectrometry results, we utilized PRM targeted proteomics to quantify absolute protein abundance. Several proteins were selected, including exosomal marker protein ALIX, immunity-related molecules (complement C3, tyrosine-protein phosphatase nonreceptor type 6 (PTPN6)), and DEPs (coronin-1a (CORO1A), vimentin (VIM), prelamin-A/C (LMNA), myosin-4 (MYH4), and histone H1.3 (H1F3)). For each protein, between one and five peptides were chosen, and then, the targeted peptides and proteins were quantitatively analyzed (Figure 5). Detailed quantification information is shown in Supplementary Table 5. Surprisingly, the PRM analysis demonstrated that PTPN6 was significantly downregulated in *Pneumocystis*-infected B cell-derived exosomes, while the TMT quantitative proteomics of this protein did not show any prominent change (fold change 0.873, $p$ value 0.011). VIM and H1F3, which were reported as DEPs in B cell exosomes, were also significantly enriched in the PCP group. In contrast, no significant differences were observed in terms of CORO1A, C3, LMNA, MYH4, and ALIX. Generally, the expression trend of these proteins using PRM analysis was in agreement with the LC-MS/MS results, although with different statistical significance.

*3.4. Exosomes Derived from Pneumocystis-Infected B Cells Promote CD4$^+$ T Cell Proliferation and Differentiation into Th1 Cells.* We next evaluated the effect of B cell-derived exosomes on major immune cells during PCP. First, CD4$^+$ T cell proliferation and IFN-$\gamma$-expressing CD4$^+$ T cell (Th1) differentiation rate were analyzed by flow cytometry. As shown in Figures 6(a) and 6(b), B cell exosomes of both groups promoted CD4$^+$ T cells to proliferate significantly. The proliferation rate in the PCP group was slightly higher than that in the CON group, although not statistically significant. In contrast, B cell exosomes from both groups decreased Th1 cell expansion. However, exosomes from PCP B cells significantly enhanced the differentiation of naive CD4$^+$ T cells into Th1 subset in comparison to CON B cells (Figures 6(c) and 6(d)).

AMs are innate immune cells residing in alveolar spaces and act as the first line of defense against exogenous

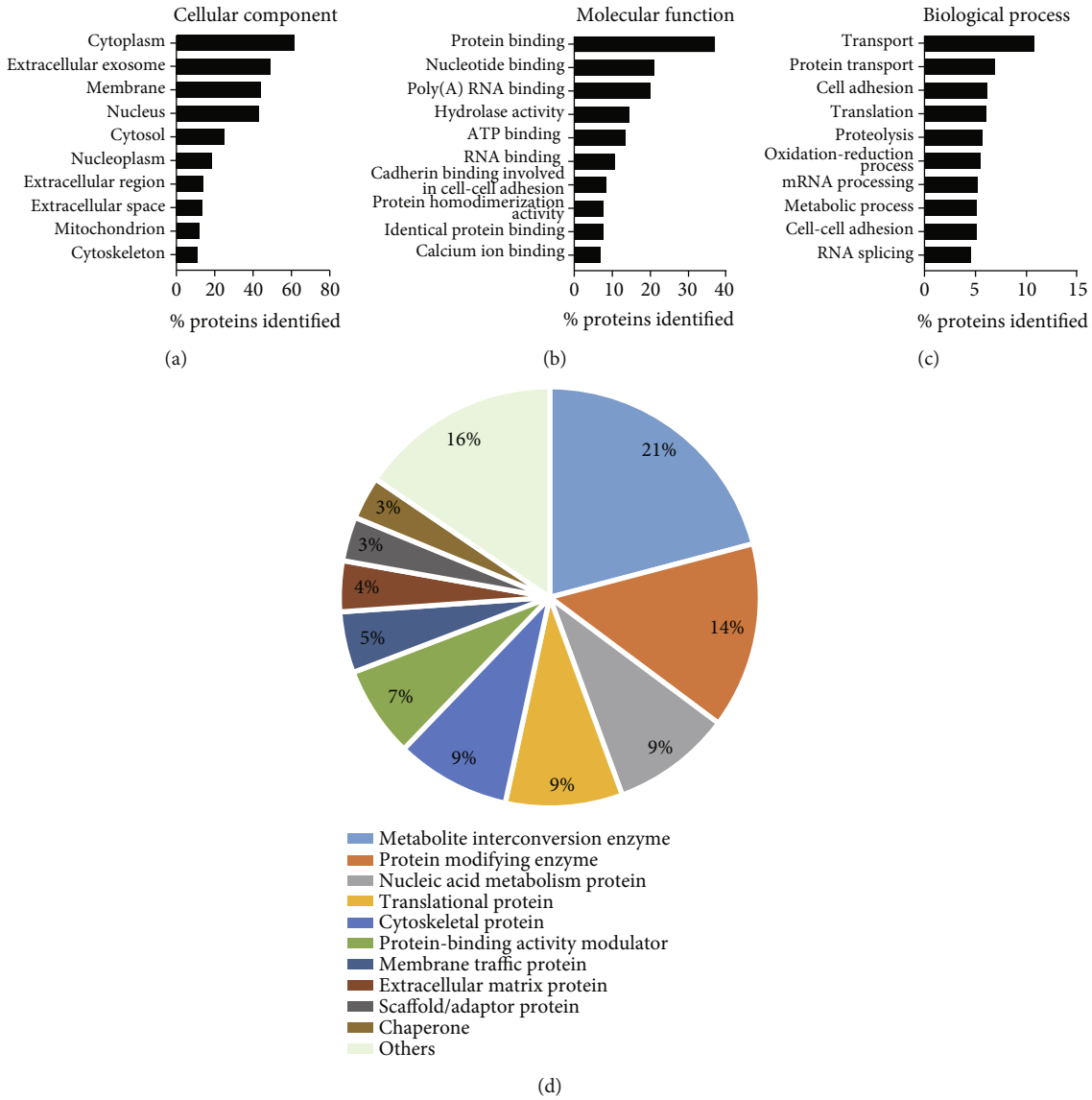


Figure 4: Continued.

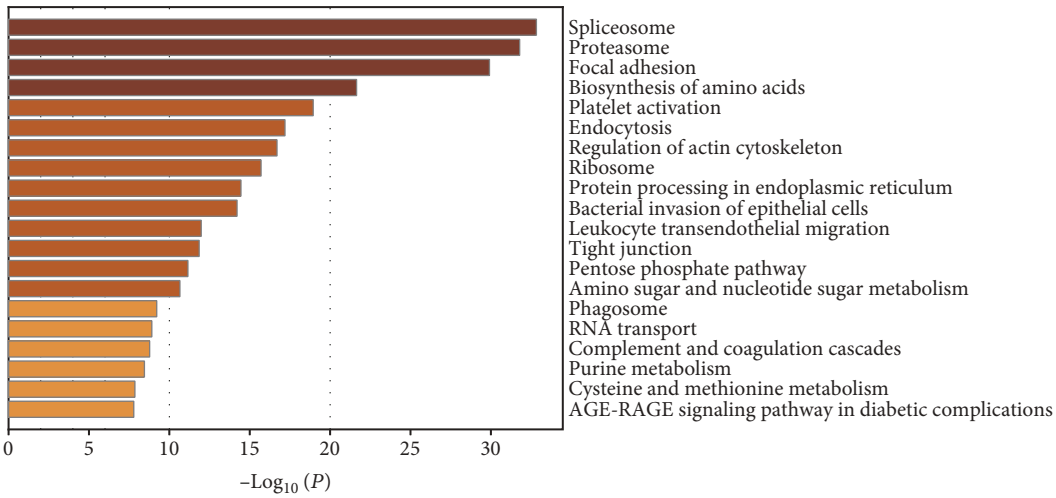


(e)

Figure 4: Bioinformatic analysis of the proteome of B cell exosomes. (a–c) Gene ontology annotation of the proteins identified in B cell exosomes based on (a) cellular component, (b) molecular function, and (c) biological process. (d) Pie chart showing Protein Analysis Through Evolutionary Relationships classification of the identified proteins from B cell exosomes. (e) The most enriched KEGG pathway of the proteome is visualized using Metascape.

pathogens. They are another indispensable effector cell population with their capacity to recognize and kill the *Pneumocystis* organism [7]. Previous studies have revealed that phagocytosis of *Pneumocystis* by AMs is the predominant mechanism in the clearance of this pathogen from lungs [33]. We therefore measured the effect of B cell exosomes derived from CON and PCP on the phagocytic function of AMs. A unique phagocytosis assay kit was applied based on the increasing fluorescence of pH-sensitive dye-labeled zymosan when these particles are ingested. Flow cytometry quantification analysis showed that while AMs internalized the particles with increasing fluorescence, exosomes derived from *Pneumocystis*-infected B cells had no significant influence on the phagocytic activity of AMs (Figures 7(a) and 7(b)). Overall, these findings suggested that B cell exosomes could potentiate $CD4^+$ T cell immune response during PCP.

## 4. Discussion

B cells have been reported to play an increasingly important role in the immune defense against PCP. While immunological studies of B cells have mainly focused on their role as antibody-producing and antigen-presenting cells [10–12], no studies have examined the EVs of B cells and their function during *Pneumocystis* infection. Exosomes and other EVs produced by immune cells can mediate host response in bacterial, viral, and fungal respiratory infection. For instance, exosomes released from *Mycobacterium tuberculosis*-infected RAW264.7 cells could promote the recruitment of macrophages [34]. Exosomes derived from respiratory syncytial virus-infected cells induce the release of cytokines and chemokines from monocytes and airway epithelial cells, suggesting their roles in activating the innate immune response [35]. Also, fungal pathogens such as *Cryptococcus neoformans* [36], *Candida albicans* [37], and *Aspergillus fumigatus* [38] modify the EV protein components of infected immune cells, and these EVs released by the cells could facilitate the host antifungal response. In this study, we isolated exosomes released from lung B cells of uninfected and PCP mice. Exosomal proteome and its effects on other cells were characterized. As *Pneumocystis murina* cannot be cultured *in vitro* [1], an *in vivo* infection mouse model was generated. Also, the data obtained from primary cells can reflect the biological process more truly than those from cell lines.

Proteins are the ultimate performer of gene function, and the secreted proteins in the extracellular microenvironment have fundamental roles in intercellular communication. To obtain an overview of the proteome profile of B cell exosomes, mass spectrometry analysis was conducted. A total of 1701 distinct proteins were identified in exosomes from both *Pneumocystis*-infected and uninfected B cells. Comparison of these proteins with the Vesiclepedia database revealed that 77.1% of these proteins were considered exosomal, confirming the abundant levels of exosomes in our samples. Conventional ER-Golgi pathway and unconventional pathway are two types of protein secretion pathways, while the latter form is further categorized into vesicular and nonvesicular pathways [39]. Exosomes, a smaller subtype of EVs, are therefore speculated to carry proteins mainly of the unconventional pathway [40]. In our data, 495 (29.10%) proteins encapsulated in B cell exosomes were predicted to be unconventionally secreted, whereas a lower proportion (18.16%) of proteins were involved in the classical pathway based on the detection of signal peptides. The result is not surprising as previous studies have also reported the presence of signal peptides in exosomes [37, 41, 42], which indicates a more complex protein sorting mechanism during the biogenesis and secretion of exosomes. Due to the endosomal origin of exosomes, the remaining nonsecretory proteins were estimated to be cytoplasmic and membrane-associated proteins. The GO cellular component analysis

Table 1: B cell markers (a) and immunity-related molecules (b) identified in the proteomic analysis.

(a)

| Uniprot accession no. | Protein name | Gene symbol |
|---|---|---|
| P19437 | B-lymphocyte antigen CD20 | Ms4a1 |
| P06800 | Receptor-type tyrosine-protein phosphatase C | Ptprc |
| P35329 | B cell receptor CD22 | Cd22 |
| P21855 | B cell differentiation antigen CD72 | Cd72 |
| Q61470 | Leukocyte antigen CD37 | Cd37 |
| P11911 | B cell antigen receptor complex-associated protein alpha chain | Cd79a |
| P15530 | B cell antigen receptor complex-associated protein beta chain | Cd79b |

(b)

| Uniprot accession no. | Protein name | Gene symbol |
|---|---|---|
| P01899 | H-2 class I histocompatibility antigen, D-B alpha chain | H2-D1 |
| P01901 | H-2 class I histocompatibility antigen, K-B alpha chain | H2-K1 |
| P14438 | H-2 class II histocompatibility antigen, A-U alpha chain (fragment) | H2-Aa |
| P14483 | H-2 class II histocompatibility antigen, A beta chain | H2-Ab1 |
| P01027 | Complement C3 | C3 |
| P01029 | Complement C4-B | C4b |
| Q9ES30 | Complement C1q tumor necrosis factor-related protein 3 | C1qtnf3 |
| P06684 | Complement C5 | C5 |
| P04186 | Complement factor B | Cfb |
| Q8CFG9 | Complement C1r-B subcomponent | C1rb |
| Q8BH35 | Complement component C8 beta chain | C8b |
| Q64735 | Complement component receptor 1-like protein | Cr1l |
| P01837 | Immunoglobulin kappa constant | Igkc |
| Q9EQS9 | Immunoglobulin superfamily DCC subclass member 4 | Igdcc4 |
| P01872 | Immunoglobulin heavy constant mu | Ighm |
| P01749 | Ig heavy chain V region 3 | Ighv1-61 |
| P04202 | Transforming growth factor beta-1 proprotein | Tgfb1 |
| P82198 | Transforming growth factor-beta-induced protein ig-h3 | Tgfbi |
| P27005 | Protein S100-A8 | S100a8 |
| P31725 | Protein S100-A9 | S100a9 |
| P51437 | Cathelicidin antimicrobial peptide | Camp |

also confirmed that a multitude of these identified proteins were annotated with cytoplasm and membrane. The proportion of predicted secretory and nonsecretory proteins was similar to that from a prior study that had investigated EV protein contents modulated by *Candida albicans* [37].

Exosomes have been implicated in cell-to-cell communication in inflammatory response [14]. We sought to determine how *Pneumocystis* infection impacts exosomes derived from B lymphocytes and modulates their protein cargo. We observed that most of the DEPs were involved in immune response, transcription regulation, and signal transduction. Notably, the proteome of PCP B cell exosomes contained more histones, both revealed by LC-MS/MS and by PRM validation analysis. The abundance may partly be attributed to the increased rate of apoptotic B cells during PCP [43]. Historically, histones in EVs have been recognized as specific contents in apoptotic vesicles released from dying cells. However, recent evidence suggests that histones are also present in exosomes and have other particular roles. For example, histones loaded into exosomes may be involved in a survival mechanism by eliminating harmful DNA to maintain cellular homeostasis without dying [44]. Another study has demonstrated that exosomal histones can mediate adhesion and interaction with other cells [45]. Importantly, we focused on exosomal histones for their roles as DAMPs, which could further activate immune cells and release inflammatory mediators [46]. Increased levels of histones in exosomes and EVs have been observed in some other infections, such as the key fungal component $\beta$-glucan infection model [47] and the Kaposi sarcoma-associated virus (KSHV) infection [48]. Hence, we hypothesized that the enrichment of histones in PCP B cell exosomes may be

Table 2: Differentially expressed proteins in B cell exosomes in response to *Pneumocystis* infection.

| Uniprot accession no. | Protein name | Gene symbol | Fold change | *p* value |
|---|---|---|---|---|
| Immune response | | | | |
| O35744 | Chitinase-like protein 3 | Chil3 | 2.076 | 7.515*E*-05 |
| Q8C2K1 | Differentially expressed in FDCP 6 | Def6 | 1.305 | 1.464*E*-02 |
| Q3SXB8 | Collectin-11 | Colec11 | 1.282 | 2.262*E*-02 |
| P11911 | B cell antigen receptor complex-associated protein alpha chain | Cd79a | 1.260 | 3.765*E*-02 |
| P01749 | Ig heavy chain V region 3 | Ighv1-61 | 1.236 | 1.096*E*-02 |
| P19467 | Mucin-13 | Muc13 | 1.423 | 2.680*E*-04 |
| Damage-associated molecular patterns | | | | |
| P43277 | Histone H1.3 | H1f3 | 2.218 | 1.969*E*-02 |
| P27661 | Histone H2AX | H2ax | 2.037 | 2.325*E*-02 |
| P43274 | Histone H1.4 | H1f4 | 1.867 | 1.018*E*-02 |
| P0C0S6 | Histone H2A.Z | H2az1 | 1.701 | 7.582*E*-03 |
| P43276 | Histone H1.5 | H1f5 | 1.660 | 4.329*E*-03 |
| Q6GSS7 | Histone H2A type 2-A | H2ac18 | 1.595 | 3.061*E*-02 |
| P15864 | Histone H1.2 | H1f2 | 1.572 | 4.342*E*-02 |
| P68433 | Histone H3.1 | H3c1 | 1.569 | 4.227*E*-03 |
| Q8CGP7 | Histone H2A type 1-K | H2ac15 | 1.564 | 4.561*E*-02 |
| P62806 | Histone H4 | H4c1 | 1.516 | 3.010*E*-03 |
| Q8CGP0 | Histone H2B type 3-B | H2bu1-ps | 1.513 | 3.093*E*-04 |
| P10854 | Histone H2B type 1-M | H2bc14 | 1.475 | 1.079*E*-03 |
| P10922 | Histone H1.0 | H1f0 | 1.465 | 3.718*E*-02 |
| P02301 | Histone H3.3C | H3f3c | 1.458 | 6.179*E*-03 |
| Transcription regulation | | | | |
| Q9CQE8 | RNA transcription, translation and transport factor protein | RTRAF | 2.014 | 4.639*E*-02 |
| O54962 | Barrier-to-autointegration factor | Banf1 | 1.746 | 2.677*E*-02 |
| Q61116 | Zinc finger protein 235 | Znf235 | 1.365 | 2.023*E*-02 |
| Q9Z277 | Tyrosine-protein kinase BAZ1B | Baz1b | 1.352 | 7.932*E*-06 |
| P42586 | Homeobox protein Nkx-2.2 | Nkx2-2 | 1.272 | 4.253*E*-02 |
| Q04750 | DNA topoisomerase 1 | Top1 | 1.237 | 1.698*E*-03 |
| Q3TWW8 | Serine/arginine-rich splicing factor 6 | Srsf6 | 0.790 | 1.047*E*-03 |
| Q9Z130 | Heterogeneous nuclear ribonucleoprotein D-like | Hnrnpdl | 0.639 | 9.385*E*-04 |
| Signal transduction | | | | |
| P70296 | Phosphatidylethanolamine-binding protein 1 | Pebp1 | 1.443 | 7.441*E*-03 |
| P56716 | Oxygen-regulated protein 1 | Rp1 | 1.843 | 7.102*E*-03 |
| Q7TSJ6 | Serine/threonine-protein kinase LATS2 | Lats2 | 1.245 | 4.905*E*-04 |
| Q60870 | Receptor expression-enhancing protein 5 | Reep5 | 1.308 | 2.552*E*-02 |
| Metabolism | | | | |
| P16331 | Phenylalanine-4-hydroxylase | Pah | 1.390 | 3.699*E*-03 |
| P00688 | Pancreatic alpha-amylase | Amy2 | 1.229 | 4.990*E*-03 |
| Vesicle trafficking | | | | |
| Q8K012 | Formin-binding protein 1-like | Fnbp1l | 1.293 | 1.909*E*-02 |
| Q3UQN2 | F-BAR domain only protein 2 | Fcho2 | 1.200 | 1.819*E*-04 |
| P50396 | Rab GDP dissociation inhibitor alpha | Gdi1 | 1.250 | 9.281*E*-03 |
| Cytoskeletal components | | | | |
| Q5SX39 | Myosin-4 | Myh4 | 2.690 | 2.488*E*-03 |
| Q91Z83 | Myosin-7 | Myh7 | 1.643 | 4.466*E*-02 |
| P20152 | Vimentin | Vim | 1.322 | 2.314*E*-02 |
| Q62418 | Drebrin-like protein | Dbnl | 0.833 | 2.465*E*-02 |

Table 2: Continued.

| Uniprot accession no. | Protein name | Gene symbol | Fold change | $p$ value |
|---|---|---|---|---|
| O89053 | Coronin-1A | Coro1a | 0.829 | 2.040$E$-03 |
| Q9QYB5 | Gamma-adducin | Add3 | 0.801 | 4.797$E$-02 |
| P48678 | Prelamin-A/C | Lmna | 1.264 | 3.074$E$-02 |
| Ribosome components | | | | |
| Q9CZT6 | Protein CMSS1 | Cmss1 | 1.362 | 4.707$E$-02 |
| P47915 | 60S ribosomal protein L29 | Rpl29 | 1.325 | 3.513$E$-03 |
| Miscellaneous | | | | |
| Q3UPH1 | Protein PRRC1 | Prrc1 | 1.542 | 1.967$E$-03 |
| O55143 | Sarcoplasmic/endoplasmic reticulum calcium ATPase 2 | Atp2a2 | 1.224 | 4.780$E$-02 |
| Q9QZR9 | Collagen alpha-4(IV) chain | Col4a4 | 1.219 | 3.126$E$-03 |
| Q921G7 | Electron transfer flavoprotein-ubiquinone oxidoreductase, mitochondrial | Etfdh | 1.204 | 1.111$E$-02 |
| P62309 | Small nuclear ribonucleoprotein G | Snrpg | 1.202 | 2.930$E$-02 |

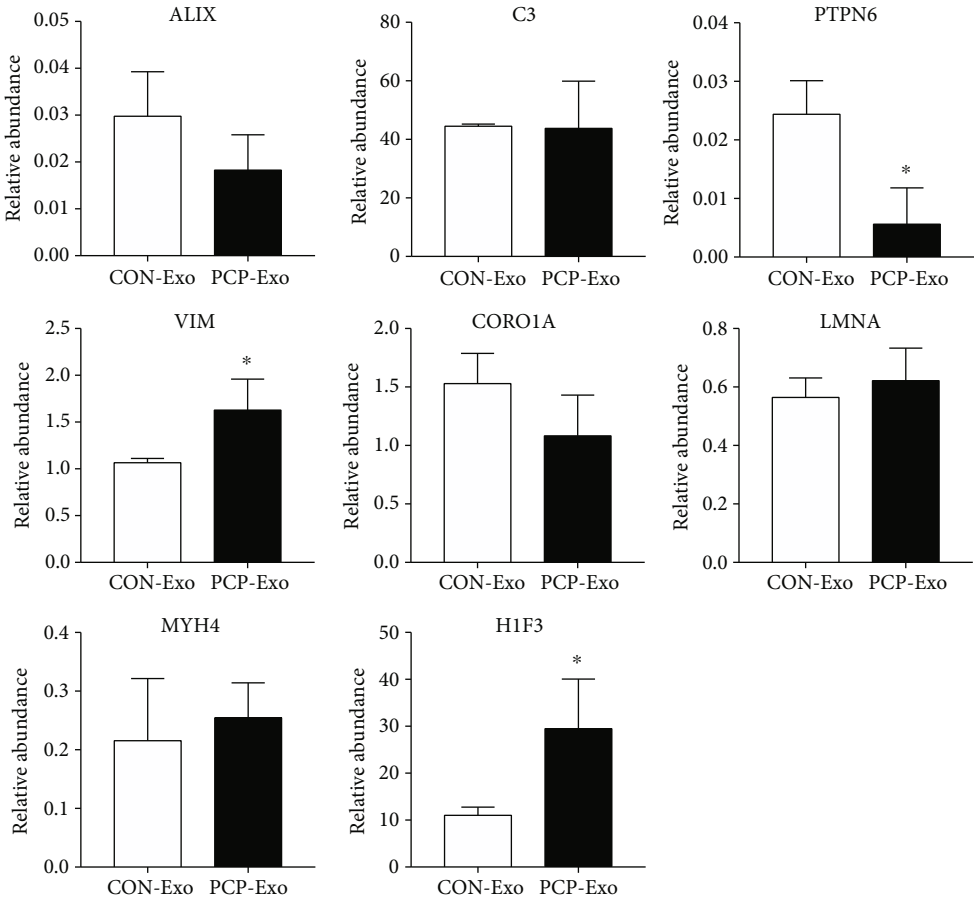


Figure 5: Validation of the selected proteins using PRM. Exosomes of CON and PCP B cells were isolated and subjected to LC-PRM/MS analysis. Relative protein abundance of eight proteins (ALIX, C3, PTPN6, VIM, CORO1A, LMNA, MYH4, and H1F3) was calculated based on the normalized peak area of peptide fragments. A two-tailed Student's $t$ test was used to detect the difference between two groups ($n = 3$). $*$indicates $p < 0.05$.

proinflammatory and could have effects on other immune cells.

PTPN6, also known as Src homology 2 domain-containing protein tyrosine phosphatase-1 (SHP-1), is a widely expressed cytoplasmic protein in all mature hematopoietic lineages. Intriguingly, PRM targeted analysis revealed that PTPN6 was significantly downregulated in PCP B cell exosomes. SHP-1 (PTPN6) exerts its regulatory role on T cells by inhibiting antigen-dependent activation and proliferation in *Leishmania* infection and other inflammatory

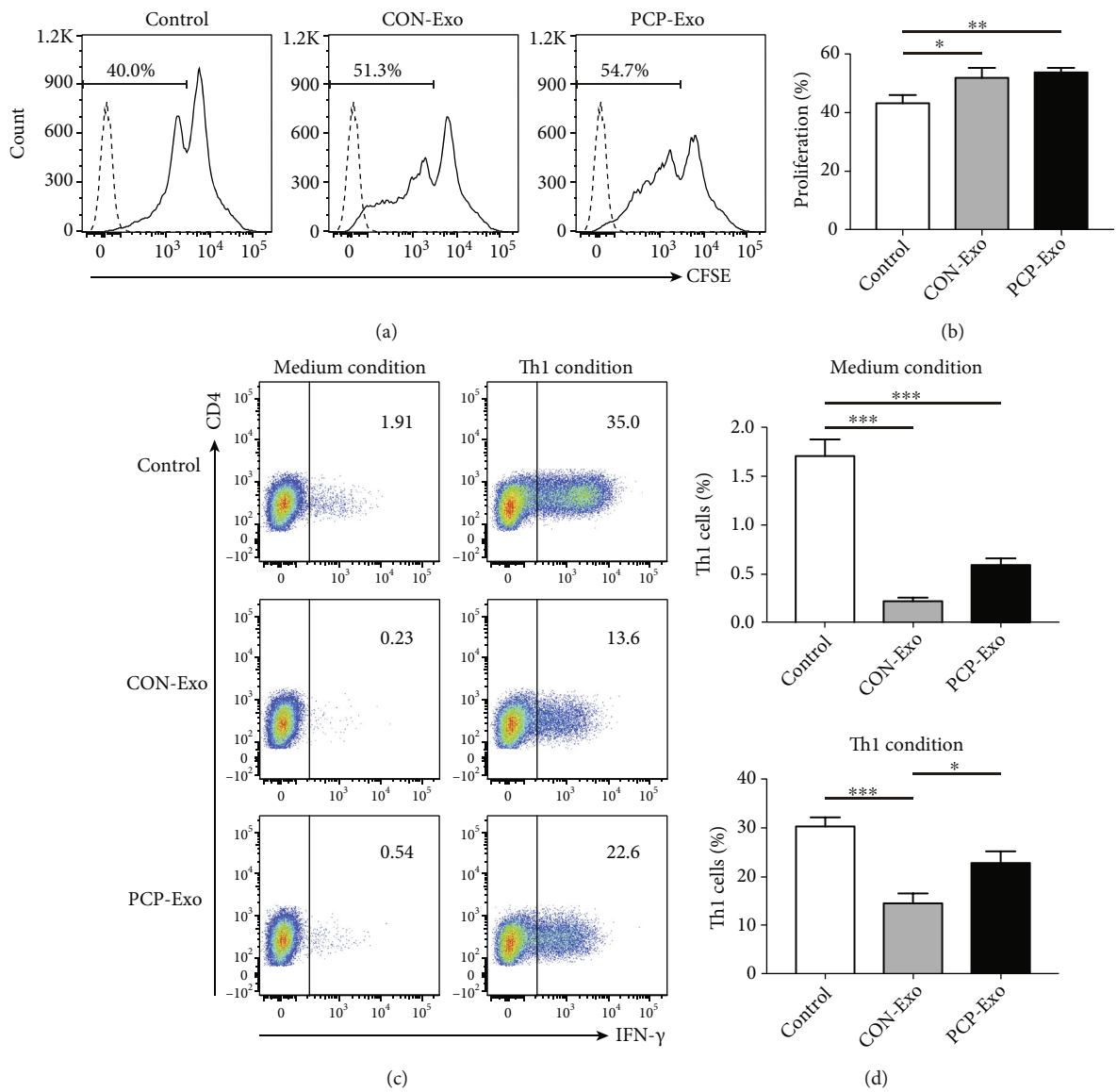


Figure 6: Effects of B cell-derived exosomes on $CD4^+$ T cells. $CD4^+$ T cells and naive $CD4^+$ T cells were purified from the spleens of two wild-type mice and treated with CON and PCP B cell exosomes or left untreated (control). Proliferation and Th1 cell differentiation rate were analyzed. (a) Representative flow cytometric histograms for CFSE of $CD4^+$ T cells receiving different treatments. Dotted lines represent CFSE unlabeled control. (b) The comparison result of (a). (c) Representative flow cytometric dot plots showing the differentiation of naive $CD4^+$ T cells into Th1 subset and the corresponding comparison result (d). Comparisons were conducted by one-way ANOVA, followed by Bonferroni post hoc test ($n = 3$). $^*p < 0.05$; $^{**}p < 0.01$; $^{***}p < 0.001$.

conditions [49, 50]. Moreover, in a tumor model of melanoma, knockdown of SHP-1 (PTPN6) expands antitumor T cell repertoire and dampens tumor growth, suggesting the potential application of SHP-1 (PTPN6) as immune checkpoint in future immune therapy [51]. A previous study showed that when B cells were infected with KSHV, PTPN6 expression in B cell-derived exosomes was also significantly downregulated [48].

Another DEP validated by PRM analysis is VIM. It belongs to the intermediate filament cytoskeletal protein ubiquitously located in nonepithelial cells, including immune cells such as lymphocytes and macrophages [37, 47, 52–54]. Despite being a cytoskeleton component, VIM could be secreted by activated phagocytes to reinforce the bactericidal activity and augment the immune response [53]. VIM secretion via EVs has also been reported in fungal infection of macrophages with higher expression level compared with uninfected cells, which is consistent with our results [37, 47]. Besides, Epstein-Barr virus infection of B cell line induces dramatic increase in VIM mRNA and protein expression, further implying a possible role of VIM in infectious diseases [54].

Based on the enrichment of proinflammatory DAMP histones and immunity-related cytoskeleton VIM and the decreased level of the inhibitory molecule PTPN6, we inferred that exosomes released from B cells in PCP may

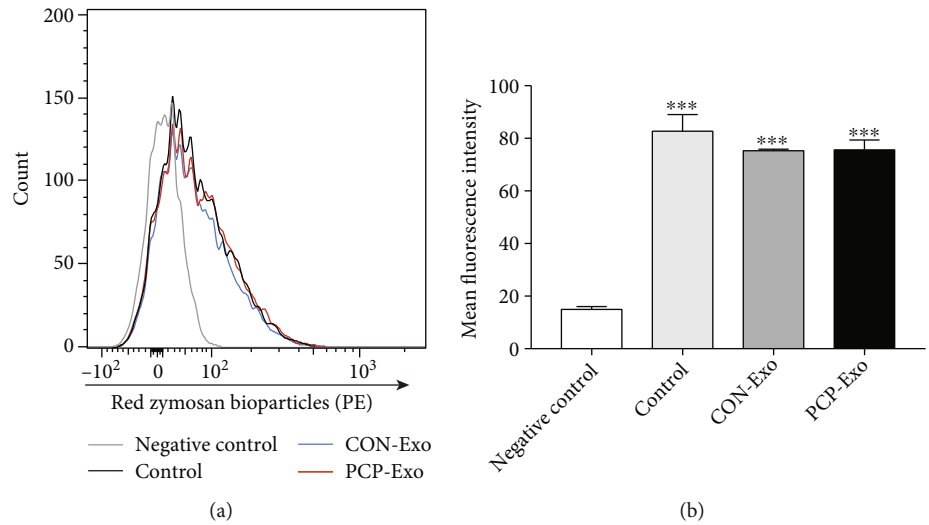


Figure 7: Effect of B cell-derived exosomes on phagocytic capacity of alveolar macrophages. AMs were isolated from five uninfected mice and treated with CON and PCP B cell exosomes or left untreated (control). AMs from different groups were incubated with dye-labeled zymosan particles to examine the phagocytic function. For negative control, only AMs were added. (a) Representative flow cytometric histogram showing the particle fluorescence within macrophages from different groups. (b) Comparison result of mean fluorescence intensity of four groups ($n = 3$). Comparison was conducted by one-way ANOVA, followed by Bonferroni post hoc test. $^{***}p < 0.001$ compared with the negative control. AMs: alveolar macrophages.

have immune effects on other immune cells. While B cells have a critical role in activating $CD4^+$ T cells in PCP, their significance in $CD8^+$ T cells has not been reported. Furthermore, the role of $CD8^+$ T cells in PCP is still questionable, with both protective and detrimental responses reported [55, 56]. Therefore, we first tested the proliferation of $CD4^+$ T cells exposed to B cell exosomes. Significantly improved proliferation of $CD4^+$ T cells by both groups of B cell exosomes was demonstrated. However, the expected immune stimulation role of *Pneumocystis*-infected B cell exosomes was not obvious. Subsequently, the differentiation of naive $CD4^+$ T cells into Th1 cells was measured. We found that although B cell exosomes generally suppressed Th1 differentiation, exosomes derived from PCP mice promoted Th1 differentiation compared with those from uninfected mice. AMs are ultimately responsible for the innate immune response against PCP. The phagocytosis assay demonstrated that fluorescence in AMs increased significantly when incubated with zymosan, implying that AMs have a role in the elimination of *Pneumocystis*. In contrast, no effect of B cell exosomes was observed on the phagocytosis of macrophages. It is still unknown whether DAMPs and other immunological molecules identified in B cell exosomes could induce phagocytosis. In general, AMs have to be activated by host cytokines, such as IFN-$\gamma$, TNF-$\alpha$, and granulocyte macrophage colony stimulating factor (GM-CSF), to maximize their phagocytic activity [7]. However, these cytokines were not identified by mass spectrometry. The relationship between B cells and macrophages during PCP was also not studied. Altogether, the alteration of the abovementioned immunological proteins in B cell exosomes in response to PCP could be responsible for the proinflammatory effect on $CD4^+$ T cells. Further functional studies should be performed to elucidate the precise mechanism.

## 5. Conclusion

In conclusion, our findings suggest that B cells can secrete exosomes abundant in immune active protein contents, and these vesicles could modulate other immune cells such as $CD4^+$ T cells in response to *Pneumocystis* infection. This work provides new insights into the pathogenesis of PCP for the possible role of exosomes derived from immune cells. Future investigations are warranted to unravel the involvement and function of exosomes from other immune effector cells during PCP.

## Data Availability

The mass spectrometry proteomics data have been deposited in the ProteomeXchange Consortium via the PRIDE partner repository with the dataset identifier PXD030103. Other data supporting the findings are available from the corresponding author upon request.

## Conflicts of Interest

The authors declare that they have no conflicts of interest.

## Authors' Contributions

Z.H.T, K. Z, and H.M.R conceived and designed the study. D. M and Q.Y.Z carried out the experiments. D. M interpreted the data, drafted the manuscript, and prepared the figures. Z.H.T and K. Z supervised the study and revised the manuscript. All of the authors have read and approved the final manuscript.

## Acknowledgments

This study was supported by Beijing Natural Science Foundation (KZ201910025031) and the National Natural Science Foundation of China (81870004).

## Supplementary Materials

Supplementary Table 1: initial culture cell number and protein amount of B cell exosomes used for mass spectrometry. Supplementary Table 2: all identified proteins of uninfected and *Pneumocystis*-infected B cell exosomes. Supplementary Table 3: SignalP and SecretomeP prediction results. Supplementary Table 4: differentially expressed proteins of B cell exosomes in response to PCP. Supplementary Table 5: quantitative information of peptides and proteins by PRM analysis. *(Supplementary Materials)*

## References

[1] G. Nevez, P. M. Hauser, and S. Le Gal, "_Pneumocystis jirovecii_," *Trends in Microbiology*, vol. 28, no. 12, pp. 1034-1035, 2020.

[2] A. Morris, J. D. Lundgren, H. Masur et al., "Current epidemiology of Pneumocystis pneumonia," *Emerging Infectious Diseases*, vol. 10, no. 10, pp. 1713–1720, 2004.

[3] A. Kanj, B. Samhouri, N. Abdallah, O. Chehab, and M. Baqir, "Host factors and outcomes in hospitalizations for _Pneumocystis jirovecii_ pneumonia in the United States," *Mayo Clinic Proceedings*, vol. 96, no. 2, pp. 400–407, 2021.

[4] A. Roux, E. Canet, S. Valade et al., "Pneumocystis jirovecii pneumonia in patients with or without AIDS, France," *Emerging Infectious Diseases*, vol. 20, no. 9, pp. 1490–1497, 2014.

[5] C. Cilloniz, C. Dominedo, and M. J. Alvarez-Martinez, "Pneumocystis pneumonia in the twenty-first century: HIV-infected versus HIV-uninfected patients," *Expert Review of Anti-Infective Therapy*, vol. 17, no. 10, pp. 787–801, 2019.

[6] J. C. Hoving and J. K. Kolls, "New advances in understanding the host immune response to _Pneumocystis_," *Current Opinion in Microbiology*, vol. 40, pp. 65–71, 2017.

[7] P. Otieno-Odhiambo, S. Wasserman, and J. C. Hoving, "The contribution of host cells to pneumocystis immunity: an update," *Pathogens*, vol. 8, no. 2, p. 52, 2019.

[8] I. Martin-Garrido, E. M. Carmona, U. Specks, and A. H. Limper, "_Pneumocystis_ pneumonia in patients treated with rituximab," *Chest*, vol. 144, no. 1, pp. 258–265, 2013.

[9] K. C. Wei, C. Sy, S. Y. Wu, T. J. Chuang, W. C. Huang, and P. C. Lai, "_Pneumocystis jirovecii pneumonia_ in HIV-uninfected, rituximab treated non- Hodgkin lymphoma patients," *Sci Rep*, vol. 8, no. 1, p. 8321, 2018.

[10] M. M. Opata, M. L. Hollifield, F. E. Lund et al., "B lymphocytes are required during the early priming of CD4+ T cells for clearance of pneumocystis infection in mice," *Journal of Immunology*, vol. 195, no. 2, pp. 611–620, 2015.

[11] F. E. Lund, K. Schuer, M. Hollifield, T. D. Randall, and B. A. Garvy, "Clearance of pneumocystis carinii in mice is dependent on B cells but not on P carinii-specific antibody," *Journal of Immunology*, vol. 171, no. 3, pp. 1423–1430, 2003.

[12] H. M. Rong, T. Li, C. Zhang et al., "IL-10-producing B cells regulate Th1/Th17-cell immune responses in Pneumocystis pneumonia," *American Journal of Physiology. Lung Cellular and Molecular Physiology*, vol. 316, no. 1, pp. L291–L301, 2019.

[13] R. Kalluri and V. S. LeBleu, "The biology, function, and biomedical applications of exosomes," *Science*, vol. 367, no. 6478, 2020.

[14] P. D. Robbins and A. E. Morelli, "Regulation of immune responses by extracellular vesicles," *Nature Reviews. Immunology*, vol. 14, no. 3, pp. 195–208, 2014.

[15] M. Rodrigues, J. Fan, C. Lyon, M. Wan, and Y. Hu, "Role of extracellular vesicles in viral and bacterial infections: pathogenesis, diagnostics, and therapeutics," *Theranostics*, vol. 8, no. 10, pp. 2709–2721, 2018.

[16] G. Raposo, H. W. Nijman, W. Stoorvogel et al., "B lymphocytes secrete antigen-presenting vesicles," *Journal of Experimental Medicine*, vol. 183, no. 3, pp. 1161–1172, 1996.

[17] A. Muntasell, A. C. Berger, and P. A. Roche, "T cell-induced secretion of MHC class II-peptide complexes on B cell exosomes," *The EMBO Journal*, vol. 26, no. 19, pp. 4263–4272, 2007.

[18] C. Admyre, B. Bohle, S. M. Johansson et al., "B cell-derived exosomes can present allergen peptides and activate allergen-specific T cells to proliferate and produce $T_H2$-like cytokines," *The Journal of Allergy and Clinical Immunology*, vol. 120, no. 6, pp. 1418–1424, 2007.

[19] S. C. Saunderson and A. D. McLellan, "Role of lymphocyte subsets in the immune response to primary B cell-derived exosomes," *Journal of Immunology*, vol. 199, no. 7, pp. 2225–2235, 2017.

[20] M. W. Klinker, V. Lizzio, T. J. Reed, D. A. Fox, and S. K. Lundy, "Human B cell-derived lymphoblastoid cell lines constitutively produce Fas ligand and secrete $MHCII^+FasL^+$ killer exosomes," *Frontiers in Immunology*, vol. 5, p. 144, 2014.

[21] F. Zhang, R. Li, Y. Yang et al., "Specific decrease in b-cell-derived extracellular vesicles enhances post- chemotherapeutic $CD8^+$ T cell responses," *Immunity*, vol. 50, no. 3, pp. 738–750.e7, 2019.

[22] A. Thompson, J. Schafer, and K. Kuhn, "Tandem mass tags: a novel quantification strategy for comparative analysis of complex protein mixtures by MS/MS," *Analytical Chemistry*, vol. 75, no. 8, pp. 1895–1904, 2003.

[23] J. R. Wisniewski, A. Zougman, N. Nagaraj, and M. Mann, "Universal sample preparation method for proteome analysis," *Nature Methods*, vol. 6, no. 5, pp. 359–362, 2009.

[24] D. W. Huang, B. T. Sherman, and R. A. Lempicki, "Systematic and integrative analysis of large gene lists using DAVID bioinformatics resources," *Nature Protocols*, vol. 4, no. 1, pp. 44–57, 2009.

[25] D. W. Huang, B. T. Sherman, and R. A. Lempicki, "Bioinformatics enrichment tools: paths toward the comprehensive functional analysis of large gene lists," *Nucleic Acids Research*, vol. 37, no. 1, pp. 1–13, 2009.

[26] H. Mi, D. Ebert, A. Muruganujan et al., "PANTHER version 16: a revised family classification, tree-based classification tool, enhancer regions and extensive API," *Nucleic Acids Research*, vol. 49, no. D1, pp. D394–D403, 2021.

[27] Y. Zhou, B. Zhou, L. Pache et al., "Metascape provides a biologist-oriented resource for the analysis of systems-level datasets," *Nature Communications*, vol. 10, no. 1, p. 1523, 2019.

[28] M. Pathan, P. Fonseka, S. V. Chitti et al., "Vesiclepedia 2019: a compendium of RNA, proteins, lipids and metabolites in

extracellular vesicles," *Nucleic Acids Research*, vol. 47, no. D1, pp. D516–D519, 2019.

[29] H. Kalra, R. J. Simpson, H. Ji et al., "Vesiclepedia: a compendium for extracellular vesicles with continuous community annotation," *PLoS Biology*, vol. 10, no. 12, article e1001450, 2012.

[30] J. J. Almagro Armenteros, K. D. Tsirigos, and C. K. Sonderby, "SignalP 5.0 improves signal peptide predictions using deep neural networks," *Nature Biotechnology*, vol. 37, no. 4, pp. 420–423, 2019.

[31] J. D. Bendtsen, L. J. Jensen, N. Blom, G. Von Heijne, and S. Brunak, "Feature-based prediction of non-classical and leaderless protein secretion," *Protein Engineering, Design & Selection*, vol. 17, no. 4, pp. 349–356, 2004.

[32] B. MacLean, D. M. Tomazela, N. Shulman et al., "Skyline: an open source document editor for creating and analyzing targeted proteomics experiments," *Bioinformatics*, vol. 26, no. 7, pp. 966–968, 2010.

[33] C. Steele, L. Marrero, S. Swain et al., "Alveolar macrophage-mediated killing of Pneumocystis carinii f. sp. muris involves molecular recognition by the Dectin-1 beta-glucan receptor," *The Journal of Experimental Medicine*, vol. 198, no. 11, pp. 1677–1688, 2003.

[34] P. P. Singh, V. L. Smith, P. C. Karakousis, and J. S. Schorey, "Exosomes isolated from mycobacteria-infected mice or cultured macrophages can recruit and activate immune cells in vitro and in vivo," *Journal of Immunology*, vol. 189, no. 2, pp. 777–785, 2012.

[35] H. S. Chahar, T. Corsello, A. S. Kudlicki, N. Komaravelli, and A. Casola, "Respiratory syncytial virus infection changes cargo composition of exosome released from airway epithelial cells," *Scientific Reports*, vol. 8, no. 1, p. 387, 2018.

[36] L. Zhang, K. Zhang, H. Li et al., "Cryptococcus neoformans-infected macrophages release proinflammatory extracellular vesicles: insight into their components by multi-omics," *MBio*, vol. 12, no. 2, 2021.

[37] J. A. Reales-Calderon, C. Vaz, L. Monteoliva, G. Molero, and C. Gil, "Candida albicans modifies the protein composition and size distribution of THP-1 macrophage-derived extracellular vesicles," *Journal of Proteome Research*, vol. 16, no. 1, pp. 87–105, 2017.

[38] I. A. Shopova, I. Belyaev, P. Dasari et al., "Human neutrophils produce antifungal extracellular vesicles against Aspergillus fumigatus," *MBio*, vol. 11, no. 2, 2020.

[39] C. Rabouille, V. Malhotra, and W. Nickel, "Diversity in unconventional protein secretion," *Journal of Cell Science*, vol. 125, no. 22, pp. 5251–5255, 2012.

[40] A. Ras-Carmona, M. Gomez-Perosanz, and P. A. Reche, "Prediction of unconventional protein secretion by exosomes," *BMC Bioinformatics*, vol. 22, no. 1, p. 333, 2021.

[41] S. Mathivanan, J. W. Lim, B. J. Tauro, H. Ji, R. L. Moritz, and R. J. Simpson, "Proteomics analysis of A33 immunoaffinity-purified exosomes released from the human colon tumor cell line LIM1215 reveals a tissue-specific protein signature," *Molecular & Cellular Proteomics*, vol. 9, no. 2, pp. 197–208, 2010.

[42] K. Ono, M. Niwa, H. Suzuki, N. B. Kobayashi, T. Yoshida, and M. Sawada, "Secretion of signal peptides via extracellular vesicles," *Biochemical and Biophysical Research Communications*, vol. 560, pp. 21–26, 2021.

[43] S. Kumar, Q. L. Matthews, and B. Sims, "Effects of cocaine on human glial-derived extracellular vesicles," *Frontiers in Cell and Development Biology*, vol. 8, 2021.

[44] A. Yokoi, A. Villar-Prados, P. A. Oliphint et al., "Mechanisms of nuclear content loading to exosomes," *Science Advances*, vol. 5, no. 11, p. 16, 2019.

[45] G. Nangami, R. Koumangoye, J. Shawn Goodwin et al., "Fetuin-A associates with histones intracellularly and shuttles them to exosomes to promote focal adhesion assembly resulting in rapid adhesion and spreading in breast carcinoma cells," *Experimental Cell Research*, vol. 328, no. 2, pp. 388–400, 2014.

[46] G. P. Collett, C. W. Redman, I. L. Sargent, and M. Vatish, "Endoplasmic reticulum stress stimulates the release of extracellular vesicles carrying danger-associated molecular pattern (DAMP) molecules," *Oncotarget*, vol. 9, no. 6, pp. 6707–6717, 2018.

[47] W. Cypryk, T. Ohman, E. L. Eskelinen, S. Matikainen, and T. A. Nyman, "Quantitative proteomics of extracellular vesicles released from human monocyte-derived macrophages upon $\beta$-glucan stimulation," *Journal of Proteome Research*, vol. 13, no. 5, pp. 2468–2477, 2014.

[48] D. G. Meckes Jr., H. P. Gunawardena, and R. M. Dekroon, "Modulation of B-cell exosome proteins by gamma herpesvirus infection," *Proceedings of the National Academy of Sciences of the United States of America*, vol. 110, no. 31, pp. E2925–E2933, 2013.

[49] H. A. Watson, S. Wehenkel, J. Matthews, and A. Ager, "SHP-1: the next checkpoint target for cancer immunotherapy?," *Biochemical Society Transactions*, vol. 44, no. 2, pp. 356–362, 2016.

[50] S. C. Khouili, E. C. L. Cook, E. Hernández-García, M. Martínez-López, R. Conde-Garrosa, and S. Iborra, "SHP-1 regulates antigen cross-presentation and is exploited by _Leishmania_ to evade immunity," *Cell Reports*, vol. 33, no. 9, article 108468, 2020.

[51] J. P. Snook, A. J. Soedel, H. A. Ekiz, R. M. O'Connell, and M. A. Williams, "Inhibition of SHP-1 expands the repertoire of anti-tumor T cells available to respond to immune checkpoint blockade," *Cancer Immunology Research*, vol. 8, no. 4, pp. 506–517, 2020.

[52] M. Nieminen, T. Henttinen, M. Merinen, F. Marttila–Ichihara, J. E. Eriksson, and S. Jalkanen, "Vimentin function in lymphocyte adhesion and transcellular migration," *Nature Cell Biology*, vol. 8, no. 2, pp. 156–162, 2006.

[53] N. Mor-Vaknin, A. Punturieri, K. Sitwala, and D. M. Markovitz, "Vimentin is secreted by activated macrophages," *Nature Cell Biology*, vol. 5, no. 1, pp. 59–63, 2003.

[54] M. Birkenbach, D. Liebowitz, F. Wang, J. Sample, and E. Kieff, "Epstein-Barr virus latent infection membrane protein increases vimentin expression in human B-cell lines," *Journal of Virology*, vol. 63, no. 9, pp. 4079–4084, 1989.

[55] J. M. Beck, R. L. Newbury, B. E. Palmer, M. L. Warnock, P. K. Byrd, and H. B. Kaltreider, "Role of CD8+ lymphocytes in host defense against _Pneumocystis carinii_ in mice," *Journal of Laboratory and Clinical Medicine*, vol. 128, no. 5, pp. 477–487, 1996.

[56] F. Gigliotti, E. L. Crow, S. P. Bhagwat, and T. W. Wright, "Sensitized CD8+ T cells fail to control organism burden but accelerate the onset of lung injury during Pneumocystis carinii pneumonia," *Infection and Immunity*, vol. 74, no. 11, pp. 6310–6316, 2006.

Hindawi
Journal of Immunology Research
Volume 2022, Article ID 5473763, 11 pages
https://doi.org/10.1155/2022/5473763

*Research Article*

# Optimized Protocol for the Isolation of Extracellular Vesicles from the Parasitic Worm *Schistosoma mansoni* with Improved Purity, Concentration, and Yield

**Marije E. Kuipers**,[1,2] **Roman I. Koning**,[3] **Erik Bos**,[3] **Cornelis H. Hokke**,[1] **Hermelijn H. Smits**,[1] **and Esther N. M. Nolte-'t Hoen**[2]

[1]*Department of Parasitology, LUMC, Leiden, Netherlands*
[2]*Department of Biomolecular Health Sciences, Faculty of Veterinary Medicine, Utrecht University, Utrecht, Netherlands*
[3]*Department of Cell & Chemical Biology, LUMC, Leiden, Netherlands*

Correspondence should be addressed to Esther N. M. Nolte-'t Hoen; e.n.m.nolte@uu.nl

Received 25 January 2022; Accepted 21 February 2022; Published 8 April 2022

Academic Editor: Ana Claudia Torrecilhas



In the past decade, the interest in helminth-derived extracellular vesicles (EVs) increased owing to their role in pathogen-host communication. However, the availability of EVs from these parasitic worms is often limited due to the restricted occurrence and culturing possibilities of these organisms. *Schistosoma mansoni* is one of several helminths that have been shown to release EVs affecting the immune response of their host. Further investigation of mechanisms underlying these EV-induced effects warrants separation of EVs from other components of the helminth excretory/secretory products. However, isolation of high-purity EVs often come to the expense of reduced EV yield. We therefore aimed to develop an optimized protocol for isolation of EVs from *S. mansoni* schistosomula and adult worms with respect to purity, concentration, and yield. We tested the use of small (1.7 ml) iodixanol density gradients and demonstrated that this enabled western blot-based analysis of the EV marker protein tetraspanin-2 (TSP-2) in gradient fractions without additional concentration steps. Moreover, the concentration and yield of EVs obtained with small iodixanol gradients were higher compared to medium-sized (4.3 ml) or conventional large-sized (12 ml) gradients. Additionally, we provide evidence that iodixanol is preferred over sucrose as medium for the small density gradients, because EVs in iodixanol gradients reached equilibrium much faster (2 hours) and iodixanol but not sucrose was suitable for purification of schistosomula EVs. Finally, we demonstrate that the small iodixanol gradients were able to separate adult worm EVs from non-EV contaminants such as the blood digestion product hemozoin. Our optimized small iodixanol density gradient allows to simultaneously separate and concentrate EVs while reducing handling time and EV loss and can be applied for EVs from helminths and other limited EV sources.

## 1. Introduction

Extracellular vesicles (EVs) are nanosized, lipid bilayer-enclosed particles containing (glycosylated) proteins, lipids, and RNAs that are released into the extracellular space by virtually all cells and organisms. EVs are widely investigated for their role in communication between cells in various diseases [1–3], in host-pathogen interactions [4, 5], and for their biomarker or therapeutic potential [6–8]. EVs from parasitic worms have emerged as important players in host-pathogen interactions and their role in parasitic diseases warrants extensive investigations [9]. Research on such EVs faces many technical challenges [9–11].

To characterize their molecular composition and function, EVs need to be isolated from biological fluids and separated from large molecular (lipo) protein complexes that overlap in size and/or buoyant density [12]. These purification steps generally reduce EV yield [13, 14], and it has been shown that adsorption of EVs to plastic surfaces, e.g., from (ultra) centrifugation tubes, results in EV

loss over time [15]. This loss of EVs could be compensated by increasing the starting material, but this poses an extra challenge when working with limited material, such as parasites. Additionally, the complex life cycle of helminths poses a technical challenge for EV research in this area. The life cycles of many helminths depend on mammalian and intermediate hosts, and one of these helminths is *Schistosoma mansoni*. Obtaining the different schistosome life stages for culture and subsequent EV isolation is challenging due to limited availability of larvae and the restricted amount of parasites obtained from sacrificed infected animals [16]. The schistosomula are transformed cercarial larvae that can only be obtained from an infected intermediate snail host. Adult worms are obtained from perfusion of the portal venous system of mice or hamsters infected with cercarial larvae, and eggs can be isolated from enzymatically digested liver and gut tissue from the infected animals. EVs are released by all three life stages as part of the complex excretory/secretory (E/S) products released by *S. mansoni* [17–19]. Studying their EVs requires separation from other proteins and lipids in these E/S products. E/S from blood feeding parasites, among which is *S. mansoni*, also contains digestion products of blood that the adult worms regurgitate when they are cultured *ex vivo* in serum-free medium [20, 21]. One of these products is hemozoin, a nontoxic, insoluble, and crystallized form of the otherwise toxic heme.

The discovery of (glyco)proteins and RNAs that are specifically enriched in schistosome EVs will accelerate research on how these EVs interact with and manipulate their hosts and on the biomarker potential of these EVs. This kind of research, however, demands the acquisition of sufficient amounts of highly purified EVs. We aimed to develop an optimized method for separating adult worm and schistosomula EVs from non-EV contaminants while keeping the EV yield as high as possible. We propose the use of small-sized iodixanol density gradients to increase concentration and yield of obtained EV isolates while reducing handling time.

## 2. Materials and Methods

*2.1. Parasite Culture.* The life cycle of *S. mansoni* (Puerto Rican strain) was maintained in golden Syrian hamsters (HsdHan-Aura) and *Biomphalaria glabrata* snails as previously described [22]. All hamster experiments were performed in accordance with the Guide for the Care and Use of Laboratory Animals of the Institute for Laboratory Animal Research and have received approval from the university Ethical Review Board (Leiden University Medical Center, Leiden, The Netherlands). Cercariae from shed snails were washed with >25 ml cold DMEM (high glucose with L-glutamine, Lonza, Basel, Switzerland) supplemented with Antibiotic Antimycotic Solution (ABAM, Sigma-Aldrich, St. Louis, MO, USA) in a 30 $\mu$m pluriStrainer (pluriSelect, Leipzig, Germany) and subsequently resuspended in 12 ml warm medium (37°C) and transformed to schistosomula by pipetting with a 10 ml serological pipet and incubation at 37°C for 20 minutes. Schistosomula (cercariae without tails) were collected using an orbital shaker and cultured at 37°C and 5% $CO_2$ for three days in DMEM + ABAM at 7,500 schistosomula/ml in 25 $cm^2$ polystyrene flasks (Greiner Bio-One, Alphen a/d Rijn, The Netherlands).

Obtained adult worms (mixed sex) from perfused hamsters were washed five times or more with >25 ml DMEM + ABAM supplemented with 10 mM HEPES (pH 7.4). Residual hair and tissue, blot clots, and dead worms were removed. Worms were cultured in DMEM + ABAM + HEPES for two days at 37°C and 5% $CO_2$ and at 10 worms/ml in 75 $cm^2$ polystyrene flasks (Corning, Sigma-Aldrich) with a maximum of 40 ml/flask. Viability of the worms was ensured during and after culture by visual inspection of worm movement and attachment of the worms' sucker to the flask bottom.

*2.2. Differential Ultracentrifugation (dUC).* Culture medium of the schistosomula and adult worms was collected in 15 ml tubes and 50 ml tubes (Greiner Bio-One), respectively, and centrifuged twice at 200 × *g* and twice at 500 × *g*, all for 10 minutes and at 4°C with low brake (SX4750A rotor and an Allegra X-15R centrifuge) (Beckman Coulter, Brea, CA, USA). After each centrifugation step, supernatants were transferred to a new tube using a serological pipet. The 500 × g supernatants were centrifuged (all in 15 ml tubes) 30 minutes at 5,000 × *g* (SX4750A rotor) and 4°C (max brake). The 5,000 × *g* supernatants were stored at -80°C till further use.

The frozen 5,000 × g supernatants (11-66 mL) were thawed overnight at 4°C, transferred to polypropylene tubes, and ultracentrifuged for 65 minutes 4°C, at 28,000 rpm (~100,000 × g, k-factor 265) in an XE-90 centrifuge using an SW 41 Ti rotor (Beckman Coulter). Subsequently, supernatant was aspirated until the liquid surface reached the conical part of the tube. If this was the final spin, the rest of the supernatant was decanted after which the walls of the tube were wiped dry with a tissue while holding the tube upside down. When a washing step was performed, pellets were resuspended in supernatant remaining in the conical part of the tube, pooled to one tube, topped up with cold PBS (B. Braun, Melsungen, Germany), and spun as before. This washing step was then repeated once more followed by the steps for the final spin. Final EV-enriched pellets were resuspended in PBS or PBS supplemented with 0.2% BSA (Sigma-Aldrich), which was made from a 5% BSA in PBS stock that was cleared from protein aggregates by overnight ultracentrifugation at 100,000 × g. Washed UC pellets for cryo electron microscopy of schistosomula were prepared as described in [23].

*2.3. Size Exclusion Chromatography (SEC).* The SEC column (qEVoriginal, 70 nm, IZON Science LTD, Christchurch, Aotearoa-New Zealand) was washed with 10 ml PBS at room temperature. Subsequently, 170 $\mu$l of ultrafiltrated adult worm culture E/S, corresponding to material from ~100 worms, was loaded onto the column followed by addition of 10 ml PBS, after which 25 consecutive eluted fractions of 500 $\mu$l were collected. Fractions were stored at -20°C till preparation for SDS-PAGE.

Table 1: Iodixanol gradient volumes and centrifugation details.

(a)

| | Rotor type | EV sample (μL) | Gradient build (iodixanol) 60% (μL) | 40% (μL) | 30% (μL) | 10% (μL) |
|---|---|---|---|---|---|---|
| Large | SW 41 Ti | 70 | 3,200 | 1,600 | 1,600 | 5,500 |
| Medium | SW 55 Ti | 70 | 1,100 | 550 | 550 | 1,980 |
| Small | TLS-55 | 70 | 440 | 220 | 220 | 792 |

(b)

| Rotor type | Rpm | Average g-force | k-Factor | Centrifugation time (h) | Total gradient volume (μL) | Fraction volume (μL) (12×) |
|---|---|---|---|---|---|---|
| SW 41 Ti | 37,000 | 169,044 | 152 | >16 | 11,970 | 997 |
| SW 55 Ti | 42,000 | 169,639 | 82 | >15 | 4,250 | 354 |
| TLS-55 | 50,000 | 166,180 | 60 | 2 | 1,742 | 145 |

*2.4. Density Gradient Ultracentrifugation.* UC pellets from 11-30 ml adult worm or 40 ml schistosomula culture supernatants were resuspended in a final volume of 70 μl PBS + 0.2%BSA. For bottom-up iodixanol gradient centrifugation, the resuspended EV pellet was mixed gently with 60% iodixanol (Optiprep, Axis-Shield PoC AS, Oslo, Norway). Blocks of 40%, 30%, and 10% were carefully layered on top using a plastic Pasteur pipet. The volumes used for small, medium, and large gradients are displayed in Table 1a. Iodixanol dilutions were made from a 50% dilution and PBS. For the sucrose gradients, a 2.5 M D(+)-sucrose (Biochemica, PanReac AppliChem, Darmstadt, Germany) stock solution was prepared and from that, 2 M and 0.4 M dilutions were made to prepare 14 linear dilutions as described previously [24]. 70 μl of EV pellet was mixed gently with 320 μl 2.5 M sucrose within the small UC tube. Subsequently, 14 fractions with decreasing sucrose densities (from 1.886 M to 0.4 M sucrose) of 105 μl were carefully added. For top-down centrifugation, the gradients were built with equal iodixanol or sucrose volumes first after which 70 μl EVs suspensions were carefully added on top of the 10% iodixanol or 0.4 M sucrose.

Centrifugation times of large (SW 41 Ti), medium (SW 55 Ti), and small (TLS-55) gradients can be found in Table 1b. Centrifugation time for the small sucrose gradients was either two or 13.5 hours on similar speed as the iodixanol small gradient. All were centrifuged in thin-wall polypropylene tubes, at 4°C with slow acceleration and slow deceleration. SW 41 Ti and SW 55 Ti rotors were used in an XE-90 ultracentrifuge and the TLS-55 rotor in an Optima TLX (Beckman Coulter). Volumes of collected fractions of the iodixanol gradients are mentioned in Table 1b. The volume of sucrose gradient fractions was 155 μl. Collected fractions were kept on ice, vortexed, and 15 μl per fraction was used to measure their refractive index (RI) by a CETI refractometer (Medline Scientific, Chalgrove, UK). Densities were calculated with the formulas 3,35∗RI-3,4665 and 2,6448∗RI-2,5263 for iodixanol and sucrose, respectively.

When comparing the different tube sizes, culture medium of the same worm culture was used and EV pellets were pooled and split evenly before building the gradients and each gradient consisted of EV material from 11 ml medium. For the washing of iodixanol density gradient fractions, two fractions were pooled: 400 μl per pool for the medium gradient and 1,650 μl per pool for the large gradient in SW41 and SW32 sized polypropylene tubes, respectively. Tubes were topped up with cold PBS (diluting the gradient fractions ~22×) supplemented with 0.1% BSA (from 5% BSA stock) or with plain PBS. Samples were centrifuged for 65 minutes, 4°C, at 32,000 rpm in an XE-90 centrifuge (average 126,444 × g and k-factor 203 for SW 41 Ti and average 125,755 × g and k-factor 204 for SW 32 Ti) after which the obtained pellets were resuspended in a volume of 1× sample buffer equal to the pooled small gradient fractions. Samples were stored at -20°C until SDS-PAGE.

*2.5. Ultrafiltration.* Adult worm culture medium from ~1,100 worms was centrifuged once at 200 × g, and the supernatant was concentrated in 3 or 10 kDa filter tubes (Amicon Ultra, Millipore, Merck, Darmstadt, Germany) according to the manufacturer's protocol. E/S in the filters was washed 3 times with PBS and finally concentrated to a volume of 1,870 μl, of which aliquots were stored at -80°C till further use.

Fractions 5-8 with a density 1.21-1.07 g/ml of bottom-up small iodixanol density gradient isolated adult worm EVs (from ~660 worms) were pooled, diluted 1 : 1 with PBS, and transferred into an 0.5 ml 10 kDa centrifugal filter unit (Amicon Ultra, Millipore, Merck) that was precoated with 20 μg trypsin-digested BSA. Iodixanol was removed in 5 centrifugation steps of 10 minutes at 14,000 × g, by which the sample was fully loaded after three steps followed by two additional washing steps with 300-400 μl PBS. The sample was concentrated to 50 μl by a final centrifugation step of 20 minutes. This final sample was collected by brief reverse centrifugation of the filter and directly used for cryo electron microscopy (EM).

*2.6. Cryo Electron Microscopy (Cryo-EM).* 300 mesh EM grids (Quantifoil R2/2, Jena, Germany) were glow-discharged by 0.2 mbar air for two minutes using the glow

discharger unit of an EMITECH K950X. Three $\mu$l of sample was applied per glow-discharged grid, and the grid was vitrified using an EMGP (Leica, Wetzlar, Germany) at room temperature and 100% humidity. For vitrification, excess sample was removed by blotting for one second to Whatman #1 filter paper directly followed by plunging the grid into liquid ethane (-183°C) after which the grid was stored under liquid nitrogen till further use. Cryo-EM imaging was performed at 120 kV on a Tecnai 12 electron microscope (Thermo Fisher Scientific, Waltham, MA, USA) after mounting the grid in a Gatan 626 cryo-holder. A 4 k × 4 k Eagle camera (Thermo Fisher Scientific) was used to record images with focus between 5-10 $\mu$m and an 18,000 × magnification (pixel size 1.2 nm).

*2.7. Trichloroacetic Acid (TCA) Precipitation.* Iodixanol density fractions were mixed with 2% (*w*/*v*) Na-deoxycholate (added 1 : 117), and proteins were precipitated by mixing each fraction with cold 100% (*w*/*v*) trichloroacetic acid (TCA) (added 1 : 10) and a 15 minutes incubation on ice. Eppendorf tubes were centrifuged at maximum speed (16,100 × g) for 10 minutes at 4°C and supernatant was discarded. Eppendorf tubes were spun briefly again to allow removal of all remaining supernatant. Protein pellets were subsequently mixed with 100% ice cold acetone (similar volume as original gradient fraction) and incubated for >10 minutes at -20°C and centrifuged as before. This acetone washing step was repeated after which the samples were dried at room temperature for 5 minutes. Fractions were mixed with 200 $\mu$l (large gradient fractions) or 100 $\mu$l (medium and small gradient fractions) 1× unreduced sample buffer.

*2.8. Western Blotting.* SEC fractions were thawed and vortexed before mixing with 4× Laemmli sample buffer under nonreducing conditions. Iodixanol and sucrose density fractions were either directly mixed with 4× sample buffer or after pooling and washing by UC. All samples were incubated 3 min 100°C directly after mixing with sample buffer, stored at -20°C, and incubated again at 100°C before loading on the SDS-PAGE gel. All samples were loaded 15 $\mu$l per lane, with an exception for the TCA samples of the small and medium gradient fractions, which were loaded 2 $\mu$l per lane. Samples and 1.5 $\mu$l of ladder (PageRuler Plus, Thermo Fisher Scientific) were separated on 12.5% gels, which were subsequently blotted onto methanol activated PVDF membranes. Membranes were blocked with PBS supplemented with 0.1% (*v*/*v*) Tween-20 and 0.2% (*w*/*v*) gelatin from cold water fish skin (Sigma-Aldrich) and overnight incubated with TSP2-2D6 (mouse IgG, 1 : 2,000) (kind gift from Professor Alex Loukas, James Cook University, Australia) monoclonal antibody. Incubated blots were washed several times with blocking buffer and incubated 45 minutes with Goat-$\alpha$Mouse-IgG-HRP (1 : 10,000, Promega, Leiden, The Netherlands) and washed again extensively. Chemiluminescence substrate (SuperSignal West Pico PLUS, Thermo Fisher Scientific) was applied, and Alliance Q9 (UVITEC, Cambridge, UK) imaged blots were analyzed and signals quantified in Fiji/ImageJ [25].

## 3. Results

*3.1. Worm EV Isolates Obtained by Differential Ultracentrifugation and Size Exclusion Chromatography Contain Non-EV Contaminants.* We first tested two size-based separation methods, differential (ultra)centrifugation (dUC) and size exclusion chromatography (SEC), for isolation of EVs released by *Schistosoma* adult worms. As an indicator for the presence of EVs we used western blot analysis for *S. mansoni* tetraspanin-2 (TSP-2), which is one of the most abundant proteins identified in adult worm EVs [26, 27]. Both in the EV-enriched 100,000 x g pellet obtained by dUC and in the EV-enriched SEC fractions, we confirmed the presence of TSP-2 containing schistosome EVs (Figures 1(a) and 1(c)). However, we observed brown coloring of both the UC pellet and the EV-containing SEC fractions (Figures 1(b) and 1(d)). We suspected that this was due to contamination with the blood digestion product hemozoin, which is pigmented and colors the worm gut dark and culture medium light brown. We confirmed the presence of hemozoin crystals in 100,000 × g EV pellets by cryo electron microscopy (cryo-EM) and observed that these crystals overlapped in size with the adult worm EV (Figure 1(e)). This suggests that small hemozoin crystals, and possibly also other non-EV particles [21], sedimented at similar *g*-forces as the worm EVs and could not be separated from EVs based on size differences. The hemozoin contamination was specific for adult worm EV isolates, as EV-enriched dUC pellets from schistosomula did not contain hemozoin (Figure 1(f)). This was expected because schistosomula are transformed from larvae released by snails and cultures of these worms do not contain blood-digestion products. These data indicate that for the design of a protocol that allows purification of EVs from both schistosome life stages, size-based separation methods do not suffice and should be combined with density gradient centrifugation.

*3.2. The Use of Small Density Gradients Increases EV Concentration and Yield.* When separation based on size is insufficient, EVs can be further purified using density gradient centrifugation [12, 14, 28]. An unwanted consequence of conventional density gradient separation, however, is the dilution of EVs in relatively large volumes of gradient medium. As a consequence, additional concentrating steps are required for further analysis of the EVs. This can be achieved by ultracentrifugation, after pooling the EV-containing density gradient fractions in a larger UC tube, dilution with PBS, and repelleting by UC [28]. This step can cause loss of EVs via adsorption to tube walls and handling time, though the addition of BSA to the PBS may reduce some of the loss [15]. Because loss of EVs is particularly undesirable when working with limited worm-derived material, we aimed to optimize density gradient-based EV isolation for low-input material. We hypothesized that using a small volume density gradient in a small tube will reduce EV loss by decreasing the plastic surface area to which EVs may be adsorbed [15]. In addition, the shorter centrifugation time needed for EVs to reach their equilibrium density in

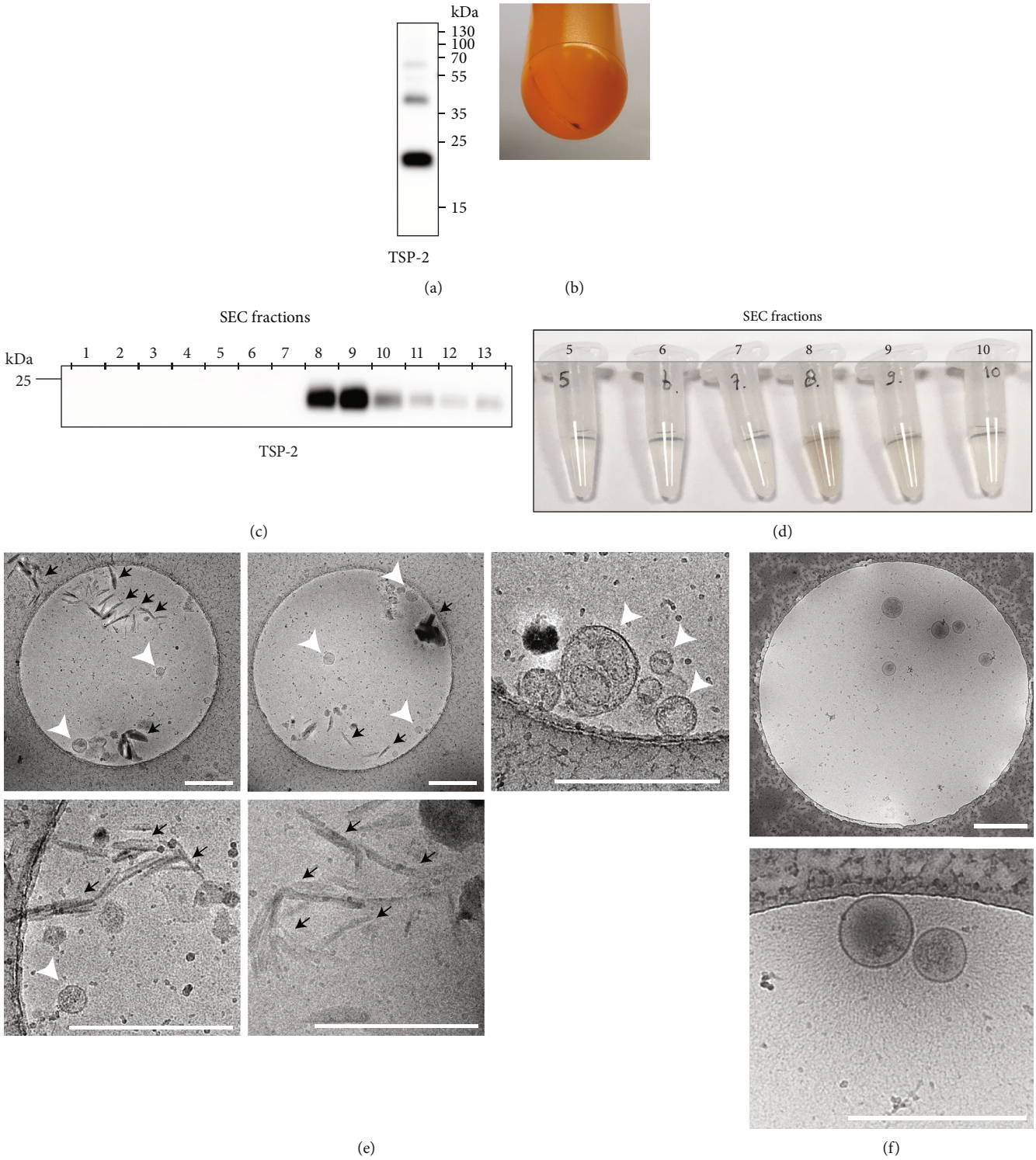


Figure 1: Adult worm EV isolates prepared by differential (ultra)centrifugation (dUC) or size exclusion chromatography (SEC) are contaminated by hemozoin. Culture supernatant of adult worms was subjected to dUC (a, b, and e) or SEC (c, d). (a) Western blot detection of the schistosome EV marker tetraspanin-2 (TSP-2) in 100,000 × g pelleted adult worm EVs. (b) Black 100,000 × g pellet of adult worm EVs indicates the presence of hemozoin. Collected SEC fractions from adult worm E/S released by ~100 worms show similar fractions containing TSP-2 (c) and hemozoin (brown fractions in d). (e) Cryo-EM analysis of washed 100,000 × g pellet from 22 ml adult worm culture shows EVs (white arrowheads) and coisolated hemozoin crystals (black arrows). (f) Cryo-EM analysis shows that pelleted schistosomula EVs from 15 ml culture medium, with characteristic "hair-like" filaments on their surface, do not contain hemozoin crystals. Scale bars (e, f) are 500 nm.

these small tubes reduces exposure time of EVs to the plastic surfaces. Finally, a small gradient introduces a concentrating factor of the EVs as fraction volumes will be smaller. We compared EV isolation efficiency in conventional large-sized (12 ml) and medium-sized (4.3 ml) gradients to a small-sized (1.7 ml) gradient. All three iodixanol gradients were built according to a similar set-up (see Table 1) but the large and medium gradients were centrifuged for >16 hours [28], and the small gradient was centrifuged for two hours [29]. These centrifugation times were sufficient for EVs to float to the ~1.07-1.10 g/ml density fractions, as based on western blot detection of schistosome TSP-2 (Figure 2(a)).

Next, we assessed whether the smaller gradient size reduced adult worm EV loss and enabled western blot-based analysis of EV proteins in gradient fractions without additional concentration steps. To be able to accurately compare EV concentrations within the gradient fractions, adult worm EVs from the same worm culture were equally divided over the three differently sized gradients. After centrifugation, 12 equal volume fractions were collected from each gradient and two consecutive fractions were pooled to allow all EV containing fractions (F5-F10) from the three different gradients to be loaded on the same SDS-page gel. First, the pools of gradient fractions were directly mixed with sample buffer, subjected to SDS-PAGE, and analyzed by western blotting for the presence of TSP-2 (Figure 2(b)). We observed that the concentration in the fractions of the medium and large-sized gradients was 41-56% and 90-94% lower compared to the small gradients, respectively (Figure 2(c)). Thus, the small gradient allows western blot analysis of EV proteins without the need to concentrate the density fractions before gel loading.

Next, we tested the effect of concentration steps on EV recovery from fractions of the medium and large gradients. Based on previous indications that this loss could be reduced in the presence of BSA, the EV containing density fractions were diluted in PBS or PBS supplemented with BSA prior to repelleting of EVs by UC. EV pellets were resuspended in the same volume as the pooled fractions from the small gradient. Western blotting of TSP-2 showed that concentrating the pooled fractions in the presence of BSA resulted in 8-20% lower concentration of EVs from the medium gradient and 24-73% lower concentration for the EVs from the large gradient, as compared to the small gradient fractions (Figure 2(d)). Concentration in the absence of BSA led to an almost complete loss of EVs. Thus, the small gradient is superior over the other sized gradients in EV concentration and yield while the handling time is reduced.

*3.3. Iodixanol but Not Sucrose Density Gradients Are Suitable for Purification of Adult Worm and Schistosomula EVs.* We aimed to optimize an EV purification protocol suitable for EVs of both adult worms and schistosomula. To verify whether both types of EVs reached equilibrium density within 2 hours of centrifugation in these small gradients, we compared loading the gradients on top of the EV-enriched pellets (EVs floating "bottom-up") to loading the EVs on top of the gradients (EVs floating "top-down"). TSP-2 detection in collected fractions showed that both schistosomula and adult worm EVs concentrated in fractions with densities characteristic for EVs (1.08-1.16 g/ml) and that this was similar in bottom-up or top-down loaded gradients (Figures 3(a) and 3(b)), indicating that equilibrium densities were reached.

Another widely used density gradient medium is sucrose, and we additionally tested whether EVs from both schistosome life stages could also be isolated by a small sucrose gradient. However, two hours of centrifugation was not sufficient for the adult worm EVs to reach equilibrium density in bottom-up sucrose gradients (Figure 3(c)). Under these conditions, part of the TSP-2 remained in the fractions with higher densities, suggesting that the EVs needed more time to reach the lower densities. Indeed, 13.5 hours centrifugation of the bottom-up gradient was needed for the adult worm EVs to reach the 1.12-1.16 g/ml density fractions (Figure 3(c)). In contrast to the EVs from the adult worms, sucrose gradients were less effective in purification of schistosomula EVs. In both bottom-up and top-down sucrose gradients, the schistosomula EVs ended up in fractions with higher densities (between 1.21 and 1.28 g/ml) compared to iodixanol gradients (Figure 3(d)). This is undesirable, since various non-EV contaminants also remain in the bottom fractions of gradients. These data suggest that the small iodixanol gradients are most optimal and time-efficient for purifying EVs from both life stages of *S. mansoni*.

*3.4. Small Iodixanol Density Gradients Separate EVs from Non-EV Contaminants.* Finally, we verified whether the small iodixanol gradients allowed separation of EVs from non-EV contaminants (Figure 1). We selected hemozoin as detectable example for non-EV contaminants, since markers for other protein contaminants are currently lacking for *Schistosoma* spp. UC pellets of adult worm culture supernatant were overlaid with the optimized small iodixanol density gradient. After two hours centrifugation, we observed a black substance in the bottom of the gradient, suggesting the presence of hemozoin (Figure 4(a)). Cryo-EM analysis of EV-containing fractions (1.07-1.21 g/ml) confirmed the absence of hemozoin among the high number of adult worm EVs in these gradient fractions (Figure 4(b)). These data indicate that the small iodixanol density gradient allowed successful separation of EVs from non-EV particles such as hemozoin. We propose that small-sized (1.7 ml) iodixanol density gradients can be used to simultaneously separate and concentrate EVs from limited sources, such as helminths, to increase EV yield while reducing handling time.

## 4. Discussion

Each EV source has its own challenge for obtaining a high-quality EV preparation with sufficient material for downstream analysis, and these challenges often include the separation of EVs from non-EV contaminants [30]. For *Schistosoma mansoni* parasites, these non-EV contaminants include many released E/S components [17, 18] and for adult worms also the blood-digestion product hemozoin

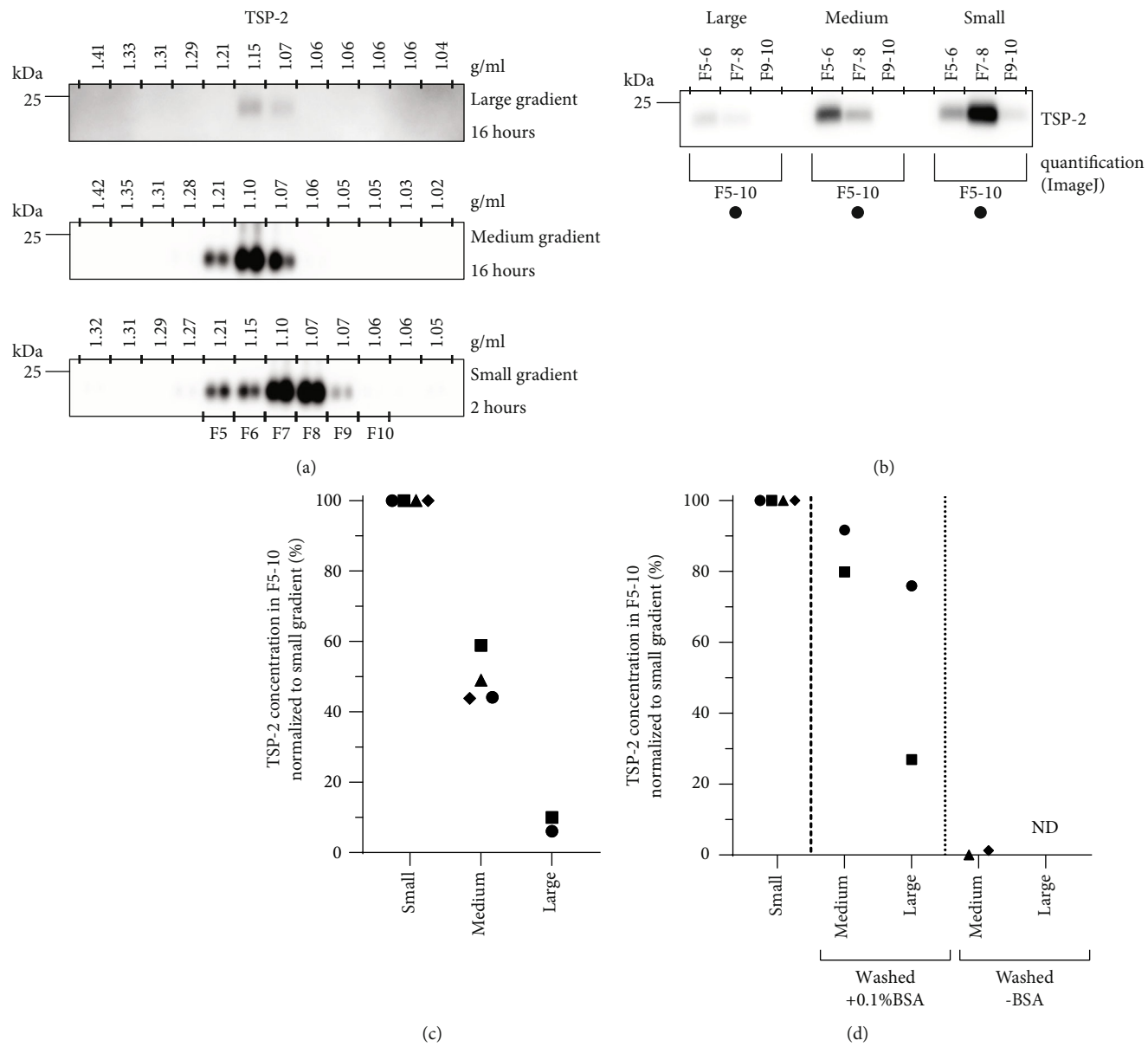


Figure 2: Comparative detection of adult worm EVs isolated with three different sizes iodixanol density gradients. (a) Western blot detection of tetraspanin-2 (TSP-2) in TCA precipitated protein isolates of fractions from adult worm EVs floated bottom-up into large (12 ml), medium (4.3 ml), or small (1.7 ml) iodixanol gradients. (b) Equal 100,000 × g EV-enriched pellets of the same adult worm cultures were loaded in the three differently sized gradients. EV-containing fractions were pooled and directly mixed with sample buffer for SDS-PAGE to compare TSP-2 detection by western blot. (c) Quantification of TSP-2 band intensities of western blots in (b). (d) EVs in pooled fractions of medium and large gradients were diluted in PBS with or without 0.1%BSA, repelleted by UC, and concentrated to equal volumes as the small gradient fractions. TSP-2 levels in concentrated EV isolates from medium- and large-sized gradients were compared to EV isolates taken directly from the small density gradient. TSP-2 western blot and quantification were performed as in (b). Data in (a) and (b) is representative for 2-4 independent experiments. Each symbol in (c) and (d) corresponds to an independent experiment.

[31]. Both non-EV E/S components and hemozoin are unwanted in EV-preparations, especially when studying host-pathogen interactions as they can affect host immune responses [32, 33]. Additional challenges for studying EVs from *S. mansoni* are imposed by the complex life cycle of this parasite. Not only do the different life stages of the parasite release EVs with different characteristics (Figures 1(e) and 1(f) and [23]), there is also limited availability of each life stage, thus restricting the material to isolate EVs from. This latter restriction makes any loss of EVs during the isolation process highly undesirable. Here, we propose the use of small iodixanol density gradients to increase EV yield compared to larger-sized gradients for separating EVs from non-EV contaminants. This protocol is applicable to EVs from the different *S. mansoni* life stages and EVs from other limited sources.

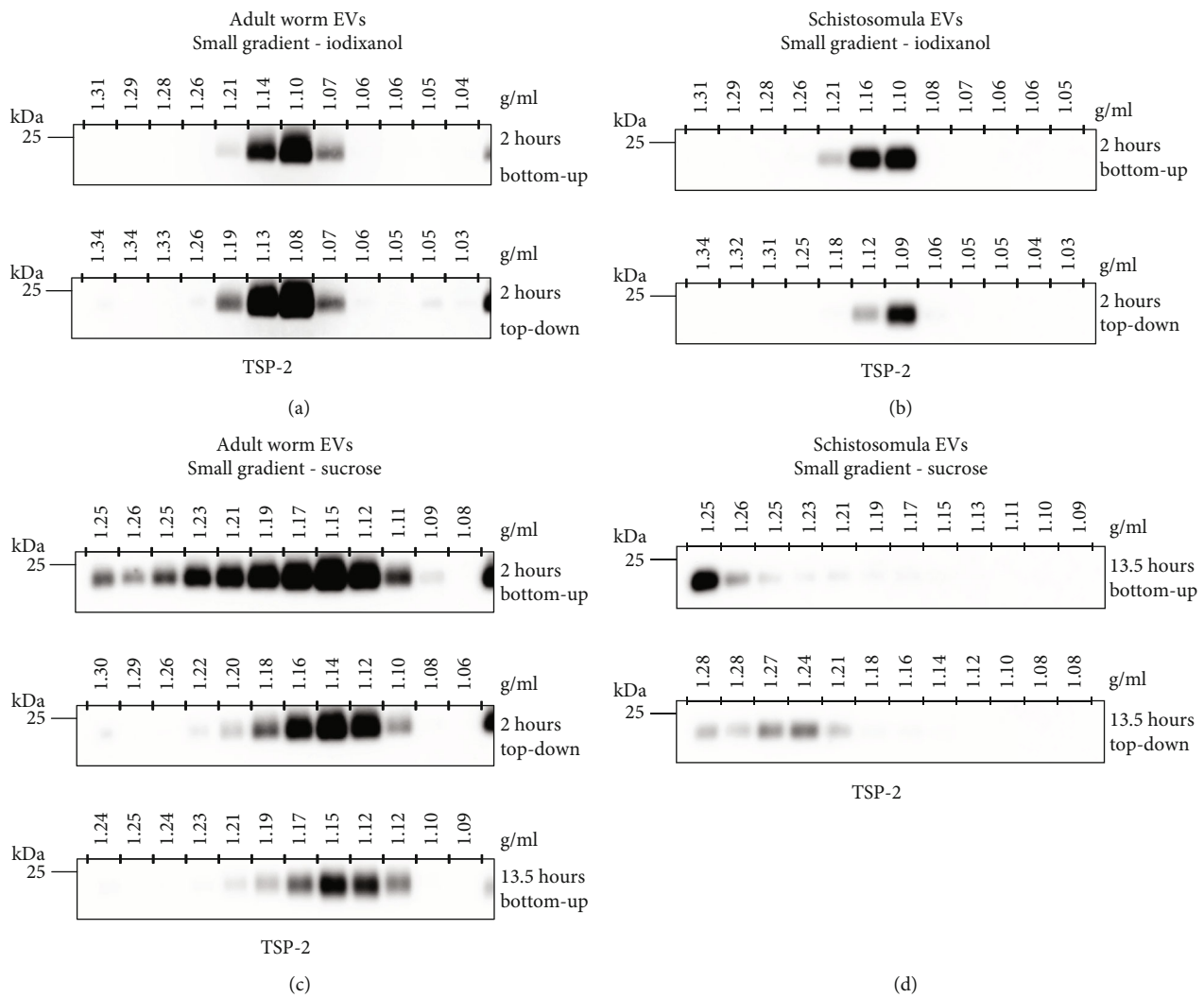


Figure 3: Iodixanol gradients are preferred over sucrose gradients for purification of adult worm and schistosomula EVs. EV-enriched UC pellets of adult worm EVs (a) or schistosomula EVs (b) were loaded at the bottom (bottom-up) or on top (top-down) of a small iodixanol density gradient and centrifuged for two hours. Western blot analysis of collected density fractions for the EV marker TSP-2 shows that both EV types reached equilibrium densities in the small gradients. (c) Adult worm EVs were loaded at the bottom or top of small sucrose density gradients. Shown are western blot detections of TSP-2 in fractions collected from two and 13.5 hours centrifuged sucrose density gradients. (d) Top-down and bottom-up sucrose gradients were used to purify schistosomula EVs. Shown are western blot detections of TSP-2 in fractions collected from 13.5 hours centrifuged gradients. Gradients were loaded with material from 11 or 10 ml culture medium from the adult worms or schistosomula, respectively. Western blots shown are representative for 2-3 independent experiments.

Methods that separate structures based on size, such as dUC and SEC, were not sufficient to separate adult worm EVs from contaminating particles such as hemozoin crystals (Figure 1). Previously, SEC was proposed as a promising method for helminth EVs [11]. In that study, dUC and SEC were compared for isolation of EVs from *Fasciola hepatica*. Since *F. hepatica* lives in the bile duct and consumes local cells and bile instead of red blood cells for survival, there will be no hemozoin among the non-EV contaminants. However, SEC often dilutes the sample and EVs may be lost upon subsequent concentration steps, which would be unwanted for limited EV sources. Furthermore, a combination of size- and density-based separation methods is preferred to prepare EV populations to the highest purity [14, 28, 30, 34].

Both sucrose and iodixanol are used as gradient media for density-based isolation of EVs. Studies comparing iodixanol and sucrose density gradients for isolation of mammalian EVs showed no clear differences in densities the EVs ended up in [35, 36]. We here provide evidence that the type of gradient medium can strongly influence in which density fraction the *S. mansoni* EVs are concentrated and that this differs between EVs from the different parasite life stages. Our data show that the EVs from schistosomula, in contrast to EVs from adult worms, did not float to the characteristic EV density fractions (~1.10-1.17 g/ml) in sucrose gradients (Figure 3(d)). Yet, these two types of EVs floated to similar density fractions in the iodixanol gradients. The preferential localization of schistosomula EVs in high sucrose densities may possibly be linked to the unique filamentous structures

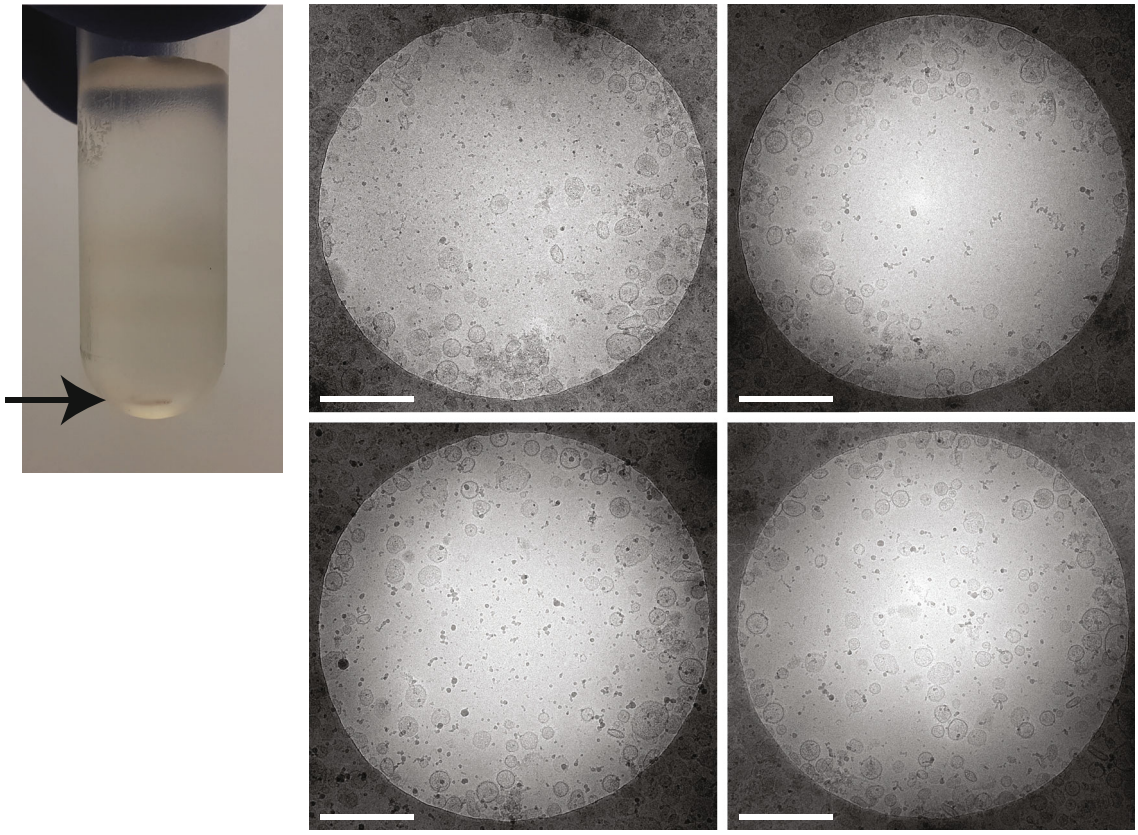

(a) (b)

Figure 4: Small iodixanol gradient separates adult worm EVs from non-EV contaminants. Adult worm EV-enriched UC pellets were overlaid with a small (1.7 ml) iodixanol density gradient and centrifuged for two hours. (a) The gradient after centrifugation shows hemozoin (black arrow) in the bottom of the tube. (b) Cryo-EM analysis of washed iodixanol gradient fractions with density 1.07-1.21 g/ml shows that EV-enriched fractions of the small gradients are devoid of hemozoin crystals. Scale bars are 500 nm.

on the schistosomula EV surface of which the actual molecular structure remains unknown [23]. We speculate that these structures contain glycans and/or mucins that interact with the sucrose, thereby influencing their localization in the gradient. There are several advantages of iodixanol over sucrose gradients for the purification of EVs. Iodixanol is isosmotic and isotonic, which is better to preserve EV structure and function. Moreover, iodixanol is far less toxic to cells than sucrose and therefore more suitable to study EV function. Our data substantiates the advantages of iodixanol over sucrose since iodixanol gradients allowed purification of EVs released by both *S. mansoni* life stages and allowed EVs to reach equilibrium density within shorter centrifugation times.

To our knowledge, this is the first report on utilizing small gradients for EV isolation, even though such gradients have been used for isolation of (multi)-protein complexes [29, 37, 38]. In these smaller gradients, EVs reach their equilibrium density after shorter centrifugation times than in conventional large volume gradients, which reduces handling time. Moreover, EVs are concentrated in a smaller volume, which makes it more feasible to directly subject density fractions to western blot analysis without additional concentration steps that may cause EV loss [15]. Another possible benefit of concentrated EV in small volume iodixanol density fractions is that these fractions could be directly added to cells, but this has not yet been studied. Though iodixanol is nontoxic, potential side-effects on cell functions would need to be controlled for. Of note, our proposed small iodixanol gradient was optimized for isolation of schistosome EVs. The exact construction of the gradient may need to be adjusted for optimal separation of EVs from other sources. Therefore, we highly encourage researchers to adjust their own established gradients to smaller-sized tubes.

EV research in the last decade taught us that choosing an appropriate EV isolation method is guided by both the research question and the type of source material. Our optimized protocol increases the concentration and yield of highly purified EVs from *S. mansoni* life stages. This may accelerate research and discoveries in the field including EV-induced immune-modulatory mechanisms and EV-associated biomarkers.

## Data Availability

N.A. This manuscript does not include omics-based data that can be archived in public databases. *EV-TRACK*. We have submitted all relevant data of our experiments to the EV-TRACK knowledgebase (EV-TRACK ID: EV220119) [39].

## Conflicts of Interest

We declare that none of the authors have competing financial or non-financial interests.

## Authors' Contributions

M.E.K. contributed to conceiving the study, designed experiments, performed the parasite cultures, EV isolations and western blots, data analysis, and drafting of the manuscript. R.I.K. and E.B. performed the cryo-EM imaging and provided feedback on the manuscript. H.H.S. and C.H.H. both contributed to conceiving the study, interpretation of results, and correcting the manuscript. E.N.M. N-'tH. contributed to conceiving the study, designed experiments, interpretation of the results, and drafting of the manuscript. All authors read and approved the final manuscript.

## Acknowledgments

The authors would like to thank Jan de Best and the rest of the life-cycle team for maintaining the availability of *S. mansoni* parasites, Professor Alex Loukas from James Cook University, Queensland (Australia) for providing the TSP-2-targeting antibodies, Sjaak van Voorden and the rest of the Medical Microbiology department (LUMC) for using their refractometer, Uvitec Alliance, ultracentrifuges and rotors, and Dr. George MC Janssen of the Center for Proteomics and Metabolomics of the LUMC for providing trypsin-digested BSA. This work was supported by the Nederlandse Organisatie voor Wetenschappelijk Onderzoek (NWO) Graduate School Program[022.006.010] (to M.E.K.).

## References

[1] E. N. Nolte-'t Hoen and M. H. Wauben, "Immune cell-derived vesicles: modulators and mediators of inflammation," *Current Pharmaceutical Design*, vol. 18, no. 16, pp. 2357–2368, 2012.

[2] M. Tkach and C. Thery, "Communication by extracellular vesicles: where we are and where we need to go," *Cell*, vol. 164, no. 6, pp. 1226–1232, 2016.

[3] F. Urabe, K. Patil, G. A. Ramm, T. Ochiya, and C. Soekmadji, "Extracellular vesicles in the development of organ-specific metastasis," *Journal of Extracellular Vesicles*, vol. 10, no. 9, 2021.

[4] M. E. Kuipers, C. H. Hokke, and H. H. Smits, "Pathogen-derived extracellular vesicle-associated molecules that affect the host immune system: an overview," *Frontiers in Microbiology*, vol. 9, p. 2182, 2018.

[5] M. H. Saad, R. Badierah, E. M. Redwan, and E. M. El-Fakharany, "A comprehensive insight into the role of exosomes in viral infection: dual faces bearing different functions," *Pharmaceutics*, vol. 13, no. 9, p. 1405, 2021.

[6] A. Hoshino, H. S. Kim, L. Bojmar et al., "Extracellular vesicle and particle biomarkers define multiple human cancers," *Cell*, vol. 182, no. 4, pp. 1044–1061.e18, 2020.

[7] T. A. P. Driedonks, S. Mol, S. Bruin et al., "Y-RNA subtype ratios in plasma extracellular vesicles are cell type- specific and are candidate biomarkers for inflammatory diseases," *Journal of Extracellular Vesicles*, vol. 9, no. 1, article 1764213, 2020.

[8] O. M. Elsharkasy, J. Z. Nordin, D. W. Hagey et al., "Extracellular vesicles as drug delivery systems: why and how?," *Advanced Drug Delivery Reviews*, vol. 159, pp. 332–343, 2020.

[9] C. M. Sánchez-López, M. Trelis, D. Bernal, and A. Marcilla, "Overview of the interaction of helminth extracellular vesicles with the host and their potential functions and biological applications," *Molecular Immunology*, vol. 134, pp. 228–235, 2021.

[10] A. Zakeri, E. P. Hansen, S. D. Andersen, A. R. Williams, and P. Nejsum, "Immunomodulation by helminths: intracellular pathways and extracellular vesicles," *Frontiers in Immunology*, vol. 9, p. 2349, 2018.

[11] C. N. Davis, H. Phillips, J. J. Tomes et al., "The importance of extracellular vesicle purification for downstream analysis: a comparison of differential centrifugation and size exclusion chromatography for helminth pathogens," *PLoS Neglected Tropical Diseases*, vol. 13, no. 2, 2019.

[12] T. Arab, A. Raffo-Romero, C. Van Camp et al., "Proteomic characterisation of leech microglia extracellular vesicles (EVs): comparison between differential ultracentrifugation and Optiprep™ density gradient isolation," *Journal of Extracellular Vesicles*, vol. 8, no. 1, 2019.

[13] A. Cvjetkovic, J. Lötvall, and C. Lässer, "The influence of rotor type and centrifugation time on the yield and purity of extracellular vesicles," *Journal of Extracellular Vesicles*, vol. 3, no. 1, 2014.

[14] Z. Onódi, C. Pelyhe, C. Terézia Nagy et al., "Isolation of high-purity extracellular vesicles by the combination of iodixanol density gradient ultracentrifugation and bind-elute chromatography from blood plasma," *Frontiers in Physiology*, vol. 9, 2018.

[15] E. G. Evtushenko, D. V. Bagrov, V. N. Lazarev, M. A. Livshits, and E. Khomyakova, "Adsorption of extracellular vesicles onto the tube walls during storage in solution," *PloS one*, vol. 15, no. 12, 2020.

[16] F. C. Lombardo, V. Pasche, G. Panic, Y. Endriss, and J. Keiser, "Life cycle maintenance and drug-sensitivity assays for early drug discovery in *Schistosoma mansoni*," *Nature Protocols*, vol. 14, no. 2, pp. 461–481, 2019.

[17] R. M. Maizels, H. H. Smits, and H. J. McSorley, "Modulation of host immunity by helminths: the expanding repertoire of parasite effector molecules," *Immunity*, vol. 49, no. 5, pp. 801–818, 2018.

[18] M. Giera, M. M. M. Kaisar, R. J. E. Derks et al., "The _Schistosoma mansoni_ lipidome: leads for immunomodulation," *Analytica Chimica Acta*, vol. 1037, pp. 107–118, 2018.

[19] S. F. Mossallam, I. F. Abou-El-naga, A. A. Bary, E. A. Elmorsy, and R. G. Diab, "Schistosoma mansoni egg-derived extracellular vesicles: a promising vaccine candidate against murine schistosomiasis," *PLoS Neglected Tropical Diseases*, vol. 15, no. 10, 2021.

[20] P. J. Skelly, A. A. Da'dara, X. H. Li, W. Castro-Borges, and R. A. Wilson, "Schistosome feeding and regurgitation," *PLoS Pathogens*, vol. 10, no. 8, article e1004246, 2014.

[21] S. L. Hall, S. Braschi, M. Truscott, W. Mathieson, I. M. Cesari, and R. A. Wilson, "Insights into blood feeding by schistosomes from a proteomic analysis of worm vomitus," *Molecular and Biochemical Parasitology*, vol. 179, no. 1, pp. 18–29, 2011.

[22] G. J. van Dam, B. J. Bogitsh, R. J. M. van Zeyl, J. P. Rotmans, and A. M. Deelder, "Schistosoma mansoni: in vitro and in vivo excretion of CAA and CCA by developing

schistosomula and adult worms," *The Journal of Parasitology*, vol. 82, no. 4, pp. 557–564, 1996.

[23] M. E. Kuipers, "DC-SIGN mediated internalisation of glycosylated extracellular vesicles from Schistosoma mansoni increases activation of monocyte-derived dendritic cells," *Journal of Extracellular Vesicles*, vol. 9, no. 1, article 1753420, 2020.

[24] E. J. van der Vlist, E. N. Nolte-'t Hoen, W. Stoorvogel, G. J. Arkesteijn, and M. H. Wauben, "Fluorescent labeling of nano-sized vesicles released by cells and subsequent quantitative and qualitative analysis by high-resolution flow cytometry," *Nature Protocols*, vol. 7, no. 7, pp. 1311–1326, 2012.

[25] J. Schindelin, I. Arganda-Carreras, E. Frise et al., "Fiji: an open-source platform for biological-image analysis," *Nature Methods*, vol. 9, no. 7, pp. 676–682, 2012.

[26] J. Sotillo, M. Pearson, J. Potriquet et al., "Extracellular vesicles secreted by _Schistosoma mansoni_ contain protein vaccine candidates," *International Journal for Parasitology*, vol. 46, no. 1, pp. 1–5, 2016.

[27] D. W. Kifle, M. S. Pearson, L. Becker, D. Pickering, A. Loukas, and J. Sotillo, "Proteomic analysis of two populations of _Schistosoma mansoni_ -derived extracellular vesicles: 15k pellet and 120k pellet vesicles," *Molecular and Biochemical Parasitology*, vol. 236, p. 111264, 2020.

[28] K. Brennan, K. Martin, S. P. FitzGerald et al., "A comparison of methods for the isolation and separation of extracellular vesicles from protein and lipid particles in human serum," *Scientific Reports*, vol. 10, no. 1, pp. 1–13, 2020.

[29] S. Aibara, J. Andréll, V. Singh, and A. Amunts, "Rapid isolation of the mitoribosome from HEK cells," *Journal of Visualized Experiments*, vol. 140, 2018.

[30] C. Thery, K. W. Witwer, E. Aikawa, M. J. Alcaraz, and J. D. Anderson, "Minimal information for studies of extracellular vesicles 2018 (MISEV2018): a position statement of the International Society for Extracellular Vesicles and update of the MISEV2014 guidelines," *Journal of Extracellular Vesicles*, vol. 7, no. 1, 2018.

[31] S. H. Xiao and J. Sun, "Schistosoma hemozoin and its possible roles," *International Journal for Parasitology*, vol. 47, no. 4, pp. 171–183, 2017.

[32] M. Truscott, D. A. Evans, M. Gunn, and K. F. Hoffmann, "Schistosoma mansoni hemozoin modulates alternative activation of macrophages via specific suppression of Retnla expression and secretion," *Infection and Immunity*, vol. 81, no. 1, pp. 133–142, 2013.

[33] G. Coakley, A. H. Buck, and R. M. Maizels, "Host parasite communications–messages from helminths for the immune system: parasite communication and cell-cell interactions," *Molecular and Biochemical Parasitology*, vol. 208, no. 1, pp. 33–40, 2016.

[34] G. Vergauwen, J. Tulkens, C. Pinheiro et al., "Robust sequential biophysical fractionation of blood plasma to study variations in the biomolecular landscape of systemically circulating extracellular vesicles across clinical conditions," *Journal of Extracellular Vesicles*, vol. 10, no. 10, 2021.

[35] S. R. Krishn, A. Singh, N. Bowler et al., "Prostate cancer sheds the $\alpha v\beta 3$ integrin in vivo through exosomes," *Matrix biology : Journal of the International Society for Matrix Biology*, vol. 77, pp. 41–57, 2019.

[36] L. Paolini, A. Zendrini, G. D. Noto et al., "Residual matrix from different separation techniques impacts exosome biological activity," *Scientific Reports*, vol. 6, no. 1, 2016.

[37] N. Tanese, "Small-scale density gradient sedimentation to separate and analyze multiprotein complexes," *Methods*, vol. 12, no. 3, pp. 224–234, 1997.

[38] M. Bagnat, S. Keränen, A. Shevchenko, A. Shevchenko, and K. Simons, "Lipid rafts function in biosynthetic delivery of proteins to the cell surface in yeast," *Proceedings of the National Academy of Sciences of the United States of America*, vol. 97, no. 7, pp. 3254–3259, 2000.

[39] J. van Deun, P. Mestdagh, P. Agostinis et al., "EV-TRACK: transparent reporting and centralizing knowledge in extracellular vesicle research," *Nature Methods*, vol. 14, no. 3, pp. 228–232, 2017.

Hindawi
Journal of Immunology Research
Volume 2022, Article ID 8092170, 15 pages
https://doi.org/10.1155/2022/8092170

*Review Article*

# Commensal and Pathogenic Bacterial-Derived Extracellular Vesicles in Host-Bacterial and Interbacterial Dialogues: Two Sides of the Same Coin

**Samira Tarashi**,[1,2] **Mohammad Saber Zamani**,[3] **Mir Davood Omrani**,[4] **Abolfazl Fateh**,[1,2] **Arfa Moshiri**,[1,2,5] **Ahmad Saedisomeolia**,[6,7] **Seyed Davar Siadat**,[1,2] **and Stan Kubow**[7]

[1]*Microbiology Research Center, Pasteur Institute of Iran, Tehran, Iran*
[2]*Mycobacteriology & Pulmonary Research Department, Pasteur Institute of Iran, Tehran, Iran*
[3]*Immunoregulation Research Center, Shahed University, Tehran, Iran*
[4]*Department of Medical Genetics, Shahid Beheshti University of Medical Sciences, Tehran, Iran*
[5]*Laboratory of Experimental Therapies in Oncology, IRCCS Istituto Giannina Gaslini, Genova, Italy*
[6]*Department of Cellular and Molecular Nutrition, School of Nutritional Sciences and Dietetics, Tehran University of Medical Sciences, Tehran, Iran*
[7]*School of Human Nutrition, McGill University, 21, 111 Lakeshore, Ste. Anne de Bellevue, QC, Canada H9X 3V9*

Correspondence should be addressed to Seyed Davar Siadat; d.siadat@gmail.com

Received 22 October 2021; Revised 17 January 2022; Accepted 1 February 2022; Published 17 February 2022

Academic Editor: Ana Claudia Torrecilhas



Extracellular vesicles (EVs) cause effective changes in various domains of life. These bioactive structures are essential to the bidirectional organ communication. Recently, increasing research attention has been paid to EVs derived from commensal and pathogenic bacteria in their potential role to affect human disease risk for cancers and a variety of metabolic, gastrointestinal, psychiatric, and mental disorders. The present review presents an overview of both the protective and harmful roles of commensal and pathogenic bacteria-derived EVs in host-bacterial and interbacterial interactions. Bacterial EVs could impact upon human health by regulating microbiota–host crosstalk intestinal homeostasis, even in distal organs. The importance of vesicles derived from bacteria has been also evaluated regarding epigenetic modifications and applications. Generally, the evaluation of bacterial EVs is important towards finding efficient strategies for the prevention and treatment of various human diseases and maintaining metabolic homeostasis.

## 1. Introduction

Extracellular vesicles (EVs) are nanosized membrane-encapsulated cell fragments shed from different domains of life, including bacteria [1]. The first evidence of bacteria-derived EVs dates back to the 1960s [2–4]. However, researchers initially failed to realize the importance of these newly discovered structures, which were mistakenly identified as unused cellular components ejected as "trash cans" [1, 5]. Another misconception was the assumption that bacteria-derived EVs constitute cellular debris solely from decomposition of dead cells, whereas in reality, the production of EVs by bacteria requires their metabolic activity [6, 7]. Different routes of formation of bacterial EVs have been indicated based on the diverse cell wall architecture of the EVs, which includes outer membrane vesicles (OMVs), inner membrane vesicles (IMVs), outer-inner membrane vesicles (O-IMVs), explosive outer membrane vesicles (EOMVs), cytoplasmic membrane vesicles (CMVs), and tube-shaped membranous structures (TSMSs). These latter

EVs contrast to bacterial EVs formed during phage endolysin-triggered cell lysis as bacteria-derived EVs originating from membrane blebbing of living cells are structurally different from EVs derived from cell lysis [8–12]. This latter distinction in the structure of EVs is associated with differences in their components, and possibly, their functions [12]. In that regard, such released membranous structures cannot replicate but are involved in the shuttling of bioactive compounds from their mother cells, including proteins, lipids, nucleic acids, and metabolites [13].

Trillions of different bacterial EVs are produced by not only pathogenic bacteria during infections but also by commensal microbiota communities that are colonized in various niches of a normal human body, particularly mucosa [14]. These nanosized bacterial vesicles act as major mediators in host-bacterial interactions by transporting different molecules, which contribute to physiological and pathophysiological processes [15–17]. Remarkably, bacteria-derived EVs are involved in interbacterial interactions [18, 19]. Additionally, these vesicles may be transferred to different organs of the host via systemic circulation to promote communication under homeostatic or pathogenic conditions [20]. Although the definitive role of bacterial EVs in affecting homeostatic and pathological conditions of the host is not yet fully understood, there is increasingly evidence supporting this connection [1].

Bacterial EVs are extensively studied *in vitro* using cell line cultures isolated from a mixture of vesicles released by different types of bacteria or from a specific microorganism. Since bacterial EVs are similar to eukaryote-derived EVs in size, it is difficult to differentiate them based on size alone [21]. Besides, the size and composition of bacterial EVs can vary drastically, depending on the growth conditions and type of strain (even within the same species) [22–24]. Moreover, knowledge of specific markers present specifically on bacterial EVs is limited. Generally, lack of a standardized methodology for purification and isolation of bacterial EVs is one of the major limitations, deterring progress in this field [21]. This lack of knowledge of specific EV markers and EV cargos, as well as EV biogenesis, is an important challenge for clinical researchers [6, 25]. Also, the evaluation of the understanding of different possible functions of bacterial EVs presents even a greater challenge. Despite limited knowledge about these bioactive molecules as compared to eukaryotic EVs, studies on bacterial EVs are continuously increasing as the possible protective or adverse effects of bacterial EVs in interbacterial and host-bacterial interactions has engendered great research interest. Therefore, this review article is aimed at addressing the current status of research on bacterial EVs by focusing on their role in host-bacterial interactions that affect host homeostasis and pathogenesis. Overall, the knowledge of the pertinent mechanisms for the above relationships may lead to the development of new therapeutics and diagnostics using bacterial EVs.

## 2. Subcategories of Bacterial Derivative Vesicles

Bacterial EVs are typically stable vesicles, which can be classified into several subcategories based on differences in the bacterial cell wall structure, Gram-positive or Gram-negative bacteria. The characteristics of different types of bacterial EVs are shown in Table 1. A peptidoglycan-rich cell wall is found in Gram-positive bacteria, while in Gram-negative bacteria, the outer and inner membranes contain lipopolysaccharides (LPS). Therefore, the biogenesis of vesicles derived from Gram-positive and Gram-negative bacteria is probably different. Although no single mechanism of bacterial EV release has been identified, one model suggests that Gram-negative bacteria randomly release EVs as side products of normal cellular processes related to the cell wall turnover. During this recycling process, the outer membrane budding and subsequent OMV formation can result from the loss of interaction between the outer membrane and peptidoglycans. Various routes can weaken this latter interaction to form OMVs. For example, imbalanced turnover of peptidoglycans, accumulation of phospholipids, and diacylation of lipid-A in LPS can induce OMV blebbing. The other mechanisms include intercalation of hydrophobic substrates such as antibiotics and bacterial signaling molecules into the outer membrane and the shedding of membrane blebs from flagella. Shedding of membrane blebs from the flagella is a unique mechanism based on the alteration of membrane-sheathed flagella by which OMVs are released when the flagella are rotating [26]. Structurally, OMVs derived from Gram-negative bacteria contain LPS [17, 27]. Moreover, a structural change in LPS may lead to membrane deformation and bacterial EV shedding [28]. Therefore, it is recognized as a major route of LPS release and inflammation induction can occur without bacterial killing [29]. It is also important to consider that the release of LPS does not constantly trigger inflammatory responses as this feature is dependent on the LPS type, including proinflammatory LPS (P-LPS) or anti-inflammatory LPS (A-LPS). P-LPS is often present in pathogenic bacteria, inducing strong proinflammatory responses, septic shock, and even death, as traditionally described. On the other hand, A-LPS is mainly formed by certain commensal microbiota, inducing antagonistic activity to inhibit proinflammatory responses [30]. The biological activity of P-LPS is associated with differential immune activation by various bacterial species, while the basic structure and chemical properties are generally similar. Interestingly, the functional difference between various LPS is affected by structural variations of O-antigen and lipid A (number of phosphate groups, number, and length of acryl chains) [31].

In a stricter clarification of bacterial EVs, some Gram-negative bacteria release a different type of EV, called inner membrane vesicles (IMVs). IMVs are formed by fissioning the protrusion of the outer and plasma membranes and entrapping the cytoplasm components. The outer IMVs (O-IMVs) are also formed as double-layered EVs, originating from cytoplasmic turgor pressure and containing most DNA fragments of Gram-negative bacteria. O-IMVs are also frequent products of weakening of the peptidoglycan layer by hydrolysis and protruding of the inner membrane into the periplasm. In this manner, cytoplasmic content such as DNA fragments are packed into O-IMVs. In addition, formation of Gram-negative bacterial EVs that are highly

Table 1: The characteristics of different types of bacterial EVs.

| Bacterial EV type | Derived from Gram-positive/Gram-negative bacteria | Derived from viable cells/cells lysis | Origination characteristics |
|---|---|---|---|
| OMV[1] | Gram-negative | Viable cells | Formed from outer membranes by budding/containing LPS, periplasmatic and cytosolic proteins, RNA and DNA, and virulence factors/A specialized bacterial secretion pathway |
| IMV[2] | Gram-negative | Viable cells | Formed by fission of a protrusion of the outer and plasma membranes |
| O-IMV[3] | Gram-negative | Viable cells/cells lysis | Formed as double bilayer EVs by cytoplasmic turgor pressure (frequently after cell lysis) which originally contain most DNA fragments and cytoplasmic contents |
| EOMV[4] | Gram-negative | Cells lysis | Formed by reassemble of membrane fragments after cell lysis and explodes/containing most DNA fragments and cytoplasmic contents |
| TSMS[5] | Gram-positive/Gram-negative | Viable cells | Formed from outer membranes in Gram-negative bacteria and unable to transfer cytoplasmic contents/formed from cytoplasmic membranes in Gram-positive bacteria and able to transfer cytoplasmic contents/an intercellular connection between neighboring cells to facilitate cellular components exchange |
| CMV[6]/microvesicle | Gram-positive | Viable cells/cells lysis | Formed by pressure, blebbing, or cell lysis from the cell wall |
| Bacterial EV derived by phage endolysin-triggered cell lysis | Gram-positive/Gram-negative | Cells lysis | Formed by enzymatic action that lyse the origin cells by phages |
| Bacterial EV derived from "hot spot" regions | Gram-positive/Gram-negative | Viable cells | Formed from specific regions that locally enriched with specific lipids and proteins involved in hypervesiculation |
| Bacterial EV derived under specific conditions | Gram-positive/Gram-negative | Viable cells/cells lysis | Formed by induced extended turgor pressure, membrane protuberances, and pinching-off of small membrane portions after accumulation of peptidoglycan or misfolded proteins in the periplasm/release of additional potential proteins into the extracellular space to combat stressors and survive |

[1]Outer membrane vesicles, [2]inner membrane vesicles, [3]outer-inner membrane vesicles, [4]explosive outer membrane vesicles, [5]tube-shaped membranous structures, and [6]cytoplasmic membrane vesicles.

contained by cytoplasmic content and DNA fragments could be mediated through explosive cell lysis. Once cell lysis is triggered and peptidoglycan is degraded, the cell explodes and the devastated cell envelope fragments round up and reassemble into "explosive outer membrane vesicles" (EOMVs) that enclose the released DNA fragments [12]. In addition, tube-shaped membranous structures (TSMSs) have been recently introduced as a particular type of bacterial EV, protruding from the cell surface of Gram-negative or Gram-positive bacteria. TSMSs are often involved in the formation of intercellular connections between neighboring cells to facilitate the exchange of various cellular components. The difference between these tube-like structures in Gram-negative and Gram-positive bacteria depends on their origin membrane and, consequently, transfer of different components. In Gram-negative bacteria, TSMSs originate from the outer membrane, which enables the intercellular transfer of membrane proteins, periplasmic metabolites, and lipids, but not cytoplasmic content. On the other hand, in Ggram-positive bacteria, the TSMSs are derived from the cytoplasmic membrane and exchange various cytoplasmic content, such as proteins and plasmid DNAs. Cytoplasmic microvesicles (CMVs) are another specific type of Gram-positive bacterial EVs. It was previously assumed that EVs cannot be released through the thick cell wall of Gram-positive bacteria. However, the formation of EVs has been indicated to occur via pressure through pores in the cell wall, a conservative blebbing mechanism from the cell membrane, or by degradation of the cell wall of Gram-positive bacteria [12, 32]. Some proteins, such as peptidoglycan-degrading enzymes, phenol-soluble modulins, and autolysins, increase the cell membrane fluidity and facilitate CMV release [9, 33, 34]. Generally, the formation of different EVs by both Gram-positive and Gram-negative bacteria is based on two principal processes, namely, shedding from living cells and endolysin-triggered cell lysis [12]. The shedding of bacterial EVs from living cells is an active metabolic process in constantly living cells, while endolysin-triggered cell lysis is based on the enzymatic activity that enables the lysis of original cells. During this process, double-stranded DNA phages lyse their host cells until phage progeny can be released; consequently, the shattered membrane fragments round up and self-assemble into EVs [12].

The profiles of bacterial EVs and the original bacterial membrane fractions do not necessarily match, as some specific cargos may be actively sorted into bacterial EVs [35]. In models of active biogenesis of bacterial EVs, the vesiculation of EVs mainly occurs in distinct areas of the cell membrane, known as "hot spots." These specific regions are locally enriched with specific lipids and proteins involved in hypervesiculation, while vesiculation inhibitory proteins, such as lipoproteins needed for cell wall integrity, are reduced [1, 36]. Also, some proteins affect vesiculation by deleting genes involved in EV formation. Nevertheless, the active biogenesis of bacterial EVs is not still fully understood, and different bacterial strains possibly use different vesiculation mechanisms [37, 38]. The fission of formed vesicles, as the final vesiculation step, is an active process that requires energy, while there is no energy source in the periplasm; therefore, it seems that conformational changes of the outer membrane proteins are involved [36]. The continuous folding of outer membrane proteins and their conformational changes provide the required energy for vesiculation.

The biogenesis of bacterial EVs can vary under specific conditions, which can affect their properties. Changes in temperature, nutrients, and stress exposure are some of these above conditions [1]. EVs are released from pathogens that encounter numerous stressors during colonization [39]. Antibiotic agents may even stimulate EV shedding through various mechanisms, depending on the antibiotic [12]. Also, several environmental stressors, such as nutrient deficiency, oxidative stress, UV radiation, pH changes, heat shock stress, osmotic pressure, hydration, and desiccation, as well as the host immune system, increase EV shedding [39]. Under these latter conditions, peptidoglycans or misfolded proteins accumulate excessively in the periplasm through the effects of physical or chemical stress-induced malfunctioning membranes. This phenomenon increases turgor pressure, membrane protuberances, and pinching-off of small membrane portions [40]. Through this mechanism, bacteria can release additional proteins into the extracellular space to combat stressors and survive [1].

Differences in bacterial EVs go beyond the cell wall structure and may also depend on their compositional differences (related to the bacterial cell origin). The EV components may include lipids and proteins (toxins and enzymes), causing differences in EV functionality [41]. As described earlier, the cargo composition of bacterial EVs is not usually similar to the bacterial origin, and specific cargos can be actively sorted within them [35]. The high plurality of bacterial EVs and the lack of universal or common markers for all bacterial EVs may be related to the diversity of bacterial origins [42]; even in cultures with similar conditions, different bacterial EVs can be identified, which is a puzzling phenomenon [43]. A consequential difference between bacterial EVs, which is particularly important for studying their interactions with various cells, is based on the commensal or pathogenic bacterial origin [6, 21]. The study of bacterial EVs has focused mainly on Gram-negative pathogenic bacteria, while the mechanisms regulating the EV release under homeostatic and pathogenic conditions remains hypothetical. A problem with bacterial EVs is difficulty understanding their primary acute or chronic functional biological properties [17]. In the following sections, the importance of commensal or pathogenic bacterial EVs in host-bacterial and interbacterial interactions to maintain homeostasis or in the development of pathogenesis of the host will be highlighted.

## 3. The Importance of Bacterial EVs in Host-Bacterial Dialogues

As mentioned earlier, bacterial EVs involve interactions between bacteria and host cells. Since the community of commensal or pathogenic bacteria and their metabolites can directly or indirectly induce positive or negative host health effects, the derived EVs are also critical to maintaining homeostasis or pathogenesis (Figure 1). There are several mechanisms involved in the uptake (Figure 2) and effects of EVs on the immune system. Briefly, the mechanisms of interactions between bacterial EVs and host cells include EV interactions with the host receptors, delivery of EV cargos to the host cell, and full incorporation of EVs into the host cell cytoplasm [6]. Several mechanisms, including endocytosis, phagocytosis, micropinocytosis, internalization through lipid rafts, direct membrane fusion, and ligand-receptor interactions, have been proposed for the uptake of EVs [17, 44]. Moreover, Toll-like receptors (TLRs) and NOD-like receptors (NLRs) are critical pattern recognition receptors (PRRs), involved in direct host-bacterial interactions through bacterial EVs [45]. The involvement of TLR2 in the internalization process of EVs derived from *Moraxella catarrhalis* and *Mycobacterium* in epithelial cells has been established [46, 47]. The interaction of *Bifidobacterium* and *Lactobacillus*-derived EVs with dendritic cells enhances TLR2/1 and TLR4 responses [48]. Similarly, cellular LPS-binding proteins (LBPs) are important in picking up bacterial EVs exposing LPS [49].

Abundant evidence has confirmed the effects of pathogen-derived EVs in host-bacterial interactions to facilitate the interaction of pathogens with their hosts by acting as intermediates, inducing pathogenic protection and host immunomodulation as extracellular virulence factors [50–53]. Bacterial EVs can also act as an effective secretory and delivery system to transfer various molecules to bacteria and host cells, regardless of the physicochemical structure [53]. These vesicles also function as a delivery system to transfer various virulence factors, including degradative enzymes and toxins, possibly leading to immunosuppression [54]. The released EVs from *Staphylococcus aureus* stimulate proinflammatory cytokines and facilitate immune responses [50]. *Clostridium perfringens*-derived EVs increase interleukin- (IL-) 6, tumor necrosis factor- (TNF-) $\alpha$, and granulocyte colony-stimulating factor (G-CSF) expression to stimulate inflammation [55]. The released EVs during infection with mycobacterial species stimulate TLR2, TLR4, and Myd88-dependent signaling pathways to induce IL-12 and TNF-$\alpha$ production involved in proinflammatory responses [56].

In contrast, EVs derived from commensal microbiota have benefits for host-bacterial interactions, such as inhibition of pathogenic colonization and regulation of immune

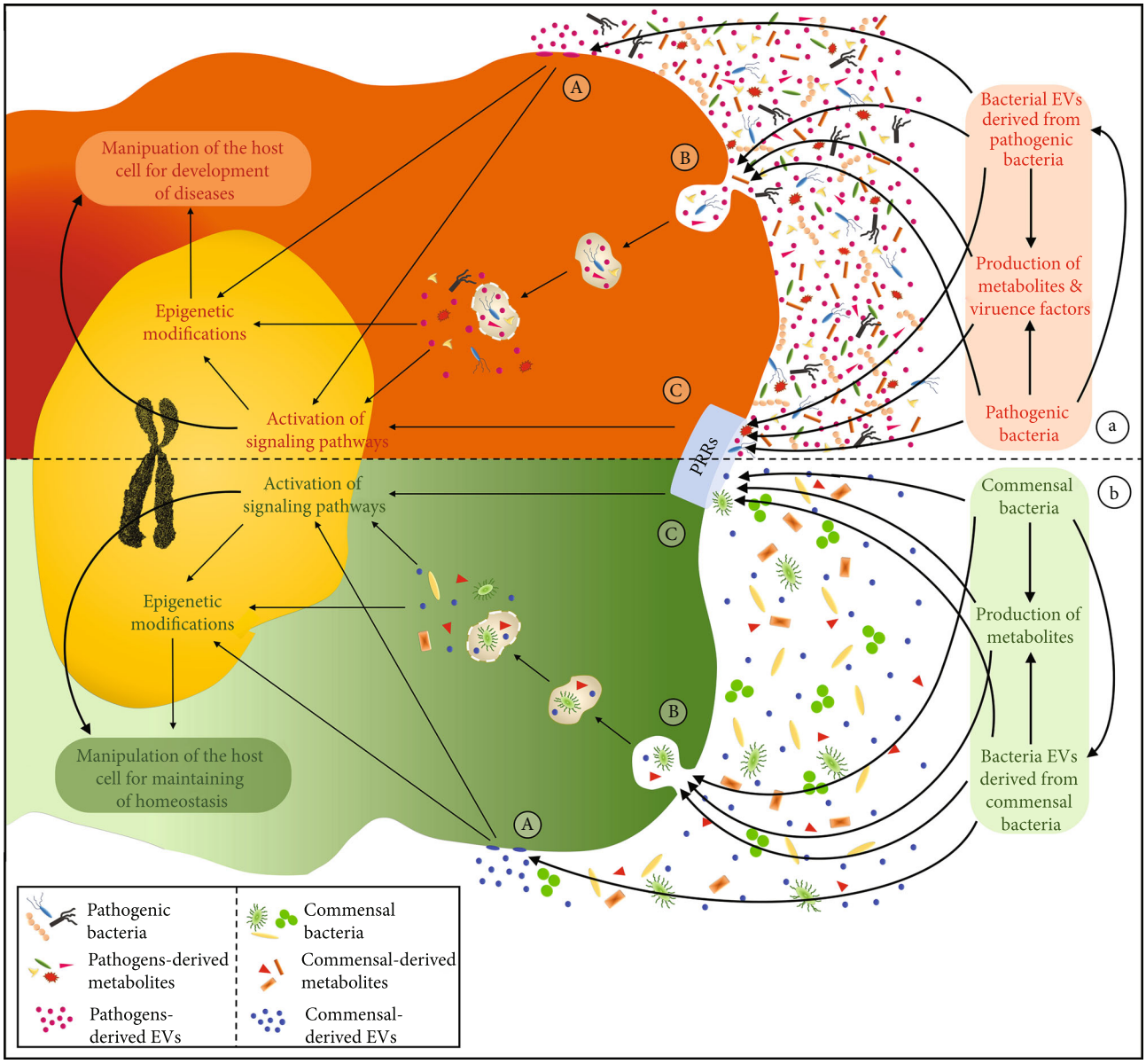


Figure 1: The schematic comparison of pathogenic or commensal bacterial EV importance in host-bacterial interactions to develop homeostasis or pathogenesis conditions. (a, A, b, A) Fusion of pathogenic or commensal bacterial EV with host cell membrane. Direct release of components in the cytoplasm and impact on signaling pathways or epigenetic modifications may develop pathogenesis or homeostasis conditions. (a, B, b, B) Direct entrance of pathogenic or commensal bacteria, their metabolites, or derived EVs to the host cell. Impact of such bacteria, metabolites, or components of bacterial EVs on signaling pathways or epigenetic modifications may also develop pathogenesis or homeostasis conditions. (a, C, b, C) Activation of PRRs by pathogenic or commensal bacteria, their metabolites, or derived EVs. Activation of PRRs to stimulate signaling pathways may directly develop pathogenesis or homeostasis conditions or indirectly develop such conditions by epigenetic modifications. Three main mechanisms of uptake of bacterial EVs by host cells are indicated in Figure 2 in details.

system responses. Under hemostatic conditions, bacterial EVs derived from the commensal microbiota community are prominent, leading to the suppression of pathogenic colonization [21]. Mounting evidence suggests the immunomodulatory and anti-inflammatory roles of commensal EVs [57, 58]. EVs released from *Akkermansia muciniphila* inhibit the production of IL-6 during colitis [59]. Also, *Bacteroides fragilis*-derived EVs, carrying polysaccharide A, are sensed by TLR2 in intestinal immune cells. Besides, *Bacteroides thetaiotaomicron*-derived EVs containing hydrolytic enzymes improve digestion by sharing these components [60].

Despite the beneficial effects of these commensal EVs, they may also disrupt host-bacterial interactions, as they can transfer virulence factors, such as antibiotic resistance genes, to pathogenic bacteria [61]. For instance, *Bacteroides thetaiotaomicron* and several other *Bacteroides* species, as a major part of the gut microbiota, encode $\beta$-lactamase. On the other hand, the produced bacterial EVs contain $\beta$-lactamases that can enhance cefotaxime resistance in both

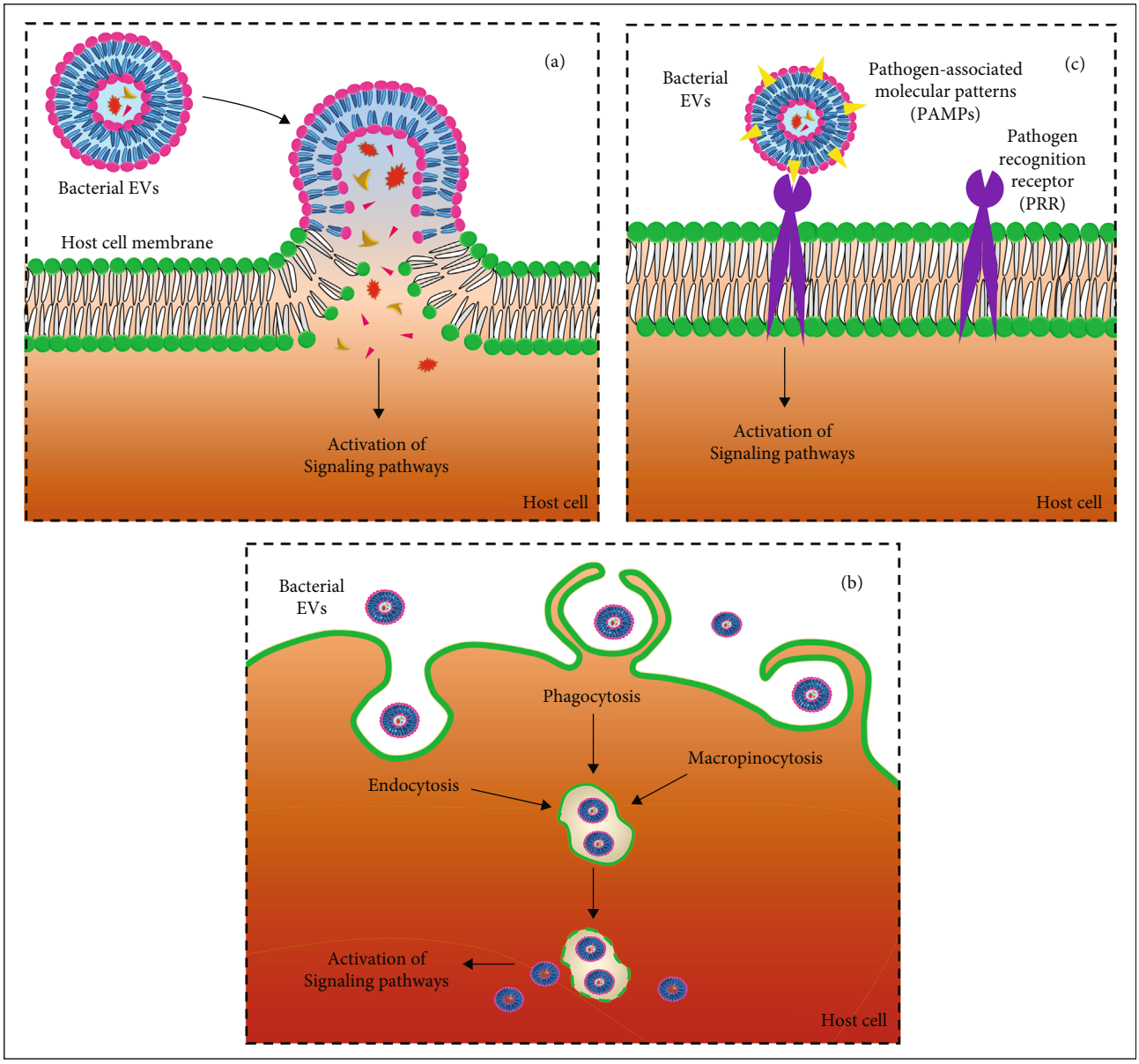


Figure 2: Three main mechanisms of EV uptake by host cells in schematic. (a) Delivery of bacterial EV contents into the host cell by direct membrane fusion or lipid rafts. (b) Direct entrance of bacterial EVs by endocytosis, phagocytosis, or micropinocytosis. (c) Ligand-receptor interaction. The order of mechanisms is in parallel to Figure 1.

commensal (such as *B. breve*) and pathogenic bacteria (such as *Salmonella typhimurium*). Therefore, the production of bacterial EVs by commensal microbiota may positively affect not only commensal microbiota but also pathogenic bacteria [61]. Overall, shedding of bacterial EVs depends on the bacteria or host cell type producing heterogenic EVs regarding size, content, and composition of EV cargos, which may ultimately affect the host immune response [5]. Various exogenous and endogenous factors can impair the composition of commensal microbiota, such as dysbiosis induction and increased colonization of pathogens and so the production of bacterial EVs may change accordingly. Abnormal bacterial EVs may facilitate host pathologies via interactions with host cells or by affecting the normal microbiota composition. There is growing evidence that bacterial EVs from dysbiotic microbiota can cross the altered epithelial barrier and enter systemic or lymphatic circulation to gain access to distant tissues and interact with immune cells in the body [62]. In this manner, bacterial EVs may interact with various axes in the body.

## 4. The Importance of Bacterial EVs in Various Axes

Mucosal and epithelial barriers in the tissues and organs represent a significant defense line to protect against harmful external stimuli. These host barriers are derived from epithelial and endothelial cells, organized by various tight junction

proteins, along with other supporting structures that maintain their integrity [63]. Disruptions in these host barrier structures have been implicated in various disorders. While several factors influence the host barrier, recently, there has been a growing interest in the role of gut bacteria-derived EVs in regulating the barrier integrity, which plays an important role in various axes of the body. In that regard, bacterial EVs have been observed in human plasma and cerebrospinal fluid [62]. Several studies have confirmed the importance of bacterial EVs in the gut-brain, gut-liver, and gut-lung axes [64–66]. Therefore, the effects of bacterial EVs on epithelial differentiation and integrity in various axes of the human body are of particular interest. It has been reported that EVs released from *Vibrio cholerae* stimulate gene expression in association with epithelial cell differentiation [67]. Likewise, isolated EVs from some commensal *Escherichia coli* strains, such as EcN and ECOR63, upregulate the tight junction proteins claudin-14 and zonula occludens- (ZO-) 1 and downregulate claudin-2 (a leaky protein) [68]. The epithelial barrier is responsible for suppressing leaky gut and endotoxemia that lead to inflammation. As described earlier, in addition to the effects of bacterial EVs on epithelial differentiation and integrity, their ability to transfer to different organs via systemic circulation has attracted the research attention [20]. Different axes, especially the gut-brain and gut-liver axes, have been proposed to promote communication in the human body under homeostatic or pathogenic conditions by transferring bacterial EVs from their origin to other organs.

Three probable mechanisms are indicated to be used by bacterial EVs to penetrate into the target and distant organs [69]. The transfer of bacterial EVs from their origin to the target organ, by directly crossing epithelial and endothelial barriers, is one of the possible mechanisms. The crosstransfer of bacterial EVs through the blood-brain barrier has been also confirmed. Different bacteria may translocate to various organs via circulation and release their EVs in the target organs; this process is the second transfer mechanism. The final possible mechanism involves the infection of immune cells by bacterial EVs in the origin organ and transfer by infected cells to the target organs. This mechanism may be similar to the defined "Trojan horse" transfer of bacteria to escape unfavorable conditions and immune system responses [70]. Some studies have highlighted the importance of bacterial EVs in different organs. A previous study confirmed the biological effect of *A. muciniphila*-derived EVs on the enhancement of serotonin production in the colon and hippocampus of mouse models and Caco-2 cell lines [64]. A similar study established that treatment of *Faecalibacterium prausnitzii* and *A. muciniphila*-derived EVs affected the expression of genes involved in serotonin release in the Caco-2 cell line [71]. Moreover, EVs from *Bacillus subtilis* were shown to be transported across Caco-2 cells to be secreted at the opposite cell surface side [72]. Besides, the positive effects of *A. muciniphila*-derived EVs on the attenuation of inflammatory cytokine expression and subsequent prevention of liver fibrosis has been described [65]. Moreover, the efficiency of EVs derived from *A. muciniphila* has been established in restoring the barrier integrity, lipid metabolism, modulation of obesity, and promotion of homeostasis [73]. The improvement of various disorders, such as metabolic diseases, cancers, gastrointestinal, mental, and psychiatric disorders, by prescription of bacterial EVs and microbiota manipulation via diet has been postulated [69, 74, 75]. Regarding the important effects of bacterial EVs on different bidirectional axes, further studies are needed to unravel novel therapeutic processes in various disorders to restore homeostasis.

Considering the putative effective roles of bacterial EVs, any changes in their production can affect their host interactions. It has been confirmed that pathogenic bacteria release significantly more EVs compared to commensal microbiota [76]. Undeniably, the infection type (acute or chronic) is important in the efficiency of bacterial EVs. Acute infectious pathogens rapidly colonize, proliferate, and spread in the host, whereas chronic infectious pathogens proliferate and spread less rapidly, cause long-term infections, and may persist for longer periods [77]. This phenomenon is of great significance in chronic infections, where persistent pathogens can release significantly more EVs during infection, thereby manipulating the host cells for immune evasion, survival, and persistence [78].

## 5. The Importance of Bacterial EVs in Epigenetic Modifications

The evaluation of the importance of bacterial EVs in host-bacterial interactions is multifaceted, and there are still many vague aspects. Recently, an interkingdom crosstalk was established between host and bacterial cells through epigenetic modifications by bacterial EVs (Figure 1). It is obvious that the induced epigenetic modifications by bacterial EVs and their components are more intricate than they first appeared. Interestingly, such vesicles may package noncoding RNAs, as well as other components, which can function as epigenetic regulators in the recipient host cells [79]. Noncoding RNAs, such as microRNAs, are among these epigenetic modifications. Evidence suggests that some bacteria, such as *Streptococcus mutans* and *E. coli*, produce vesicles containing microRNA-like molecules that may impair the "eukaryotic miRNA machinery" to their favor [80, 81]. Also, further evaluation of *E. coli* and *V. cholerae* revealed that RNA is a component of many bacterial EVs and highlighted the potential role of RNA-containing bacterial EVs in the host-bacterial interactions [82]. It is well-established that various bacterial EV components are aligned with histone proteins (such as H3K4Me1, H3K4Me3, and H3K27Ac), chromatin-modifying enzymes, transcription factors, or constitute ribonucleoprotein complexes in host cells for epigenetic regulation [79].

The homeostatic and pathological conditions caused by epigenetic interactions of commensal microbiota or pathogenic bacterial EVs with eukaryotic genomes are not fully understood. Bacterial EVs preserve these fragile cargos against degradation by enzymes and are responsible for selecting host cells [1]. Indirect epigenetic modifications and chromatin accessibility of promoters and transcription start sites (TSSs) of genes (by stimulating bacterial EVs)

are associated with commensal microbiota *E. coli* and pathogenic *V. cholerae* in coculturing with colorectal carcinoma cells [67]. Global 5-methylcytosine (5mC) hypermethylation has been also observed in the salivary samples of periodontitis patients, induced by significantly increased levels of EVs from periodontal pathogens (*Porphyromonas gingivalis*, *Fusobacterium nucleatum*, *Eikenella corrodens*, and *Treponema denticola*) [83]. Likewise, salivary bacterial EVs seem to be associated with DNA methylation in IL-8, IL-6, IL-10, IL-1$\beta$, and TNF-$\alpha$ gene promoters in gingivitis patients [84]. Moreover, the transfer and delivery of methyltransferases (DNMT1, DNMT3A, and DNMT3B) by eukaryotic EVs and gene expression regulation through alteration of DNA methylation have been confirmed in the literature [85]. Therefore, bacterial EVs may carry various cell fragments from their origin as epigenome regulators. This host-bacterial interaction supports long-distance bacteria-derived vehicles that may potentially control the host cell response, depending on the tendency of operating bacteria, commensal microbiota, or pathogenic bacteria. These bacterial vesicles may affect epigenetic modifications not only in the host-bacterial interactions but also in interbacterial dialogues that warrant more attention.

## 6. The Importance of Bacterial EVs in Interbacterial Dialogues

Regarding the host-bacterial interactions, bacterial EVs are involved in the interactions of bacterial communities. A complex interaction has been established between commensal or pathogenic bacterial communities and the released bacterial EVs, as an important contributor to different bacterial interactions or competition strategies [86]. The specific bacterial EV cargo components may be also responsible for a particular EV function in the bacterial community, such as antibiotic resistance, biofilm formation, quorum sensing, and virulence factors [17, 87, 88]. These functions of EVs have been reported in both commensal microbiota and pathogenic communities to meet specific goals and increase their survival [20]. Bacterial EVs mediate antibiotic resistance by facilitating horizontal gene transfer, trapping antimicrobial agents, and carrying related enzymes to suppress antibiotic activities. For instance, some carbapenem-resistant strains of *Acinetobacter baumannii* may release EVs containing OXA-24 carbapenemase gene to horizontally transfer carbapenem resistance to other susceptible strains [89]. This horizontal gene transfer is not only a delivery system in bacterial communities but also a way to protect DNA against degradation under environmental stress [90]. The induction of antibiotic resistance may be also induced by trapping of antimicrobial agents in the EV compartments to survive longer in the microbial community. Some studies have confirmed the longer survival of bacteria producing EVs compared to their wild-type counterparts under antibiotic exposure [91, 92]. *S. aureus* and *Haemophilus influenzae*-derived EVs transfer $\beta$-lactamase to protect *S. epidermis*, *E. coli*, *S. enterica*, and group A streptococci against ampicillin and amoxicillin activities in the bacterial community [25, 93]. Similarly, *Bacteroides* species, as predominant genera in the gut microbiota, produces EVs containing cephalosporinases to induce $\beta$-lactam resistance [61]. Also, EVs carrying the related enzymes are involved in bacterial protection against possible inactivation [94]. In *M. catarrhalis*, $\beta$-lactamase packaging in EVs suppresses neutralization by serum IgG [95].

Additionally, numerous components of biofilm matrices (such as alkaline protease, PrpL, and CdrA), quorum-sensing molecules (such as quinolines and lactones), toxins and degradative enzymes, and virulence factors (such as alkaline phosphatase, phospholipase C, lipase, and serine protease) may be carried by bacterial EVs to communicate and coordinate the bacterial community activities [96–98]; carrying such molecules and enzymes can increase the killing of competing bacteria, bacterial invasion, and bacterial adhesion [41, 99, 100]. The extraction of anthrax toxin from the released *Bacillus anthracis*-derived EVs confirms this finding [101]. However, further studies are needed to fully understand the importance of bacterial EVs in interbacterial dialogues.

## 7. Bacterial EV Applications

Although many functions of bacterial EVs have not been elucidated, various properties of bacterial EVs in host-bacterial and interbacterial dialogues modulate defensive or pathogenic functions of EVs. Moreover, bacterial vesicles can be applied to maintain and improve homeostatic conditions. Generally, bacterial EVs are a different type of non-classical secretory systems with more advanced functions than only the transfer of some cargos to the target sites [1]. In other words, treatment with commensal microbiota-derived EVs for different disorders may further induce the beneficial effects of normal microbiota, as confirmed in leaky gut syndrome [102]. Several beneficial members of commensal microbiota have been introduced into the market as "probiotics," because of their effects on refining homeostasis [103]. It has been proposed that the derived EVs can mediate the effectiveness of probiotic bacteria, while decreasing the safety concerns and potential risks of consuming living bacteria, as they are nonreplicating [104]. Therefore, such potential activity can also appear in bacterial EVs and introduced them as "postbiotics." The ability of bacterial EVs to pass through epithelial, endothelial, and blood-brain barriers has highlighted the potential advantages of these delivery molecules in targeted therapy of various infections, diseases, and disorders, especially the gut-brain axis disorders, such as psychopathic disorders [69]. In this regard, application of bacterial EVs has been suggested for the treatment of some disorders such as ulcers caused by *Helicobacter pylori* and inflammatory bowel disease (IBD) [104]. The fundamental functions of these EVs may be associated with their properties as direct and targeted antigen delivery vectors [73]. Therefore, researchers have focused on bacterial EVs as a new biotechnology tool, particularly in cancer treatment.

As mentioned earlier, bacterial EVs mimic their origin cell structure and also contain different immunostimulatory molecules, which have been identified and taken up by immune cells to stimulate immune responses that are

beneficial for tumor treatment. In that regard, these nano-sized bacterial structures can accumulate in tumors to stimulate and gain local immunity through enhanced permeation and retention effects [105]. The potential of manipulated bacterial EVs is to selectively target tumor cells that may be a novel and specific EV-based therapy [106]. Also, targeting human epidermal growth factor receptor 2 (HER2), which is frequently present in tumor cells, is one of the most important approaches to reduce the tumor burden by manipulating *E. coli*-derived EVs to transfer antitumor components [107]. Bacterial EVs are also directly involved in cancer therapies by altering the microenvironment surrounding the tumor cells. These derived vesicles are specifically involved in extracellular signaling. The administration of bacterial EVs derived from *S. aureus*, *S. enterica*, and *L. acidophilus* can stimulate the expression of tumor-suppressor genes and activate anti-tumor immune responses in tumor tissues [108]. Likewise, bacterial EVs have been introduced as smart vehicles for targeted drug delivery in fundamental biological research. Bacterial EVs are simple targeted delivery systems, which can be coated with targeting ligands by genetically engineering the origin bacteria. Therefore, drug accumulation is facilitated at the target site.

Additionally, bacterial EVs can passively accumulate in tumor sites through enhanced permeation and retention effects because of their size, which is essential for drug delivery to the tumor site. Also, bacterial EVs act as drug delivery vehicles, where the loaded drug protects against denaturation and degradation until reaching the target site. Finally, bacterial EVs as drug delivery vehicles may be known as "foreign" agents, eliciting inflammatory responses and causing diverse effects in the body. Accordingly, detoxified bacterial EVs are suggested to diminish reactogenicity, inflammatory responses, and self-damage; the safety of these bacterial EVs has been confirmed in a mouse model [109, 110].

On the other hand, bacterial EVs can be easily identified and taken up by neutrophils. In other words, circulating neutrophils can be used as cellular carriers to transport bacterial EVs for targeted drug delivery [111]. Overall, advances in the use of bacterial EVs in drug delivery systems have increased their potential clinical applications. Regarding the characteristics of bacterial EVs, with delivery of a sublethal dose of antibiotics, *A. baumannii* infection was successfully treated with the fewest indiscriminate side effects in the commensal microbiota in a mouse model [112]. Also, these effective bacterial vectors can be applied in the direct codelivery of antigens and adjuvants to host cells. Bacterial EVs are suitable adjuvants that induce immune responses to target antigens through different approaches. Three main examples of these approaches include genetic engineering of bacteria to express the target antigens, loading of target antigens on surfaces or in bacterial EVs, and mixing with the target antigens. Following immunization, bacterial EV adjuvants initiate more robust immune responses in terms of quality and quantity as compared to immunization with only purified proteins and antigens [105]. Generally, adjuvants play a role in increasing antigen presentation and uptake, antigen delivery to lymph nodes, and direct stimulation of immunity [113].

Bacterial EVs have been also introduced as a novel vaccine delivery technology to trigger long-lasting and robust immune responses [114]. A vaccine must at least contain the target antigens and several pathogen-associated molecular patterns (PAMPs) and have an appropriate size comparable to the pathogen. Interestingly, bacterial EVs simultaneously have all of the three properties described above [105, 115]. The released EVs from some bacterial species, present in the commensal microbiota or pathogenic bacterial community, may act as a permanent natural vaccine by triggering both innate and adaptive immune responses [57, 116]. For instance, the EVs isolated from *Neisseria meningitidis*, *A. baumannii*, *S. pneumoniae*, *B. anthracis*, and even *M. tuberculosis* can induce a protective immune response to inhibit the development of infection [21, 116]. To date, the administration of only one bacterial EV-based vaccine (MeNZB vaccine) has been approved for human use [117]. MeNZB vaccine has been effectively and safely implemented to combat meningococcal serotype B disease, caused by *N. meningitides*, to control the disease epidemic in New Zealand [118].

Primarily, bacterial EVs are used as adjuvants to trigger an immune response to meningitis B vaccine. They can also deliver some antigens, especially to the target pathogens, such as PorA [119, 120]. PorA is highly variable between different *N. meningitidis* strains and has been introduced as the main immunogenic protein in EVs. Therefore, immunization with bacterial EV vaccines is strain-specific, and use of single strain-derived EVs can restrict vaccine application in an epidemic triggered by several strains. Depending on the need, bacterial EV-based vaccines containing multivalent PorA have been established using the released EVs from bioengineered *N. meningitidis* strains, including multiple *PorA* genes [121, 122]. Along with porins, other minor proteins in bacterial EVs also induce pathogen-specific immunization [123]. Apart from the bacterial EV vaccination approved for *N. meningitidis*, similar vaccines against other pathogens such as *H. pylori*, *S. typhimurium*, *V. cholera*, and *Shigella flexneri* have been evaluated in animal models, as well; however, none of them have been approved for clinical trials [124, 125]. It is predicted that a multitude of vaccines based on bacterial EVs, with low toxicity and high efficiency, will be developed in future clinical trials [105]. Besides, control of the particle properties of EV-based vaccines may improve their immunization effects. During the immunization process, maturation of dendritic cells and presentation of antigens in lymph nodes are crucial for provoking a strong antigen-specific immune response. This immunization process can be modulated by the properties of vaccine particles, such as their size, rigidity, and shape [126]. The size of vaccine particles determines their trafficking mode from the site of administration to the lymph nodes. Vaccine particles with a size of 20-100 nm are mainly transferred to lymph nodes through lymphatic circulation, and larger particles are differently encapsulated and carried to lymph nodes by antigen-presenting cells [127]. Since the properties of synthetic nanoparticles are finely adjustable, nanoparticle-based

bacterial EV vaccines can provoke a more robust antigen-specific immune response. Some examples of nanoparticle-based vaccines include coated bacterial EVs onto gold nanoparticles (BM-AuNPs), coated bacterial EVs onto bovine serum albumin nanoparticles (BN-EVs), and loading bacterial EVs into nanoparticles (NP-EVs), which are more stable and stronger immunostimulants than pure bacterial EVs [128–130]. Overall, different types of nanoparticles show different properties, and selection of the finest nanoparticles can augment the immunization of bacterial EV-based vaccines.

On the other hand, due to EV extraction from bacteria and their structural similarity, these components may act as decoys against bacteriophages. Bacteriophages may bind to LPS and be neutralized. This phenomenon decreases the potential efficacy of bacterial EVs and, subsequently, reduces their therapeutic efficacy. Some electron microscopy evidence confirms this finding for *E. coli*, *Salmonella*, and *V. cholera* [131, 132]. Some strategies have been suggested to overcome this limitation. The first strategy is concealing bacterial EVs with antifouling agents, such as poly(ethylene glycol), to reduce their immunological recognition by inhibiting protein binding [109]. The second strategy is to use complement system inhibitors to improve bacterial EV detection by the host cells. Such inhibitors are coated on the EV surface or administered before EV inoculation [133, 134]. The final approach is mimicking biological systems that may be potentially useful to evade recognition by immune cells. It seems that preparation of a hybrid membrane covered with bacterial EVs, along with some host cell membranes, such as platelets, leukocytes, and red blood cells is possible [135, 136].

Additionally, bacterial EVs mimic a bacterial structure to competitively bind to the target cells and suppress adhesion and infection caused by the main pathogens. Initiation of various infections is often induced by bacterial adhesion to target cells; therefore, antiadhesion therapies can decelerate the progression of infection [137, 138]. On the other hand, nonadhering infectious agents are recognized and neutralized more efficiently by immune cells [139]. Due to the presence of various intact bacterial adhesions on the EVs, these vesicles can be useful in antiadhesion therapies.

In the literature, the blockade of *H. pylori* adhesion to gastric epithelial cells has been reported by application of *H. pylori*-derived EVs [140]. Today, the potential applications of bacterial EVs, besides their known traditional applications, are being clarified. For example, use of these bioactive molecules in biosensing and biomedical imaging applications is becoming an interesting topic in biotechnology sciences [141]. Overall, the application of bacterial EVs is far more extensive and needs to be investigated in various contexts.

## 8. Conclusion

The current knowledge of bacterial EVs is very limited considering the vast spectrum of bacterial EVs in host-bacterial and interbacterial interactions, and further research is warranted. The investigation of bacterial EVs under different homeostatic and pathogenic conditions can also resolve many problems concerning host susceptibility. The importance of EVs derived from bacterial cells, associated with bacterial infection types and acute/chronic infections, has been also recently highlighted.

Overall, shedding of EVs is related to the adjustment of bacterial populations to unfavorable or changing conditions and controls the interaction of bacteria with their host cells and other bacteria. The ability of bacterial EVs to pass through epithelial, endothelial, and blood-brain barriers emphasizes the potential advantages of these delivery molecules in the targeted therapy of various infections, diseases, and disorders. Some bacterial EVs even engage in a mechanism of epigenetic modification, antibiotic resistance, and immune escape strategy. Moreover, the evaluation of EVs from commensal bacteria or different pathogens can provide an opportunity to improve personalized medicine in the near future.

## Data Availability

No data were used to support this study.

## Conflicts of Interest

The authors have no relevant affiliations or financial involvement with any organization or entity with a financial interest in or financial conflict with the subject matter discussed in the manuscript. No writing assistance was utilized in the production of this manuscript.

## Acknowledgments

The authors are grateful to the personnel of Mycobacteriology and Pulmonary Research Department, Pasteur Institute of Iran for their assistance in this project. We thank those authors whose deserving research was not cited in this manuscript.

## References

[1] E. Woith, G. Fuhrmann, and M. F. Melzig, "Extracellular vesicles-connecting kingdoms," *International Journal of Molecular Sciences*, vol. 20, no. 22, p. 5695, 2019.

[2] D. Bishop and E. J. B. J. Work, "An extracellular glycolipid produced byEscherichia coligrown under lysine-limiting conditions," *Biochemical Journal*, vol. 96, no. 2, pp. 567–576, 1965.

[3] K. Knox, J. Cullen, and E. J. B. J. Work, "An extracellular lipopolysaccharide-phospholipid-protein complex produced by Escherichia coli grown under lysine-limiting conditions," *Biochemical Journal*, vol. 103, no. 1, pp. 192–201, 1967.

[4] H. A. Bladen and J. F. Waters, "Electron microscopic study of some strains of bacteroides," *Journal of Bacteriology*, vol. 86, no. 6, pp. 1339–1344, 1963.

[5] N. Spencer and L. Yeruva, "Role of bacterial infections in extracellular vesicles release and impact on immune response," *Biomedical Journal*, vol. 44, no. 2, pp. 157–164, 2021.

[6] Y. Liu, K. A. Y. Defourny, E. J. Smid, and T. Abee, "Gram-positive bacterial extracellular vesicles and their impact on health and disease," *Frontiers in Microbiology*, vol. 9, 2018.

[7] L. Brown, A. Kessler, P. Cabezas-Sanchez, J. L. Luque-Garcia, and A. Casadevall, "Extracellular vesicles produced by the Gram-positive bacteriumBacillus subtilisare disrupted by the lipopeptide surfactin," *Molecular Microbiology*, vol. 93, no. 1, pp. 183–198, 2014.

[8] L. Turnbull, M. Toyofuku, A. L. Hynen et al., "Explosive cell lysis as a mechanism for the biogenesis of bacterial membrane vesicles and biofilms," *Nature Communications*, vol. 7, no. 1, pp. 1–13, 2016.

[9] M. Toyofuku, G. Cárcamo-Oyarce, T. Yamamoto et al., "Prophage-triggered membrane vesicle formation through peptidoglycan damage in Bacillus subtilis," *Nature Communications*, vol. 8, no. 1, 2017.

[10] C. Pérez-Cruz, L. Delgado, C. López-Iglesias, and E. Mercade, "Outer-inner membrane vesicles naturally secreted by Gram-negative pathogenic bacteria," *PLOS ONE*, vol. 10, no. 1, article e0116896, 2015.

[11] X. Wei, C. N. Vassallo, D. T. Pathak, and D. Wall, "Myxobacteria produce outer membrane-enclosed tubes in unstructured environments," *Journal of Bacteriology*, vol. 196, no. 10, pp. 1807–1814, 2014.

[12] M. Toyofuku, N. Nomura, and L. Eberl, "Types and origins of bacterial membrane vesicles," *Nature Reviews Microbiology*, vol. 17, no. 1, pp. 13–24, 2019.

[13] M. I. Ramirez and A. J. M. I. Marcilla, "Pathogens and extracellular vesicles: new paths and challenges to understanding and treating diseases," *Molecular Immunology*, vol. 139, pp. 155-156, 2021.

[14] R. Sender, S. Fuchs, and R. Milo, "Revised estimates for the number of human and bacteria cells in the body," *PLOS Biology*, vol. 14, no. 8, article e1002533, 2016.

[15] A. Sheikh, J. Taube, and K. L. Greathouse, "Contribution of the microbiota and their secretory products to inflammation and colorectal cancer pathogenesis: the role of Toll-like receptors," *Carcinogenesis*, vol. 42, no. 9, pp. 1133–1142, 2021.

[16] M. Wang, Y. Nie, and X.-. L. Wu, "Membrane vesicles from a Dietzia bacterium containing multiple cargoes and their roles in iron delivery," *Environmental Microbiology*, vol. 23, no. 2, pp. 1009–1019, 2021.

[17] R. A. Ñahui Palomino, C. Vanpouille, P. E. Costantini, and L. Margolis, "Microbiota–host communications: Bacterial extracellular vesicles as a common language," *PLOS Pathogens*, vol. 17, no. 5, article e1009508, 2021.

[18] L. Kern, S. K. Abdeen, A. A. Kolodziejczyk, and E. Elinav, "Commensal inter-bacterial interactions shaping the microbiota," *Current Opinion in Microbiology*, vol. 63, pp. 158–171, 2021.

[19] E. Nudleman, D. Wall, and D. J. S. Kaiser, "Cell-to-cell transfer of bacterial outer membrane lipoproteins," *Science*, vol. 309, no. 5731, pp. 125–127, 2005.

[20] M. Muraca, L. Putignani, A. Fierabracci, A. Teti, and G. Perilongo, "Gut microbiota-derived outer membrane vesicles: under-recognized major players in health and disease?," *Discovery Medicine*, vol. 19, no. 106, pp. 343–348, 2015.

[21] L. Macia, R. Nanan, E. Hosseini-Beheshti, and G. E. Grau, "Host- and microbiota-derived extracellular vesicles, immune function, and disease development," *International Journal of Molecular Sciences*, vol. 21, no. 1, 2020.

[22] J.-H. Kim, E.-J. Jeun, C.-P. Hong et al., "Extracellular vesicle-derived protein from Bifidobacterium longum_ alleviates food allergy through mast cell suppression," *Journal of Allergy and Clinical Immunology*, vol. 137, no. 2, pp. 507–516.e8, 2016.

[23] H. Taboada, N. Meneses, M. F. Dunn et al., "Proteins in the periplasmic space and outer membrane vesicles of Rhizobium etli CE3 grown in minimal medium are largely distinct and change with growth phase," *Microbiology*, vol. 165, no. 6, pp. 638–650, 2019.

[24] T. Wagner, B. Joshi, J. Janice et al., "Enterococcus faecium produces membrane vesicles containing virulence factors and antimicrobial resistance related proteins," *Journal of Proteomics*, vol. 187, pp. 28–38, 2018.

[25] J. Lee, E.-Y. Lee, S.-H. Kim et al., "Staphylococcus aureus extracellular vesicles carry biologically active $\beta$-lactamase," *Antimicrobial Agents and Chemotherapy*, vol. 57, no. 6, pp. 2589–2595, 2013.

[26] M.-S. Aschtgen, J. B. Lynch, E. Koch, J. Schwartzman, M. McFall-Ngai, and E. Ruby, "Rotation of Vibrio fischeri flagella produces outer membrane vesicles that induce host development," *Journal of Bacteriology*, vol. 198, no. 16, pp. 2156–2165, 2016.

[27] A. J. McBroom, A. P. Johnson, S. Vemulapalli, and M. J. Kuehn, "Outer membrane vesicle production by Escherichia coli is independent of membrane instability," *Journal of Bacteriology*, vol. 188, no. 15, pp. 5385–5392, 2006.

[28] W. Elhenawy, M. Bording-Jorgensen, E. Valguarnera, M. F. Haurat, E. Wine, and M. F. Feldman, "LPS remodeling triggers formation of outer membrane vesicles in Salmonella," *mBio*, vol. 7, no. 4, 2016.

[29] Y. Gao, J. Lee, G. Widmalm, and W. Im, "Modeling and simulation of bacterial outer membranes with lipopolysaccharides and enterobacterial common antigen," *The Journal of Physical Chemistry B*, vol. 124, no. 28, pp. 5948–5956, 2020.

[30] T.-L. Lin, C.-C. Shu, Y.-M. Chen et al., "Like cures like: pharmacological activity of anti-inflammatory lipopolysaccharides from gut microbiome," *Frontiers in Pharmacology*, vol. 11, 2020.

[31] L. Mazgaeen and P. Gurung, "Recent advances in lipopolysaccharide recognition systems," *International Journal of Molecular Sciences*, vol. 21, no. 2, p. 379, 2020.

[32] P. Briaud and R. K. J. I. Carroll, "Extracellular vesicle biogenesis and functions in gram-positive bacteria," *Infection and Immunity*, vol. 88, no. 12, 2020.

[33] P. Briaud and R. K. Carroll, "The mechanism behind bacterial lipoprotein release: phenol-soluble modulins mediate Toll-like receptor 2 activation via extracellular vesicle release from Staphylococcus aureus," *Infection and Immunity*, vol. 9, no. 6, 2018.

[34] X. Wang, C. D. Thompson, C. Weidenmaier, and J. C. Lee, "Release of Staphylococcus aureus extracellular vesicles and their application as a vaccine platform," *Nature Communications*, vol. 9, no. 1, pp. 1–13, 2018.

[35] C. Schwechheimer, C. J. Sullivan, and M. J. Kuehn, "Envelope control of outer membrane vesicle production in Gram-negative bacteria," *Biochemistry*, vol. 52, no. 18, pp. 3031–3040, 2013.

[36] A. Kulp and M. J. Kuehn, "Biological functions and biogenesis of secreted bacterial outer membrane vesicles," *Annual Review of Microbiology*, vol. 64, pp. 163–184, 2010.

[37] S. Roier, D. R. Leitner, J. Iwashkiw et al., "Correction: iimmunization with nontypeable Haemophilus influenzae outer membrane vesicles induces cross-protective immunity in mice," *PLoS ONE*, vol. 7, no. 8, 2012.

[38] R. A. Ñahui Palomino, C. Vanpouille, L. Laghi et al., "Extracellular vesicles from symbiotic vaginal lactobacilli inhibit HIV-1 infection of human tissues," *Nature Communications*, vol. 10, no. 1, 2019.

[39] N. Mozaheb and M.-P. Mingeot-Leclercq, "Membrane vesicle production as a bacterial defense against stress," *Frontiers in Microbiology*, vol. 11, 2020.

[40] A. J. McBroom and M. J. Kuehn, "Release of outer membrane vesicles by Gram-negative bacteria is a novel envelope stress response," *Molecular Microbiology*, vol. 63, no. 2, pp. 545–558, 2007.

[41] J. H. Kim, "Gram-negative and Gram-positive bacterial extracellular vesicles," in *Seminars in Cell & Developmental Biology*, Elsevier, 2015.

[42] N. Orench-Rivera and M. J. Kuehn, "Environmentally controlled bacterial vesicle-mediated export," *Cellular Microbiology*, vol. 18, no. 11, pp. 1525–1536, 2016.

[43] P. D. Singorenko, V. Chang, A. Whitcombe et al., "Isolation of membrane vesicles from prokaryotes: a technical and biological comparison reveals heterogeneity," *Journal of Extracellular Vesicles*, vol. 6, no. 1, 2017.

[44] E. A. Taha, K. Ono, and T. Eguchi, "Roles of extracellular HSPs as biomarkers in immune surveillance and immune evasion," *International Journal of Molecular Sciences*, vol. 20, no. 18, 2019.

[45] S. A. Badi, A. Moshiri, A. Fateh et al., "Microbiota-derived extracellular vesicles as new systemic regulators," *Frontiers in Microbiology*, vol. 8, 2017.

[46] V. Schaar, S. P. W. de Vries, M. L. A. Perez Vidakovics et al., "Multicomponent Moraxella catarrhalis outer membrane vesicles induce an inflammatory response and are internalized by human epithelial cells," *Cellular Microbiology*, vol. 13, no. 3, pp. 432–449, 2011.

[47] A. Palacios, S. Gupta, G. M. Rodriguez, and R. Prados-Rosales, "Extracellular vesicles in the context of Mycobacterium tuberculosis infection," *Molecular Immunology*, vol. 133, pp. 175–181, 2021.

[48] J. van Bergenhenegouwen, A. D. Kraneveld, L. Rutten, N. Kettelarij, J. Garssen, and A. P. Vos, "Extracellular vesicles modulate host-microbe responses by altering TLR2 activity and phagocytosis," *PLoS ONE*, vol. 9, no. 2, article e89121, 2014.

[49] M. Toyofuku, Y. Tashiro, Y. Hasegawa, M. Kurosawa, and N. Nomura, "Bacterial membrane vesicles, an overlooked environmental colloid: biology, environmental perspectives and applications," *Advances in Colloid and Interface Science*, vol. 226, pp. 65–77, 2015.

[50] N. R. Tartaglia, K. Breyne, E. Meyer et al., "Staphylococcus aureus extracellular vesicles elicit an immunostimulatory response in vivo on the murine mammary gland," *Frontiers in Cellular and Infection Microbiology*, vol. 8, 2018.

[51] H. Y. Kim, Y. Lim, S.-. J. An, and B.-. K. Choi, "Characterization and immunostimulatory activity of extracellular vesicles from Filifactor alocis," *Molecular Oral Microbiology*, vol. 35, 2020.

[52] Z. Yin, J. Fan, J. Xu et al., "Immunoregulatory roles of extracellular vesicles and associated therapeutic applications in lung cancer," *Frontiers in Immunology*, vol. 11, 2020.

[53] A. Guerrero-Mandujano, C. Hernández-Cortez, J. A. Ibarra, and G. Castro-Escarpulli, "The outer membrane vesicles: secretion system type zero," *Traffic*, vol. 18, no. 7, pp. 425–432, 2017.

[54] I. A. MacDonald and M. J. Kuehn, "Offense and defense: microbial membrane vesicles play both ways," *Research in Microbiology*, vol. 163, no. 9-10, pp. 607–618, 2012.

[55] Y. Jiang, Q. Kong, K. L. Roland, and R. Curtiss, "Membrane vesicles of Clostridium perfringens type A strains induce innate and adaptive immunity," *International Journal of Medical Microbiology*, vol. 304, no. 3-4, pp. 431–443, 2014.

[56] P. P. Singh, V. L. Smith, P. C. Karakousis, and J. S. Schorey, "Exosomes isolated from mycobacteria-infected mice or cultured macrophages can recruit and activate immune cells in vitro and in vivo," *The Journal of Immunology*, vol. 189, no. 2, pp. 777–785, 2012.

[57] M. Sandkvist, E. Cascales, and P. J. Christie, "Outer membrane vesicle-host cell interactions," *Microbiology Spectrum*, vol. 7, no. 1, 2019.

[58] J. C. Caruana and S. A. Walper, "Bacterial membrane vesicles as mediators of microbe–microbe and microbe–host community interactions," *Frontiers in Microbiology*, vol. 11, 2020.

[59] C.-S. Kang, M. Ban, E.-J. Choi et al., "Extracellular vesicles derived from gut microbiota, especially Akkermansia muciniphila, protect the progression of dextran sulfate sodium-induced colitis," *Plos One*, vol. 8, no. 10, article e76520, 2013.

[60] L. E. Comstock, "Importance of glycans to the host-bacteroides mutualism in the mammalian intestine," *Cell Host & Microbe*, vol. 5, no. 6, pp. 522–526, 2009.

[61] R. Stentz, N. Horn, K. Cross et al., "Cephalosporinases associated with outer membrane vesicles released by Bacteroides spp. protect gut pathogens and commensals against $\beta$-lactam antibiotics," *Journal of Antimicrobial Chemotherapy*, vol. 70, no. 3, pp. 701–709, 2015.

[62] J. Tulkens, G. Vergauwen, J. Van Deun et al., "Increased levels of systemic LPS-positive bacterial extracellular vesicles in patients with intestinal barrier dysfunction," *Gut*, vol. 69, no. 1, pp. 191–193, 2020.

[63] Y. J. N. Bhattarai, "Microbiota-gut-brain axis: Interaction of gut microbes and their metabolites with host epithelial barriers," *Neurogastroenterology & Motility*, vol. 30, no. 6, article e13366, 2018.

[64] R. Yaghoubfar, A. Behrouzi, F. Ashrafian et al., "Modulation of serotonin signaling/metabolism by Akkermansia muciniphila and its extracellular vesicles through the gut-brain axis in mice," *Scientific Reports*, vol. 10, no. 1, pp. 1–12, 2020.

[65] S. K. A. Raftar, F. Ashrafian, A. Yadegar et al., "The protective effects of live and pasteurized Akkermansia muciniphila and its extracellular vesicles against HFD/CCl4-induced liver Injury," *Microbiology Spectrum*, vol. 9, no. 2, 2021.

[66] B. Jafari, R. A. K. Nejad, F. Vaziri, and S. D. Siadat, "Evaluation of the effects of extracellular vesicles derived from Faecalibacterium prausnitzii on lung cancer cell line," *Biologia*, vol. 74, no. 7, pp. 889–898, 2019.

[67] S. Vdovikova, S. Gilfillan, S. Wang, M. Dongre, S. N. Wai, and A. Hurtado, "Modulation of gene transcription and epigenetics of colon carcinoma cells by bacterial membrane vesicles," *Scientific Reports*, vol. 8, 2018.

[68] C.-S. Alvarez, J. Badia, M. Bosch, R. Giménez, and L. Baldomà, "Outer membrane vesicles and soluble factors released by probiotic Escherichia coli Nissle 1917 and commensal ECOR63 enhance barrier function by regulating expression of tight junction proteins in intestinal epithelial cells.," *Frontiers in Microbiology*, vol. 7, 2016.

[69] C. M. Cuesta, C. Guerri, J. Ureña, and M. Pascual, "Role of microbiota-derived extracellular vesicles in gut-brain communication," *International Journal of Molecular Sciences*, vol. 22, no. 8, 2021.

[70] M. Rodrigues, J. Fan, C. Lyon, M. Wan, and Y. Hu, "Role of extracellular vesicles in viral and bacterial infections: pathogenesis, diagnostics, and therapeutics," *Theranostics*, vol. 8, no. 10, pp. 2709–2721, 2018.

[71] R. Yaghoubfar, A. Behrouzi, E. Zare Banadkoki et al., "Effect of Akkermansia muciniphila, Faecalibacterium prausnitzii, and their extracellular vesicles on the serotonin system in intestinal epithelial cells," *Probiotics and Antimicrobial Proteins*, vol. 13, no. 6, pp. 1546–1556, 2021.

[72] A. P. D. Rubio, J. Martínez, M. Palavecino et al., "Transcytosis of Bacillus subtilis extracellular vesicles through an in vitro intestinal epithelial cell model," *Scientific Reports*, vol. 10, no. 1, 2020.

[73] F. Ashrafian, A. Shahriary, A. Behrouzi et al., "Akkermansia muciniphila-derived extracellular vesicles as a mucosal delivery vector for amelioration of obesity in mice.," *Frontiers in Microbiology*, vol. 10, p. 2155, 2019.

[74] Y. Chen, Y. Xu, H. Zhong et al., "Extracellular vesicles in inter-kingdom communication in gastrointestinal cancer," *American Journal of Cancer Research*, vol. 11, no. 4, pp. 1087–1103, 2021.

[75] A. Chronopoulos and R. J. O. Kalluri, "Emerging role of bacterial extracellular vesicles in cancer," *Oncogene*, vol. 39, no. 46, pp. 6951–6960, 2020.

[76] N. B. Zakharzhevskaya, A. A. Vanyushkina, I. A. Altukhov et al., "Outer membrane vesicles secreted by pathogenic and nonpathogenic Bacteroides fragilis represent different metabolic activities," *Scientific Reports*, vol. 7, no. 1, pp. 1–16, 2017.

[77] S. Furukawa, S. Kuchma, and G. A. O'toole, "Keeping their options open: acute versus persistent infections," *Journal of Bacteriology*, vol. 188, no. 4, pp. 1211–1217, 2006.

[78] M. Villares, J. Berthelet, and J. B. Weitzman, "The clever strategies used by intracellular parasites to hijack host gene expression," *In Seminars in Immunopathology*, vol. 42, no. 2, pp. 215–226, 2020.

[79] A. Celluzzi and A. Masotti, "How our other genome controls our epi-genome," *Trends in Microbiology*, vol. 24, no. 10, pp. 777–787, 2016.

[80] S.-M. Kang, J. W. Choi, Y. Lee, S. H. Hong, and H. J. Lee, "Identification of microRNA-size, small RNAs in Escherichia coli," *Curr Microbiol*, vol. 67, no. 5, pp. 609–613, 2013.

[81] H.-J. Lee and S. H. Hong, "Analysis of microRNA-size, small RNAs in Streptococcus mutans by deep sequencing," *FEMS Microbiology Letters*, vol. 326, no. 2, pp. 131–136, 2012.

[82] A. E. Sjöström, L. Sandblad, B. E. Uhlin, and S. N. Wai, "Membrane vesicle-mediated release of bacterial RNA," *RNA*, vol. 5, no. 1, pp. 1–10, 2015.

[83] P. Han, P. M. Bartold, C. Salomon, and S. Ivanovski, "Salivary outer membrane vesicles and DNA methylation of small extracellular vesicles as biomarkers for periodontal status: a pilot study," *Int J Mol Sci*, vol. 22, no. 5, p. 2423, 2021.

[84] P. Han, A. Lai, C. Salomon, and S. Ivanovski, "Detection of salivary small extracellular vesicles associated inflammatory cytokines gene methylation in gingivitis," *Int J Mol Sci*, vol. 21, no. 15, p. 5273, 2020.

[85] D. A. Dakhlallah, J. Wisler, M. Gencheva et al., "Circulating extracellular vesicle content revealsde novoDNA methyltransferase expression as a molecular method to predict septic shock," *J Extracell Vesicles*, vol. 8, no. 1, p. 1669881, 2019.

[86] R. M. Stubbendieck, C. Vargas-Bautista, and P. D. Straight, "Bacterial communities: interactions to scale," *Frontiers in Microbiology*, vol. 7, p. 1234, 2016.

[87] M. J. Uddin, J. Dawan, G. Jeon, T. Yu, X. He, and J. Ahn, "The role of bacterial membrane vesicles in the dissemination of antibiotic resistance and as promising carriers for therapeutic agent delivery," *Microorganisms*, vol. 8, no. 5, p. 670, 2020.

[88] K. Koeppen, A. Nymon, R. Barnaby et al., "Let-7b-5p in vesicles secreted by human airway cells reduces biofilm formation and increases antibiotic sensitivity of P. aeruginosa," *Proceedings of the National Academy of Sciences*, vol. 118, no. 28, 2021.

[89] C. Rumbo, E. Fernández-Moreira, M. Merino et al., "Horizontal transfer of the OXA-24 carbapenemase gene via outer membrane vesicles: a new mechanism of dissemination of carbapenem resistance genes in Acinetobacter baumannii," *ASM Journals on CD*, vol. 55, no. 7, pp. 3084–3090, 2011.

[90] D. Zocco, S. Bernardi, M. Novelli et al., "Isolation of extracellular vesicles improves the detection of mutant DNA from plasma of metastatic melanoma patients," *Scientific Reports*, vol. 10, no. 1, pp. 1–12, 2020.

[91] E. Kanshin, S. Wang, L. Ashmarina et al., "The stoichiometry of protein phosphorylation in adipocyte lipid droplets: analysis by N-terminal isotope tagging and enzymatic dephosphorylation," *Proteomics Clinical Applications*, vol. 9, no. 22, pp. 5067–5077, 2009.

[92] A. J. Manning and M. J. Kuehn, "Contribution of bacterial outer membrane vesicles to innate bacterial defense," *BMC Microbiology*, vol. 11, no. 1, pp. 1–15, 2011.

[93] V. Schaar, I. Uddback, T. Nordstrom, and K. Riesbeck, "Group A streptococci are protected from amoxicillin-mediated killing by vesicles containing lactamase derived from Haemophilus influenzae," *J Antimicrob Chemother*, vol. 69, no. 1, pp. 117–120, 2014.

[94] N. J. Alves, K. B. Turner, I. L. Medintz, and S. A. Walper, "Protecting enzymatic function through directed packaging into bacterial outer membrane vesicles," *Scientific Reports*, vol. 6, no. 1, pp. 1–10, 2016.

[95] V. Schaar, M. Paulsson, M. Morgelin, and K. Riesbeck, "Outer membrane vesicles shield Moraxella catarrhalis lactamase from neutralization by serum IgG," *J Antimicrob Chemother*, vol. 68, no. 3, pp. 593–600, 2013.

[96] M. Toyofuku, K. Morinaga, Y. Hashimoto et al., "Membrane vesicle-mediated bacterial communication," *The ISME Journal*, vol. 11, no. 6, pp. 1504–1509, 2017.

[97] C. Rueter and M. Bielaszewska, "Secretion and delivery of intestinal pathogenic Escherichia coli virulence factors via outer membrane vesicles," *Frontiers in Cellular and Infection Microbiology*, vol. 10, p. 91, 2020.

[98] S. R. Schooling and T. J. Beveridge, "Membrane vesicles: an overlooked component of the matrices of biofilms," *Journal of Bacteriology*, vol. 188, no. 16, pp. 5945–5957, 2006.

[99] M. E. Kuipers, C. H. Hokke, and H. H. Smits, "Pathogen-derived extracellular vesicle-associated molecules that affect the host immune system," *Frontiers in Microbiology*, vol. 9, p. 2182, 2018.

[100] X. Chang, S. L. Wang, S. B. Zhao et al., "Extracellular vesicles with possible roles in gut intestinal tract homeostasis and IBD," *Mediators of Inflammation*, vol. 2020, Article ID 1945832, 2020.

[101] L. Abrami, L. Brandi, M. Moayeri et al., "Hijacking multivesicular bodies enables long-term and exosome-mediated long-distance action of anthrax toxin," *Cell Reports*, vol. 5, no. 4, pp. 986–996, 2013.

[102] M. J. Fábrega, L. Aguilera, R. Giménez et al., "Activation of immune and defense responses in the intestinal mucosa by outer membrane vesicles of commensal and probiotic Escherichia coli strains," *Frontiers in Microbiology*, vol. 7, p. 705, 2016.

[103] D. Cheng, J. Song, M. Xie, and D. Song, "The bidirectional relationship between host physiology and microbiota and health benefits of probiotics: a review," *Trends Food Sci Technol*, vol. 91, pp. 426–435, 2019.

[104] J. A. Molina-Tijeras, J. Gálvez, and M. E. J. N. Rodríguez-Cabezas, "The immunomodulatory properties of extracellular vesicles derived from probiotics: a novel approach for the management of gastrointestinal diseases," *Nutrients*, vol. 11, no. 5, p. 1038, 2019.

[105] M. Li, H. Zhou, C. Yang et al., "Bacterial outer membrane vesicles as a platform for biomedical applications: an update," *J Control Release*, vol. 323, pp. 253–268, 2020.

[106] W. J. Gilmore, E. L. Johnston, L. Zavan, N. J. Bitto, and M. Kaparakis-Liaskos, "Immunomodulatory roles and novel applications of bacterial membrane vesicles," *Molecular Immunology*, vol. 134, pp. 72–85, 2021.

[107] A. Nanou, L. L. Zeune, F. C. Bidard, J. Y. Pierga, and L. W. M. M. Terstappen, "HER2 expression on tumor-derived extracellular vesicles and circulating tumor cells in metastatic breast cancer," *BCR*, vol. 22, no. 1, pp. 1–11, 2020.

[108] O. Y. Kim, N. T. H. Dinh, H. T. Park, S. J. Choi, K. Hong, and Y. S. Gho, "Bacterial protoplast-derived nanovesicles for tumor targeted delivery of chemotherapeutics," *Clinical Materials*, vol. 113, pp. 68–79, 2017.

[109] Q. Chen, H. Bai, W. Wu et al., "Bioengineering bacterial vesicle-coated polymeric nanomedicine for enhanced cancer immunotherapy and metastasis prevention," *Nano Letters*, vol. 20, no. 1, pp. 11–21, 2020.

[110] V. Gujrati, S. Kim, S. H. Kim et al., "Bioengineered bacterial outer membrane vesicles as cell-specific drug-delivery vehicles for cancer therapy," *American Chemical Society nano*, vol. 8, no. 2, pp. 1525–1537, 2014.

[111] M. Li, S. Li, H. Zhou et al., "Chemotaxis-driven delivery of nano-pathogenoids for complete eradication of tumors post-phototherapy," *Nature Communications*, vol. 11, no. 1, pp. 1–16, 2020.

[112] W. Huang, Q. Zhang, W. Li et al., "Development of novel nanoantibiotics using an outer membrane vesicle-based drug efflux mechanism," *Journal Control Release*, vol. 317, pp. 1–22, 2020.

[113] S. G. Reed, M. T. Orr, and C. B. Fox, "Key roles of adjuvants in modern vaccines," *Nature Medicine*, vol. 19, no. 12, pp. 1597–1608, 2013.

[114] M. Morishita, M. Horita, A. Higuchi, M. Marui, H. Katsumi, and A. Yamamoto, "Characterizing different probiotic-derived extracellular vesicles as a novel adjuvant for immunotherapy," *Molecular Pharmaceutics*, vol. 18, no. 3, pp. 1080–1092, 2021.

[115] M. F. Bachmann and G. T. J. N. R. I. Jennings, "Vaccine delivery: a matter of size, geometry, kinetics and molecular patterns," *Nature Reviews Immunology*, vol. 10, no. 11, pp. 787–796, 2010.

[116] W. Huang, Q. Zhang, W. Li et al., "Anti-outer membrane vesicle antibodies increase antibiotic sensitivity of pan-drug-resistant Acinetobacter baumannii," *Frontiers in virology*, vol. 10, p. 1379, 2019.

[117] N. J. Bitto and M. Kaparakis-Liaskos, "The therapeutic benefit of bacterial membrane vesicles," *International Journal of Molecular Sciences*, vol. 18, no. 6, p. 1287, 2017.

[118] P. Oster, D. Lennon, J. O'Hallahan, K. Mulholland, S. Reid, and D. Martin, "MeNZB™: a safe and highly immunogenic tailor-made vaccine against the New Zealand Neisseria meningitidis serogroup B disease epidemic strain," *Vaccine*, vol. 23, no. 17-18, pp. 2191–2196, 2005.

[119] O. Koeberling, I. Delany, and D. M. Granoff, "A critical threshold of meningococcal factor H binding protein expression is required for increased breadth of protective antibodies elicited by native outer membrane vesicle vaccines," *Clinical and Vaccine Immunology*, vol. 18, no. 5, pp. 736–742, 2011.

[120] B. van de Waterbeemd, G. P. M. Mommen, J. L. A. Pennings et al., "Quantitative proteomics reveals distinct differences in the protein content of outer membrane vesicle vaccines," *Journal of Proteome Research*, vol. 12, no. 4, pp. 1898–1908, 2013.

[121] C. Peeters, H. C. Rümke, L. C. Sundermann et al., "Phase I clinical trial with a hexavalent PorA containing meningococcal outer membrane vesicle vaccine," *Vaccine*, vol. 14, no. 10, pp. 1009–1015, 1996.

[122] I. Claassen, J. Meylis, P. van der Ley et al., "Production, characterization and control of a Neisseria meningitidis hexavalent class 1 outer membrane protein containing vesicle vaccine," *Vaccine X*, vol. 14, no. 10, pp. 1001–1008, 1996.

[123] J. Holst, D. Martin, R. Arnold et al., "Properties and clinical performance of vaccines containing outer membrane vesicles from Neisseria meningitidis," *Vaccine*, vol. 27, pp. B3–B12, 2009.

[124] A. Camacho, J. de Souza, S. Sánchez-Gómez, M. Pardo-Ros, J. M. Irache, and C. Gamazo, "Mucosal immunization with Shigella flexneri outer membrane vesicles induced protection in mice," *Vaccine*, vol. 29, no. 46, pp. 8222–8229, 2011.

[125] R. Acevedo, A. Callicó, Y. Aranguren et al., "Immune adjuvant effect of V. cholerae O1 derived proteoliposome coadministered by intranasal route with Vi polysaccharide from Salmonella typhi," *Immunology*, vol. 14, no. S1, pp. 1–4, 2013.

[126] N. Benne, J. van Duijn, J. Kuiper, W. Jiskoot, and B. Slütter, "Orchestrating immune responses: how size, shape and rigidity affect the immunogenicity of particulate vaccines," *Journal Control Release*, vol. 234, pp. 124–134, 2016.

[127] T. J. Moyer, A. C. Zmolek, and D. J. Irvine, "Beyond antigens and adjuvants: formulating future vaccines," *The Journal of Clinical Investigation*, vol. 126, no. 3, pp. 799–808, 2016.

[128] L. Zhang, W. Gao, R. H. Fang, and C. M. J. Hu, "Modulating antibacterial immunity via bacterial membrane-coated nanoparticles," 2019, U.S. Patent 10,383,830.

[129] A. Camacho, J. M. Irache, J. de Souza, S. Sánchez-Gómez, and C. Gamazo, "Nanoparticle-based vaccine for mucosal

protection against Shigella flexneri in mice," *Vaccine*, vol. 31, no. 32, pp. 3288–3294, 2013.

[130] C.-M. J. Hu, R. H. Fang, B. T. Luk, and L. Zhang, "Nanoparticle-detained toxins for safe and effective vaccination," *Nat Nanotechnol*, vol. 8, no. 12, pp. 933–938, 2013.

[131] T. Reyes-Robles, R. S. Dillard, L. S. Cairns et al., "Vibrio cholerae outer membrane vesicles inhibit bacteriophage infection," *Journal of Bacteriology*, vol. 200, no. 15, article e00792-17, 2018.

[132] M. S. Stephan, N. K. Broeker, A. Saragliadis, N. Roos, D. Linke, and S. Barbirz, "In vitro analysis of O-antigen-specific bacteriophage P22 inactivation by Salmonella outer membrane vesicles," *Frontiers in Microbiology*, vol. 11, p. 2304, 2020.

[133] S. M. Moghimi and Z. S. J. N. N. Farhangrazi, "Nanomedicine and the complement paradigm," *Biology and Medicine*, vol. 9, no. 4, pp. 458–460, 2013.

[134] J. Szebeni, L. Baranyi, S. Sávay et al., "Complement activation-related cardiac anaphylaxis in pigs: role of C5a anaphylatoxin and adenosine in liposome-induced abnormalities in ECG and heart function," *American Journal of Physiology-Heart and Circulatory Physiology*, vol. 290, no. 3, pp. H1050–H1058, 2006.

[135] D. Dehaini, X. Wei, R. H. Fang et al., "Erythrocyte-platelet hybrid membrane coating for enhanced nanoparticle functionalization," *Advanced Functional Materials*, vol. 29, no. 16, article 1606209, 2017.

[136] D. Wang, H. Dong, M. Li et al., "Erythrocyte–cancer hybrid membrane camouflaged hollow copper sulfide nanoparticles for prolonged circulation life and homotypic-targeting photothermal/chemotherapy of melanoma," *American Chemical Society Nano*, vol. 12, no. 6, pp. 5241–5252, 2018.

[137] C. Berne, C. K. Ellison, A. Ducret, and Y. V. Brun, "Bacterial adhesion at the single-cell level," *Microbiology*, vol. 16, no. 10, pp. 616–627, 2018.

[138] A. Asadi, S. Razavi, M. Talebi, and M. Gholami, "A review on anti-adhesion therapies of bacterial diseases," *Infection*, vol. 47, no. 1, pp. 13–23, 2019.

[139] M. R. Knowles and R. C. Boucher, "Mucus clearance as a primary innate defense mechanism for mammalian airways," *The Journal of Clinical Investigation*, vol. 109, no. 5, pp. 571–577, 2002.

[140] Y. Zhang, Y. Chen, C. Lo et al., "Inhibition of pathogen adhesion by bacterial outer membrane-coated nanoparticles," *Angewandte Chemie International Edition*, vol. 58, no. 33, pp. 11404–11408, 2019.

[141] V. Gujrati, J. Prakash, J. Malekzadeh-Najafabadi et al., "Bioengineered bacterial vesicles as biological nano-heaters for optoacoustic imaging," *Nature Communications*, vol. 10, no. 1, pp. 1–10, 2019.

Hindawi
Journal of Immunology Research
Volume 2022, Article ID 9038808, 9 pages
https://doi.org/10.1155/2022/9038808

*Research Article*

# Urinary Exosomal Long Noncoding RNA TERC as a Noninvasive Diagnostic and Prognostic Biomarker for Bladder Urothelial Carcinoma

**Chen Chen,[1] Anquan Shang,[1] Zujun Sun,[1] Yuting Gao,[1] Jingjuan Huang,[1] Yili Ping,[1] Wenjing Chang,[1] Chenzheng Gu,[1] Junjun Sun,[1] Ping Ji,[1] Yi Yuan,[1] Renquan Lu,[2,3] and Dong Li[1]**

[1]*Department of Laboratory Medicine, Shanghai Tongji Hospital, School of Medicine, Tongji University, Shanghai 200065, China*
[2]*Department of Clinical Laboratory, Fudan University Shanghai Cancer Center, Shanghai, China*
[3]*Department of Oncology, Shanghai Medical College, Fudan University, Shanghai, China*

Correspondence should be addressed to Renquan Lu; renquanlu@fudan.edu.cn and Dong Li; lidong@tongji.edu.cn

Received 1 November 2021; Accepted 23 December 2021; Published 25 January 2022

Academic Editor: Wagner Batista



*Purpose*. Bladder cancer is one of the most common urological malignancies worldwide, and approximately 90% of bladder cancer cases are histologically typed as bladder urothelial carcinoma (BLCA). Exosomes are 30 to 200 nm extracellular vesicles that transport microRNAs, long noncoding RNAs (lncRNAs), mRNAs, circular RNAs, and proteins across tissues and through circulation. Urinary exosomes may contain genetic information from tumor cells. Herein, we explored the clinical significance of urinary exosomal lncRNA telomerase RNA component (*TERC*) levels to provide an urgently needed diagnostic and prognostic biomarker for BLCA. *Materials and Methods*. In this study, we used RNA-sequencing of samples from four BLCA patients and three healthy controls to identify that *TERC* was differentially expressed in urinary exosomes. We then used quantitative PCR in different types of clinical samples to validate the biomarker and analyzed results using receiver operating characteristic curves. *Results*. We found that *TERC* was significantly upregulated in urinary exosomes from BLCA patients compared with those from healthy controls ($P < 0.0001$). Urinary exosomal *TERC* showed higher sensitivity (78.65%) and accuracy (77.78%) than existing indicators including nuclear matrix protein-22 and urine cytometry. Using the cut-off value 4.302, the area under the curve for urinary exosomal *TERC* was 0.836 (95% confidence interval: 0.768–0.891, $P < 0.0001$). Furthermore, this noninvasive assay could distinguish low-grade and high-grade tumors ($P = 0.0153$). *Conclusions*. *TERC* is enriched in urinary exosomes from BLCA patients. Urinary exosomal *TERC* could become a diagnostic and prognostic biomarker for BLCA that allows clinicians to realize noninvasive detection of BLCA.

## 1. Introduction

Globally, bladder cancer is one of the most common urological malignancies, with approximately 90% of cases histologically defined as bladder urothelial carcinoma (BLCA). In 2020, the incidence of bladder cancer ranked tenth among all malignant tumors, and its incidence and mortality ranked second among male urinary system malignancies [1]. The gold standard for diagnosing bladder cancer remains tissue biopsy *via* cystoscopy. The colloidal gold immunochromatographic assay (GICA) for nuclear matrix protein- (NMP-) 22 and bladder tumor antigen are clinical methods approved by the US Food and Drug Administration; however, their sensitivity is too low, and hematuria always leads to false positive results [2–4]. Thus, there is an urgent need for a more meaningful diagnostic index for bladder cancer that balances sensitivity and specificity.

Exosomes are potential diagnostic samples from liquid biopsy because they can transport mRNAs, microRNAs, long noncoding RNAs (lncRNAs), circular RNAs, lipids, and proteins throughout bodily fluids [5, 6]. The exosomal lipid bilayer protects the contents from RNases and

proteases [7]. lncRNAs are defined as transcripts of >200 nucleotides and have been demonstrated to play critical roles in many biological and pathological processes rather than being "transcriptional noise" [8]. It has been reported that exosomes can selectively package certain lncRNAs that are abundantly present in exosomes [9, 10]. BLCA tumor cells continuously release exosomes that contain lncRNAs into urine. Urinary exosomal lncRNAs can directly reflect the malignant state and have the possibility to be diagnostic and prognostic biomarkers for BLCA [11–14].

Using deep RNA-sequencing of urinary exosomes, we found that the lncRNA telomerase RNA component (*TERC*, 451 nt in length) was differently expressed between four BLCA patients and three healthy controls. *TERC* and telomerase reverse transcriptase (TERT) compose telomerase. In most human tumors, telomerase is activated to maintain telomere length, extend lifespan, and reduce apoptosis of tumor cells [15]. Many previous studies have reported the roles of *TERC* in telomere biology and in promoting tumorigenesis and inflammation, but there are still few reports regarding the diagnostic and/or prognostic value of exosomal *TERC* expression [16–19].

## 2. Materials and Methods

*2.1. Patients and Volunteers.* Samples were collected from BLCA patients with histopathologically confirmed diagnosis between October 2019 and May 2021 at Shanghai Tongji Hospital and Fudan University Shanghai Cancer Center. The clinical information of patients is provided in Supplementary File 1. In total, healthy participants were sought. The Ethics Committee of Shanghai Tongji Hospital (No. 2021-KYSB-064) and Fudan University Shanghai Cancer Center (No. 050432-4-1911D) authorized this study.

*2.2. Isolation of Exosomes.* Exosomes for sequencing were isolated from 150 mL of urine using differential centrifugation. The isolation procedure was as follows, taking the supernatant from each step: urine was centrifuged at $600 \times g$ for 20 min, $2000 \times g$ for 30min, and $10000 \times g$ for 1h and then filtered through a 0.22 $\mu$m filter. Finally, ultracentrifugation at $100000 \times g$ for 2h was performed, and the supernatant was discarded. All centrifugation steps were performed at 4°C. Exosome pellets were resuspended in 50 $\mu$L of 0.22 $\mu$m filtered phosphate-buffered saline.

Exosomes used for validation were isolated from human urine in strict accordance with the instructions of the exosome extraction kit (BestBio, Shanghai, China). 8 mL of urine was centrifuged at $3000 \times g$ for 15 min at 4°C, and the supernatant was then centrifuged at $10000 \times g$ for 20 min at 4°C. The supernatant was then mixed with solution A and stored 4°C overnight. The mixture was centrifuged at $10000 \times g$ for 1 h at 4°C and exosome pellets were resuspended in 500 $\mu$L TRIzol-LS (Life Technologies, Carlsbad, CA, USA).

*2.3. Transmission Electron Microscopy (TEM).* Exosome suspensions were placed on 400-mesh carbon-coated copper grids and negatively stained with 2% phosphotungstic acid solution. TEM was performed to view and capture images (Thermo Fisher Scientific, Waltham, MA, USA).

Table 1: Primer sequences are listed in the table.

| | | |
|---|---|---|
| TERC | Forward | 5′-GTGGTGGCCATTTTTTGTCTAAC-3′ |
| | Reverse | 5′-TGCTCTAGAATGAACGGTGGAA-3′ |
| GAPDH | Forward | 5′-TGATGACATCAAGAAGGTGG-3′ |
| | Reverse | 5′-TTGTCATACCAGGAAATGAGC-3′ |
| 18S | Forward | 5′-CGTTCTTAGTTGGTGGAGCG-3′ |
| | Reverse | 5′-CGCTGAGCCAGTCAGTGTAG-3′ |

*2.4. Nanoparticle Tracking Analysis (NTA).* The NanoSight LM10 system (Malvern Instruments Ltd., Malvern, UK) was used to detect the concentration and size distribution of particles.

*2.5. Western Blot Analysis.* Exosome suspensions were mixed with the appropriate volume of 5x SDS loading buffer, the mixture was boiled for 15 min at 100°C, and then, the supernatant was collected for western blot analysis. The primary antibodies included anti-TSG101 (Abcam, Cambridge, UK), anti-HSP70, anti-Annexin V, and anti-CD9 (all from Cell Signaling Technology, Danvers, MA, USA). The secondary antibody used was peroxidase-conjugated goat anti-rabbit IgG (Millipore, Burlington, MA, USA).

*2.6. RNA-Sequencing.* RNA-sequencing (RNA-seq) was performed by Shanghai Kangcheng Biotechnology Company (Shanghai, China) using an Illumina Novaseq 6000 system (San Diego, CA, USA). Differences in transcript levels were analyzed and used to screen out the differentially expressed lncRNAs between the BLCA patient and healthy control groups. The comparison scheme was fold change $> 1.5$, $P$ value ($F$ test) $\leq 0.05$, and mean FPKM $\geq 0.5$ in each sample.

*2.7. RNA Extraction and Real-Time Quantitative PCR (qPCR).* TRIzol-LS reagent was used to extract total exosomal RNA, cDNA was synthesized using the PrimeScript™ RT reagent kit with gDNA Eraser (Takara, Dalian, Japan), and qPCR was performed using the TB Green Premix Ex Taq II (Tli RNaseH Plus) (Takara) on an Applied Biosystems 7300 real-time PCR system (Waltham, MA, USA). Table 1 shows the sequences of primers used in this study.

*2.8. GICA and Enzyme-Linked Immunosorbent Assay (ELISA) Analyses of NMP-22.* Urine exosomal NMP-22 was detected using the Alere NMP22® BladderChek® Test based on GICA and ELISA kits from Hualian Biotechnology (Wuhan, China). The assays were performed in accordance with the kit instructions.

*2.9. Statistical Analysis.* Data are presented as mean ± SD. The Mann–Whitney $U$ test, Pearson's $\chi^2$ test, and Pearson's correlation analysis were used to assess differences or

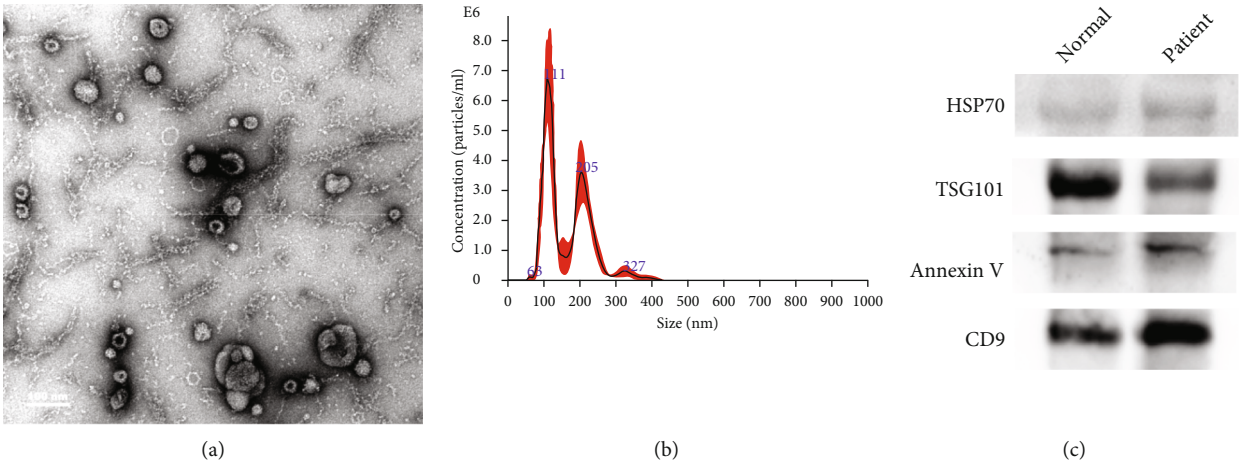


Figure 1: Characterization of urinary exosomes. (a) Transmission electron microscopy image of exosomes isolated from urine; scale bar: 100 nm. (b) Particles were observed in the size range of 50 to 200 nm by nanoparticle tracking analysis. (c) Western blot analysis of the exosomal protein markers HSP70, TSG101, Annexin V, and CD9. Exosomes were derived from healthy controls and bladder urothelial carcinoma patients.

correlation. $P < 0.05$ was considered statistically significant. Receiver operating characteristic (ROC) curves were used to determine the sensitivity and specificity of indicators. All statistical analyses were performed using GraphPad Prism 8 (GraphPad Software, Inc., Sand Diego, CA, USA) and MedCalc version 15.2.2 (MedCalc Software Ltd., Ostend, Belgium). Analysis of Kaplan–Meier survival curves was performed using data from the PrognoScan database for BLCA (GSE13507).

## 3. Results

*3.1. Identification of Exosomes Derived from Urine Samples.* According to the 2018 checklist for minimum information for studies of extracellular vesicles (MISEV2018) [20], we used a combination of TEM, NTA, and western blot analysis to identify exosomes. TEM showed that urinary exosomes were of round shape with cup-like concavity (Figure 1(a)). The size distributions of exosomes were analyzed by NTA. As shown in Figure 1(b), the size (diameter) of urinary exosomes ranged from approximately 50 to 200 nm (mean: 165.2 nm). Positive expression of four exosomal protein markers was confirmed by western blot analysis (Figure 1(c)) including of two cytosolic proteins (TSG101 and Annexin V) and two transmembrane proteins (HSP70 and CD9). Only strictly identified urine exosomes were used for further analysis and research [21].

*3.2. RNA-Sequencing of Urinary Exosomes.* To identify differentially expressed BLCA-specific molecules, we performed RNA-sequencing on urine exosomes from four BLCA patients and three healthy controls [22]. The results revealed 106 differentially expressed lncRNAs between urine exosomes from BLCA patients and healthy donors, among which 103 were upregulated and three were downregulated (Figures 2(a) and 2(b)). Among the upregulated lncRNAs, we found high abundance of *TERC*, which has been previously reported to be related to "tumor growth."

*3.3. Increased TERC Expression in Urine Exosomes from BLCA Patients.* We performed qPCR to evaluate relative *TERC* expression in different types of clinical samples. We found that *18S* levels were more stable and abundant in urinary exosomes than the conventional housekeeping gene *GAPDH* and was more suitable as an internal reference gene for lncRNAs in exosomes. The absolute expression levels of genes are listed in Supplementary File 2. First, we detected *TERC* expression in urine exosomes from the three healthy controls and four BLCA patients used for sequencing (Figure 3(a)). In this small sample, we verified that *TERC* expression was higher in urinary exosomes from BLCA patients than from healthy controls, which was consistent with the RNA-sequencing results.

*TERC* was then detected in urine exosomes from 94 healthy controls, 46 patients with urinary benign lesions, and 128 BLCA patients (Figure 3(c)). The findings suggested that urinary exosomal *TERC* expression in BLCA patients was significantly higher compared with that in healthy controls and patients with urinary benign lesions ($P < 0.0001$), indicating that urinary exosomal *TERC* may have diagnostic value for BLCA. As shown in Figure 3(b), there was no difference between *TERC* expression of tumors ($n = 39$) and that of adjacent tissues ($n = 23$).

*3.4. Urinary Exosomal TERC Had Better Diagnostic Value than NMP-22 (ELISA and GICA) and Urine Cytology.* We examined *TERC* levels in urine exosomes from 89 BLCA patients and 63 healthy controls to determine its diagnostic utility. ROC curve analysis using the cut-off value 4.302 showed that *TERC* was a promising diagnostic biomarker with an area under the curve (AUC) of 0.836 (95% confidence interval [CI]: 0.768–0.891, $P < 0.0001$). The sensitivity and specificity of *TERC* were 78.65% and 77.78%, respectively (Figure 4(a)). Meanwhile, we detected NMP-22 from urine samples using ELISA; the results are listed in Supplementary File 2. The AUC, sensitivity, and specificity of NMP-22 (ELISA) were 0.696 (95% CI: 0.616–0.768, $P <$

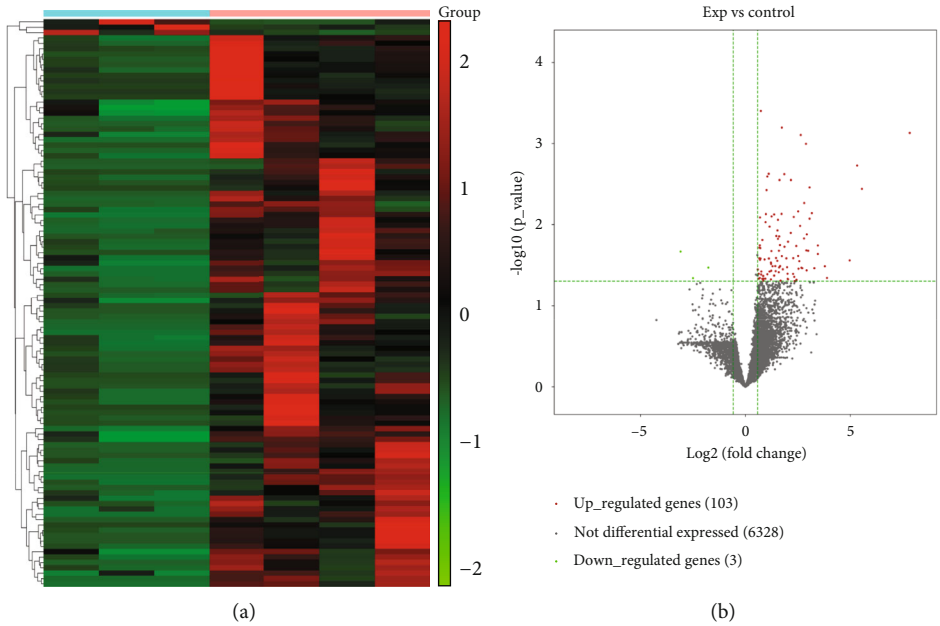


Figure 2: Heat map and volcano plot of differentially expressed long noncoding RNAs (DE-lncRNAs) from urinary exosomes. (a) Heat map of all DE-lncRNAs from urinary exosomes of healthy controls and bladder urothelial carcinoma (BLCA) patients. Results of the differential analysis are shown ($P \leq 0.05$), with color from green to red indicating low to high fragments per kilobase of exon per million mapped fragments (FPKM) of DE-lncRNAs. (b) Volcano plot of RNA-sequencing results. Green dots represent downregulated genes and red dots represent upregulated genes.

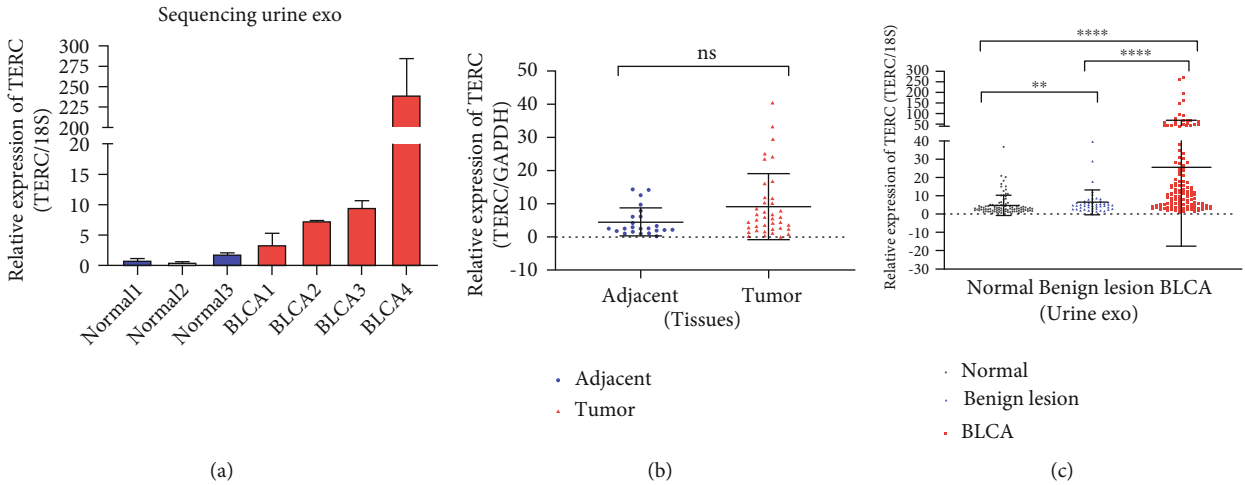


Figure 3: Relative telomerase RNA component (TERC) expression levels in bladder urothelial carcinoma (BLCA) patients. (a) TERC expression levels in urinary exosome samples from the three healthy controls and four BLCA patients used for RNA-sequencing are shown as mean ± SD. (b, c) Real-time quantitative PCR detection of TERC in different sample types including urine exosomes and tissues (ns: $P > 0.05$, $^{**}P < 0.01$, $^{****}P < 0.0001$). Relative expression levels in tissues were normalized to *GAPDH*, while *18S* was used as the internal reference gene in exosomes. Groups were compared with the nonparametric Mann–Whitney *U* test.

0.0001), 60.67%, and 74.6%, respectively (Figure 4(b)). The AUC of combining the indicators reached 0.861 (95% CI: 0.795–0.911) (Figure 4(c)). Additionally, we analyzed NMP-22 (GICA) and urine cytology in 128 patients and 94 healthy controls. The results illustrated the high specificities of NMP-22 (GICA) and urine cytology (96.809% and 98.936%, respectively), but their sensitivities (31.25% and 43.75%, respectively) were much lower than that of urine exosomal *TERC* (78.65%) (Tables 2 and 3). In summary, these results demonstrated that urinary exosomal *TERC* had better diagnostic abilities than the existing indicators (NMP-22 [ELISA and GICA] and urine cytology).

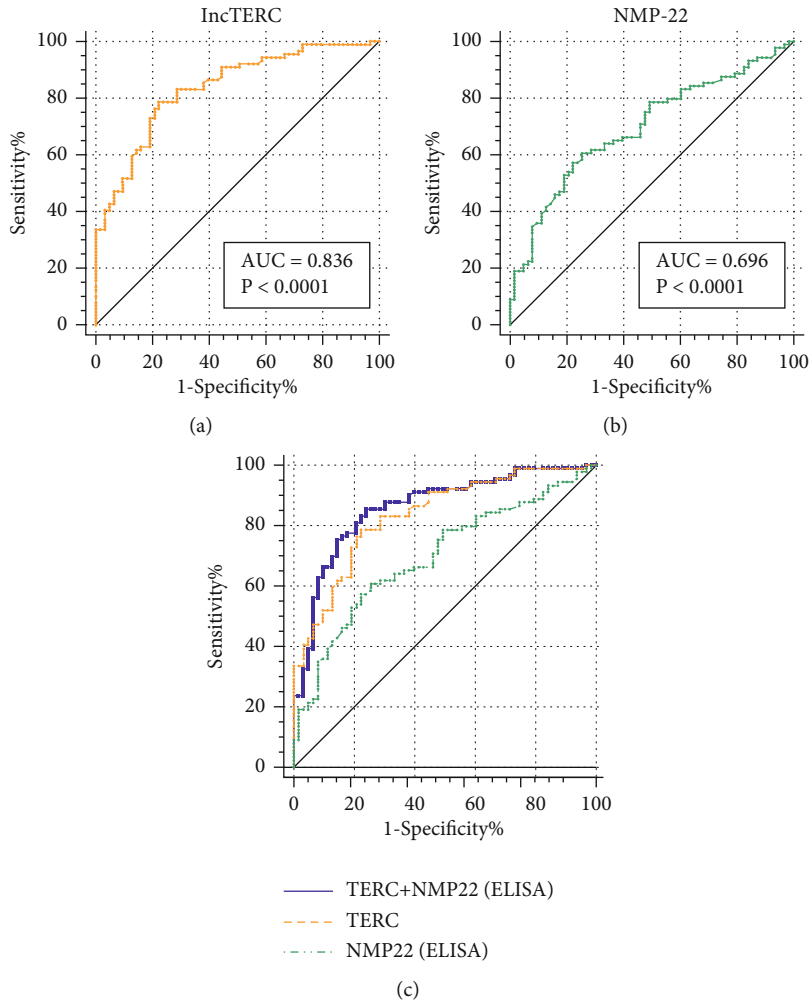


Figure 4: Diagnostic ability of exosomal telomerase RNA component (TERC) and nuclear matrix protein- (NMP-) 22 for bladder urothelial carcinoma (BLCA). (a–c) Receiver operating characteristic curve analysis of exosomal TERC and NMP-22 (ELISA) and the combination of these indicators revealed area under the curve values of 0.836, 0.696, and 0.861.

Table 2: Statistics of NMP-22 (GICA) and urine cytology in BLCA patients and normal individuals.

| | | BLCA | Normal |
|---|---|---|---|
| NMP-22 (GICA) | Positive | 40 | 3 |
| | Negative | 88 | 91 |
| Urine cytology | Positive | 56 | 1 |
| | Negative | 72 | 93 |

Table 3: Diagnostic efficacy of NMP-22 (GICA) and urine cytology.

| | NMP-22 (GICA) | Urine cytology |
|---|---|---|
| Sensitivity | 31.250% | 43.750% |
| Specificity | 96.809% | 98.936% |
| Positive likelihood ratio | 9.792 | 41.125 |
| Negative likelihood ratio | 0.710 | 0.569 |
| Positive predictive value | 93.023% | 98.246% |
| Negative predictive value | 50.838% | 56.364% |

*3.5. Urine Exosomal TERC Was Associated with Tumor Grade, and Bioinformatics Analysis Showed Prognostic Predictive Value for BLCA.* Patients' clinical characteristics including age, sex, TNM stage, histological grade, metastasis, and recurrence are summarized in Table 4. Pearson's $\chi^2$ test was performed to explore associations between exosomal *TERC* levels and clinical pathological characteristics. Patients were divided into the low- ($n = 64$) and high-expression ($n = 64$) groups, using the median value of *TERC* expression as the cut-off value. The findings indicated that the level of *TERC* expression was associated with tumor grade ($P = 0.0153$), while other clinical features such as metastasis and recurrence were not significantly correlated with *TERC*. Thus, we conclude that high TERC expression is associated with BLCA disease progression. Meanwhile, we analyzed Kaplan–Meier curves of disease-specific survival (DSS) and overall survival (OS) according to *TERC* expression using the PrognoScan database (http://dna00.bio.kyutech.ac.jp/PrognoScan/index.html) based on GSE13507. The hazard

Table 4: The characteristics of bladder urothelial carcinoma patients.

| Variables | Total | Expression of TERC | | $\chi^2$ | *P* value |
|---|---|---|---|---|---|
| | | High | Low | | |
| Age | | | | 0.82 | 0.3651 |
| ≤60 | 49 | 22 | 27 | | |
| >60 | 79 | 42 | 37 | | |
| Sex | | | | 3.099 | 0.0783 |
| Male | 98 | 44 | 54 | | |
| Female | 30 | 19 | 11 | | |
| TNM | | | | 1.315 | 0.2515 |
| Ta~T1 | 105 | 50 | 55 | | |
| T2~T4 | 23 | 14 | 9 | | |
| Grade | | | | 5.88 | 0.0153[a] |
| Low | 20 | 5 | 15 | | |
| High | 108 | 59 | 49 | | |
| Lymphatic metastasis | | | | 1.026 | 0.3110 |
| Negative | 110 | 53 | 57 | | |
| Positive | 18 | 11 | 7 | | |
| Recurrence | | | | 1.233 | 0.2668 |
| Primary | 103 | 54 | 49 | | |
| Recurrent | 25 | 10 | 15 | | |

ratios (HRs) for DSS and OS were 1.79 and 1.51, respectively (Figures 5(a) and 5(b)). These results indicated that urinary exosomal *TERC* was a significant risk predictor with the potential to be a prognostic biomarker for BLCA.

[a]$P < 0.05$, Pearson's $\chi^2$ test for the variables above in patients.

*3.6. Urine Exosomal TERC Expression Was Not Correlated with Paired Tissues, and It Stably Exists after Freeze-Thaw Cycles due to Protection from the Lipid Bilayer.* To investigate the relationship in *TERC* expression between different types of samples, *TERC* levels were measured by qPCR in paired tissues and urine exosomes from BLCA patients [23]. Pearson's correlation analysis demonstrated that urine exosomal *TERC* levels were not correlated with the *TERC* levels in corresponding tissues; the correlation coefficients ($r$) were 0.00954 (Figure 6(a)).

Additionally, we divided urine samples into five aliquots of equal volume and placed each at −80°C for one to five freeze-thaw cycles [24]. The results revealed that exosomal *TERC* levels were stable after multiple freeze-thaw cycles (Figure 6(b)). This suggested that storing urine at −80°C even with multiple freeze-thaw cycles will not affect exosomal *TERC*, which was superior to detecting *TERC* in urine sediment cells [25, 26]. In summary, urinary exosomal *TERC* has the potential to be a stable and noninvasive diagnostic and prognostic biomarker for BLCA.

## 4. Discussion

Bladder cancer is one of the most frequent malignancies of the urinary system, with 90% of cases pathologically classified as BLCA. The cause of BLCA tumorigenesis is currently unclear and may include smoking, repeated infection, exposure to compounds, or genetic factors [27, 28]. The gold standard for diagnosing bladder cancer is pathological tissue biopsy, which is invasive and uncomfortable. This study introduced a novel assay that does not require expedited or other special handling procedures, and an 8 mL urine sample is more than enough for the analysis.

We identified that the lncRNA *TERC* was differentially upregulated in urinary exosomes of BLCA patients by RNA-sequencing. The important components of the telomerase are TERT and *TERC*. As previously reported, identifying *TERT* promoter mutations in the urine may substantially aid in the early detection of bladder cancer [29, 30]. However, exosomal *TERC* has thus far not been investigated as a diagnostic or prognostic biomarker for bladder cancer.

We found that *TERC* expression levels were not significantly different between tumor and adjacent nontumor tissues from BLCA patients but were significantly upregulated in urinary exosomes from BLCA patients compared with those from healthy controls. Furthermore, urinary exosomal *TERC* expression could distinguish between urinary benign diseases (inflammation, stones, and obstruction) and bladder cancer ($P < 0.0001$). *TERC* can circulate in whole body fluids under the envelopment of exosomes. Additionally, *TERC* could significantly distinguish high- versus low-grade BLCA ($P = 0.0153$), and Kaplan–Meier survival curves demonstrated its prognostic value. Importantly, multiple freeze-thaw cycles of urine did not affect the stability of exosomal *TERC*.

The exosome is the star molecule of liquid biopsy, and research into them is still in the early stages. Our findings are limited by current science and technology in terms of achieving rapid and efficient detection of exosomal RNA. To extract urinary exosomes, we employ the polyethylene glycol (PEG) precipitation technique, which normally involves around 10 hours of pretreatment (centrifugation and resting) and 1 hour of centrifugation at $10000 \times g$, and the exosome precipitation will be achieved using a standard high-speed centrifuge. Although costly ultracentrifuges are not needed, they still have the drawback of being time-consuming and multistep. At this stage, urine exosomal *TERC* can only be used as an adjunct to cystoscopy, with diagnostic efficacy superior to existing NMP-22, BTA, and other indicators, allowing for patient review and follow-up. From experimental research to clinical application, not only medical but also engineering, science, and other interdisciplinary collaborations are required, and completely automated batch detection of urine exosomal *TERC* is still a long way off.

In the future, more data on the detection of urine exosomal *TERC* will be collected via multicenter and large sample studies, and patients will be followed for a longer period of time to validate its diagnostic and prognostic value.

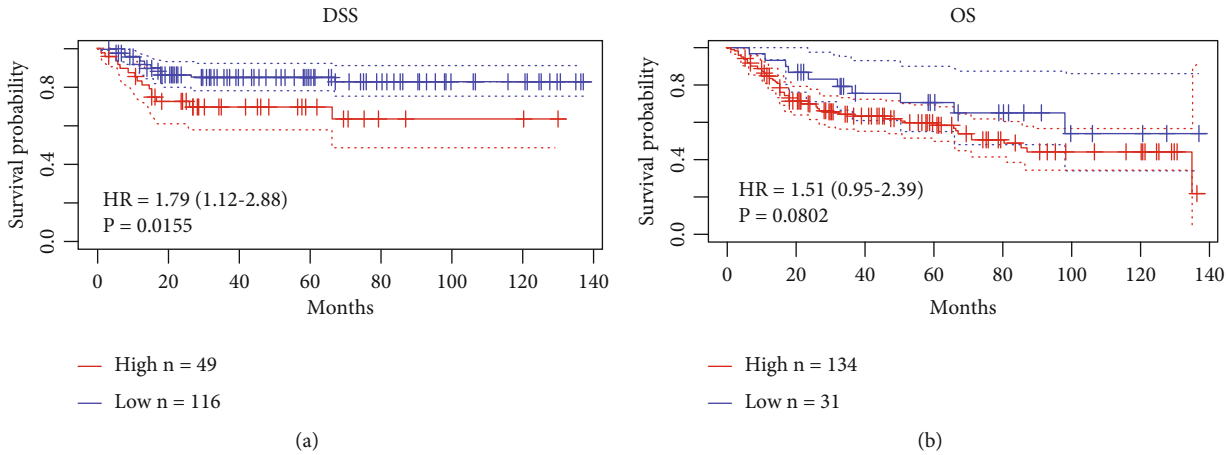


Figure 5: Analysis of Kaplan–Meier survival curves from the PrognoScan database. (a) The disease-specific survival (DSS) curve of TERC (hazard ratio [HR]: 1.79, 95% confidence interval [CI]: 1.12–2.88, $P = 0.0155$). (b) The overall survival (OS) curve of TERC (HR: 1.51, 95% CI: 0.95–2.39, $P = 0.0802$). HR > 1 indicates a risk factor associated with poor patient outcomes.

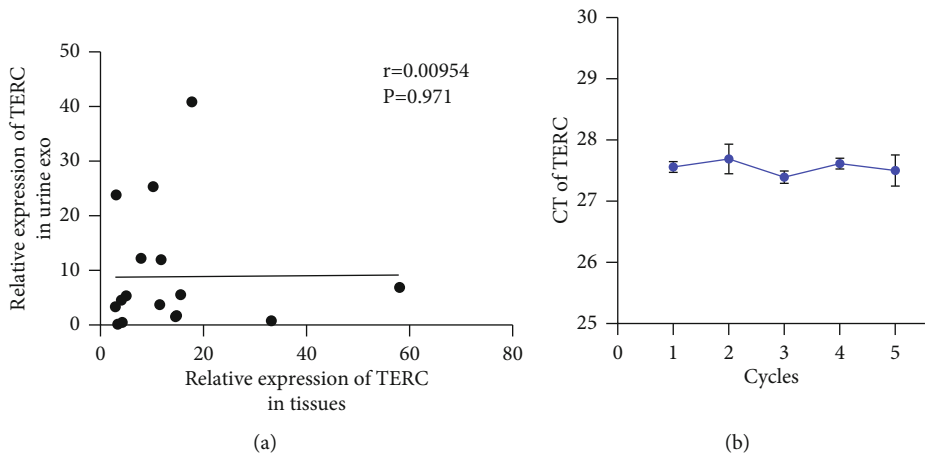


Figure 6: Correlation analysis of telomerase RNA component (TERC) levels in different sample types and its stability in exosomes. (a) TERC expression in tissues was uncorrelated with that in urine exosomes ($r = 0.00954$, $P = 0.971$). (c) Exosomal TERC levels after one to five freeze-thaw cycles of urine samples. Results are presented as mean ± SD.

## 5. Conclusions

In summary, the long noncoding RNA *TERC* was first found in urine exosomes in this article, and we demonstrated that urinary exosomal *TERC* can be used as a diagnostic and prognostic biomarker for BLCA with the added benefit of reducing unnecessary injuries from tissue biopsies. This study provides a convenient, stable, repeatable, and noninvasive index for clinicians and BLCA patients. Thus, our discovery will have profound implications for diagnosis and monitoring of bladder urothelial carcinoma.

## Data Availability

The datasets during and/or analyzed during the current study are available from the corresponding authors on reasonable request.

## Conflicts of Interest

The authors declare that there are no conflicts of interest regarding the publication of this paper.

## Acknowledgments

The work was supported by the Department of Clinical Laboratory of Fudan University Shanghai Cancer Center, and I would like to show great gratitude to Prof. Lu Renquan for supplying us with information on many bladder cancer patients. This work was supported by the Science and Technology Innovation Action Plan of the Shanghai Science and Technology Commission (grant number 19411964800), the National Natural Science Foundation of China (grant numbers 81873975, 82072362, 82002222, 82002223), the Shanghai Public Health System Construction Three-Year Action Plan (2020–2022) Key Disciplines (grant number GWV-

10.1-XK04), the Clinical Research Project of Tongji Hospital of Tongji University (grant number ITJ(ZD)1905, ITJ(QN)1905, ITJ(QN)2005), the Shanghai Post-Doctoral Excellence Program (grant number 2020409), and the Postdoctoral Science Foundation of China (grant numbers 2020M681399, 2020M681400).

## Supplementary Materials

*Supplementary 1*. Supplementary File 1: the clinical information of patients.

*Supplementary 2*. Supplementary File 2: the absolute levels of genes and NMP-22 (ELISA).

## References

[1] H. Sung, J. Ferlay, R. L. Siegel et al., "Global cancer statistics 2020: GLOBOCAN estimates of incidence and mortality worldwide for 36 cancers in 185 countries," *CA: A Cancer Journal for Clinicians*, vol. 71, no. 3, pp. 209–249, 2021.

[2] M. Zibelman, A. M. Asghar, D. C. Parker et al., "Cystoscopy and systematic bladder tissue sampling in predicting pT0 bladder cancer: a prospective trial," *The Journal of Urology*, vol. 205, no. 6, pp. 1605–1611, 2021.

[3] E. C. Hwang, H. S. Choi, S. I. Jung, D. D. Kwon, K. Park, and S. B. Ryu, "Use of the NMP22 BladderChek test in the diagnosis and follow-up of urothelial cancer: a cross-sectional study," *Urology*, vol. 77, no. 1, pp. 154–159, 2011.

[4] M. F. Sarosdy, R. W. deVere White, M. S. Soloway et al., "Results of a multicenter trial using the BTA test to monitor for and diagnose recurrent bladder cancer," *The Journal of Urology*, vol. 154, no. 2, pp. 379–384, 1995.

[5] R. Zhou, K. K. Chen, J. Zhang et al., "The decade of exosomal long RNA species: an emerging cancer antagonist," *Molecular Cancer*, vol. 17, no. 1, p. 75, 2018.

[6] D. M. Pegtel and S. J. Gould, "Exosomes," *Annual Review of Biochemistry*, vol. 88, pp. 487–514, 2019.

[7] L. E. Qu, J. Ding, C. Chen et al., "Exosome-transmitted lncARSR promotes sunitinib resistance in renal cancer by acting as a competing endogenous RNA," *Cancer Cell*, vol. 29, no. 5, pp. 653–668, 2016.

[8] B. Uszczynska-Ratajczak, J. Lagarde, A. Frankish, R. Guigó, and R. Johnson, "Towards a complete map of the human long non-coding RNA transcriptome," *Nature Reviews. Genetics*, vol. 19, no. 9, pp. 535–548, 2018.

[9] J. Cheng, J. Meng, L. Zhu, and Y. Peng, "Exosomal noncoding RNAs in glioma: biological functions and potential clinical applications," *Molecular Cancer*, vol. 19, no. 1, 2020.

[10] U. Gezer, E. Özgür, M. Cetinkaya, M. Isin, and N. Dalay, "Long non-coding RNAs with low expression levels in cells are enriched in secreted exosomes," *Cell Biology International*, vol. 38, no. 9, pp. 1076–1079, 2014.

[11] Y. Zhan, L. Du, L. Wang et al., "Expression signatures of exosomal long non-coding RNAs in urine serve as novel non-invasive biomarkers for diagnosis and recurrence prediction of bladder cancer," *Molecular Cancer*, vol. 17, no. 1, p. 142, 2018.

[12] H. J. Li, X. Gong, Z. K. Li et al., "Role of long non-coding RNAs on bladder cancer," *Frontiers in Cell and Development Biology*, vol. 9, article 672679, 2021.

[13] M. Xue, W. Chen, A. Xiang et al., "Hypoxic exosomes facilitate bladder tumor growth and development through transferring long non-coding RNA-UCA1," *Molecular Cancer*, vol. 16, no. 1, 2017.

[14] C. Chen, Y. Luo, W. He et al., "Exosomal long noncoding RNA LNMAT2 promotes lymphatic metastasis in bladder cancer," *The Journal of Clinical Investigation*, vol. 130, no. 1, pp. 404–421, 2020.

[15] D. Chakravarti, K. A. LaBella, and R. A. DePinho, "Telomeres: history, health, and hallmarks of aging," *Cell*, vol. 184, no. 2, pp. 306–322, 2021.

[16] J. A. Baena-del Valle, Q. Zheng, D. M. Esopi et al., "MYC drives overexpression of telomerase RNA (hTR/TERC) in prostate cancer," *The Journal of Pathology*, vol. 244, no. 1, pp. 11–24, 2018.

[17] Y. Cheng, P. Liu, Q. Zheng et al., "Mitochondrial trafficking and processing of telomerase RNA TERC," *Cell Reports*, vol. 24, no. 10, pp. 2589–2595, 2018.

[18] M. L. Cayuela, J. M. Flores, and M. A. Blasco, "The telomerase RNA component Terc is required for the tumour-promoting effects of Tert overexpression," *EMBO Reports*, vol. 6, no. 3, pp. 268–274, 2005.

[19] H. Liu, Y. Yang, Y. Ge, J. Liu, and Y. Zhao, "TERC promotes cellular inflammatory response independent of telomerase," *Nucleic Acids Research*, vol. 47, no. 15, pp. 8084–8095, 2019.

[20] C. Théry, K. W. Witwer, E. Aikawa et al., "Minimal information for studies of extracellular vesicles 2018 (MISEV2018): a position statement of the International Society for Extracellular Vesicles and update of the MISEV2014 guidelines," *Journal of extracellular vesicles*, vol. 7, no. 1, article 1535750, 2018.

[21] H. Zhou, P. S. Yuen, T. Pisitkun et al., "Collection, storage, preservation, and normalization of human urinary exosomes for biomarker discovery," *Kidney International*, vol. 69, no. 8, pp. 1471–1476, 2006.

[22] Y. Li, J. Zhao, S. Yu et al., "Extracellular vesicles long RNA sequencing reveals abundant mRNA, circRNA, and lncRNA in human blood as potential biomarkers for cancer diagnosis," *Clinical Chemistry*, vol. 65, no. 6, pp. 798–808, 2019.

[23] S. K. Tan, C. Pastori, C. Penas et al., "Serum long noncoding RNA HOTAIR as a novel diagnostic and prognostic biomarker in glioblastoma multiforme," *Molecular Cancer*, vol. 17, no. 1, p. 74, 2018.

[24] R. Zheng, M. Du, X. Wang et al., "Exosome-transmitted long non-coding RNA PTENP1 suppresses bladder cancer progression," *Molecular Cancer*, vol. 17, no. 1, 2018.

[25] M. Müller, H. Krause, R. Heicappell, J. Tischendorf, J. W. Shay, and K. Miller, "Comparison of human telomerase RNA and telomerase activity in urine for diagnosis of bladder cancer," *Clinical cancer research*, vol. 4, no. 8, pp. 1949–1954, 1998.

[26] L. Mezzasoma, C. Antognelli, C. del Buono et al., "Expression and biological-clinical significance of hTR, hTERT and CKS2 in washing fluids of patients with bladder cancer," *BMC Urology*, vol. 10, no. 1, 2010.

[27] N. I. Guidance, "Bladder cancer: diagnosis and management of bladder cancer," *BJU international*, vol. 120, no. 6, pp. 755–765, 2017.

[28] L. M. Mikhaleva, V. V. Pechnikova, A. M. Pshikhachev et al., "Bladder cancer: update on risk factors, molecular and ultrastructural patterns," *Current Medicinal Chemistry*, vol. 28, 2021.

[29] Y. Hayashi, K. Fujita, G. J. Netto, and N. Nonomura, "Clinical application of TERT promoter mutations in urothelial carcinoma," *Frontiers in Oncology*, vol. 11, article 705440, 2021.

[30] M. I. Hosen, N. Forey, G. Durand et al., "Development of sensitive droplet digital PCR assays for detecting urinary TERT promoter mutations as non-invasive biomarkers for detection of urothelial cancer," *Cancers*, vol. 12, no. 12, p. 3541, 2020.

Hindawi
Journal of Immunology Research
Volume 2021, Article ID 7809637, 13 pages
https://doi.org/10.1155/2021/7809637

*Research Article*

# Long-Term *In Vitro* Passaging Had a Negligible Effect on Extracellular Vesicles Released by *Leishmania amazonensis* and Induced Protective Immune Response in BALB/c Mice

**Talita Vieira Dupin,[1] Natasha Ferraz de Campos Reis,[1] Elizabeth Cristina Perez,[2] Rodrigo Pedro Soares,[3] Ana Claudia Torrecilhas,[1] and Patricia Xander[1]**

[1]*Laboratório de Imunologia Celular e Bioquímica de Fungos e Protozoários, Departamento de Ciências Farmacêuticas, Universidade Federal de São Paulo, Campus Diadema, Diadema, Brazil*
[2]*Pós Graduação em Patologia Ambiental e Experimental, Universidade Paulista, São Paulo, Brazil*
[3]*Instituto René Rachou/FIOCRUZ, Belo Horizonte, Brazil*

Correspondence should be addressed to Patricia Xander; patricia.xander@unifesp.br

Received 5 July 2021; Revised 7 November 2021; Accepted 25 November 2021; Published 24 December 2021

Academic Editor: Roberta Antonia Diotti



Depending on *Leishmania* species and the presence/absence of virulence factors, *Leishmania* extracellular vesicles (EVs) can differently stimulate host immune cells. This work is aimed at characterizing and evaluating the protective role of EVs released by *Leishmania amazonensis* promastigotes under different maintenance conditions. Initially, using a control strain, we standardized 26°C as the best release temperature to obtain EVs with a potential protective role in the experimental leishmaniasis model. Then, long-term (LT-P) promastigotes of *L. amazonensis* were obtained after long-term *in vitro* culture (100 *in vitro* passages). *In vivo*-derived (IVD-P) promastigotes of *L. amazonensis* were selected after 3 consecutive experimental infections in BALB/c mice. Those strains developed similar lesion sizes except for IVD-P at 8 weeks post infection. No differences in EV production were detected in both strains. However, the presence of LPG between LT-P and IVD-P EVs was different. Groups of mice immunized with EVs emulsified in the adjuvant and challenged with IVD-P parasites showed decreased lesion size and parasitic load compared with the nonimmunized groups. The immunization regimen with two doses showed high IFN-$\gamma$ and IgG2a titers in challenged mice with either IVD-P or LT-P EVs. IL-4 and IL-10 were detected in immunized mice, suggesting a mixed Th1/Th2 profile. EVs released by either IVD-P or LT-P induced a partial protective effect in an immunization model. Thus, our results uncover a potential protective role of EVs from *L. amazonensis* for cutaneous leishmaniasis. Moreover, long-term maintenance under *in vitro* conditions did not seem to affect EV release and their immunization properties in mice.

## 1. Introduction

Leishmaniasis is a neglected disease distributed in tropical and subtropical regions, especially in developing countries [1]. It is estimated that 700,000 to 1 million new cases and 26,000 to 65,000 deaths annually are due to infection by the parasite [1]. The cutaneous form is the most common among leishmaniasis, with most cases reported in the Americas, Mediterranean region, Middle East, and Central Asia [1, 2]. Currently, leishmaniasis has no efficacious vaccine for humans, there are few therapeutic options for treatment, and the control of vector and reservoir hosts are not practical or eco-friendly [3].

Macrophages are important cells in response to *Leishmania* infection [4]. After phagocytosis, the formation and maturation of phagolysosome-containing parasites are crucial for parasite killing [5]. Classically activated macrophages (M1) are able to destroy *Leishmania* parasites since they exhibit high microbicidal capacity with the production of high levels of reactive oxygen species (ROS) and nitric

oxide (NO) [6, 7]. On the other hand, macrophages can provide an environment for *Leishmania* replication. Alternatively, activated macrophages (M2) show an anti-inflammatory profile contributing to tissue regeneration and wound healing [6]. The role of distinct macrophage populations in the control of *Leishmania* infection still needs to be better clarified.

The control of the parasite by the mammalian host is related to developing an IFN-$\gamma$-producing $CD4^+$ Th1 profile [4], whereas susceptibility is associated to a Th2 response [4]. IFN-$\gamma$ cytokine has an important effect on macrophages since it activates these cells to produce high amounts of microbicidal molecules (such as NO), contributing to parasite elimination [4]. Thus, approaches targeting an effective immune response are promising strategies for treatment/prevention of leishmaniasis.

Different methodologies have been assessed for developing an effective human vaccine for leishmaniasis [8]. Potential candidate vaccines have explored the use of dead parasites [9], genetically modified parasites [10, 11], or molecular systems, such as viruses expressing *Leishmania* genes [12, 13], recombinant proteins [14], and plasmid DNA-based vaccines [15]. Despite efforts, there is still no approved vaccine for the prevention of human leishmaniasis.

Extracellular vesicles (EVs) are an innovative route for delivering antigenic material, providing a promising alternative for vaccine development [16]. They can deliver proteins, lipids, nucleic acids, DNA, and RNA from one cell to another [17, 18]. They may modulate immune responses, facilitating infection, among other functions [19]. EVs released by promastigote forms of *L. amazonensis* activated macrophages via TLR2/4 and by NF-$\kappa$B translocation, and this effect was higher than those elicited by *Leishmania infantum* and *Leishmania braziliensis* EVs [20–22]. *In vitro*, EVs from *L. amazonensis* promastigotes induced IL-6 and IL-10 by murine bone marrow-derived macrophages (BMDM) [20]. Similar effects were observed in THP-1 macrophage cell human lineages that increased the production of NO, TNF-$\alpha$, IL-6, and IL-10 after treatment with EVs released by *L. amazonensis* promastigotes [21]. On the other hand, EVs of *L. amazonensis* amastigotes released in the parasitophorous vacuole of macrophages led to an inhibition of NO production by infected macrophages [22]. Thus, further studies are needed to better understand the role of these EVs on macrophage activation.

Currently, it is still unknown if long-term *in vitro* culture will affect EVs released by *L. amazonensis* and their immunization properties, especially during vaccination protocols. As a part of a wider study on *L. amazonensis*, EVs from parasites bearing different maintenance conditions were evaluated and characterized. BALB/c mice were immunized with these EVs and their protective effects were evaluated. This work brings new possibilities for using parasite EVs to modulate the immune system, enabling the development of interesting alternatives for treating and preventing cutaneous leishmaniasis.

## 2. Materials and Methods

*2.1. Animals.* Female BALB/c mice (6 to 8 weeks old) were purchased from the Center for the Development of Experimental Models for Medicine and Biology (CEDEME) (Universidade Federal de São Paulo (UNIFESP), São Paulo, SP, Brazil). Animals were maintained under specific pathogen-free conditions recommended by the National Council for Control Animal Experimentation (CONCEA) of Brazil. During the experimental period, mice were fed with a sterilized commercial rodent diet and filtered water *ad libitum*. Animals were housed in microisolator cages in a room with a maintained 12 h light/dark cycle. The parameter temperature, humidity, and air quality were monitored and controlled. Animal procedures were approved by the Committee on Ethics of Animal Experiments (CEUA) of UNIFESP under protocol number 2068080319. All efforts were made to minimize the animals' suffering.

*2.2. Parasites.* The *L. amazonensis* reference strain (MHOM/BR/1973/M2269) was kindly provided by Dra. Clara Lucia Barbieri (UNIFESP). Promastigotes were cultured in M199 medium (Gibco, Life Technologies Brand, Grand Island, NY, USA) supplemented with 4.2 mM sodium bicarbonate, 4.2 mM HEPES, 1 mM adenine, 5 mg/mL hemin (bovine type I) (Sigma, St. Louis, MO, USA), and 10% inactivated fetal bovine serum (FBS) (Gibco). Parasites were cultured at 26°C until they reach the stationary growth phase and used in experimental infection of mice or to obtain EVs.

*2.3. Experimental Infection of BALB/c Mice with L. amazonensis Promastigotes.* Parasites were cultured as promastigotes until the stationary phase. After washing with sterile PBS, parasites were resuspended at a concentration of $1 \times 10^6$ parasites/20 $\mu$L and then subcutaneously inoculated at the right hind footpad in BALB/c mice. The diameter of foot lesions was evaluated weekly by monitoring the induration diameter with a digital caliper. After 6–8 weeks of infection, the entire paws were aseptically removed from euthanatized mice and individually homogenized in M199 medium. The parasite burden was evaluated by the limiting dilution method [23].

*2.4. Long-Term (LT-P) and In Vivo-Derived (IVD-P) Promastigotes.* Long-term (LT-P) promastigotes of *L. amazonensis* were obtained after long-term *in vitro* culture with M199 medium plus 10% FBS. *In vitro* passages were performed every five days until completing 100 *in vitro* passages (Figure 1). *In vivo*-derived (IVD-P) promastigotes of *L. amazonensis* were selected after subsequent parasite recovery from 3 consecutive experimental infections in BALB/c mice. Parasites were recovered from lesions in the footpad (Figure 1). Aliquots containing the same passage in culture were frozen for conducting the proposed experiments. For freezing, $2 \times 10^7$/mL promastigotes were added in a solution with fresh medium with 5% ($v/v$) dimethyl sulfoxide (DMSO). Stocks of 1 mL were maintained in liquid nitrogen.

*2.5. Isolation and Characterization of EVs Released by L. amazonensis Promastigotes.* A total of $1 \times 10^8$ *L. amazonensis* (control strain with intermediate virulence profile) [20, 24] promastigotes from stationary cultures were incubated with 1 mL of RPMI 1640 medium plus 2% D-dextrose for 4 h [20, 21]. Parasites were incubated at 26 or 37°C (26°C corresponds

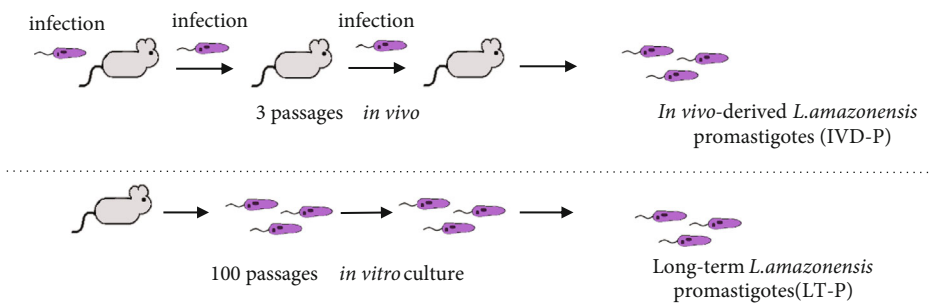


Figure 1: Scheme for obtaining *L. amazonensis* parasites with different virulence profiles (IVD-P and LT-P).

to the vector temperature; 37°C corresponds to the host vertebrate temperature) for 4 h [20]. Afterwards, the supernatants were subjected to serial centrifugation, as follows: 500 × g for 10 min at 4°C, 1,500 × g for 10 min at 4°C, 10,000 × g for 10 min at 4°C, and 2 ultracentrifugations at 100,000 × g for 1 h at 4°C. Then, the pellets were diluted in sterile PBS [20]. EVs from LT-P or IVD-P were obtained from $1 \times 10^8$ promastigotes of LT-P or IVD-P from stationary cultures incubated in 1 mL of RPMI 1640 medium plus 2% D-dextrose for 4 h at 26°C. After supernatant collection, EVs were obtained by serial centrifugations and ultracentrifugations, as described above.

Size and concentrations of EVs were analyzed by nanoparticle tracking analysis (NTA) in a NanoSight Equipment NS300 Instrument (Malvern, Instruments Ltd., Malvern, United Kingdom). The apparatus was equipped with a CCD camera and a 405 nm laser. Each sample was diluted 10- to 100-fold in filtered PBS and captured in triplicate for 1 min (20 frames per second) at 20°C. The camera level was set to 14, and the threshold was always the same. The results were analyzed in the NTA software (version 2.3 build 0017) [20]. Protein concentration was determined by using a Micro BCA Protein Assay Kit (Thermo Scientific, Waltham, MA, United States), according to the manufacturer's procedures.

Enzyme-linked immunosorbent assay (ELISA) was performed with EVs to evaluate the presence of gp63 or LPG. ELISA was performed in 96-well plates sensitized overnight at 4°C with 4 $\mu$g/mL of each EVs (corresponding to $5.4 \times 10^6$ particles of LT-P and $3.2 \times 10^6$ particles of IVD-P) released from LT-P or IVD-P. Blocking was performed with 5% nonfat dry milk in PBS for 1 h at 37°C. Monoclonal antibody CA7AE (1: 500) [25] anti-LPG or monoclonal antibody anti-gp63 (1 : 500) (mouse mAb #235) were added, and the plates were incubated for 1 h at 37°C (both mAbs kindly provided by Rodrigo P. Soares, Instituto René Rachou/FioCruz, MG, Brazil). Plates were washed with 0.05% PBS-Tween 20 and incubated with anti-IgG conjugated to peroxidase (SeraCare, KPL, Milford, MA, United States) (1 : 10,000). The reaction was revealed with TMB substrate solution (Pierce Biotechnology, Thermo Fisher, Rockford, IL, United States) and stopped with 2 N $H_2SO_4$. Absorbance was analyzed at 450 nm in an ELISA reader (BioTek, Winooski, VT, United States).

*2.6. BALB/c Mice Immunization with EVs.* First, animals were intraperitoneally immunized with 4 $\mu$g of EVs (corresponding to $5.4 \times 10^6$ of particles) obtained from *L. amazonensis* promastigote reference strain incubated at 26 or 37°C without adjuvant. Control groups were immunized with PBS.

To evaluate the protective potential of EVs from LT-P and IVD-P, BALB/c mice were immunized intraperitoneally with 4 $\mu$g of EVs (corresponding to $5.4 \times 10^6$ particles of LT-P and $3.2 \times 10^6$ particles of IVD-P). The Alum adjuvant (Adj) (Thermo) was added in the immunization protocols with EVs from LT-P and IVD-P to improve the immune response and to induce the antibody production. Control groups were immunized with alum adjuvant or PBS. Each group was composed of 5–8 animals. Immunizations were carried out at 15-day intervals.

After 2 weeks of the last immunization, mice were infected in the footpad with $1 \times 10^6$ *L. amazonensis* stationary promastigotes of IVD-P. Infection was monitored for 6–8 weeks by measuring the edema with a caliper. Parasite burden was determined by the limiting dilution method. Animals were bled before immunizations, before parasite challenge and during euthanasia. Figure 2 shows the workflow performed for immunizations and blood sample collection. Figure 2(a) shows the immunization protocol for 2 doses, and Figure 2(b) represents the design for 3 doses.

*2.7. Evaluation of Antibody Production.* Sera of all mice were collected before the first immunization, before the challenge with the parasites, and at the time of euthanasia. After immunization protocol, the anti-EV antibody production was evaluated by ELISA. Therefore, ninety-six well plates (Costar, Corning Incorporated, NY, United States) were sensitized with 50 $\mu$L/well of *L. amazonensis* EVs with a final concentration of 6 $\mu$g/mL (corresponding to $8.1 \times 10^6$ particles/mL of LT-P and $4.8 \times 10^6$ particles of IVD-P). After 6–8 weeks of challenge with the parasites, sera were tested by ELISA to evaluate the presence of anti-*Leishmania* antibodies. Thus, 50 $\mu$L of *L. amazonensis* promastigotes' total extract was added in 96-well plates at a 10 $\mu$g/mL concentration. Total extract was obtained with parasites submitted to 10 freeze-thaw cycles. Plates sensitized with EVs or total extract were incubated for 1 h at 37°C. Then, the remaining sites were blocked with 1% PBS-BSA solution for 1 h at 37° C. Wells were washed with 0.1% PBS-Tween 20. The serum samples were diluted in PBS-BSA 1% at 1 : 50 dilution, and subsequently, serial dilution was performed. The plates were incubated for 1 h at 37°C, and then, the anti-IgG1 or anti-IgG2a (Thermo Fisher) conjugated to peroxidase diluted 1 : 10,000

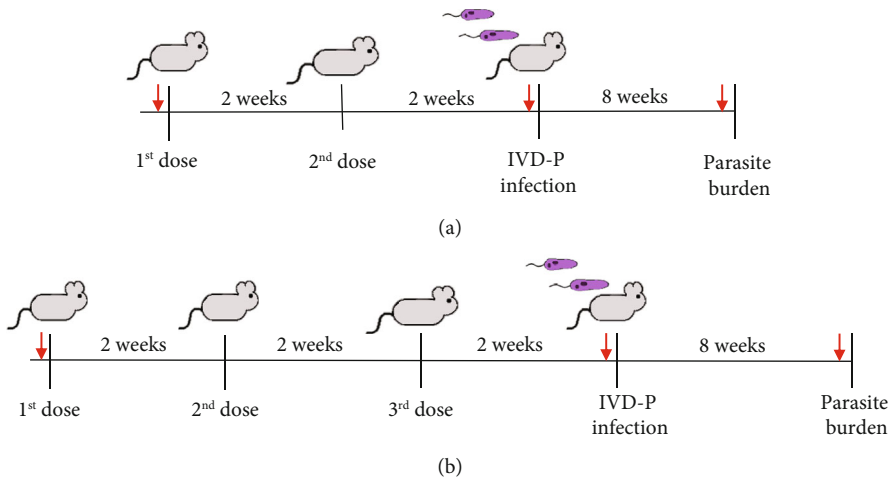


Figure 2: Immunization protocols of BALB/c mice with EVs released by LT-P or IVD-P *L. amazonensis* promastigotes. After 2 weeks of the last immunization, BALB/c mice were infected in the hind footpad with $1 \times 10^6$ IVD-P. (a) Protocol with 2 doses and (b) protocol with 3 doses. Red arrows represent blood collection (before the first immunization, before the challenge with the parasites, and at the euthanasia).

(KPL) were added. The plates were incubated for 1 h at 37°C and revealed with TMB. The reaction was stopped after the appearance of color with 100 $\mu$L/well of 4 $NH_2SO_4$. The results were evaluated by spectrophotometric reading in an ELISA reader (BioTek) at 450 nm.

*2.8. Cytokine Production.* Spleen cells derived from animals immunized with EVs from LT-P or IVD-P were aseptically removed and used to evaluate cytokine production. Cells from mice immunized with adjuvant were used as negative control. Splenocytes were added in 96-well culture plates with a concentration of $1 \times 10^6$ cells/well. Cells were incubated for 5 days with medium alone, EVs (25 $\mu$g/mL), or concanavalin-A (positive control). Supernatants were collected, stored at −80°C, and used to evaluate cytokine production.

Th1/Th2/Th17 BD cytometric bead array (CBA) (BD Biosciences) was used to evaluate cytokines in the supernatants of spleen cells from immunized animals. All procedures were performed according to the manufacturer. BD FACS Accuri C6 flow cytometer (BD Biosciences) was used for the acquisitions, and a total of 2,400 events were acquired for each preparation. Data were analyzed by FCAP ArrayTM software (BD Bioscience). Cytokine concentrations were determined based on the calibration curves constructed with known cytokine standards.

*2.9. Statistical Analysis.* All statistical analyzes were performed using the GraphPad Prism 8.0 software (GraphPad Software, La Jolla, CA, United States). The results are shown as the mean ± standard deviation (SD). Data that assumed a Gaussian distribution were analyzed with parametric tests. Therefore, comparison of multiple groups was carried out with the analysis of variance (ANOVA) followed by the Tukey post test. Two-way ANOVA followed by the Sidak post test was used to analyze a bunch of independent comparisons. Student's *t*-tests were used to evaluate the comparison between two groups. Nonparametric data were analyzed with Mann-Whitney for comparing two groups, and Kruskal-Wallis followed by the Dunn test was used to compare three or more groups. $^*P$ values < 0.05 were considered significant.

## 3. Results

*3.1. EVs Obtained from L. amazonensis Promastigotes Incubated at Different Temperatures Showed Partial Protection in Immunized BALB/c Mice.* BALB/c mice were immunized with 2 doses of EVs from *L. amazonensis*. EVs were obtained from parasites incubated at 26 or 37°C for 4 h [20]. After 2 weeks of the last immunization, mice were subcutaneously challenged in the footpad with $1 \times 10^6$ *L. amazonensis* promastigotes. The lesion size increased in all challenged groups, but the group of mice immunized with EVs obtained at 26°C showed a significant smaller lesion in comparison to the nonimmunized group ($P < 0.05$, Figure 3(a)). After 6 weeks, the mice were euthanized, and the infected hind footpads were removed. The parasite load showed a decrease (statistically nonsignificant) in the group immunized with EVs obtained at 26°C compared with the other groups (Figure 3(b)).

The analysis of IgG1 and IgG2a antibody subtypes contributes to assessing Th1/Th2 response profiles since IgG1 titers are related to the Th2 profile while IgG2a titers are associated with Th1. Thus, the sera collected after the second immunization with EVs were used to detect IgG1 or IgG2a isotype antibody anti-EVs. After the second immunization with EVs, a significant increase in the levels of IgG2a in comparison with the levels of IgG1 was detected ($^*P < 0.05$; $^{**}P < 0.01$; $^{****}P < 0.001$) (Figure 3(c)). After 6 weeks of infection, the levels of IgG1 and IgG2a antitotal extract of *L. amazonensis* promastigotes were evaluated. After 6 weeks of challenge with the parasites, animals showed higher levels of IgG2a compared with IgG1 ($^*P < 0.05$; $^{**}P < 0.01$) (Figure 3(d)), except the nonimmunized infected group that showed an increase in IgG1 levels (Figure 3(d)). These results suggest that immunized animals showed a higher

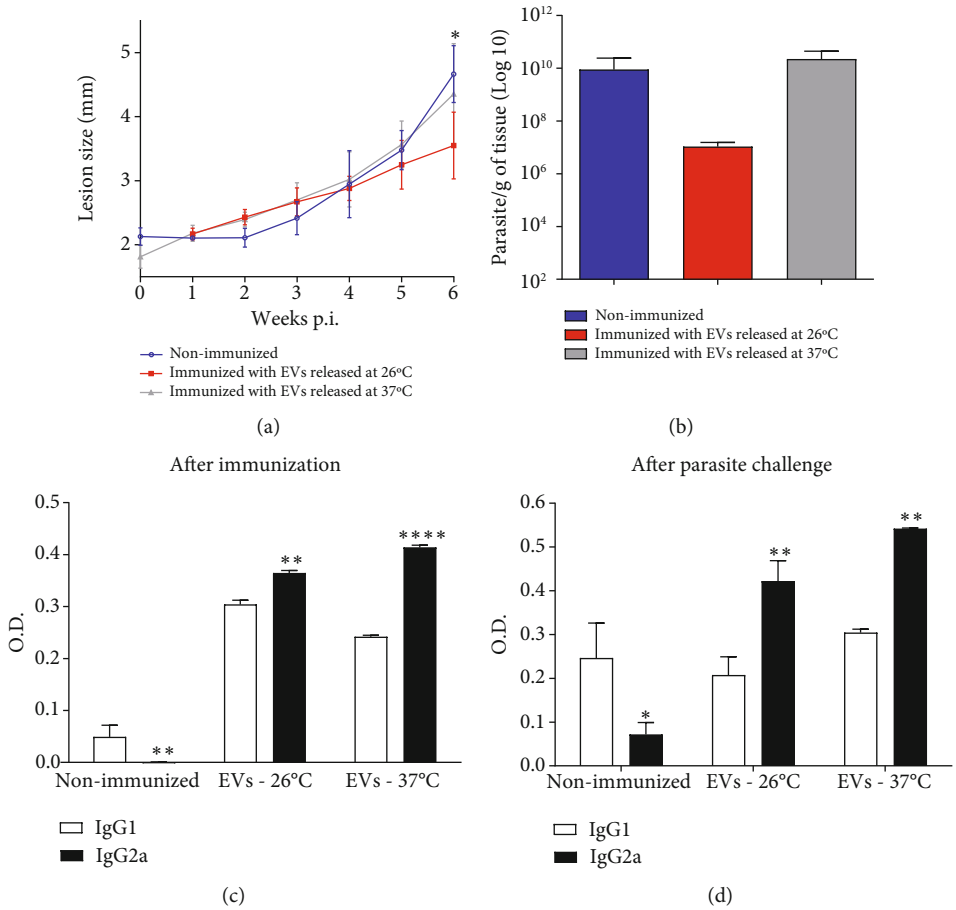


Figure 3: Immunization with EVs released by promastigotes of the reference strain of *L. amazonensis* incubated at 26 or 37°C. BALB/c mice were handled with the 2 doses protocol of EVs from *L. amazonensis* reference strain. (a) The lesion size (millimeter (mm)) measurements. Each point represents the average of the individual measurement ($n = 5$). ANOVA followed by a post hoc Tukey's test was performed $^{*}P < 0.05$. Nonimmunized mice compared with mice immunized with EVs obtained at 26°C. (b) Parasite load ($n = 5$). Bars denote the average of 5 measurements, and error bars denote the SD. ANOVA followed by a post hoc Tukey's test. (c) Production of IgG1 and IgG2a isotype antibody anti-EVs after two doses of EV immunizations. (d) Measurement of the IgG1 and IgG2a isotype antitotal extract of *L. amazonensis* in mice immunized and infected with the parasite. Bars represent the average of 5 measurements, and error bars show the SD. Two-way ANOVA followed by a post hoc Sidak test ($^{*}P < 0.05$, $^{**}P < 0.01$,and$^{****}P < 0.001$ IgG1 versus IgG2a in each group). EVs −26°C—mice immunized twice with EVs obtained from *L. amazonensis* promastigotes incubated for 4 h at 26°C; EVs −37°C—mice immunized with 2 doses of EVs obtained from *L. amazonensis* promastigotes incubated for 4 h at 37°C. Data are representative of 3 independent experiments.

induction of Th1 response, compared with the nonimmunized group.

Altogether, these data demonstrated that EVs released by promastigotes of *L. amazonensis* can induce a Th1 response. In addition, the immunization with EVs from parasites incubated at 26°C led to a significant reduction in the lesion size ($^{*}P < 0.05$) and a decrease (though not significant) in the parasite load. Thus, we established this temperature (26°C) as ideal to obtain EVs to use in the subsequent immunization protocols.

*3.2. Obtaining L. amazonensis Parasites with Different Virulence Profiles.* EVs can carry distinct molecules and virulence factors that can differently stimulate the immune response. Thus, we generated *L. amazonensis* with different virulence profiles (LT-P and IVD-P) to evaluate their EVs in immunization protocols. First, we confirmed the differences in the infection profile of LT-P and IVD-P by experimental cutaneous leishmaniasis. After 7 weeks of infection, the lesion size of mice infected with the LT-P was statistically smaller than that of the group infected with the IVD-P on the 7$^{th}$ week ($^{***}P < 0.001$) (Figure 4(a)). The parasitic load was significantly lower in the group infected with LT-P *L. amazonensis* compared with the group infected with the virulent parasite ($^{*}P < 0.05$) (Figure 4(b)).

*3.3. Characterization of EVs from LT-P and IVD-P.* EVs released by IVD-P and LT-P were obtained according to [20] with parasites incubated at 26°C since this temperature showed better results in immunization protocols (Figure 3). No differences in total protein concentration in EVs from IVD-P and LT-P were detected (Figure 5(a)). Concentration and size distribution of EVs released by IVD-P and LT-P were similar and are shown in Figure 5(b). LPG and gp63

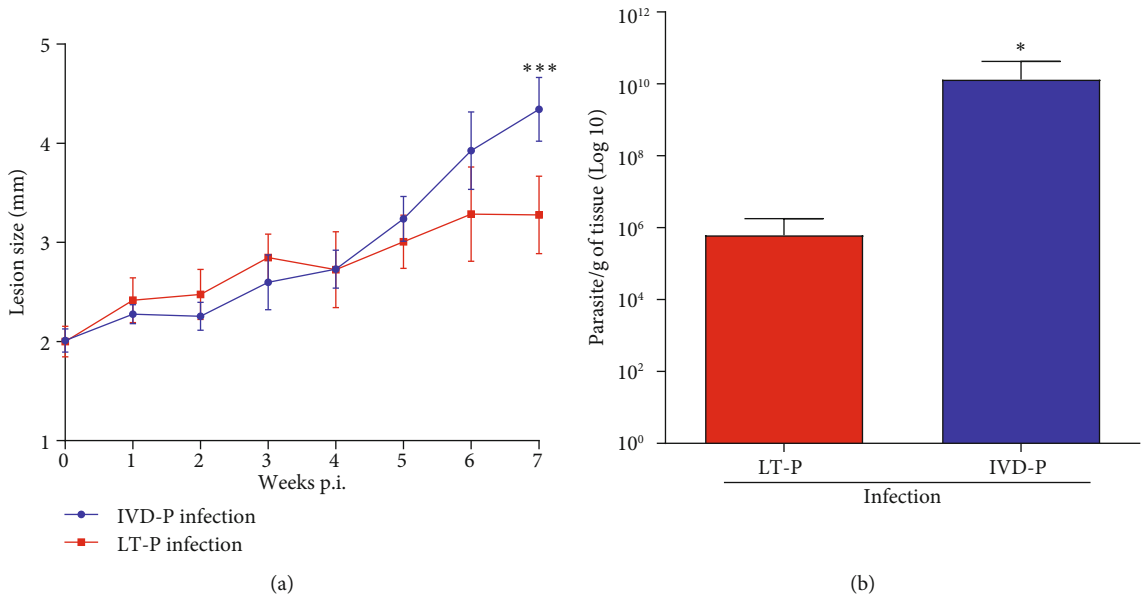


Figure 4: Evaluation of BALB/c mice infection with IVD-P or LT-P. (a) Lesion size (millimeter (mm)) measurements ($n = 5$). Each point represents the average of the measurements ($n = 5$). Student's $t$-test $^{***}P < 0.001$. (b) Parasite load in the hind footpad ($n = 5$). Bars denote the average of 5 measurements, and error bars denote the SD. Mann-Whitney test ($^{*}P < 0.05$). Data are representative of 2 independent experiments.

were detected in EVs released by IVD-P and LT-P (Figures 5(c) and 5(d)). However, a significant lower recognition of mAb anti-LPG was observed in EVs released by IVD-P as compared with EVs from LT-P ($^{**}P < 0.01$) (Figure 5(c)).

*3.4. Protective Responses of EVs Released by LT-P or IVD-P.* The possible protective role of EVs released by LT-P or IVD-P parasites was assessed in BALB/c mice immunized intraperitoneally with each EVs. To improve the immune response, EVs were injected in the presence of adjuvant (Adj). Animals received 2 doses of EVs, and after 8 weeks of infection, a significant reduction in lesion size was observed in animals immunized with LT-P compared with the nonimmunized group or mice immunized with Adj alone ($^{*}P < 0.05; ^{**}P < 0.01$) (Figure 6(a)). A significant reduction in parasite burden was observed in both groups immunized with EVs ($^{*}P < 0.05$) (Figure 6(b)).

After two doses of EVs, we detected a significant increase in IgG2a levels in comparison with IgG1 ($^{***}P < 0.001$) (Figure 6(c)). After 8 weeks of infection, animals immunized with EVs maintained higher levels of IgG2a compared with IgG1, except the adjuvant group that showed an increase in IgG1 levels ($^{**}P < 0.01; ^{***}P < 0.001$) (Figure 6(d)). These results suggest a partial protection and an induction of Th1 response in animals immunized with EVs released by LT-P and IVD-P.

The promising results obtained with 2 immunizations with EVs led us to assess whether an additional dose to the immunization protocol could synergize and led to a more protective effect. Thus, 3 immunizations were performed in the presence of adjuvant with an interval of 2 weeks between doses. After parasite challenge, a significant reduction in lesion size was observed in animals immunized with EVs compared with the nonimmunized or immunized with adjuvant alone groups ($^{*}P < 0.05$; $^{\#\#}P < 0.01; ^{***}P < 0.001$) (Figure 7(a)). A significant decrease in parasite load was observed in the group immunized with EVs from LT-P, compared with the nonimmunized group ($^{*}P < 0.05$) (Figure 7(b)).

After 3 doses, a significant increase in IgG2a levels was detected in the group immunized with EVs from LT-P ($^{*}P < 0.05$) (Figure 7(c)). No differences between the levels of IgG1 and IgG2a were observed in animals immunized with EVs from IVD-P (Figure 7(c)). After 8 weeks of challenge with the parasite, animals immunized with EVs from LT-P showed a significant decrease in IgG2a levels, compared with IgG1 levels ($^{***}P < 0.001$) (Figure 7(d)). Again, no differences were observed between IgG1 and IgG2a in the group immunized with EVs from IVD-P (Figure 7(d)). Our data suggest a mixture of Th1/Th2 responses in animals immunized with 3 doses of EVs from IVD-P and infected with *L. amazonensis* and the Th2 profile in animals immunized with the same immunization scheme with EVs from LT-P.

*3.5. Cytokine Production by Spleen Cells Isolated from Immunized Mice.* The cellular immune response induced after immunization with EVs was evaluated by the cytokine production in splenocytes restimulated *in vitro* with the homologous EVs (i.e., splenocytes from animals immunized with EVs released by LT-P were restimulated *in vitro* with EVs from LT-P). Positive controls were performed with splenocytes from all groups stimulated with concanavalin-A (data not shown). Cytokines were analyzed in animals submitted to the protocol with 2 immunizations because this scheme showed the best results in reducing the parasite load. Analysis of the culture supernatants demonstrated a significant increase in IL-10 (Figure 8(a)) and IFN-$\gamma$ (Figure 8(b)) levels by splenocytes isolated from mice immunized with

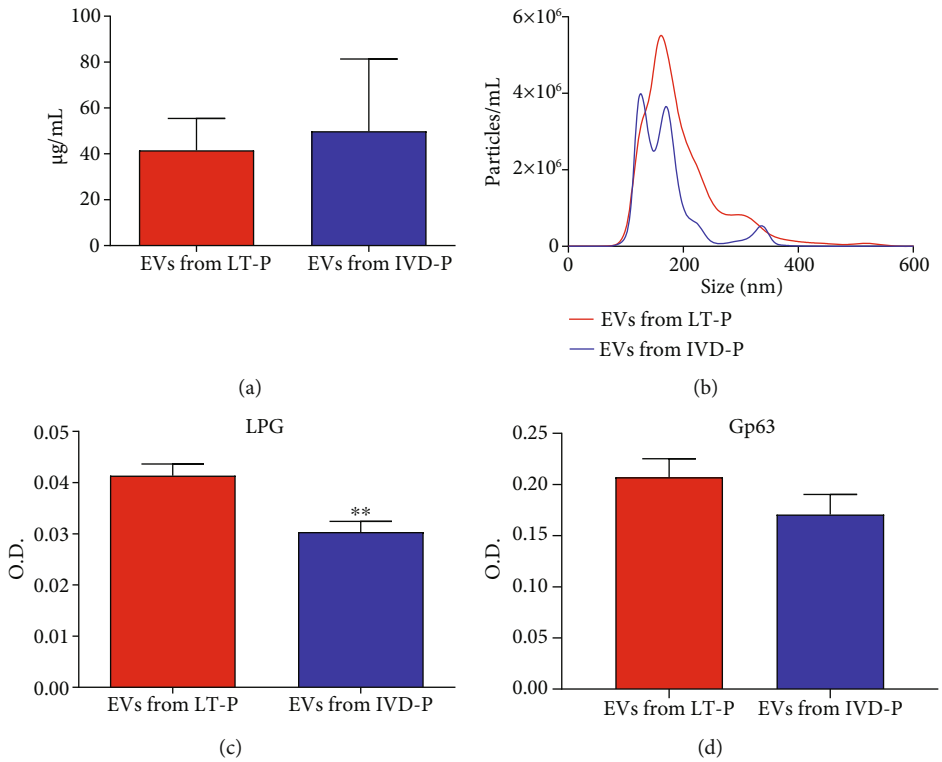


Figure 5: Characterization of EVs released *by L. amazonensis* promastigotes with distinct virulence profiles (IVD-P and LT-P). (a) Protein quantification ($\mu$g/mL). Bars represent the average of 3 measurements, and error bars shows the SD. (b) Size profile and concentration (particles/mL) measurements. (c) Detection of LPG and (d) LPG in EVs (4 $\mu$g/sample). Bars denote the average of 3 measurements, and error bars show the SD. Unpaired $t$-test $^{**}P < 0.01$.

EVs from LT-P and IVD-P and restimulated *in vitro*, as compared with the adjuvant group ($^{**}P < 0.01$; $^{****}P < 0.001$). No differences were seen in TNF-$\alpha$ levels (Figure 8(c)), but a significant increase in IL-6 (Figure 8(d)) and IL-4 (Figure 8(e)) productions was detected in mice immunized with EVs ($^{*}P < 0.05$). This data means that immunization with 2 doses of EVs induced a Th1-related cytokine (IFN-$\gamma$) but also promoted an increase in the production of cytokines of the Th2 profile (IL-10 and IL-4).

## 4. Discussion

Immunization with EVs in therapies and vaccination protocols have increased in recent years [26]. Studies have suggested that the effects of EVs on parasite experimental models depend on the disease and the characteristics of the pathogen. BALB/c mice pretreated with EVs released by *Trypanosoma cruzi* and subsequently challenged with the parasite showed cardiac complications, increased amastigote nests, showing that these EVs can contribute to parasite infection [27]. On the other hand, the immunization with EVs from nematode *Trichuris muris* was protective in C57BL/6 mice after parasite challenge. Immunized mice showed a reduction in parasite load and increased levels of IgG1, the protective isotype for extracellular pathogens [28]. Our work showed that BALB/c mice immunized with EVs released by *L. amazonensis* cultivated under distinct conditions led to a modulation of parasite load, antibodies, and cytokines.

First, we investigated the influence of temperature in immunization protocols since the temperature can contribute to the changes in EV releasing and their properties [29]. EVs released by *L. amazonensis* incubated at different temperatures induced different cytokine production by B-1 cells and macrophages [20]. A higher production of IL-6 and IL-10 was detected in macrophages stimulated with EVs from parasites cultured at 26°C [20]. Our results demonstrated that EVs obtained with parasites cultured at 26°C showed a potential protective role in immunization protocols with a significant decrease in lesion size ($^{*}P < 0.05$) and parasite load reduction. The significant increase in the production of specific antibody IgG2a anti-EVs suggests a modulation to a Th1 profile in mice immunized with EVs from parasites incubated at 26°C ($^{*}P < 0.05$; $^{**}P < 0.01$; $^{****}P < 0.001$). The ability to stimulate cytokine production in macrophages may have contributed to the better performance of EVs obtained at 26°C in our immunization protocol [20, 21]. Thus, we included 26°C as the best temperature to obtain EVs for our immunization protocols.

One of the well-known strategies for developing vaccines, including for leishmaniasis, is the use of attenuated parasites by genetic modification or by cultivation for long periods in culture (reviewed in [30]). Immunization studies with these live attenuated parasites have shown promising results against cutaneous leishmaniasis (reviewed in [30]).

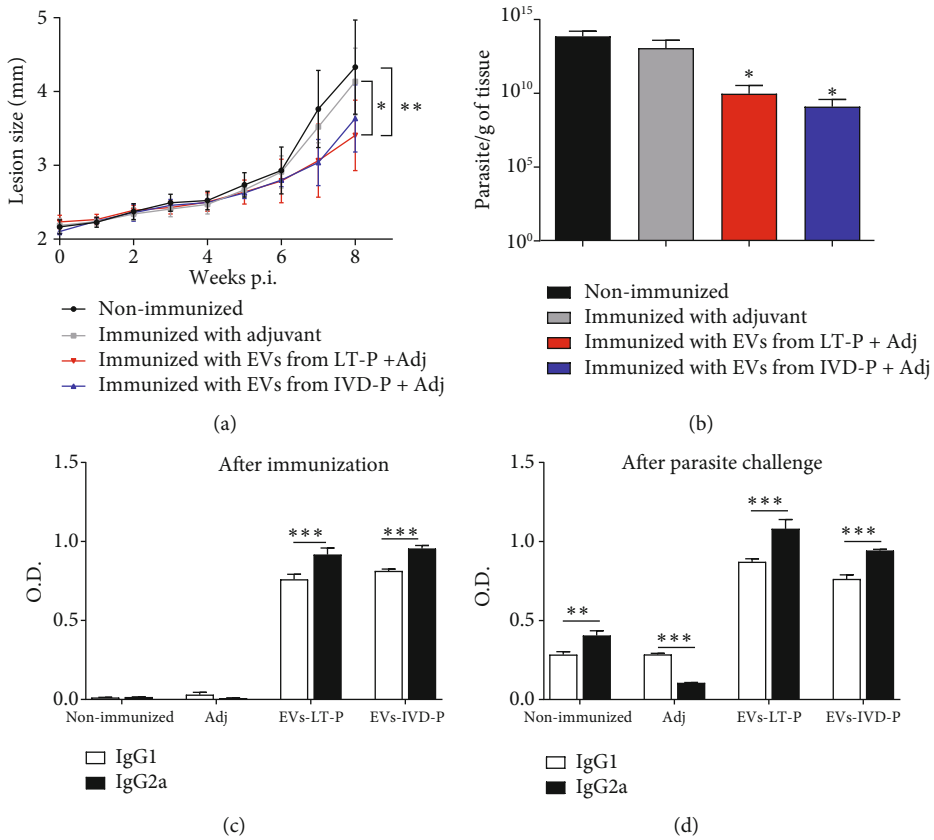


Figure 6: BALB/c mice were managed with the two-dose protocol. (a) Footpad size (millimeter (mm)) measurements ($n = 7$). Each point represents the average of the measurements. ANOVA followed by a post hoc Tukey's test; $^{*}P < 0.05$: adj compared with mice immunized with LT-P; $^{**}P < 0.01$: nonimmunized infected mice compared with the group immunized with LT-P. (b) Parasite load ($n = 7$). Bars denote the average of measurements, and error bars denote the SD. Kruskal-Wallis test followed by Dunn's test; $^{*}P < 0.05$ compared with the nonimmunized group. (c) Production of IgG1 and IgG2a isotype antibody anti-EVs after 2 doses of EV immunizations. (d) Measurement of the IgG1 and IgG2a isotype antitotal extract of *L. amazonensis* in mice immunized and challenged with the parasite. Bars represent the average of 7 measurements, and error bars show the SD. Two-way ANOVA followed by post hoc Sidak's test ($^{**}P<0.01$ and $^{***}P < 0.001$ IgG1 versus IgG2a in each group). Nonimmunized: nonimmunized infected mice; Adj: mice immunized with adjuvant; EVs-LT-P: mice immunized with EVs released by LTP-P; EVs-IVD-P: group of mice immunized with EVs from IVD-P. Data are representative of 3 independent experiments.

However, some disadvantages and some issues still need to be better evaluated, such as the behavior of the attenuated parasite in immunocompromised individuals and the possibility of recombination between genetically attenuated and wild-type parasites in the host and/or in the vector [30]. Thus, using EVs from *Leishmania* that can act as vehicles to deliver parasite antigens can be an exciting alternative for immunization protocols. A distinguished feature of *L. amazonensis* EVs for immunization protocols is their higher proinflammatory activity via TLR4/TLR2 [21]. These EVs induced higher levels of NO and cytokines in macrophages (TNF-$\alpha$ and IL-6) via TLR4/TLR2 compared with EVs from dermotropic *L. braziliensis* and viscerotropic *L. infantum* [21]. In addition, bone marrow-derived macrophages (BMDM) treated with EVs from *L. amazonensis* had an increase in IL-6 and IL-10 cytokines [20]. This initial proinflammatory effect on macrophages can contribute to the induction of an increase in the Th1 response observed in animals immunized with EVs.

In our work, parasites were cultivated for a long period to obtain isolates with different infectivity. Our data showed that the BALB/c infection with the LT-P decreased the parasite load and reduced the lesion size compared with mice infected with the parasite recovered from the lesion size (IVD-P). Similar studies with *L. infantum* and *L. amazonensis* kept for long periods in culture also reduced parasite infectivity [31, 32]. Although the loss of infectivity has been observed in our study and by [32], attenuation of *L. amazonensis* using the *in vitro* passage was not as evident as demonstrated for other pathogens [33–35]. However, this model offers interesting tools for understanding some mechanisms involved in *Leishmania* infection and studying unknown virulence factors. Furthermore, Magalhães et al. [32] demonstrated that protein expression of *L. amazonensis*-attenuated parasites showed a decrease in molecules related to biological and metabolic functions, infectivity, and motility of the flagellum [32], indicating that this method is capable of causing significant changes in protein expression related to virulence.

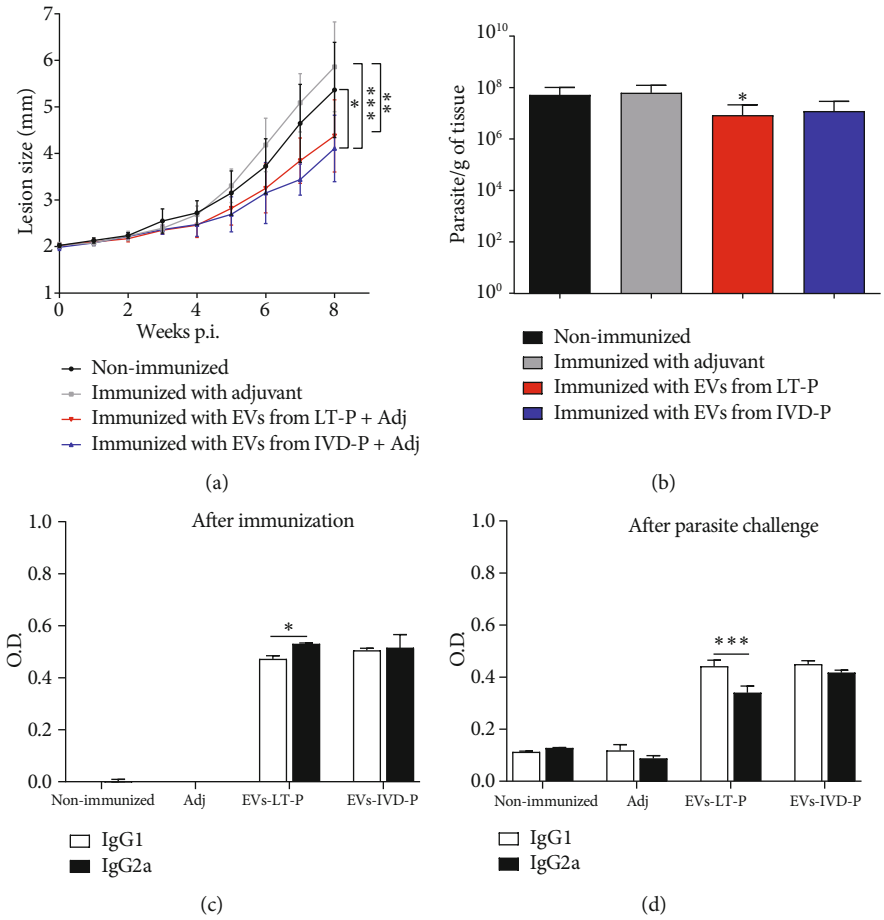


Figure 7: BALB/c mice were treated with the 3-dose protocol. (a) Lesion size (millimeter (mm)) measurements ($n = 9$). Each point represents the average of the measurements. ANOVA followed by post hoc Tukey's test; $^{*}P < 0.05$: nonimmunized infected mice compared with IVD-P; $^{**}P < 0.01$: adj compared with mice immunized with LT-P; $^{***}P < 0.001$: adj compared with the group immunized with IVD-P. (b) Parasite load ($n = 9$). Bars denote the average of 9 measurements, and error bars denote the SD. Kruskal-Wallis test followed by Dunn's test, $^{*}P < 0.05$ compared with nonimmunized mice. (c) Production of IgG1 and IgG2a isotype antibody anti-EVs. (d) Measurements of the IgG1 and IgG2a isotype anti-total extract of *L. amazonensis* in mice immunized and infected with the parasite. Bars represent the average of 9 measurements, and error bars show the SD. Two-way ANOVA followed by post hoc Sidak's test ($^{*}P<0.05$ and $^{***}P < 0.001$ IgG1 versus IgG2a in each group). Nonimmunized: nonimmunized infected mice; Adj: mice immunized with adjuvant; EVs-LT-P: mice immunized with EVs released by LTP-P; EVs-IVD-P: group of mice immunized with EVs from IVD-P. Data are representative of 2 independent experiments.

EVs are now recognized as new players during parasite-host interaction [16, 19, 36–41]. Given that EVs carry parasite content, we addressed the possibility that EVs from isolates with distinct infectivity could differentially stimulate the immune system. Using immunization protocols with EVs from LT-P or IVD-P, we observed a significant reduction in the parasite load and lesion size compared with non-immunized animals. However, no significant differences in parasite load were seen between animals immunized with EVs from LT-P and IVD-P. In conclusion, differences in infectivity did not significantly contribute to the protection induced by their respective EVs.

In contrast to our results, previous treatment of mice with EVs from *Leishmania donovani* or EVs from *Leishmania major* led to an exacerbation of infection after a challenge with respective parasites [42]. The ability of *L. amazonensis* EVs to induce an inflammatory response in human and murine macrophages may reinforce their use in immunization protocols [20, 21]. In addition, the presence of LPG and gp63 in EVs from both *L. amazonensis* profiles (LT-P and IVD-P) can partially explain the protection patterns observed. Expression of LPG was lower in IVD-P than in the LT-P resulting in functional differences in splenocyte stimulation. For example, LT-P (high gp63 and high LPG) induced higher levels of IFN-$\gamma$ whereas those from IDV-P (high gp63 and low LPG) induced higher levels of IL-6 and IL-4. A previous work showed that LPG from *L. amazonensis* (strain BH125) was able to induce the NO, TNF-$\alpha$, and IL-6 productions by peritoneal murine macrophages [43]. Thus, this molecule can contribute to an initial inflammatory response in immunization, impacting the course of the experimental infection. Besides gp63 and LPG, *Leishmania* EVs carry different parasite antigens that can stimulate the immune response [44–47]. Proteomic

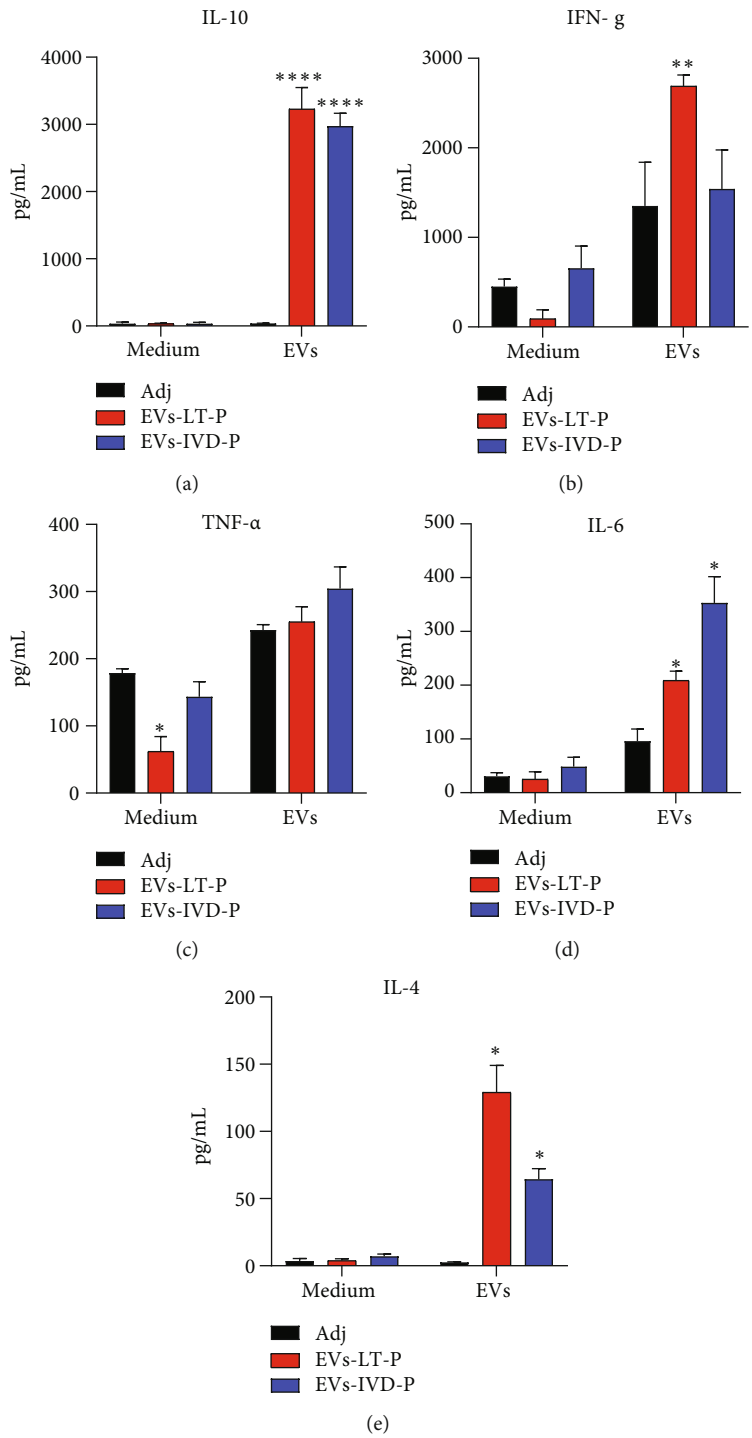


Figure 8: Cytokine responses in mice immunized with EVs from LT-P and IVD-P. BALB/c mice ($n = 5$ per group) were immunized with EVs LT-P and EVs IVD-P mixed with adjuvant. Controls received adjuvant alone (Adj). Two weeks after the last dose, spleen cells were collected and cultured with medium alone (medium) or stimulated with each homologous EVs used for immunization (EVs). (a) Measurement of IL-10, (b) IFN-$\gamma$, (c) TNF-$\alpha$, (d) IL-6, and (e) IL-4 cytokine levels in cell supernatants. The bars indicate that the mean and the error bars denote the standard deviation of the groups. Statistics were performed using two-way ANOVA, followed by the Tukey post test. * indicates significant difference in relation to the groups of mice immunized with EVs and adjuvant alone ($^{*}P < 0.05$, $^{**}P < 0.01$, and $^{****}P < 0.0001$).

studies demonstrated the presence of some important virulence factors in EVs released by *Leishmania*, such as cysteine peptidase, EF-1 alpha, enolase, HSP70, and peroxidoxin [47]. The presence of these molecules can also influence the stimulation of Th1/Th2 response profiles observed in our immunization model. Thus, proteomic analyzes of LT-P and IVD-P EVs

may help understand possible mechanisms involved in the immune response against EVs detected in our immunization protocols.

Immunization with *L. amazonensis* EVs showed a potential protective role with a decrease in parasite load after two or three doses. However, a more pronounced decrease (reduction in approximately 4 logs) in parasite load in animals immunized with two doses of EVs was observed. Immunization with two doses induced higher IFN-$\gamma$ levels by splenocytes, a cytokine involved with the protective response. A higher level of IgG2a antibodies with two immunizations was also detected before and after the challenge with the parasite, suggesting an induction of Th1 profile using this protocol. Although the presence of IL-10 and IL-4 had increased, the presence of proinflammatory cytokines (IL-6 and IFN-$\gamma$) may be related to the lower parasite load observed in animals immunized with two doses. Two hypotheses can be speculated to better performance with two doses: the alum adjuvant and the EV constitution. The alum adjuvant is known to stimulate the Th2 response. So, the addition of one more dose could have stimulated the Th2 profile, related to a no protective response. Some constituents present in EVs also could be modulating the Th2 response. These important questions are under investigation in our laboratory.

Based on literature, the dose and immune response relationship in vaccines is not fully understood and lower doses have been somehow more immunogenic than higher ones (reviewed in [48]). For example, in a preclinical study with tuberculosis vaccines, this phenomenon was reported [49]. The higher immunogenicity to tuberculosis antigens was seen with doses from 5 to 15 $\mu$g of antigens, but there was a decrease in this parameter with 50 and 150 $\mu$g [49]. In addition, the type of immunization regimen has an impact on protection. A study using a vaccine prototype against malaria showed that the use of fractionated doses and the dose spacing significantly increased the protection against infection [50]. Therefore, our study contributed to this proposal that it is important to consider studying the vaccine prototype application regime under a new perspective to better understand the immunological response in vaccine models.

Altogether, our data revealed the potential protective effects of EVs released by *L. amazonensis* in an experimental cutaneous leishmaniasis model. Although the immunization with EVs showed a partial effect on eliminating the parasite, the promising results obtained with two immunizations led to a lower parasite load and polarization response to the Th1 profile in animals challenged with the parasites. Changes in the protocols including new adjuvants and/or parasite strains may improve such responses. Some publications demonstrated promising results using vaccine preparations with *Leishmania* total antigens [8, 51]. *Leishmania* EVs are not incorporated in those protocols since the parasites are often washed to obtain the extracts. The incorporation of EVs into these preparations could lead to an additional protective benefit. Thus, our work can bring new and interesting possibilities for studying EVs in leishmaniasis as possible candidates for immunization protocols.

## 5. Conclusions

In this work, EVs from *L. amazonensis* cultured under different temperatures and EVs from parasites with different infectivity were produced and characterized. These EVs showed potential a protective role in the immunization model, inducing the production of Th-1 related cytokine and specific antibodies against the parasites. Furthermore, the long-term *in vitro* culture did not change the ability to induce partial protection in experimental cutaneous leishmaniasis. Our results are aimed at contributing to a better understanding of the role of EVs in the parasite-host interaction and validating a protective approach in an immunization model with parasite antigens.

## Data Availability

Data supporting the findings are available from the corresponding author upon request.

## Conflicts of Interest

The authors declare no conflicts of interest.

## Acknowledgments

We are indebted to Professor Wagner Luiz Batista for all suggestions to improve the manuscript. This work was supported by the Fundação de Amparo à Pesquisa do Estado de São Paulo (grant number 2019/21614-3). Scholarships were provided by the Fundação de Amparo à Pesquisa do Estado de São Paulo (2021/01556-9), Conselho Nacional de Desenvolvimento Científico e Tecnológico (CNPq), and Coordenação de Aperfeiçoamento de Pessoal de Nível Superior (CAPES).

## References

[1] S. P. Georgiadou, K. P. Makaritsis, and G. N. Dalekos, "Leishmaniasis revisited: current aspects on epidemiology, diagnosis and treatment," *Journal of Translational Internal Medicine*, vol. 3, no. 2, pp. 43–50, 2015.

[2] G. Herrera, N. Barragán, N. Luna et al., "An interactive database of *Leishmania* species distribution in the Americas," *Scientific Data*, vol. 7, no. 1, p. 110, 2020.

[3] S. Burza, S. L. Croft, and M. Boelaert, "Leishmaniasis," *Lancet*, vol. 392, no. 10151, pp. 951–970, 2018.

[4] P. Scott and F. O. Novais, "Cutaneous leishmaniasis: immune responses in protection and pathogenesis," *Nature Reviews. Immunology*, vol. 16, no. 9, pp. 581–592, 2016.

[5] D. Liu and J. E. Uzonna, "The early interaction of *Leishmania* with macrophages and dendritic cells and its influence on the host immune response," *Frontiers in Cellular and Infection Microbiology*, vol. 2, p. 83, 2012.

[6] F. Tomiotto-Pellissier, B. T. . S. Bortoleti, J. P. Assolini et al., "Macrophage polarization in leishmaniasis: broadening horizons," *Frontiers in Immunology*, vol. 9, p. 2529, 2018.

[7] P. P. Carneiro, J. Conceição, M. Macedo, V. Magalhães, E. M. Carvalho, and O. Bacellar, "The role of nitric oxide and reactive oxygen species in the killing of Leishmania braziliensis

by monocytes from patients with cutaneous leishmaniasis," *PLoS One*, vol. 11, no. 2, article e0148084, 2016.

[8] M. Moafi, H. Rezvan, R. Sherkat, and R. Taleban, "*Leishmania* vaccines entered in clinical trials: a review of literature," *International Journal of Preventive Medicine*, vol. 10, no. 1, p. 95, 2019.

[9] M. C. Teixeira, G. G. . S. Oliveira, P. O. M. Santos et al., "An experimental protocol for the establishment of dogs with long-term cellular immune reactions to Leishmania antigens," *Memórias do Instituto Oswaldo Cruz*, vol. 106, no. 2, pp. 182–189, 2011.

[10] S. C. Pandey, A. Kumar, and M. Samant, "Genetically modified live attenuated vaccine: a potential strategy to combat visceral leishmaniasis," *Parasite Immunology*, vol. 42, no. 9, article e12732, 2020.

[11] L. Pirdel and S. Farajnia, "A non-pathogenic recombinant Leishmania expressing lipophosphoglycan 3 against experimental infection with Leishmania infantum," *Scandinavian Journal of Immunology*, vol. 86, no. 1, pp. 15–22, 2017.

[12] M. Osman, A. Mistry, A. Keding et al., "A third generation vaccine for human visceral leishmaniasis and post kala azar dermal leishmaniasis: first-in-human trial of ChAd63-KH," *PLoS Neglected Tropical Diseases*, vol. 11, no. 5, article e0005527, 2017.

[13] A. M. V. Queiroz, J. W. . F. Oliveira, C. J. Moreno, D. M. A. Guérin, and M. S. Silva, "VLP-based vaccines as a suitable technology to target trypanosomatid diseases," *Vaccines (Basel)*, vol. 9, no. 3, p. 220, 2021.

[14] D. P. Lage, P. A. F. Ribeiro, D. S. Dias et al., "A candidate vaccine for human visceral leishmaniasis based on a specific T cell epitope-containing chimeric protein protects mice against *Leishmania infantum* infection," *NPJ Vaccines*, vol. 5, no. 1, p. 75, 2020.

[15] M. Samant, R. Gupta, S. Kumari et al., "Immunization with the DNA-encoding N-terminal domain of proteophosphoglycan of Leishmania donovani generates Th1-type immunoprotective response against experimental visceral leishmaniasis," *Journal of Immunology*, vol. 183, no. 1, pp. 470–479, 2009.

[16] M. Khosravi, E. S. Mirsamadi, H. Mirjalali, and M. R. Zali, "Isolation and functions of extracellular vesicles derived from parasites: the promise of a new era in immunotherapy, vaccination, and diagnosis," *International Journal of Nanomedicine*, vol. 15, pp. 2957–2969, 2020.

[17] H. Kalra, G. P. Drummen, and S. Mathivanan, "Focus on extracellular vesicles: introducing the next small big thing," *International Journal of Molecular Sciences*, vol. 17, no. 2, p. 170, 2016.

[18] G. Raposo and W. Stoorvogel, "Extracellular vesicles: exosomes, microvesicles, and friends," *The Journal of Cell Biology*, vol. 200, no. 4, pp. 373–383, 2013.

[19] S. Montaner, A. Galiano, M. Ã.-. Trelis et al., "The role of extracellular vesicles in modulating the host immune response during parasitic infections," *Frontiers in Immunology*, vol. 5, p. 433, 2014.

[20] F. M. C. Barbosa, T. V. Dupin, M. . S. Toledo et al., "Extracellular vesicles released by Leishmania (Leishmania) amazonensis promote disease progression and induce the production of different cytokines in macrophages and B-1 cells," *Frontiers in Microbiology*, vol. 9, p. 3056, 2018.

[21] P. M. Nogueira, A. de Menezes-Neto, V. M. Borges et al., "Immunomodulatory properties of Leishmania extracellular vesicles during host-parasite interaction: differential activation of TLRs and NF-$\kappa$B translocation by dermotropic and viscerotropic species," *Frontiers in Cellular and Infection Microbiology*, vol. 10, p. 380, 2020.

[22] I. P. Sauter, K. G. Madrid, J. B. de Assis et al., "TLR9/MyD88/TRIF signaling activates host immune inhibitory CD200 in Leishmania infection," *JCI insight*, vol. 4, no. 10, 2019.

[23] H. C. Lima, J. A. Bleyenberg, and R. G. Titus, "A simple method for quantifying *Leishmania* in tissues of infected animals," *Parasitology Today*, vol. 13, no. 2, pp. 80–82, 1997.

[24] M. D. S. Toledo, A. Cronemberger-Andrade, F. M. C. Barbosa et al., "Effects of extracellular vesicles released by peritoneal B-1 cells on experimental Leishmania (Leishmania) amazonensis infection," *Journal of Leukocyte Biology*, vol. 108, no. 6, pp. 1803–1814, 2020.

[25] D. L. Tolson, S. J. Turco, R. P. Beecroft, and T. W. Pearson, "The immunochemical structure and surface arrangement of _Leishmania donovani_ lipophosphoglycan determined using monoclonal antibodies," *Molecular and Biochemical Parasitology*, vol. 35, no. 2, pp. 109–118, 1989.

[26] C. Wen, R. C. Seeger, M. Fabbri, L. Wang, A. S. Wayne, and A. Y. Jong, "Biological roles and potential applications of immune cell-derived extracellular vesicles," *Journal of Extracellular Vesicles*, vol. 6, no. 1, article 1400370, 2017.

[27] A. Trocolitorrecilhas, R. Tonelli, W. Pavanelli et al., "*Trypanosoma cruzi*: parasite shed vesicles increase heart parasitism and generate an intense inflammatory response," *Microbes and Infection*, vol. 11, no. 1, pp. 29–39, 2009.

[28] R. K. Shears, A. J. Bancroft, G. W. Hughes, R. K. Grencis, and D. J. Thornton, "Extracellular vesicles induce protective immunity against Trichuris muris," *Parasite Immunology*, vol. 40, no. 7, article e12536, 2018.

[29] C. I. Vasconcelos, A. Cronemberger-Andrade, N. Souza-Melo et al., "Stress induces release of extracellular vesicles by *Trypanosoma cruzi* trypomastigotes," *Journal of Immunology Research*, vol. 2021, Article ID 2939693, 12 pages, 2021.

[30] A. Zabala-Peñafiel, D. Todd, H. Daneshvar, and R. Burchmore, "The potential of live attenuated vaccines against cutaneous leishmaniasis," *Experimental Parasitology*, vol. 210, article 107849, 2020.

[31] D. Moreira, N. Santarém, I. Loureiro et al., "Impact of continuous axenic cultivation in Leishmania infantum virulence," *PLoS Neglected Tropical Diseases*, vol. 6, no. 1, article e1469, 2012.

[32] R. D. Magalhães, M. C. Duarte, E. C. Mattos et al., "Identification of differentially expressed proteins from Leishmania amazonensis associated with the loss of virulence of the parasites," *PLoS Neglected Tropical Diseases*, vol. 8, no. 4, article e2764, 2014.

[33] D. G. Castilho, A. F. A. Chaves, P. Xander et al., "Exploring potential virulence regulators in Paracoccidioides brasiliensis isolates of varying virulence through quantitative proteomics," *Journal of Proteome Research*, vol. 13, no. 10, pp. 4259–4271, 2014.

[34] T. Duangurai, O. Reamtong, A. Rungruengkitkun et al., "*In vitro* passage alters virulence, immune activation and proteomic profiles of *Burkholderia pseudomallei*," *Scientific Reports*, vol. 10, no. 1, p. 8320, 2020.

[35] C. D. M. Veríssimo, V. J. Maschio, A. P. F. Correa, A. Brandelli, and M. B. Rott, "Infection in a rat model reactivates attenuated virulence after long-term axenic culture of

Acanthamoeba spp," *Memórias do Instituto Oswaldo Cruz*, vol. 108, no. 7, pp. 832–835, 2013.

[36] R. Soares, P. Xander, A. O. Costa et al., "Highlights of the São Paulo ISEV workshop on extracellular vesicles in cross-kingdom communication," *Journal of Extracellular Vesicles*, vol. 6, no. 1, article 1407213, 2017.

[37] G. Coakley, R. M. Maizels, and A. H. Buck, "Exosomes and other extracellular vesicles: the new communicators in parasite infections," *Trends in Parasitology*, vol. 31, no. 10, pp. 477–489, 2015.

[38] G. Dong, A. L. Filho, and M. Olivier, "Modulation of host-pathogen communication by extracellular vesicles (EVs) of the protozoan parasite Leishmania," *Frontiers in Cellular and Infection Microbiology*, vol. 9, p. 100, 2019.

[39] M. E. Kuipers, C. H. Hokke, H. H. Smits, and E. N. M. Nolte-'t Hoen, "Pathogen-derived extracellular vesicle-associated molecules that affect the host immune system: an overview," *Frontiers in Microbiology*, vol. 9, p. 2182, 2018.

[40] A. Marcilla, L. Martin-Jaular, M. Trelis et al., "Extracellular vesicles in parasitic diseases," *Journal of Extracellular Vesicles*, vol. 3, no. 1, article 25040, 2014.

[41] A. J. Szempruch, L. Dennison, R. Kieft, J. M. Harrington, and S. L. Hajduk, "Sending a message: extracellular vesicles of pathogenic protozoan parasites," *Nature Reviews. Microbiology*, vol. 14, no. 11, pp. 669–675, 2016.

[42] J. M. Silverman, J. Clos, E. Horakova et al., "Leishmania exosomes modulate innate and adaptive immune responses through effects on monocytes and dendritic cells," *Journal of Immunology*, vol. 185, no. 9, pp. 5011–5022, 2010.

[43] P. M. Nogueira, R. R. Assis, A. C. Torrecilhas et al., "Lipophosphoglycans from Leishmania amazonensis strains display immunomodulatory properties via TLR4 and do not affect sand fly infection," *PLoS Neglected Tropical Diseases*, vol. 10, no. 8, article e0004848, 2016.

[44] K. Hassani, M. T. Shio, C. Martel, D. Faubert, and M. Olivier, "Absence of metalloprotease GP63 alters the protein content of Leishmania exosomes," *PLoS One*, vol. 9, no. 4, article e95007, 2014.

[45] J. M. Silverman, S. K. Chan, D. P. Robinson et al., "Proteomic analysis of the secretome of Leishmania donovani," *Genome Biology*, vol. 9, no. 2, p. R35, 2008.

[46] J. M. Silverman, J. Clos, C. C. de'Oliveira et al., "An exosome-based secretion pathway is responsible for protein export fromLeishmaniaand communication with macrophages," *Journal of Cell Science*, vol. 123, no. 6, pp. 842–852, 2010.

[47] G. Dong, V. Wagner, A. Minguez-Menendez, C. Fernandez-Prada, and M. Olivier, "Extracellular vesicles and leishmaniasis: current knowledge and promising avenues for future development," *Molecular Immunology*, vol. 135, pp. 73–83, 2021.

[48] S. J. Rhodes, G. M. Knight, D. E. Kirschner, R. G. White, and T. G. Evans, "Dose finding for new vaccines: the role for immunostimulation/immunodynamic modelling," *Journal of Theoretical Biology*, vol. 465, pp. 51–55, 2019.

[49] S. J. Rhodes, A. Zelmer, G. M. Knight et al., "The TB vaccine H56 + IC31 dose-response curve is peaked not saturating: data generation for new mathematical modelling methods to inform vaccine dose decisions," *Vaccine*, vol. 34, no. 50, pp. 6285–6291, 2016.

[50] J. A. Regules, S. B. Cicatelli, J. W. Bennett et al., "Fractional third and fourth dose of RTS, S/AS01 malaria candidate vaccine: a phase 2a controlled human malaria parasite infection and immunogenicity study," *The Journal of Infectious Diseases*, vol. 214, no. 5, pp. 762–771, 2016.

[51] M. J. Germanó, E. S. Lozano, M. V. Sanchez et al., "Evaluation of different total Leishmania amazonensis antigens for the development of a first-generation vaccine formulated with a Toll-like receptor-3 agonist to prevent cutaneous leishmaniasis," *Memórias do Instituto Oswaldo Cruz*, vol. 115, article e200067, 2020.

Hindawi
Journal of Immunology Research
Volume 2021, Article ID 2958394, 19 pages
https://doi.org/10.1155/2021/2958394

*Research Article*

# Human Adenovirus Serotype 3 Infection Modulates the Biogenesis and Composition of Lung Cell-Derived Extracellular Vesicles

**Ayodeji O. Ipinmoroti,[1] Brennetta J. Crenshaw,[1] Rachana Pandit,[1] Sanjay Kumar,[2] Brian Sims,[2] and Qiana L. Matthews[1,3]**

[1]*Microbiology Program, Department of Biological Sciences, College of Science, Technology, Engineering and Mathematics, Alabama State University, Montgomery, AL 36104, USA*
[2]*Departments of Pediatrics and Cell, Developmental and Integrative Biology, Division of Neonatology, University of Alabama at Birmingham, Birmingham, AL 35294, USA*
[3]*Department of Biological Sciences, College of Science, Technology, Engineering and Mathematics, Alabama State University, Montgomery, AL 36104, USA*

Correspondence should be addressed to Qiana L. Matthews; qmatthews@alasu.edu

Received 1 September 2021; Revised 16 October 2021; Accepted 1 November 2021; Published 9 December 2021

Academic Editor: Ana Claudia Torrecilhas



Adenovirus (Ad) is a major causal agent of acute respiratory infections. However, they are a powerful delivery system for gene therapy and vaccines. Some Ad serotypes antagonize the immune system leading to meningitis, conjunctivitis, gastroenteritis, and/or acute hemorrhagic cystitis. Studies have shown that the release of small, membrane-derived extracellular vesicles (EVs) may offer a mechanism by which viruses can enter cells via receptor-independent entry and how they influence disease pathogenesis and/or host protection considering their existence in almost all bodily fluids. We proposed that Ad3 could alter EV biogenesis, composition, and trafficking and may stimulate various immune responses *in vitro*. In the present study, we evaluated the impact of *in vitro* infection with Ad3 vector on EV biogenesis and composition in the human adenocarcinoma lung epithelial cell line A549. Cells were infected in an exosome-free media at different multiplicity of infections (MOIs) and time points. The cell viability was determined using 3-(4,5-dimethylthiazol-2-yl)-2,5-diphenyl tetrazolium bromide (MTT) and fluorometric calcein-AM. EVs were isolated via ultracentrifugation. Isolated EV proteins were quantified and evaluated via nanoparticle tracking, transmission electron microscopy, sodium dodecyl sulfate-polyacrylamide gel electrophoresis, and immunoblotting assays. The cell viability significantly decreased with an increase in MOI and incubation time. A significant increase in particle mean sizes, concentrations, and total EV protein content was detected at higher MOIs when compared to uninfected cells (control group). A549 cell-derived EVs revealed the presence of TSG101, tetraspanins CD9 and CD63, and heat shock proteins 70 and 100 with significantly elevated levels of Rab5, 7, and 35 at higher MOIs (300, 750, and 1500) when compared to the controls. Our findings suggested Ad3 could modulate EV biogenesis, composition, and trafficking which could impact infection pathogenesis and disease progression. This study might suggest EVs could be diagnostic and therapeutic advancement to Ad infections and other related viral infections. However, further investigation is warranted to explore the underlying mechanism(s).

## 1. Introduction

Human Adenovirus (HAdV) is a nonenveloped, icosahedral double-stranded DNA virus derived from the adenoid tissue origin [1–7]. They are known to cause upper/lower respiratory tract infections. This commonly leads to acute respiratory infection, such as pneumonia in children to severe lung disease in adults with high morbidity. There are more

than 50% mortality rate in untreated severe cases [1, 8, 9]. Recurrent outbreaks of HAdV disease have been reported worldwide especially among immunocompromised individuals [1, 5, 10]. Most of these outbreaks involving young populations or individuals with underlying respiratory conditions can be severe, with high morbidity and death rates [11]. Based on their phylogeny and genomic sequence, HAdVs have been classified into seven different species (Groups A-G) with over 70 serotypes causing various types of infections which include lower and upper respiratory infection, ocular conjunctivitis/keratoconjunctivitis (Groups B-E), and gastroenteritis (Groups F and G) [1, 4, 5, 12–14]. The group B human adenovirus type 3 (HAdV3) is known to be a causative agent of respiratory tract infection, pharyngoconjunctivitis, keratoconjunctivitis, gastroenteritis, and severe infection of the central nervous system [1, 15, 16]. Cumulative research evidence has revealed HAdV3 as the most isolated HAdV responsible for most recurrent respiratory tract infection outbreaks worldwide [15]. It has been recorded in both children and adults, resulting in severe morbidity and mortality, especially among pediatrics and neonate age groups [16]. HAdV3 infection also triggers sequelae of pulmonary infections including bronchiolitis, unilateral hyperlucent lung function, and abnormal pulmonary function [16]. HAdV3 predominantly infects the upper respiratory tract by attaching to cluster of differentiation (CD) 46 or desmoglein 2 receptors of healthy cells [7]. HAdV3 has caused fatal outcomes especially in patients with an immune disorder. It has been classified as one of the most frequent serotypes associated with respiratory disease outbreaks in various countries [7, 10]. Research has revealed that HAdV infection causes degeneration of adenoid tissues and tissue culture cells. It has been demonstrated as the first virus to initiate persistent infection in humans [5, 7, 17]. The study of small heterogeneous cell-derived EVs released during early and late phases of viral infection is rapidly growing. They have been shown to strengthen the insufficient evidence supporting viral entry and viral pathogenesis owing to the fact they are present in blood, urine, saliva, amniotic fluid, breast milk, seminal fluid, and malignant effusions [18, 19]. EVs, such as exosomes have been implicated in the pathogenesis of HAdV infection [6, 20, 21]. Other types of infection include human immunodeficiency virus (HIV) [22] and HIV-associated dementia and some other metabolic comorbidities of HIV infection [23–26]. Extensively regulated intercellular interaction and communication of biological mediators, transport of a variety of biologically important molecules, such as lipids, carbohydrates, proteins, mRNAs, miRNAs, small DNA molecules, and signal transmission through EVs between metabolically active cells are vital factors involved in their adaptation to various intercellular and intracellular modification in both biophysiological and biochemical processes such as homeostasis, response to injury, and viral infection among others [27, 28]. There are three main categories of EVs; this classification was based on their biogenesis and release [18, 29–31]. EVs, which have been demonstrated to have the most biological functions, are less than 150 nm in diameter [32]. Hence, the predominantly studied EVs are the exosomes. Exosomes are small EVs of endosomal origin that are formed via transformation of intraluminal vesicles within multivesicular bodies in endosomal compartments. Their size ranges between 50 and 150 nm in diameter [27, 33]. They have been demonstrated as enhancement elements in viral transmission and spread between infected and healthy cells usually via pathogen-associated molecular patterns and antigen masking in viral invasion, which is one of the many ways to evade immune activation. The proviral effects of EVs also include inhibition of innate and adaptive antiviral mechanisms, such as interferon and natural killer cell activation in innate response and Th1 suppression in adaptive response [33]. Some bodies of evidence have shown that retroviruses (e.g., HIV) could hijack the mechanistic pathway of EV formation and release, transporting a similar set of host cell components as EVs to bystander cells, thereby facilitating disease progression and expanding their colonies [27]. EVs have been implicated in tumor growth, drug resistance, and graft rejection advancement in clinical therapy [21, 28, 34–37]. Unique features and applications of EVs include pretherapeutic EX-mimetics (EV mimics) used as drug carriers. To comprehend the application of EVs in targeted drug delivery, it is important to understand their biology and their basic functions [30]. Immunological studies have revealed that EVs secreted by cells infected with wild-type hepatitis B virus upregulated autoimmune inhibitor CD274 encoded programmed death ligands (PD-L1) and exhibit immunosuppressive effects on activation marker CD69. Certain viruses such as HIV and hepatitis B virus could transfer their viral-coding RNAs, small RNAs, and proteins to bystander cells by packaging within EVs, thereby facilitating disease progression by manipulating the immune system, establishing a tumor microenvironment in the case of Epstein-Barr virus [24, 25, 32, 38–40]. Proteomics, RNA, and DNA sequencing of EVs have been employed in the study of some viruses' pathogenesis [41]. However, only a few studies have been designed to examine HAdVs and their impact on EV formation. Conventional diagnoses of HAdV infection are based on positive outcomes from multiplex polymerase chain reaction products of bronchial lavage fluid or phlegm samples obtained from the respiratory tract of HAdV-infected individuals. However, these methods are not without their constraints which may include delay in response to infection treatment requirements [2]. This limitation could be due to inefficient behavioral study as a function of the inept detection of specific biomarkers involved in the disease pathogenesis. Therefore, it is reasonable to speculate that investigation of EV production, cargo loading, release, and communication with bystander cells post-HAdV infection would give us clues into developing more efficient and direct diagnostic and therapeutic measures relative to HAdV and similar viral infections. Hence, in the present study, we evaluated the impact of HAdV3 on EV biogenesis, composition, and trafficking using A549 cells as a model system. Our findings demonstrated that HAdV3-mediated secretion of EVs was dose- and time-dependent which resulted in enhanced expression of critical biomarkers, suggesting importance of EVs in immune modulation, virus progression, and clearance. Our result suggests that EVs secreted

from HAdV3-infected human bronchi epithelial cells play vital roles in immune modulation and transfer of certain signals that could influence viral progression. Therefore, EVs could be a diagnostic and therapeutic agent to treat HAdV-associated diseases. In addition, their proviral and antiviral function could offer more knowledge of their importance in immunotherapy and vaccine development.

## 2. Materials and Methods

*2.1. Cell Culture.* A549 were used in this study. A549 cells were obtained from (American Type Culture Collection, Manassas, VA, USA). The cells were cultured in Dulbecco's modified Eagle medium nutrient mixture/F-12 medium (DMEM-F12) (Fisher Scientific, Grand Island, NY, USA) containing L-glutamine supplemented with 10% Corning regular fetal bovine serum (FBS) (Fisher Scientific, Grand Island, NY, USA), 1% penicillin/streptomycin (Fisher Scientific, Grand Island, NY, USA), and 0.2% amphotericin-B (0.5 $\mu$g/mL) (Fisher Scientific, Grand Island, NY, USA). For virus infection, DMEM exosome-free media was prepared with exosome-depleted FBS using DMEM/F12 medium containing L-glutamine supplemented with 2% exosome-free Corning FBS, 1% penicillin/streptomycin, and 0.2% amphotericin-B (0.5 $\mu$g/mL) (Fisher Scientific, Grand Island, NY, USA). Cells were cultured at 37°C in a humidified atmosphere supplemented with 5% $CO_2$.

*2.2. Viral Stocks.* HAdV3 viral stocks used in this study were previously generated. Preparation of the final viral stock concentration was indexed at $2 \times 10^9$ vp/$\mu$L.

*2.3. Infection of A549 Cells.* Cells were trypsinized and counted, a day before infection. Cell densities between 70 and 80% confluences at the time of infection were considered fit for the assay. Cells were seeded in cell culture dishes ($5.0 \times 10^5$ cell/dish) and incubated at 37°C and 5% $CO_2$ overnight before infection. Dilution of nonreplicative HAdV3 ($2 \times 10^9$ vp/$\mu$L) using an exo-free medium with or without serum (25 $\mu$L in total) was homogenized gently. Overnight cell supernatant was discarded, and cells were infected at 300, 750, and 1500 MOIs, respectively; uninfected cells were used as control. Plates were incubated for 24, 48, and 72 hours (h), and each time point was evaluated as an independent experiment. Infected cell supernatant was collected and stored for EV isolation at the end of incubation period [42].

*2.4. Cell Viability Using Calcein-AM.* Post-infection viability of A549 cells was assessed. Briefly, calcein-AM dye was dissolved using high-quality anhydrous dimethyl sulfoxide (DMSO) at 1 mg/mL. A final concentration of 2 $\mu$g/mL working solution was diluted in sterile phosphate-buffered saline (PBS) solution. Cells were cultured and infected as previously described. The working solution of calcein-AM was added to each dish containing infected and control cells after each time point. Cells were incubated in the dark for 30 minutes (min) at 37°C in a humidified 5% $CO_2$ and observed in staining solution using the GFP channel on the fluorescence microscope.

*2.5. MTT Assays.* Cell viability was assessed relative to viral particles using an MTT assay. A549 cells were seeded independently in 96-well tissue culture plates (10,000 cells/well) and maintained in culture for 24 h before treatment. Consequently, the growth medium was discarded and replaced with a serum-free medium. Cells were stimulated with HAdV3 at different concentrations as previously mentioned. Infected cells were incubated at different time points (24, 48, or 72 h, respectively). Cells were treated with 50 $\mu$L of 5 mg/mL tetrazolium salt (3-(4,5-dimethylthiazol-2-yl)-2,5-diphenyl tetrazolium bromide, (MTT))/1× PBS and incubated for 4 h at 37°C in a 5% $CO_2$ incubator. After incubation, 100 $\mu$L of stop solution (DMSO) was added to each well. The color formation was read at 570 nm and a reference wavelength of 630 nm and stored at 4°C. All samples were evaluated in triplicate [24, 42].

*2.6. Isolation and Purification of EVs from Culture Supernatant.* EVs were isolated and purified from DMEM/F12 exosome-free cell culture media. In brief, EVs were isolated as previously described [24, 25, 42, 43]. The media was collected after infection and spun down at 1,300 revolutions per minute (rpm) at 4°C for 10 min, using a Sorvall RT 6000 refrigerated centrifuge. The supernatant was collected, and the pellet was discarded. The collected supernatant was spun again at 3,900 rpm at 4°C for 10 min using a Sorvall RT 6000 refrigerated centrifuge and then filtered through a 10 mL syringe with a 25 mM syringe filter, with a porosity of 0.22 $\mu$M. The volume of filtered supernatant was primed with PBS and centrifuged at 10,800 rpm for 45 min in an SW41T1 swinging bucket rotor at 4°C using a Beckman Coulter Optima L-70K Ultracentrifuge. The supernatant was collected and centrifuged for 32,000 rpm for 70 min in an SW41T1 swinging bucket rotor at 4°C using a Beckman Coulter Optima L-70K Ultracentrifuge. Approximately 500 $\mu$L of purified EVs was collected below the meniscus of the centrifuge tube. Collected EVs were quantified using the Bradford–Lowry quantitation method [24, 42, 44].

*2.7. Evaluation of EV Sizes and Concentration (NanoSight Tracking Analysis).* To evaluate the size distribution and concentration of A549 cell-derived EVs (particle per mL), nanoparticle tracking analysis (NTA) was performed using NanoSight-LM10, Malvern Instrument, Inc., Malvern, UK. EV particle sizes were analyzed based on Brownian motion and light scattering. The samples were prepared at a dilution of 1 : 100 in PBS (1×) and loaded in a 0.3 mL disposable syringe. The NTA assesses particles based on the size and concentration of samples. The mean values of the replicate were recorded and processed for each reading frame of the five independent experiments.

*2.8. Transmission Electron Microscopy (TEM).* The size and morphology of EVs were analyzed via TEM [45]. For TEM sample preparation, fixed EV samples were loaded on the EM grid and incubated for 1 min at room temp (RT) and immediately stained with 7 $\mu$L of filtered uranyl acetate (UA) solution on the surface of the EM grid. After 15 seconds (s), samples were observed under TEM (Tecnai)

120 kV (FEI, Hillsboro, USA) at 80 kV within 24 h as compared to the negatively stained grids. Digital images were captured with a BioSprint 29 CCD Camera (AMT, Woburn, MA, USA) [44].

*2.9. Dot Blot Analysis.* Expressions of exosomal markers, apoptotic markers, and heat shock proteins (Hsps) in EVs and cell lysates were evaluated via dot blot analysis. Briefly, 5 $\mu$g of EV protein or cell lysates was added to the reducing buffer in a 1 : 1 ratio and boiled for 10 min at 95°C. Samples were dotted on nitrocellulose membrane and were allowed to dry for 5-10 min. The membrane was blocked for nonspecific binding with 5% nonfat dry milk for 30-45 min at RT. The membranes were incubated with the primary antibodies of CD9 (1 : 500) (Fisher Scientific, Grand Island, NY, USA), CD63 (1 : 500) (Santa Cruz Biotechnology, Dallas, Texas), flotillin-1 (1 : 500) (Fisher Scientific, Grand Island, NY, USA), cleaved caspase-1 (1 : 500) (Fisher Scientific, Grand Island, NY, USA), H2A.x (1 : 500) (Cell Signaling Technology Inc., Danvers, MA, USA), Hsp70 (1 : 500) (BioFisher Scientific, Rockford, IL, USA), Hsp100 (1 : 500) (DSHB, Iowa City, IA, USA), TLR7 (1 : 500) (Abnova, Neihu District, Taipei City, Taiwan), Rab35 (1 : 500) (BioFisher Scientific, Rockford, IL, USA), Rab5 (1 : 500) (Fisher Scientific, Grand Island, NY, USA), Rab7 (1 : 500) (Fisher Scientific, Grand Island, NY, USA; DSHB, Iowa City, IA, USA), IL-1$\beta$ (1 : 500) (Bioss Antibodies Inc., Woburn, MA, USA), TSG101 (1 : 500) (Fisher Scientific, Grand Island, NY, USA), and Alix (1 : 500) (Fisher Scientific, Grand Island, NY, USA), overnight at 4°C. The membranes were washed three times 10 min each with 1× Tris buffered saline-Tween-20 buffer containing 0.2% Tween-20 (TBST). Horseradish peroxidase- (HRP-) conjugated secondary antibodies (goat anti-rabbit (1 : 500-1 : 1,000) (Novus Biologicals LLC, Centennial, CO, USA) or goat anti-mouse (1 : 500-1 : 1,000) (Fisher Scientific, Grand Island, NY, USA)) diluted in 2% blocking buffer were incubated with membranes for 1 h at RT. The membranes were washed 3 times 10 min each with TBST-20. Targeted proteins were detected using SuperSignal West Femto Maximum Sensitivity Substrate (Invitrogen, MA, USA), and images were developed using Bio-Rad ChemiDoc™ XRS+ System (Bio-Rad Laboratories, Hercules, CA, USA).

*2.10. Sodium Dodecyl Sulfate-Polyacrylamide Gel Electrophoresis (SDS-PAGE) and Western Blot Analysis.* Purified EVs or cell lysates were added to reducing buffer in 1 : 1 ratio and boiled for 10 min at 95°C. Samples were loaded in a 4-20% 1.5 mm Bio-Rad precast gel and allowed to migrate at 100 V. Proteins were transferred to a nitrocellulose membrane in a transfer chamber at 45 mA overnight. The membrane was blocked in 5% nonfat dry milk prepared in 0.2% Tween-20 and 1× TBS for 30-45 min at RT. Primary antibodies CD9 (1 : 250), Hsp70 (1 : 250), NF-$\kappa$B (1 : 250), and IRF-8 (1 : 250) (DSHB, Iowa City, IA, USA) were used in probing the membranes overnight at 4°C. Nitrocellulose blots were washed three times in wash buffer (0.2% Tween-20 in 1× TBS) for 10 min and incubated with HRP-conjugated secondary antibody (1 : 500-1 : 2000) diluted in blocking solution for 1 h at RT with gentle shaking. The membrane was washed three times in wash buffer for 10 min and developed using SuperSignal West Femto Maximum Sensitivity Substrate (vendor). The signal was detected using Bio-Rad ChemiDoc XRS+ System (Bio-Rad Laboratories, Hercules, CA, USA) [24].

*2.11. Statistical Analysis.* Statistical analyses were performed using one-way analysis of variance (ANOVA) with Tukey post hoc analysis. Statistical significance is indicated by the mean ± SD as follows: for multigroup comparisons, one-way ANOVA was used. Statistical significance was established to be $^{*}p < 0.05$, $^{**}p < 0.01$, $^{***}p < 0.001$, and $^{****}p < 0.0001$.

## 3. Results

*3.1. HAdV3 Triggered Cell Death.* A549 cells were treated with nonreplicative HAdV3 at MOIs of 300, 750, and 1500 diluted in a freshly prepared exosome-free medium. The fluorometric live/dead viability/cytotoxicity analysis imaging revealed that cell viability of HAdV3-infected A549 reduced substantially at higher MOIs relative to uninfected cells after 48 h and 72 h time points (Figure 1(a)). Evaluation of cell viability post-infection assessed using MTT showed a significant decrease in cell viability after HAdV3 infection at the highest concentration (MOI 1500) after 24 h infection (Figure 1(b)) and at MOI 750 and 1500 after 48 h and 72 h infection (Figures 1(c) and 1(d)) compared to the uninfected cells. The reduction in cell viability with increased MOIs relative to the control cells indicates that HAdV3 infection triggers cell death in human lung cells.

*3.2. HAdV3 Altered A549-Derived EV Concentration and Morphology.* To test the effect of HAdV3 on A549 cell-derived EVs, we infected cells in exosome-free complete DMEM/F12. Medium only was used as a control; EVs were isolated and purified from cell supernatant using a standard ultracentrifugation procedure [25, 42–44]. Isolated EV size and particles per mL were evaluated via TEM and NTA, respectively. EVs isolated from untreated cells and infected cells at MOI 300 were morphologically similar (Figure 2(a)). A549-derived EVs were in the size range (30-150 nm) of the previously documented size array of exosomes and were consistent with previous studies (Figures 2(b) and 2(c)) [42]. Results showed a reduction in EVs derived from infected cells (particle per mL) relative to the uninfected control EVs, although sizes were not significantly altered (Figures 2(d) and 2(e)). NTA was used to validate the EVs derived from A549 cells. Isolated EVs from untreated cells have a mean diameter size of 150 nm ± 30 nm and mean concentration of $2.0 \times 10^9 \pm 4.00 \times 10^6$ particles/mL ($^{*}p \leq 0.01$) (Figures 2(b) and 2(c)). EVs derived from infected cells at MOI 300, 750, and 1500 have a mean size of 116.2 nm ± 56.2 nm, respectively, and a mean concentration of $3.42 \times 10^6 \pm 3.91 \times 10^5$ particles/mL, respectively.

*3.3. Regulation of Intracellular Membrane Trafficking GTPases in Response to Infection.* To test whether variation in EV sizes and numbers was associated with Rab GTPases,

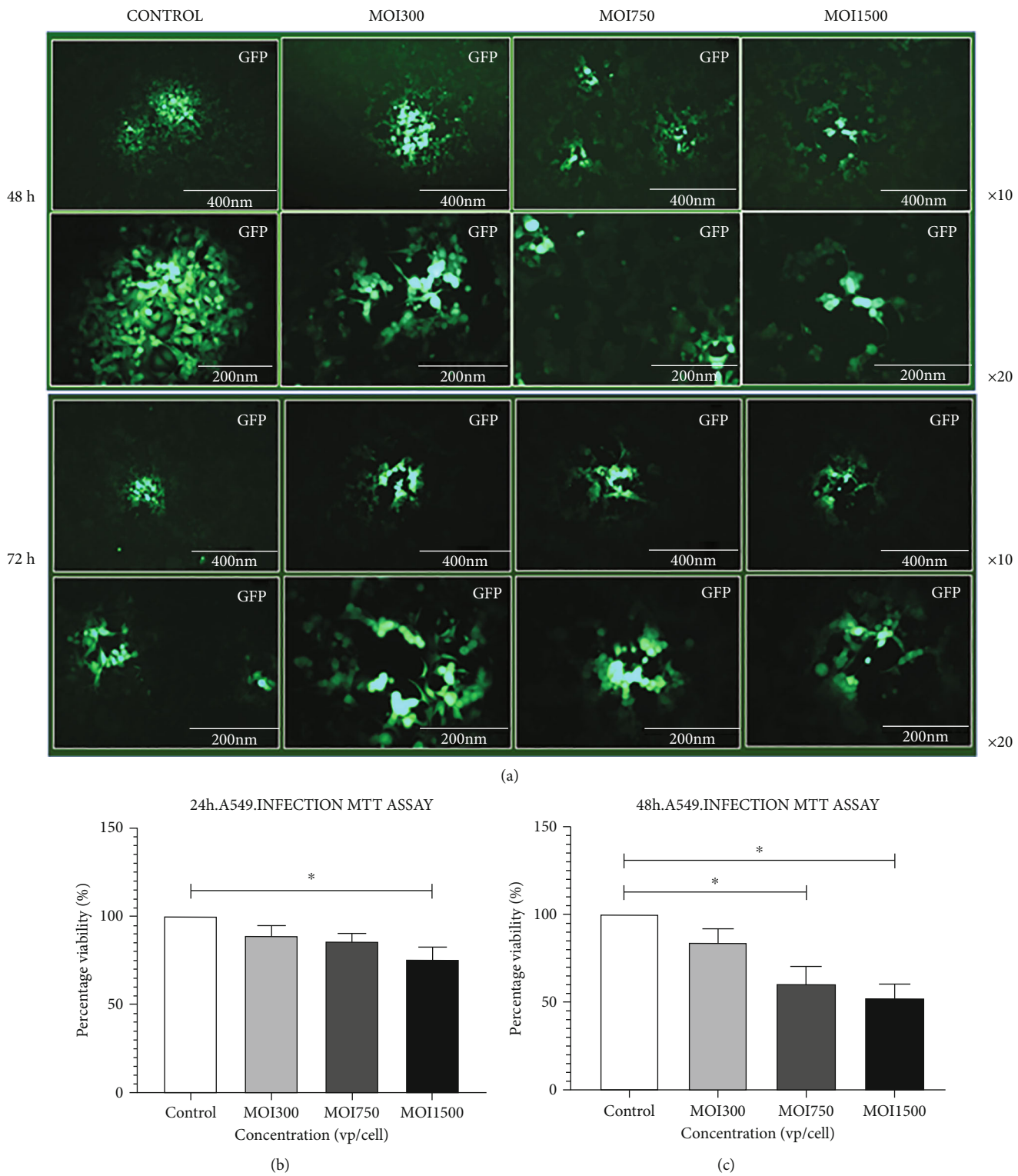


Figure 1: Continued.

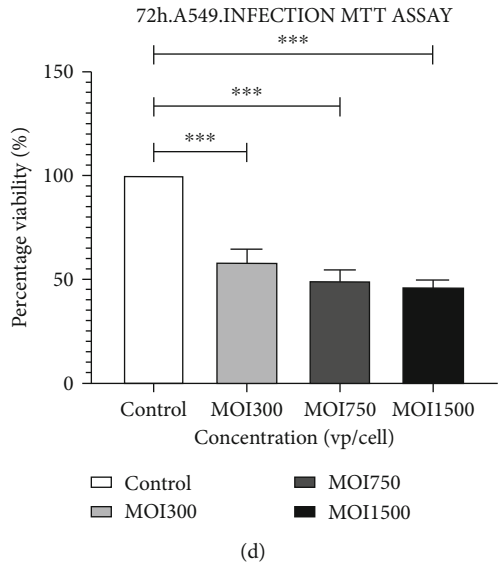


Figure 1: The effect of HAdV3 on A549 viability. (a) Intracellular esterase activity of viable A549 cells. Cells were labeled with nonfluorescent calcein-AM dye which is converted to green fluorescent molecules as a result of ester hydrolysis. The images were acquired at the indicated time after incubation. (b) Postinfection quantification of viable A549 cells after incubation with 3-(4,5-dimethylthiazol-2-yl)-25-diphenyltetra bromide after 24 h (c) 48 h, and (d) 72 h. The cells were incubated with dye solution at 37°C for 3-4 h; absorbance was read at 570 nm. Data shows the mean ± SEM from four independent experiments performed using one-way analysis of variance (ANOVA) with Tukey post hoc analysis. Statistical significance is indicated by the mean ± SD as follows: $^{*}p < 0.05$, $^{**}p < 0.01$, $^{***}p < 0.001$, and $^{****}p < 0.0001$.

we examined the expression of Rab5, Rab7, and Rab35 in A549 cells and their EVs. Rab proteins belong to the Ras superfamily of small Rab GTPases [46–48]. Rab5 and Rab7 are present in the plasma membrane and early endosomes and regulate vesicular trafficking during early endocytosis, whereas Rab35 is associated with protein sorting, secretion, and targeting [49]. The Rab family has been implicated in both endosomal sorting complex required for transport-(ESCRT-) dependent and independent formation pathways. Rab5, Rab7, and Rab35 are principal components of ESCRT-driven formation of intraluminal vesicles and the basal regulation of early to late endosome transition, including docking and fusion of multivesicular endosomes with the plasma membrane during the secretion of ILVs as exosomes [46–49]. The activity of Rab5 precedes endocytosis and autophagy in the endocytic cycle, while Rab35 is an essential component of the degradative process in the pathway [46, 48]. Conversely, studies have shown that other members of the Rab family such as Rab31 regulate ESCRT-independent EV pathway by driving ILV formation and suppressing multivesicular endosome degradation [46, 47]. Therefore, Rab proteins represent significant components of EV biogenesis, sorting, and secretion machinery. Our experimental findings showed that at 48 and 72 h, Rab5 expression was slightly elevated; meanwhile, Rab7 expressions in EVs increased with increased HAdV3 viral particle per cell (MOI 750, $^{***}p \leq 0.001$; MOI 1500, $^{***}p \leq 0.001$) compared with those in the control group (Figures 3(b) and 3(c)). Furthermore, Rab35 expression was upregulated significantly in EVs at MOI 750 and 1500 at 48 and 72 h when compared to uninfected cells (Figure 3(d)) ($p \leq 0.0001$, $p \leq 0.0001$, $p \leq 0.0001$, and $p \leq 0.0001$), suggesting that Rab proteins may have a role in EV production.

*3.4. Evaluation of Membrane Trafficking Marker in Cell Lysate.* The Rab families are small GTPases and are well characterized based on their roles in the regulation of intracellular trafficking during endocytosis, endosome formation, and secretion [28]. Rab proteins are precisely localized to the cytoplasmic surface of the intracellular compartments of cells carrying them, such as the endoplasmic reticulum. During a transfection *in vitro* fusion assay using enriched membrane prep Rab5 was shown to influence the regulation of endocytosis [28]. We found that Rab5 was slightly reduced irrespective of time point and viral dosage, but Rab7 level on the other hand significantly increased, mostly after 72 h of infection at MOI 750 ($p \leq 0.001$) but declined at MOI 1500 ($^{*}p \leq 0.05$) (Figures 4(a)–4(c)). Rab35 level significantly increased at MOI 750 and MOI 1500 (Figure 4(d)) ($p \leq 0.0001$). These findings suggested that GTPases Rab5, 7, and 35 are critical proteins in the endocytic pathway.

*3.5. EV Characterization Revealed the Presence of Classical Markers.* EVs were isolated and characterized for exosomal markers, such as CD9, CD63, and TSG101 as previously described. CD9 and CD63 are tetraspanins that play a major role in cellular functions such as motility, proliferation, fusion, adhesion, and platelet activation among others. TSG101 plays an important role in cell growth and differentiation. It is a vital element of the ESCRT-1-dependent pathway; but may also play a vital role in the negative regulation of cell growth. For these studies, we isolated EVs from

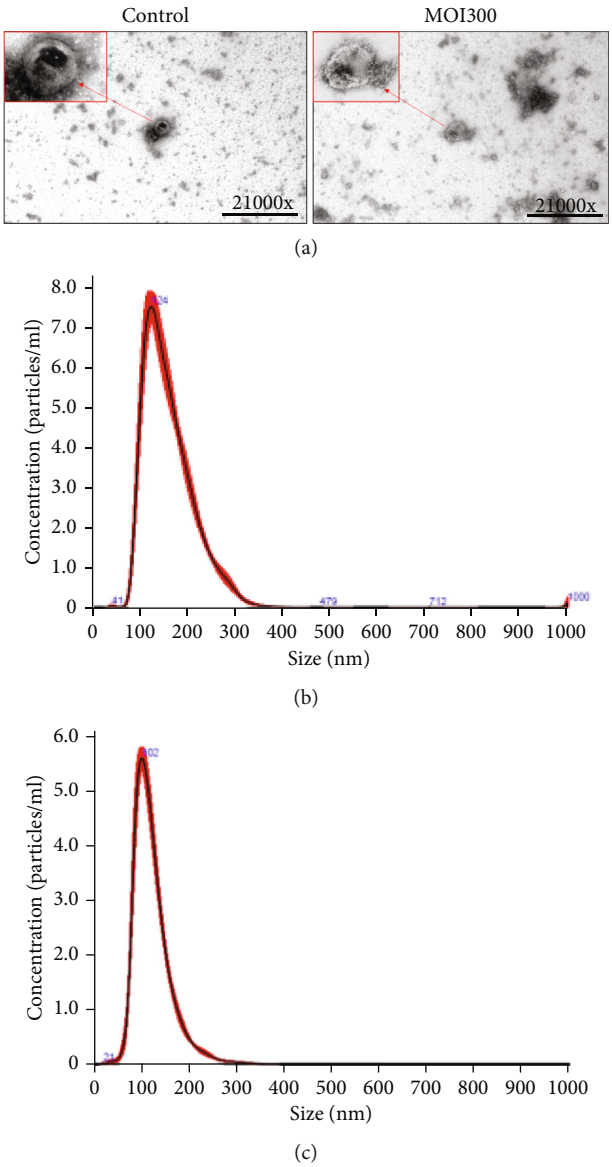


Figure 2: Continued.

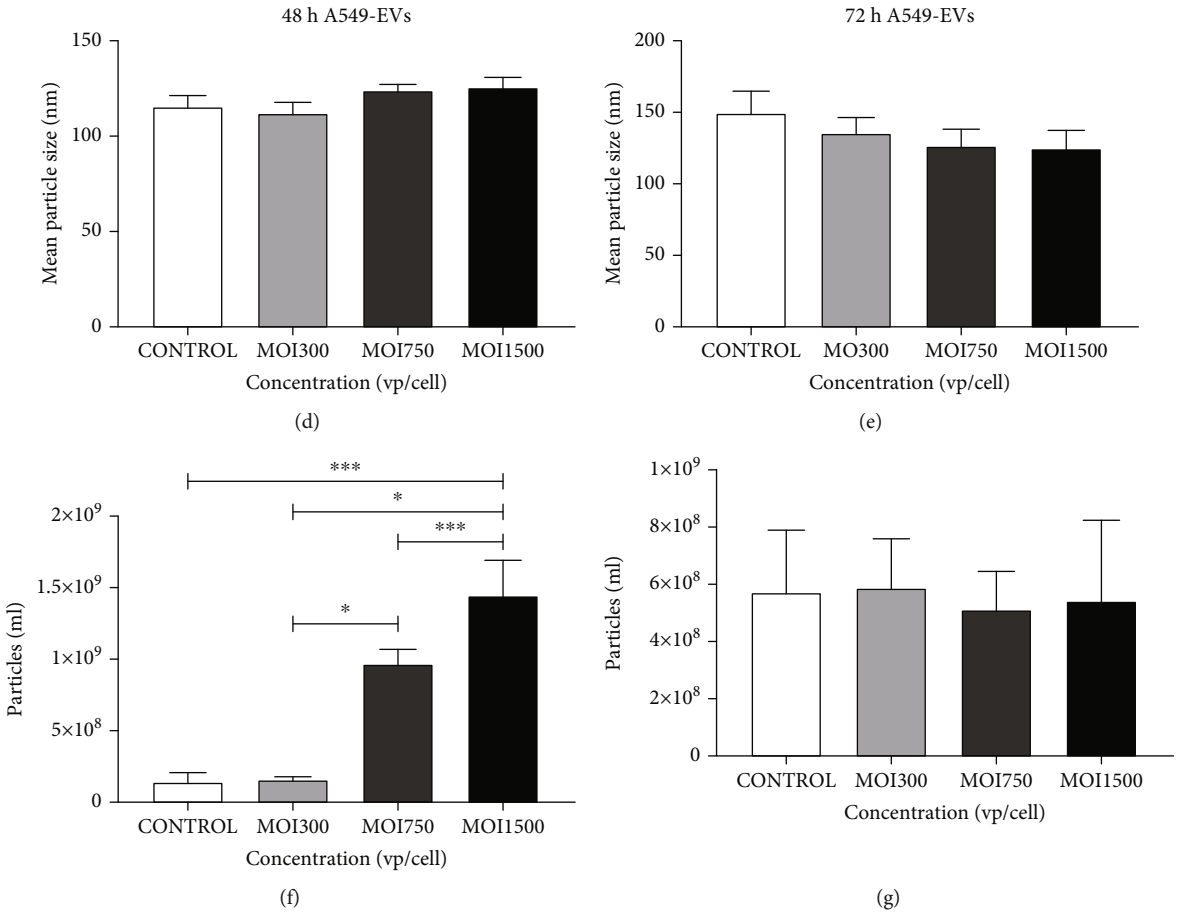


Figure 2: Morphological characterization of HAdV3-infected A549-derived exosomes. (a) TEM analysis of HAdV3-infected A549-derived exosomes. Images showing morphologies of EVs isolated from uninfected and MOI 300. (b) NTA showing distribution pattern of uninfected EVs (c) at MOI 300. (d) The graph showing assessment of EVs' mean particle sizes after 48 h of infection and (e) 72 h of infection. (f) The graph showing quantification of HAdV3-infected A549-derived EVs per mL after 48 h and (g) 72 h of infection. Data show the mean ± SEM from four independent experiments. Data shows the mean ± SEM from four independent experiments and performed using one-way analysis of variance (ANOVA) with Tukey post hoc analysis. Statistical significance is indicated by the mean ± SD as follows: $^{*}p < 0.05$, $^{**}p < 0.01$, $^{***}p < 0.001$, and $^{****}p < 0.0001$.

human lung adenocarcinoma cells (A549). We verified successful EV isolation by performing detection analyses which include dot blot, SDS-PAGE, and western blot to examine the expression of common and classical exosomal proteins. HAdV3-infected A549-derived EVs showed significantly increased expressions of CD9, CD63, and TSG101 relative to EVs derived from untreated cells after 48 h and 72 h infection ($p \leq 0.0001$, $p \leq 0.001$, and $p \leq 0.001$) (Figures 5(a)–5(c)). Glyceraldehyde 3-phosphate dehydrogenase (GAPDH) is an abundant glycolytic enzyme present naturally on the EV surface that is important in the assembly, secretion, and aggregation of EVs. They are overly expressed in some cases when there is a production of large EV clusters [50]. Due to their abundance and conserved nature in EVs, we assessed GADPH as a control in our isolated EVs. Our results indicated no significant difference in GAPDH levels at all MOIs and time points relative to uninfected cell-derived EVs (Figure 5(d)). Summarily, these results indicate that HAdV3 infection affects the abundance of tetraspanins in a dose-dependent manner and modulates the ESCRT-dependent pathway, which makes it a potential factor in evaluating EV subpopulations.

*3.6. Stress Response Marker Expression Increased in Response to HAdV3 Infection.* Heat shock proteins (Hsps) are an evolutionarily conserved group of proteins expressed in all eukaryotes and some prokaryotes [28]. They act as molecular chaperones, assisting the proper folding and/or refolding of newly synthesized proteins. In addition, they play cytoprotective roles under stress and trauma conditions. Their expression levels increase many-fold when cells are exposed to pathogens (e.g., viruses), drugs, heavy metals, and heat. Analysis of isolated EVs for the presence of Hsp70 and Hsp100 confirmed their presence with a slightly elevated level of Hsp100. However, a significant increase in Hsp70 expression was observed relative to EVs derived from uninfected cells ($^{***}p \leq 0.000$) (Figures 6(b) and 6(c)). Moreover, the abundance of Hsp70 in EVs was verified using western blot (Figure 7(b)). We found that HAdV3 infection had no significant effect on the expression of Hsp100 as revealed

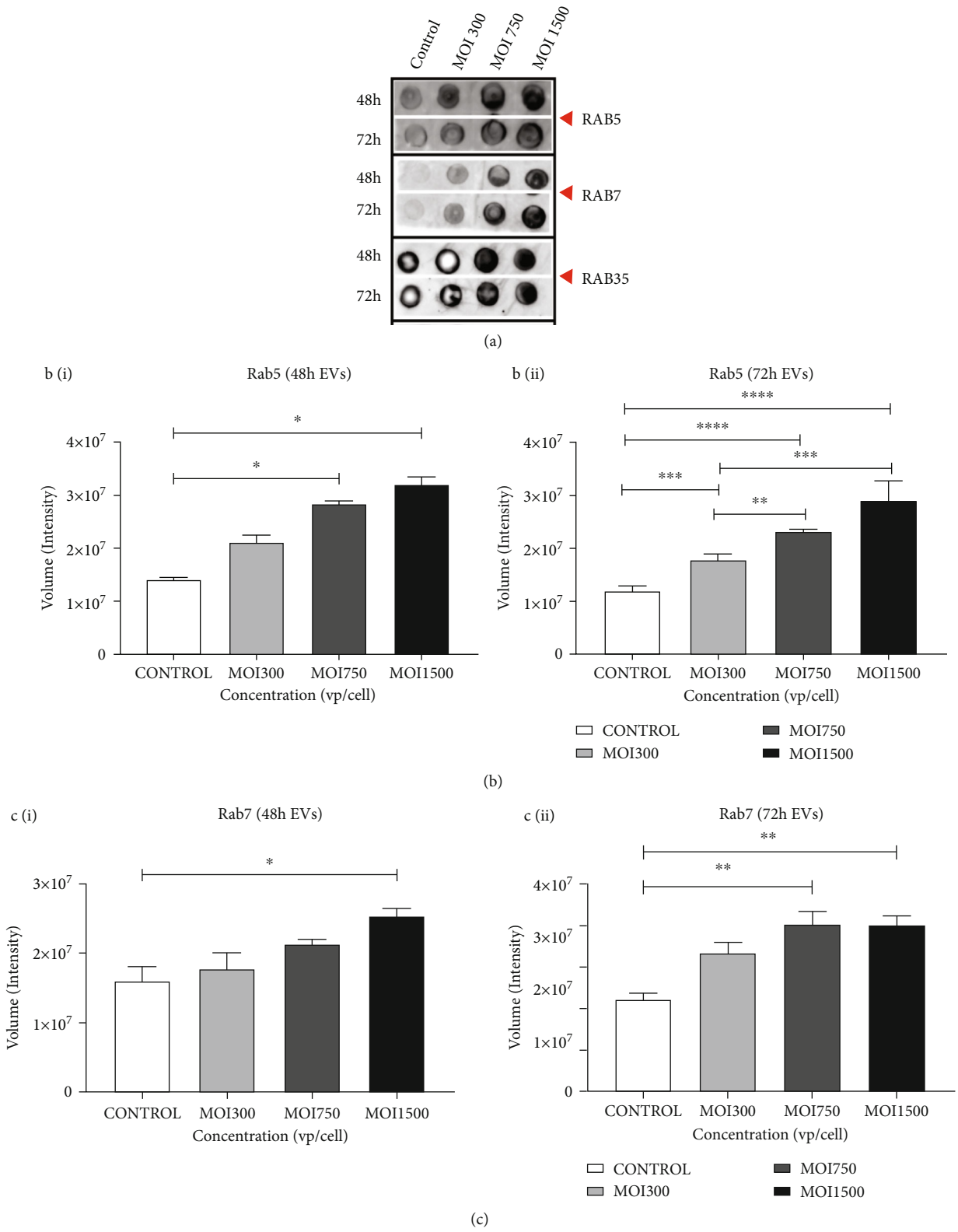


Figure 3: Continued.

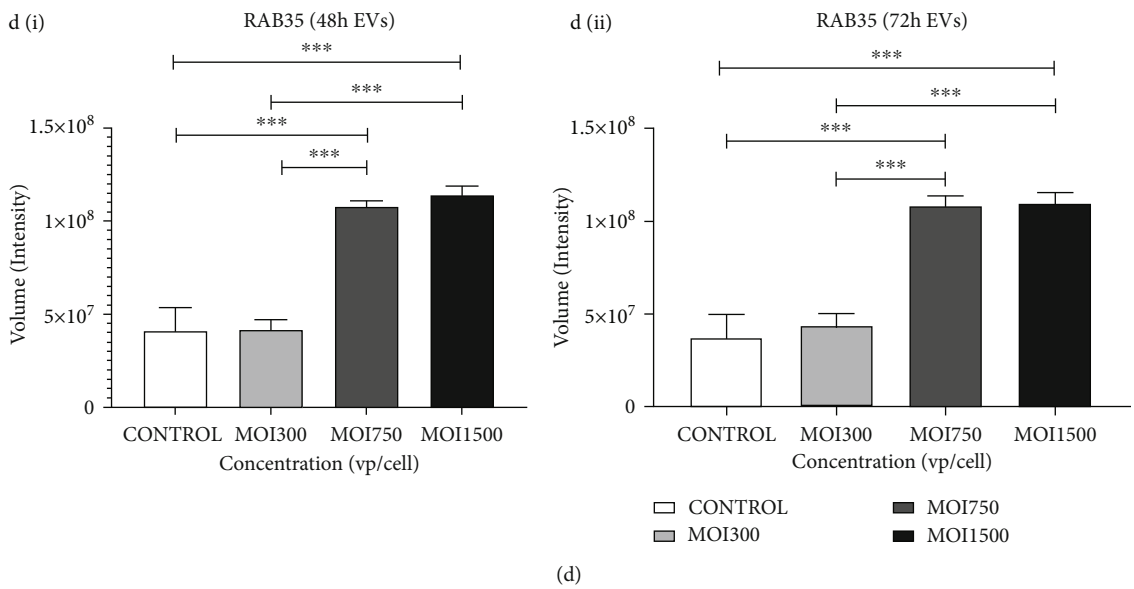


Figure 3: The effect of HAdV3 infection on intracellular trafficking GTPase. (a) Dot blot analysis showing expression of Rab5, Rab7, and Rab35 after 48 h and 72 h infection. EVs were probed for the presence of Rab proteins. (b) (i) Graphs showing quantification of Rab5 level after 48 h and (ii) 72 h of infection. (c) (i) Rab7 after 48 h and (ii) 72 h of infection. (d) (i) Rab35 after 48 h and (ii) 72 h of infection. Data show the mean ± SEM from three independent experiments. Dots shown in the figure are representative of four independent experiments. Data shows the mean ± SEM from four independent experiments and performed using one-way analysis of variance (ANOVA) with Tukey post hoc analysis. Statistical significance is indicated by the mean ± SD as follows: $^{*}p < 0.05$, $^{**}p < 0.01$, $^{***}p < 0.001$, and $^{****}p < 0.0001$.

in the dot blot analysis. These findings suggest that Hsps are regulated during HAdV3 infection. We speculate that the heat shock protein modulation might be a response to increased cell death.

*3.7. HAdV3 Induced Pathogen Recognition and Proinflammatory Response.* We measured the expression of toll-like receptor (TLR)7 in A549 cell-derived EV post-infection. TLR7 is a key regulator that induces activation of NF-$\kappa$B. It controls the expression of immune and inflammatory response-related genes [28]. We found that at MOI 300, 750, and 1500, HAdV3 significantly increased the expression of TLR7 in a dose-dependent approach after 48 h and 72 h ($p \leq 0.001$ and $p \leq 0.0008$) (Figure 6(c)). These results are consistent with previous reports that TLR7 activation modulates and reduces the damaging effects of inflammation [28]. We further examined the effect of HAdV3 exposure on the expression of histone H2A.x (Figure 6(e)), a well-known marker of double-stranded DNA damage [28]. MOI 300 and 750 significantly increase histone H2A.x expression after 48 h and more at 72 h ($^{**}p \leq 0.002$) but declined significantly at MOI 1500 when compared to the untreated supporting previous findings [28] ($p \leq 0.01$). These results suggest that there is evidence of cell injury/death which could be dose and time dependent.

*3.8. Infection Modulates Apoptotic Activation.* Caspases are usually activated in response to cells undergoing stress and are triggered in a variety of conditions (i.e., infections and/or chemical stimuli). The proteolytic cleavage of caspases is a unique characteristic of apoptotic cell death. The presence of cleaved caspase 1 indicates the active form of the protein, which causes an apoptotic cascade. Levels of cleaved caspase 1 in A549-derived EVs were significantly upregulated in a time- and dose-dependent manner at 48 and 72 h ($^{**}p \leq 0.001$ and $^{**}p \leq 0.001$) (Figure 6(d)). Our results indicate that HAdV3 infection modulates the trafficking of apoptotic proteins within EVs. We found that HAdV3 induced a significant increase in expression of cleaved caspase-1 with increased MOI and when compared to the untreated cells.

*3.9. EV Cargoes Include Innate Immune Response Modulator.* We determine the level of inflammatory marker interleukin (IL)-1$\beta$, a transcription activator in the innate immune response to viral infection induced upon infection of A549 cells with HAdV3. HAdV3 infection induced a significant increase in IL-1$\beta$ protein levels in infected A549-derived EVs when compared to control-derived EVs ($^{***}p \leq 0.0009$, $^{**}p \leq 0.003$, and $^{**}p \leq 0.004$) (Figures 7(a) and 7(c)). To further examine EV cargo, we validated the presence of transmembrane tetraspanins CD9 and oxidative stress activation protein Hsp70 using the western blot technique. Also, we examine immune activation modulators interferons (IRF)3 and 8 which take part in antigen processing and presentation. We detected a significant increase in IRF3 levels at all MOIs after 48 h and 72 h infection. Additionally, there was a slight increase in IRF8 gene expressions at 48 and 72 h time points (Figure 7(b)). Results confirmed the expressions of Hsp70 and CD9. Moreover, the results showed that HAdV3 infection of A549 modulates major immune responses *in vitro* which was revealed in IL-1$\beta$ and IRF-3 expression.

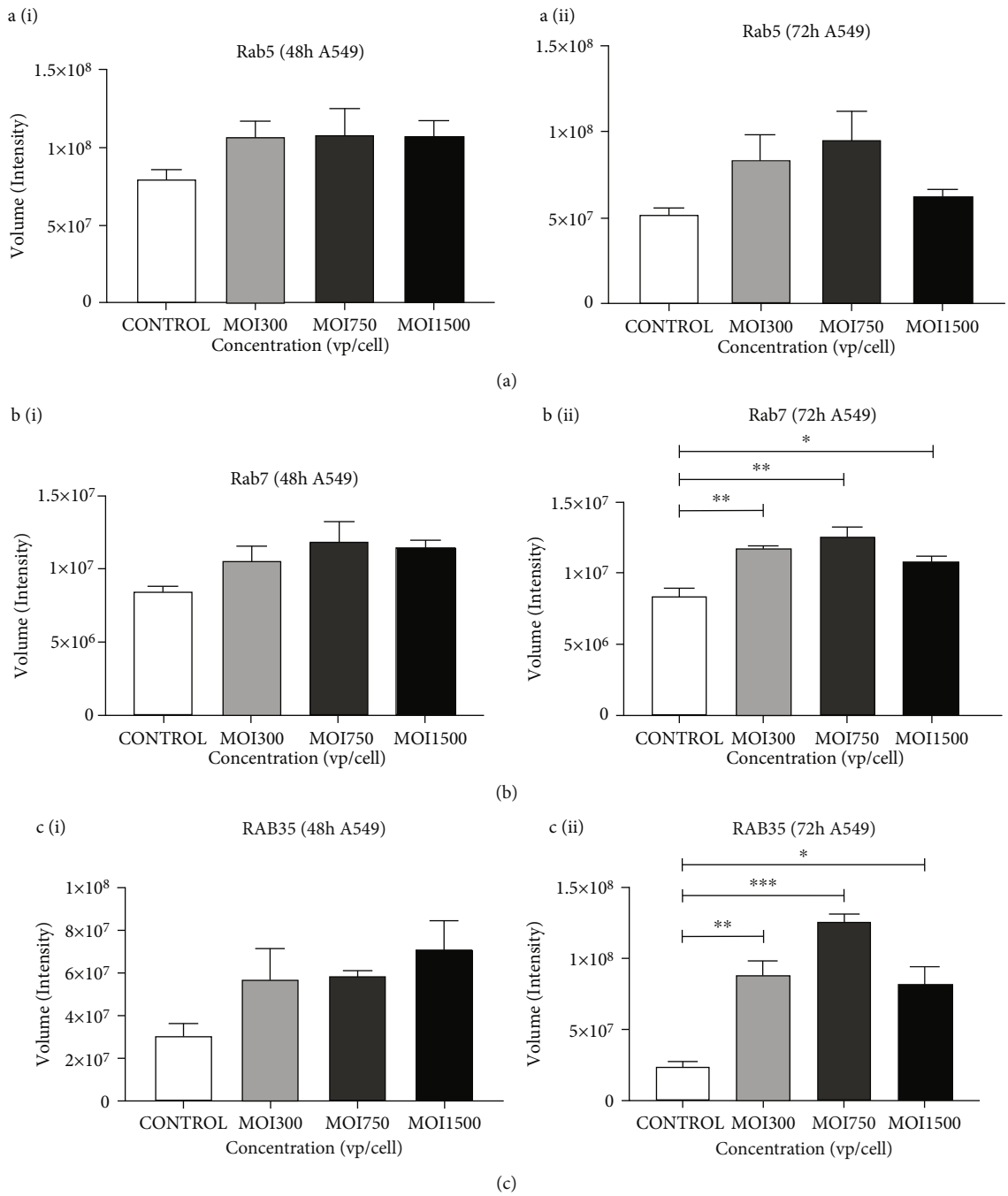


Figure 4: The effect of HAdV3 infection on intracellular trafficking GTPase in A549 lysate. (a) Quantification of dot blot analysis showing expression of Rab5, Rab7, and Rab35 after 48 h and 72 h infection. A549 cell lysate was probed for the presence of Rab proteins. (a) (i) Graphs showing quantification of Rab5 level after 48 h and (ii) 72 h of infection. (b) (i) Rab7 after 48 h and (ii) 72 h of infection. (c) (i) Rab35 after 48 h and (ii) 72 h of infection. Dots shown in the figure are representative of four independent experiments. Data shows the mean ± SEM from four independent experiments and performed using one-way analysis of variance (ANOVA) with Tukey post hoc analysis. Statistical significance is indicated by the mean ± SD as follows: $^{*}p < 0.05$, $^{**}p < 0.01$, $^{***}p < 0.001$, and $^{****}p < 0.0001$.

## 4. Discussion

EVs isolated from HAdV3-infected A549 cells are known to convey viral proteins that play vital roles in viral infection progression and transfer to bystander cells. The concept of EV-mediated viral infection advancement has been previously reported [51–54]. Cells infected with adenovirus have been shown to release infectious EV enclosing viral particles [6]. Our present findings showed that HAdV3 infection impacted A549-derived EV biogenesis, composition, and trafficking in cells. Our present findings showed significantly modulated exosomal markers and reduction in A549 cell viability at MOI 300, 750, and 1500 after 72 h infection relative to uninfected cells. This indicates that HAdV3 infection

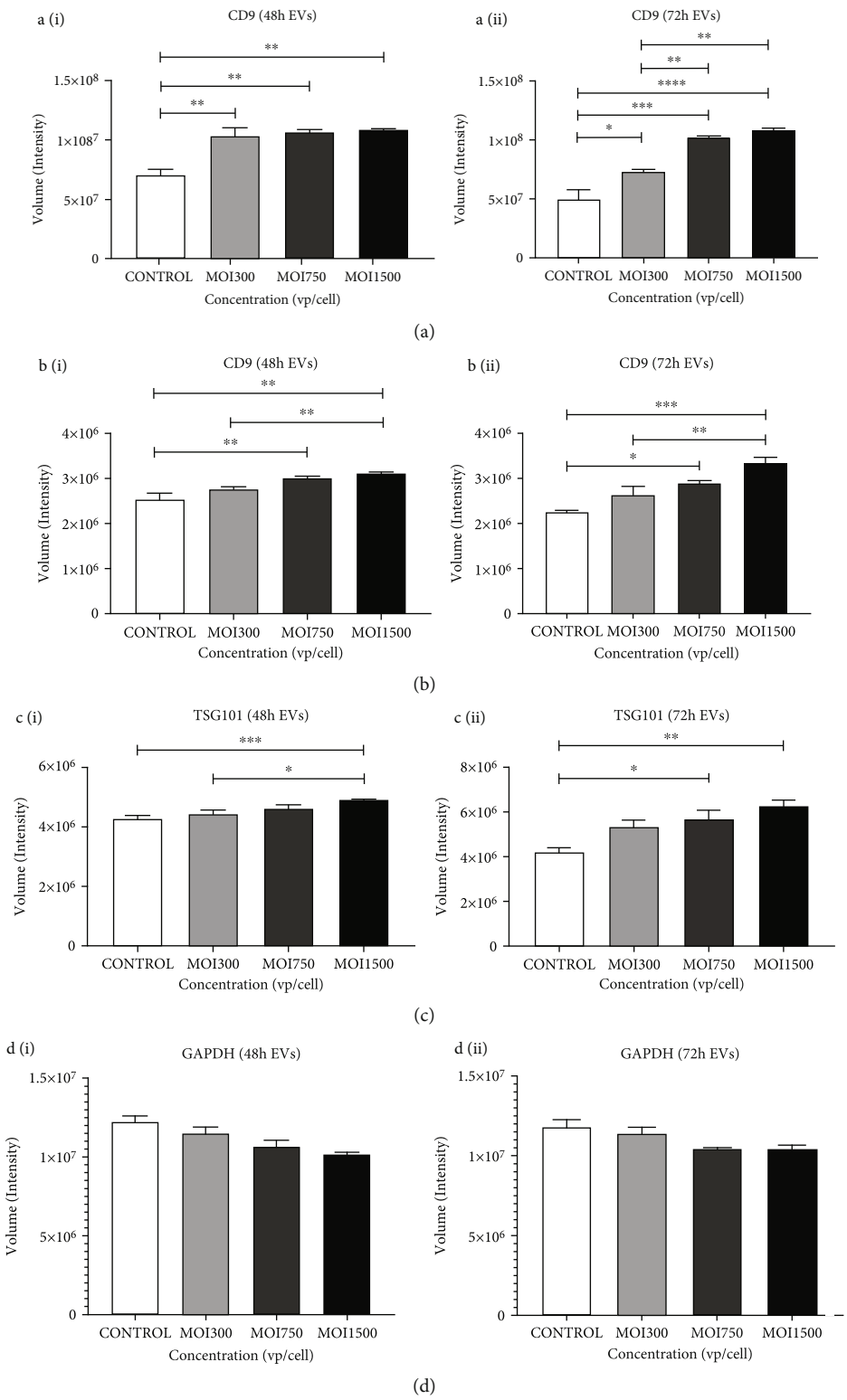


Figure 5: The effect of HAdV3 infection on isolated EV classical markers. Quantification of dot blot analysis showing expression of CD9, CD63, TSG101, and GAPDH expression after 48 h and 72 h infection. EVs were probed for the presence of classical markers. (a) (i) Graph showing quantification of CD9 level after 48 h and (ii) 72 h of infection. (b) (i) CD63 after 48 h and (ii) 72 h of infection .(c) (i) TSG101 after 48 h and (ii) 72 h of infection. (d) (i) GAPDH after 48 h and (ii) 72 h of infection. Dots shown in the figure are representative of four independent experiments. Data show mean ± SEM from three independent experiments. Data show the mean ± SEM from four independent experiments. Data shows the mean ± SEM from four independent experiments and performed using one-way analysis of variance (ANOVA) with Tukey post hoc analysis. Statistical significance is indicated by the mean ± SD as follows: $^{*}p < 0.05$, $^{**}p < 0.01$, $^{***}p < 0.001$, and $^{****}p < 0.0001$.

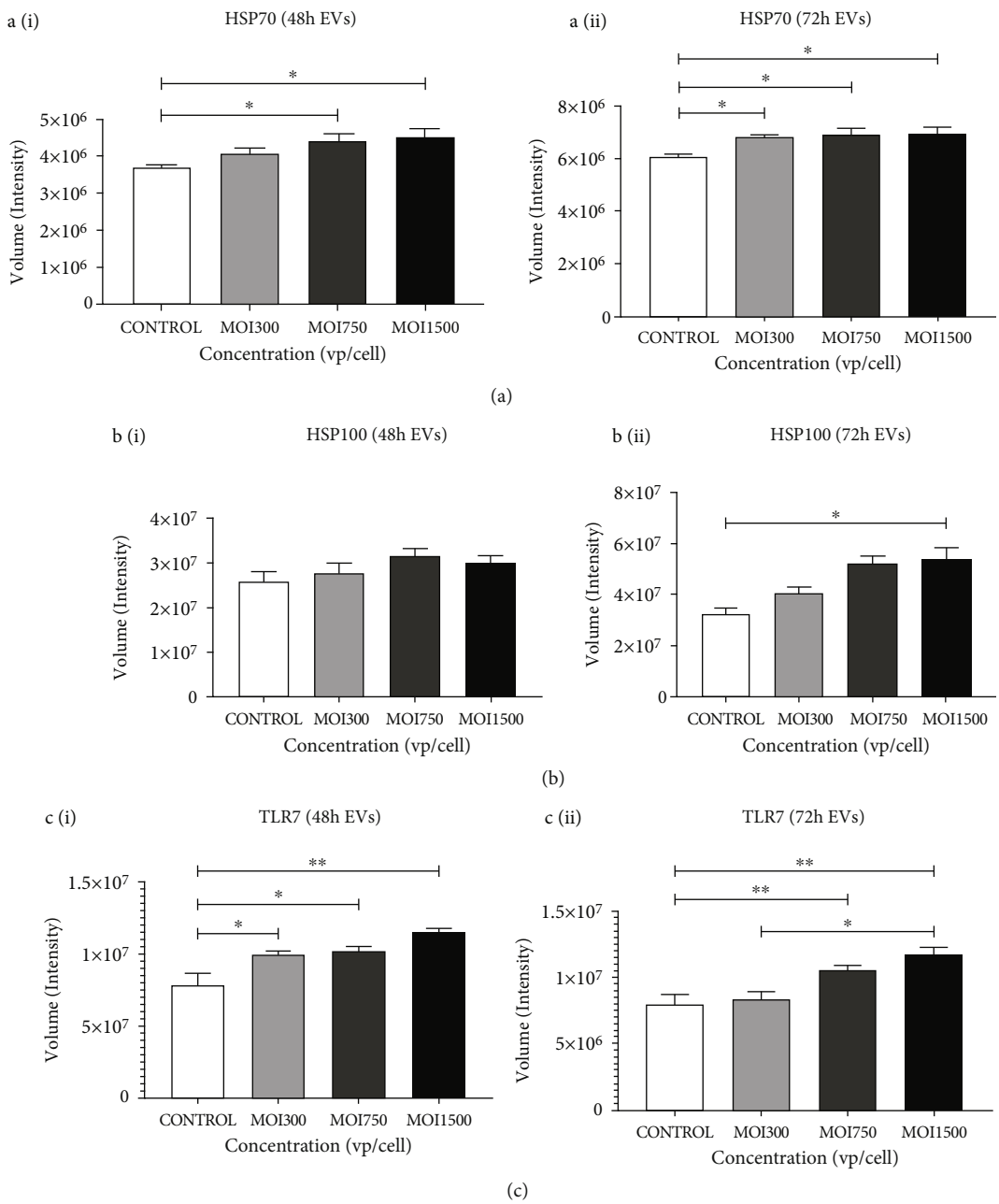


Figure 6: Continued.

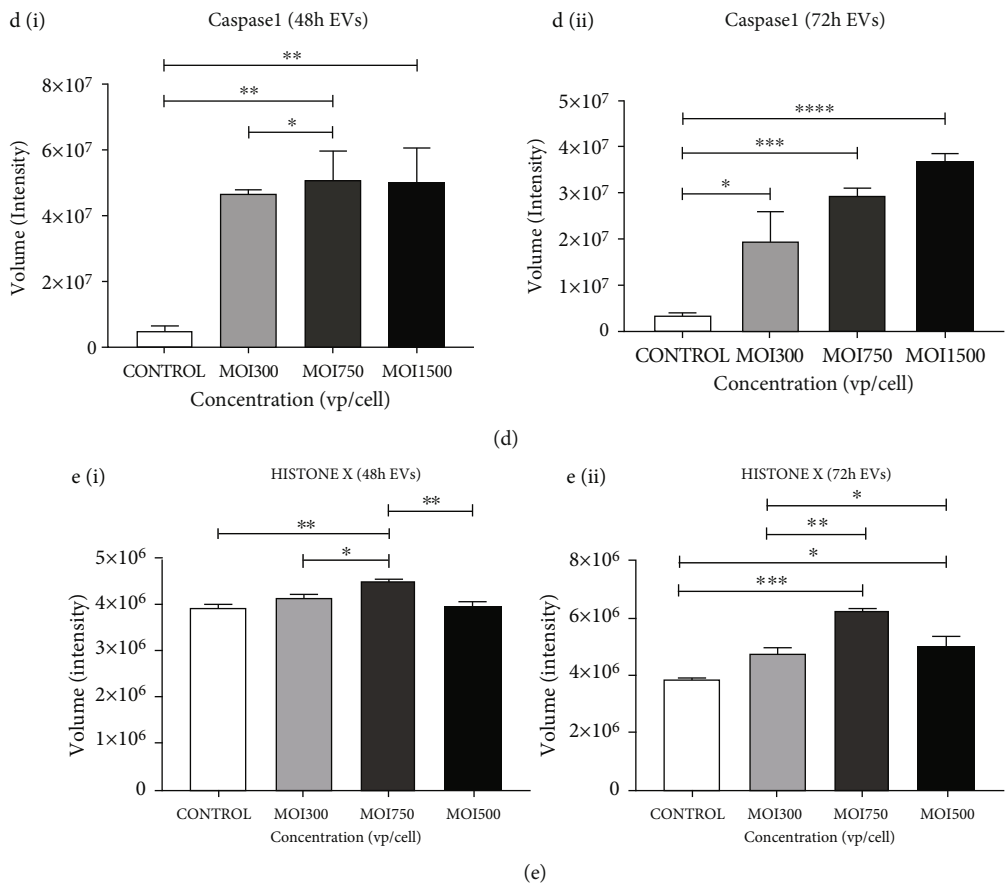


Figure 6: The effect of HAdV3 infection on heat shock protein, Toll-like receptor, and caspase. Quantification of dot blot analysis showing expression of Hsp70, Hsp100, TLR7, caspase 1, and H2A-X expression after 48 h and 72 h infection. EVs were probed for the presence of proteins. (a) (i) Graphs showing quantification of Hsp70 level after 48 h and (ii) 72 h of infection. (b) (i) Hsp100 after 48 h and (ii) 72 h of infection. (c) (i) TLR7 after 48 h and (ii) 72 h of infection. (d) (i) Caspase 1 after 48 h and (ii) 72 h of infection. (e) (i) H2A-X after 48 h and (ii) 72 h of infection. Dots shown in the figure are representative of four independent experiments. Data shows the mean ± SEM from four independent experiments and performed using one-way analysis of variance (ANOVA) with Tukey post hoc analysis. Statistical significance is indicated by the mean ± SD as follows: $^{*}p < 0.05$, $^{**}p < 0.01$, $^{***}p < 0.001$, and $^{****}p < 0.0001$.

of A549 cells induced cell death-associated response which was confirmed via caspase and Hsp activation. Microscopic analysis of isolated EVs suggests that their morphological characteristics, such as size and shape are identical to those already documented. There was no significant difference in the sizes of HAdV3-infected A549 -derived EVs relative to the control. However, there was a significant increase in particles per mL of EVs in the infected group compared to the uninfected, suggesting that HAdV3 infection could impact the release of EVs. Unlike RNA viruses that are known to assemble within the host cell cytoplasm, DNA viruses, such as HAdV3 completes their formation and assembly in the host cell nucleus where they are eventually released via cell lysis [28, 55]. The series of events that would lead to successful encapsulation or packaging of HAdV within EVs will involve migration of virus from the nucleus of host cell before lysis. Viral DNA or protein could be targeted towards being packaged within intraluminal vesicles and then released into the extracellular space [1]. We also found that classical markers CD9, TSG101, and CD63 levels increased in infected EVs in a dose-dependent manner. This is an important finding because tetraspanins, such as CD9 and CD63 expression within EVs can act as a receptor for EVs into bystander cells. In addition, tetraspanins are also involved in cargo loading and sorting of molecules within EVs [28]. Therefore, it is possible that HAdV3 infection stimulates the formation of intraluminal vesicles and facilitates EV release. Rab5 and Rab7 are characteristically associated with the early endosome and late endosomes. Overexpression of Rab5 has been shown to increase the rate of endocytosis and the recycling of the transferrin receptor necessary for iron uptake. Although Rab5 could regulate endocytosis at the level of early endosome-plasma membrane fusion, the mechanism remains yet to be understood. Conversely, Rab7 has been known to regulate the intracellular trafficking involving early to late endosome formation [28]. Studies have shown that both Rab5 and Rab7 significantly stimulate uptake of horseradish peroxidase by germ cells such as oocytes. Rab35 is also a small GTPase that is involved in various cellular processes, including membrane trafficking, cytokinesis, lipid homeostasis, immunity, and phagocytosis. They are known to facilitate membrane trafficking of early endosomes across the plasma membrane to the cell surface. Other roles include regulating epithelial

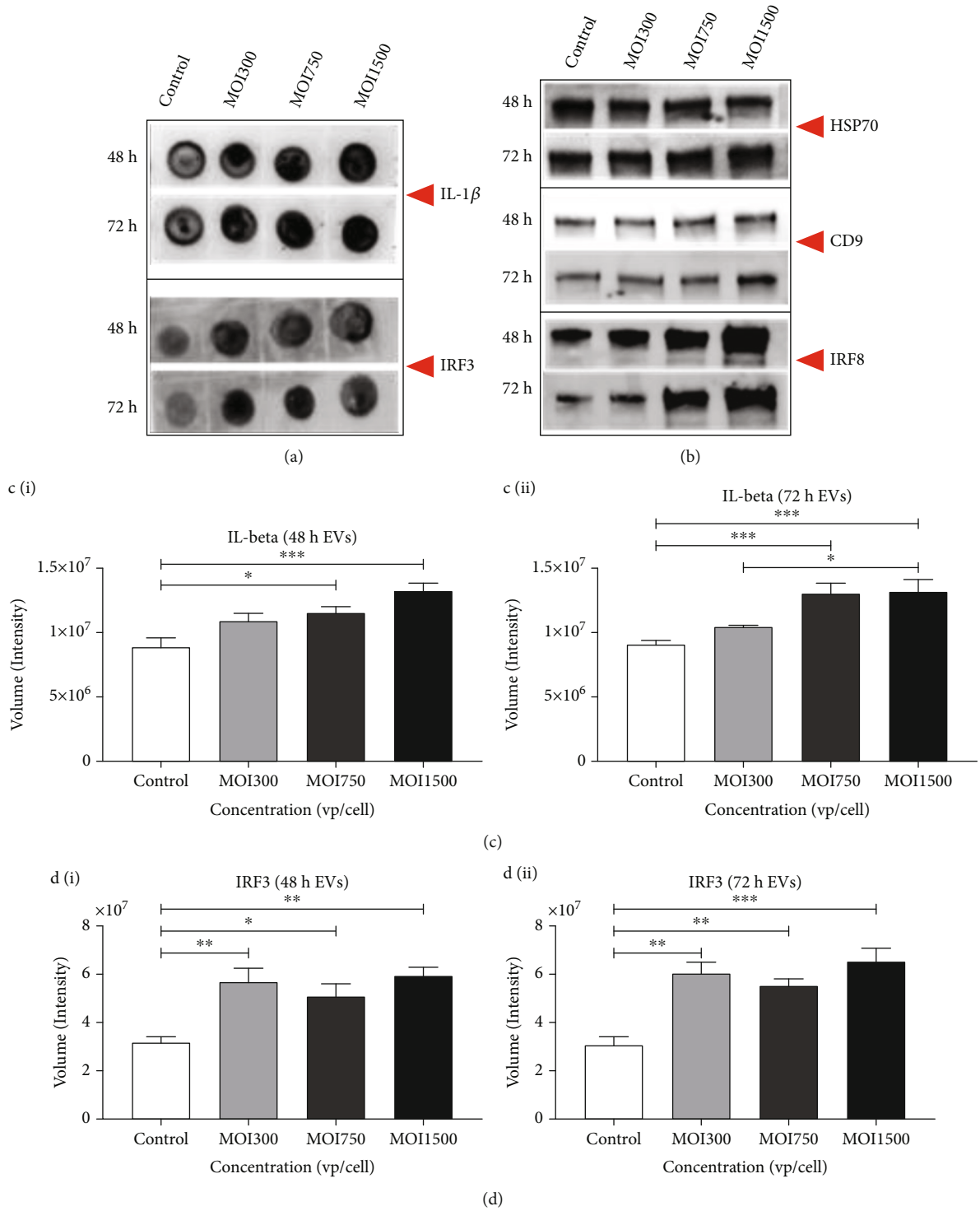


Figure 7: The effect of HAdV3 infection on proinflammatory interleukin and interferon. (a) Dot blot analysis showing expression of IL-1$\beta$ and TLR7 after 48 h and 72 h infection. EVs were probed for the expression of IL-1$\beta$ and TLR7 proteins. (b) Western blot analysis showing Hsp70, CD9, and IRF8 expression after 48 h and 72 h of infection. (c) (i) Graph showing quantification of IL-1$\beta$ after 48 h and (ii) 72 h of infection. (d) (i) IRF-3 after 48 h and (ii) 72 h of infection. Dots shown in the figure are representative of four independent experiments. Data shows the mean ± SEM from four independent experiments and performed using one-way analysis of variance (ANOVA) with Tukey post hoc analysis. Statistical significance is indicated by the mean ± SD as follows: $^{*}p < 0.05$, $^{**}p < 0.01$, $^{***}p < 0.001$, and $^{****}p < 0.0001$.

polarity and epithelia interpolation. Disruption of circulating Rab35 has been linked to some types of neurological disease, such as Parkinson's disease. Herein, we reported that Rab5, 7, and 35 levels were altered in the cell lysate during HAdV3 infection. The data presented in this study illustrated a significant increase in Rab5 and Rab7 protein

expression in EVs at 48 h and 72 h in a dose-dependent manner. However, their levels decreased at MOI 1500 at 48 and 72 h in cell lysates. This result was not unanticipated, as it is similar to what was observed in a previous study [28] showing that exposure decreased Rab7 in hepatocytes. We also found a slight modulation of DIS3, a putative catalytic component of the RNA-exosome complex with a $3'$-$5'$ exonuclease activity known to contribute to cellular RNA processing and degradation usually in response to inflammation (data not shown, see Supplementary Figures 8a and 8f), although this was different from a study carried out by Jones et al. (2021) where complex of RRP44/DIS3 level was elevated in response to lipopolysaccharide administration in mice [56]. This difference in results might be a result of synergy in the complex of RRP44/DIS3 or due to intricacies in immune response *in vivo* in comparison to *in vitro* response because RRP44 in EVs of eukaryotic cells are known to play a major role in the recognition and degradation of targeted RNA [56, 57].

A549-derived EVs at 48 and 72 h infection contained significant levels of Hsps 70 and 100. Our studies demonstrated a vast range of expressions within Hsp70. One very important role of Hsp70 is its ability to prevent detrimental proinflammatory responses. It is believed that increased expression of Hsp70 with an increase in infection time is an effort to increase the chance of cell survival [28]. Hsp70 is known as one of the most sensitive Hsps and it is considered an important regulator of response to thermal stress. Other Hsps, such as Hsp22, 27, 60, and 90$\beta$, were detected in the A549 cell but negligible quantity (data not shown). Studies have shown that Hsps play vital roles in carcinogenesis and could be a suitable marker for cancer detection and treatment [58]. Detection of caspase 1 revealed increased protein level in infected EVs post-infection at 48 and 72 h infection in a dose-dependent approach. Caspases have been known to be an important player in EV-mediated cell-to-cell communication and the transfer of biomolecules [59, 60]. Results showed a significant increase in cleaved caspase 1 expression at increased viral particle per cell. We also documented a significant increase in caspase 9 expression notably after 72 h infection in highly infected cell-derived EVs. Caspase 9 is an important protein essential to intrinsic apoptosis pathway function [61]. Data presented by our study suggests that EVs released from HAdV3-infected A549 cells bear stress and apoptotic markers which were evident in the cell viability and morphology after infection and that HAdV3-induced death in A549 cells could be chiefly through an intrinsic apoptosis program rather than extrinsic [60–62]. We assessed another important EV surface molecule that is commonly found on certain cell types but is crucial for distinguishing EVs' parent cells. Syncytin-1, a member of the endogenous retroviral group encoded by human endogenous retrovirus genes, is present at the surface of EVs produced by placenta-derived syncytiotrophoblast and a major player in EV uptake. We investigate their expression since they also play a major role in EV uptake by bystander cells. Syncytin-1 expression in A549-derived EVs was significantly increased at all doses of HAdV3 after 48 h and 72 h infection (see Supplementary Figure 8c). This result indicates that EVs that are released by infected cells might be actively taken up by neighboring cells, a process that might have been influenced by syncytin expression on EV surface [63].

## 5. Conclusion

The inconsistency and inability to establish a universally efficient technique for endogenous EV purification and identification coupled with complexities in the detection of biomarkers at the subcellular level are a few of the various challenges that need to be overcome in order to fully address the relevance of EVs in disease diagnosis and their potential therapeutic applications. Our study employed high- and low-speed ultracentrifugation methods which seem to be proficient in preserving isolated EVs' integrity. We found that *in vitro* HAdV3 infection significantly impacts cell viability and survival, which was confirmed in HAdV3-infected A549 EV triggering stress responses and apoptotic signals. Furthermore, HAdV3 infection did trigger an increase in tetraspanins and endosome formation-related marker(s). In summary, we offer the perspective that *in vitro* viral infection of A549 cell culture produced EVs in response to infection and that EVs produced could play a vital role in viral progression. This study demonstrates that during viral-induced stress, A549-derived EVs can effectively package markers and proteins that are indicative of viral effects on lung cell physiology. Further study to investigate the mechanism of EV uptake using the bystander assay with virally derived EV is important. The outcome of this study could increase the understanding of EVs in viral infection and highlight its prospective importance in therapeutic application.

## Data Availability

The original data will be maintained by the corresponding author. Information pertaining to the datasets will be made available upon written request.

## Disclosure

The funders had no role in the study design, data collection, and analysis, the decision to publish, or the preparation of the manuscript.

## Conflicts of Interest

The authors declare that they have no conflicts of interest.

## Authors' Contributions

Writing the original draft was done by A.I. Writing the review and editing was done by S.K. Writing the review and editing was done by B.S. Writing the review and editing was done by Q.L.M. B.J.C. and R.P. contributed to the experimental design. A.I. executed the experiments. All authors contributed to the article and approved the submitted version.

## Acknowledgments

Special recognition is due to the High-Resolution Imaging Facility Service Center who provided NTA at the University of Alabama at Birmingham. This work was funded by the National Institutes of Health (# 1R15DA045564-01) and the National Science Foundation (# IOS-1900377).

## Supplementary Materials

Dot blot analyses of caspase 9, syncytin, LAMP-H, MHC-I, and DIS3. *(Supplementary Materials)*

## References

[1] B. J. Crenshaw, L. B. Jones, C. R. Bell, S. Kumar, and Q. L. Matthews, "Perspective on adenoviruses: epidemiology, pathogenicity, and gene therapy," *Biomedicine*, vol. 7, no. 3, p. 61, 2019.

[2] F. Huang, J. Bai, J. Zhang et al., "Identification of potential diagnostic biomarkers for pneumonia caused by adenovirus infection in children by screening serum exosomal microRNAs," *Molecular Medicine Reports*, vol. 19, no. 5, pp. 4306–4314, 2019.

[3] A. Yoshimura, "Adenovirus-induced leakage of co-endocytosed macromolecules into the cytosol," *Cell Structure and Function*, vol. 10, no. 4, pp. 391–404, 1985.

[4] Q. L. Matthews, "Capsid-incorporation of antigens into adenovirus capsid proteins for a vaccine approach," *Molecular Pharmaceutics*, vol. 8, no. 1, pp. 3–11, 2011.

[5] J. R. Radke and J. L. Cook, "Human adenovirus infections: update and consideration of mechanisms of viral persistence," *Current Opinion in Infectious Diseases*, vol. 31, no. 3, pp. 251–256, 2018.

[6] M. Garofalo, A. Villa, N. Rizzi et al., "Extracellular vesicles enhance the targeted delivery of immunogenic oncolytic adenovirus and paclitaxel in immunocompetent mice," *Journal of Controlled Release*, vol. 294, pp. 165–175, 2019.

[7] H. V. Trinh, G. Lesage, V. Chennamparampil et al., "Avidity binding of human adenovirus serotypes 3 and 7 to the membrane cofactor CD46 triggers infection," *Journal of Virology*, vol. 86, no. 3, pp. 1623–1637, 2012.

[8] A. L. Farrow, B. J. Peng, L. Gu, A. Krendelchtchikov, and Q. L. Matthews, "A novel vaccine approach for Chagas disease using rare adenovirus serotype 48 vectors," *Viruses*, vol. 8, no. 3, p. 78, 2016.

[9] G. Sailaja, H. HogenEsch, A. North, J. Hays, and S. K. Mittal, "Encapsulation of recombinant adenovirus into alginate microspheres circumvents vector-specific immune response," *Gene Therapy*, vol. 9, no. 24, pp. 1722–1729, 2002.

[10] W. J. Lee, H. D. Jung, H. M. Cheong, and K. Kim, "Molecular epidemiology of a post-influenza pandemic outbreak of acute respiratory infections in Korea caused by human adenovirus type 3," *Journal of Medical Virology*, vol. 87, no. 1, pp. 10–17, 2015.

[11] L. James, M. O. Vernon, R. C. Jones et al., "Outbreak of human adenovirus type 3 infection in a pediatric long-term care facility–Illinois, 2005," *Clinical Infectious Diseases*, vol. 45, no. 4, pp. 416–420, 2007.

[12] E. E. Thacker, L. Timares, and Q. L. Matthews, "Strategies to overcome host immunity to adenovirus vectors in vaccine development," *Expert Review of Vaccines*, vol. 8, no. 6, pp. 761–777, 2009.

[13] S. Boppana, A. Fiore-Gartland, A. Bansal, and P. Goepfert, "Cross-reactive CD8 T-cell responses elicited by adenovirus type 5-based HIV-1 vaccines contributed to early viral evolution in vaccine recipients who became infected," *Journal of Virology*, vol. 94, no. 2, 2020.

[14] D. E. Chondronasiou, T. J. Eisden, A. Stam et al., "Improved induction of anti-melanoma T cells by adenovirus-5/3 fiber modification to target human DCs," *Vaccines*, vol. 6, no. 3, p. 42, 2018.

[15] A. K. Adhikary, "Genomic diversity of human adenovirus type 3 isolated in Fukui, Japan over a 24-year period," *Journal of Medical Microbiology*, vol. 66, no. 11, pp. 1616–1622, 2017.

[16] E. Haque, U. Banik, T. Monwar, L. Anthony, and A. K. Adhikary, "Worldwide increased prevalence of human adenovirus type 3 (HAdV-3) respiratory infections is well correlated with heterogeneous hypervariable regions (HVRs) of hexon," *PLoS One*, vol. 13, no. 3, article e0194516, 2018.

[17] J. H. Campos, R. P. Soares, K. Ribeiro, A. Cronemberger Andrade, W. L. Batista, and A. C. Torrecilhas, "Extracellular vesicles: role in inflammatory responses and potential uses in vaccination in cancer and infectious diseases," *Journal of Immunology Research*, vol. 2015, Article ID 832057, 14 pages, 2015.

[18] A. O. Ipinmoroti and Q. L. Matthews, "Extracellular vesicles: roles in human viral infections, immune-diagnostic, and therapeutic applications," *Pathogens*, vol. 9, no. 12, p. 1056, 2020.

[19] C. Wen, R. C. Seeger, M. Fabbri, L. Wang, A. S. Wayne, and A. Y. Jong, "Biological roles and potential applications of immune cell-derived extracellular vesicles," *Journal of Extracellular Vesicles*, vol. 6, no. 1, article 1400370, 2017.

[20] M. Garofalo, A. Villa, N. Rizzi, L. Kuryk, V. Mazzaferro, and P. Ciana, "Systemic administration and targeted delivery of immunogenic oncolytic adenovirus encapsulated in extracellular vesicles for cancer therapies," *Viruses*, vol. 10, no. 10, p. 558, 2018.

[21] Y. Zhang, J. Wu, H. Zhang, J. Wei, and J. Wu, "Extracellular vesicles-mimetic encapsulation improves oncolytic viro-immunotherapy in tumors with low Coxsackie and adenovirus receptor," *Frontiers in Bioengineering and Biotechnology*, vol. 8, article 574007, 2020.

[22] N. A. Kutchy, E. S. Peeples, S. Sil et al., "Extracellular vesicles in viral infections of the nervous system," *Viruses*, vol. 12, no. 7, p. 700, 2020.

[23] N. Mukhamedova, A. Hoang, D. Dragoljevic et al., "Exosomes containing HIV protein Nef reorganize lipid rafts potentiating inflammatory response in bystander cells," *PLoS Pathogens*, vol. 15, no. 7, article e1007907, 2019.

[24] B. Sims, A. L. Farrow, S. D. Williams et al., "Role of TIM-4 in exosome-dependent entry of HIV-1 into human immune cells," *International Journal of Nanomedicine*, vol. Volume 12, pp. 4823–4833, 2017.

[25] B. Sims, A. L. Farrow, S. D. Williams, A. Bansal, A. Krendelchtchikov, and Q. L. Matthews, "Tetraspanin blockage reduces exosome-mediated HIV-1 entry," *Archives of Virology*, vol. 163, no. 6, pp. 1683–1689, 2018.

[26] B. Sims, L. Gu, A. Krendelchtchikov, and Q. L. Matthews, "Neural stem cell-derived exosomes mediate viral entry," *International Journal of Nanomedicine*, vol. 9, pp. 4893–4897, 2014.

[27] S. Kodidela, K. Gerth, S. Haque et al., "Extracellular vesicles: a possible link between HIV and Alzheimer's disease-like pathology in HIV subjects?," *Cell*, vol. 8, no. 9, p. 968, 2019.

[28] L. Mashouri, H. Yousefi, A. R. Aref, A. M. Ahadi, F. Molaei, and S. K. Alahari, "Exosomes: composition, biogenesis, and mechanisms in cancer metastasis and drug resistance," *Molecular Cancer*, vol. 18, no. 1, p. 75, 2019.

[29] R. P. McNamara, L. M. Costantini, T. A. Myers et al., "Nef secretion into extracellular vesicles or exosomes is conserved across human and simian immunodeficiency viruses," *MBio*, vol. 9, no. 1, article e02344, 2018.

[30] S. G. Antimisiaris, S. Mourtas, and A. Marazioti, "Exosomes and exosome-inspired vesicles for targeted drug delivery," *Pharmaceutics*, vol. 10, no. 4, p. 218, 2018.

[31] B. J. Crenshaw, L. Gu, B. Sims, and Q. L. Matthews, "Exosome biogenesis and biological function in response to viral infections," *The Open Virology Journal*, vol. 12, no. 1, pp. 134–148, 2018.

[32] M. Kakizaki, Y. Yamamoto, S. Yabuta, N. Kurosaki, T. Kagawa, and A. Kotani, "The immunological function of extracellular vesicles in hepatitis B virus-infected hepatocytes," *PLoS One*, vol. 13, no. 12, article e0205886, 2018.

[33] P. S. Perez, M. A. Romaniuk, G. A. Duette et al., "Extracellular vesicles and chronic inflammation during HIV infection," *The Journal of Infectious Diseases*, vol. 8, no. 1, article 1687275, 2019.

[34] A. Benito-Martin, A. di Giannatale, S. Ceder, and H. Peinado, "The new deal: a potential role for secreted vesicles in innate immunity and tumor progression," *Frontiers in Immunology*, vol. 6, p. 66, 2015.

[35] M. Garofalo, H. Saari, P. Somersalo et al., "Antitumor effect of oncolytic virus and paclitaxel encapsulated in extracellular vesicles for lung cancer treatment," *Journal of Controlled Release*, vol. 283, pp. 223–234, 2018.

[36] S. Maacha, A. A. Bhat, L. Jimenez et al., "Extracellular vesicles-mediated intercellular communication: roles in the tumor microenvironment and anti-cancer drug resistance," *Molecular Cancer*, vol. 18, no. 1, p. 55, 2019.

[37] G. Benichou and A. Prunevieille, "Graft-derived exosomes. When small vesicles play a big role in transplant rejection," *American Journal of Transplantation*, vol. 18, no. 7, pp. 1585-1586, 2018.

[38] C. Keryer-Bibens, C. Pioche-Durieu, C. Villemant et al., "Exosomes released by EBV-infected nasopharyngeal carcinoma cells convey the viral latent membrane protein 1 and the immunomodulatory protein galectin 9," *BMC Cancer*, vol. 6, no. 1, p. 283, 2006.

[39] P. Nagpal, D. B. Descalzi-Montoya, and N. Lodhi, "The circuitry of the tumor microenvironment in adult and pediatric Hodgkin lymphoma: cellular composition, cytokine profile, EBV, and exosomes," *Cancer Reports*, vol. 4, no. 2, article e1311, 2021.

[40] S. Y. Teow, K. Liew, A. S. Khoo, and S. C. Peh, "Pathogenic role of exosomes in Epstein-Barr virus (EBV)-associated cancers," *International Journal of Biological Sciences*, vol. 13, no. 10, pp. 1276–1286, 2017.

[41] R. A. Barclay, P. Khatkar, G. Mensah et al., "An omics approach to extracellular vesicles from HIV-1 infected cells," *Cells*, vol. 8, no. 8, p. 787, 2019.

[42] S. Kumar, Q. L. Matthews, and B. Sims, "Effects of cocaine on human glial-derived extracellular vesicles," *Frontiers in Cell and Development Biology*, vol. 8, article 563441, 2021.

[43] C. R. Bell, L. B. Jones, B. J. Crenshaw et al., "The role of lipopolysaccharide-induced extracellular vesicles in cardiac cell death," *Biology*, vol. 8, no. 4, p. 69, 2019.

[44] S. Kumar, B. J. Crenshaw, S. D. Williams, C. R. Bell, Q. L. Matthews, and B. Sims, "Cocaine-specific effects on exosome biogenesis in microglial cells," *Neurochemical Research*, vol. 46, no. 4, pp. 1006–1018, 2021.

[45] M. J. van Gils, E. M. Bunnik, B. D. Boeser-Nunnink et al., "Longer V1V2 region with increased number of potential N-linked glycosylation sites in the HIV-1 envelope glycoprotein protects against HIV-specific neutralizing antibodies," *Journal of Virology*, vol. 85, no. 14, pp. 6986–6995, 2011.

[46] W. M. Henne, N. J. Buchkovich, and S. D. Emr, "The ESCRT pathway," *Developmental Cell*, vol. 21, no. 1, pp. 77–91, 2011.

[47] D. Wei, W. Zhan, Y. Gao et al., "RAB31 marks and controls an ESCRT-independent exosome pathway," *Cell Research*, vol. 31, no. 2, pp. 157–177, 2021.

[48] F. Zhou, Z. Wu, M. Zhao et al., "Rab5-dependent autophagosome closure by ESCRT," *The Journal of Cell Biology*, vol. 218, no. 6, pp. 1908–1927, 2019.

[49] P. Sheehan, M. Zhu, A. Beskow, C. Vollmer, and C. L. Waites, "Activity-dependent degradation of synaptic vesicle proteins requires Rab35 and the ESCRT pathway," *The Journal of Neuroscience*, vol. 36, no. 33, pp. 8668–8686, 2016.

[50] G. H. Dar, C. C. Mendes, W.-L. Kuan et al., *GAPDH Controls Extracellular Vesicle Biogenesis and Enhances Therapeutic Potential of EVs in Silencing the Huntingtin Gene in Mice via siRNA Delivery*, bioRxiv, 2020.

[51] R. Bello-Morales and J. A. Lopez-Guerrero, "Extracellular vesicles in herpes viral spread and immune evasion," *Frontiers in Microbiology*, vol. 9, p. 2572, 2018.

[52] N. Altan-Bonnet, "Extracellular vesicles are the Trojan horses of viral infection," *Current Opinion in Microbiology*, vol. 32, pp. 77–81, 2016.

[53] I. E. Andras, A. Leda, M. G. Contreras et al., "Extracellular vesicles of the blood-brain barrier: role in the HIV-1 associated amyloid beta pathology," *Molecular and Cellular Neurosciences*, vol. 79, pp. 12–22, 2017.

[54] H. M. van Dongen, N. Masoumi, K. W. Witwer, and D. M. Pegtel, "Extracellular vesicles exploit viral entry routes for cargo delivery," *Microbiology and Molecular Biology Reviews*, vol. 80, no. 2, pp. 369–386, 2016.

[55] O. Pornillos, J. E. Garrus, and W. I. Sundquist, "Mechanisms of enveloped RNA virus budding," *Trends in Cell Biology*, vol. 12, no. 12, pp. 569–579, 2002.

[56] L. B. Jones, S. Kumar, C. R. Bell et al., "Lipopolysaccharide administration alters extracellular vesicles in cell lines and mice," *Current Microbiology*, vol. 78, no. 3, pp. 920–931, 2021.

[57] J. C. Zinder, E. V. Wasmuth, and C. D. Lima, "Nuclear RNA exosome at 3.1 Å reveals substrate specificities, RNA paths, and allosteric inhibition of Rrp44/Dis3," *Molecular Cell*, vol. 64, no. 4, pp. 734–745, 2016.

[58] T. N. Bukong, F. Momen-Heravi, K. Kodys, S. Bala, and G. Szabo, "Exosomes from hepatitis C infected patients transmit HCV infection and contain replication competent viral RNA in complex with Ago2-miR122-HSP90," *PLoS Pathogens*, vol. 10, no. 10, article e1004424, 2014.

[59] R. Kakarla, J. Hur, Y. J. Kim, J. Kim, and Y. J. Chwae, "Apoptotic cell-derived exosomes: messages from dying cells," *Experimental & Molecular Medicine*, vol. 52, no. 1, pp. 1–6, 2020.

[60] S. J. Park, J. M. Kim, J. Kim et al., "Molecular mechanisms of biogenesis of apoptotic exosome-like vesicles and their roles as damage-associated molecular patterns," *Proceedings of the National Academy of Sciences of the United States of America*, vol. 115, no. 50, pp. E11721–E11730, 2018.

[61] A. M. Cochran and J. Kornbluth, "Extracellular vesicles from the human natural killer cell line NK3.3 have broad and potent anti-tumor activity," *Developmental Biology*, vol. 9, article 698639, 2021.

[62] H. Wu, M. Fu, J. Liu et al., "The role and application of small extracellular vesicles in gastric cancer," *Molecular Cancer*, vol. 20, no. 1, p. 71, 2021.

[63] A. Vargas, S. Zhou, M. Ethier-Chiasson et al., "Syncytin proteins incorporated in placenta exosomes are important for cell uptake and show variation in abundance in serum exosomes from patients with preeclampsia," *The FASEB Journal*, vol. 28, no. 8, pp. 3703–3719, 2014.

Hindawi
Journal of Immunology Research
Volume 2021, Article ID 2939693, 12 pages
https://doi.org/10.1155/2021/2939693

*Research Article*

# Stress Induces Release of Extracellular Vesicles by *Trypanosoma cruzi* Trypomastigotes

**Camilla Ioshida Vasconcelos,[1] A Cronemberger-Andrade,[2] Normanda Souza-Melo,[3] Juliana Terzi Maricato,[4] Patrícia Xander,[1] Wagner Luiz Batista,[1] Rodrigo Pedro Soares,[5] Sergio Schenkman,[3] and Ana Claudia Torrecilhas[1]**

[1]*Departamento de Ciências Farmacêuticas, UNIFESP, Rua São Nicolau, 210, 09913-030, Diadema, São Paulo, Brazil*
[2]*Cell Therapy Institute, Spinal Cord Injury and Tissue Regeneration Center Salzburg (SCI-TReCS), Paracelsus Medical University (PMU), 5020 Salzburg, Austria*
[3]*Departamento de Microbiologia, Imunologia e Parasitologia, UNIFESP, Rua Pedro de Toledo, 669, 04039-032 São Paulo, Brazil*
[4]*Departamento de Microbiologia, Imunologia e Parasitologia, UNIFESP, Rua Botucatu, 862, 04023-062 São Paulo, Brazil*
[5]*Instituto René Rachou/FIOCRUZ-MG, Av. Augusto de Lima, 1715, 30190-009 Belo Horizonte, Minas Gerais, Brazil*

Correspondence should be addressed to Sergio Schenkman; sschenkman@unifesp.br
and Ana Claudia Torrecilhas; ana.torrecilhas@unifesp.br

Received 14 June 2021; Accepted 26 August 2021; Published 24 September 2021

Academic Editor: Ilaria Roato



All extracellular forms of *Trypanosoma cruzi*, the causative agent of Chagas disease, release extracellular vesicles (EVs) containing major surface molecules of the parasite. EV release depends on several mechanisms (internal and external). However, most of the environmental conditions affecting this phenomenon are still unknown. In this work, we evaluated EV release under different stress conditions and their ability to be internalized by the parasites. In addition, we investigated whether the release conditions would affect their immunomodulatory properties in preactivated bone marrow-derived macrophages (BMDM). Sodium azide and methyl-cyclo-$\beta$-dextrin (CDB) reduced EV release, indicating that this phenomenon relies on membrane organization. EV release was increased at low temperatures (4°C) and acidic conditions (pH 5.0). Under this pH, trypomastigotes differentiated into amastigotes. EVs are rapidly liberated and reabsorbed by the trypomastigotes in a concentration-dependent manner. Nitrosative stress caused by sodium nitrite in acid medium or *S*-nitrosoglutathione also stimulated the secretion of EVs. EVs released under all stress conditions also maintained their proinflammatory activity and increased the expression of iNOS, Arg 1, IL-12, and IL-23 genes in IFN-$\gamma$ and LPS preactivated BMDM. In conclusion, our results suggest a budding mechanism of release, dependent on the membrane structure and parasite integrity. Stress conditions did not affect functional properties of EVs during interaction with host cells. EV release variations under stress conditions may be a physiological response against environmental changes.

## 1. Introduction

The flagellated protozoan *Trypanosoma cruzi* is the etiological agent of Chagas disease, affecting 8 million people worldwide. Approximately 100 million people are at risk of infection, causing about 2,000 deaths per year. These circumstances make this disease a serious health problem [1, 2]. In the bloodstream of the mammalian vertebrate host, trypomastigote forms invade various cell types, differentiate into amastigotes, and proliferate in their cytoplasm.

Trypomastigotes derived from infected mammalian cell cultures release extracellular vesicles (EVs) in the culture medium. They express major protozoan surface molecules [2], including mucin-like glycoproteins, glycosylphosphatidyl inositol phospholipids (GIPLs), and members of the gp85/*trans*-sialidase (TS) superfamily of glycoproteins [3].

EV release promotes parasite infectivity and modulates the host's innate and acquired immune responses [4–10]. However, mechanisms involved in EV release by the parasites facing adverse environmental conditions are still poorly understood. Those may include diverse body fluids (e.g., blood), extracellular matrix, and contact with chemical agents. As a part of a wider study on *T. cruzi* EVs, we sought to characterize their release under different conditions (temperature, pH, and chemical agents). We also evaluated if *T. cruzi* EVs released under stress conditions were functionally affected during interaction with bone marrow-derived macrophages.

## 2. Material and Methods

*2.1. Animal Ethics.* The experimental procedures used in this study were approved by the Animal Use Ethics Committee (CEUA) of the Federal University of São Paulo (http://www.unifesp.br/reitoria/ceua) under protocol # 9254110216.

*2.2. Parasite Cultures.* Trypomastigotes (Y-strain) were obtained from the supernatant of infected LLC-$MK_2$ cells maintained in low-glucose DMEM (Vitrocell Embriolife), supplemented with 10% fetal bovine serum (SFB) (Vitrocell Embriolife). Trypomastigotes were collected from the cell culture medium from the fifth to the ninth day after infection by centrifugation ($1{,}000 \times g$ for 15 min). They were washed with PBS, and the pellet containing the parasites was resuspended in 1 mL DMEM. Parasite concentration was estimated using a Neubauer (Reichert) chamber.

*2.3. EV Release Assays.* Trypomastigotes ($1 \times 10^7$) were incubated for 2 h in DMEM with/without FBS containing 5% glucose, at distinct temperatures and pH levels, and/or in the presence of metabolic inhibitors and nitroxidative compounds ($NaN_3$ and $NaNO_2$) and methyl-$\beta$cyclodextrin (CBD). The assays were always performed in triplicate. After incubation, trypomastigotes were centrifuged ($1{,}000 \times g$ for 15 min) (MiniSpin plus, Eppendorf) and supernatants were collected for measuring EVs' size and concentration. To determine viability, 90 $\mu$L of the parasite's suspension was added to each well of a 96-well plate and mixed with 10 $\mu$L of the PrestoBlue (Thermo Fisher Scientific). Plates were incubated (37°C, 2 h), and fluorescence was detected by excitation at 560 nm and emission at 590 nm (Synergy HT, BioTek). Parasites incubated without any agent were used as negative controls, and the results were expressed as relative fluorescence units. In parallel, trypomastigotes were centrifuged ($3{,}000 \times g$, 5 min) and the supernatant was discarded. The pellet was resuspended in PBS, dried on glass coverslips, fixed in methanol, and washed with 2X running water. Then, parasites were stained with Giemsa (Merck) diluted 1 : 10 in running water and mounted with Entellan (Merck). Images were acquired under an optical microscope. 300 parasites/slide were counted, and *T. cruzi* morphology was analyzed (Imager.A2, Zeiss).

*2.4. Isolation of T. cruzi Trypomastigote EVs.* The total shed material released by the trypomastigotes was centrifuged ($10{,}000 \times g$, 15 min). After centrifugation, the supernatant was filtered using a 0.22 $\mu$m filter (Sarstedt) and ultracentrifuged ($100{,}000 \times g$, 1 h, 4°C) (Sorvall WX Ultra Series 80, rotor T890, Thermo Scientific). The pellet containing EVs was resuspended in 5 mL of sterile PBS and submitted to a new ultracentrifugation under the same conditions. EVs were recovered from the pellet, resuspended in sterile PBS, and stored at 4°C. The procedures follow the Minimal Information for Studies of Extracellular Vesicles 2018 [11].

*2.5. Scanning Electronic Microscopy (SEM).* Poly L-lysine solution (200 $\mu$L) at 0.01% (Sigma-Aldrich), prefiltered through a 0.22 $\mu$m pore size filter, was added onto circular coverslips (13 mm, Glasscyto). After 30 min, the poly L-lysine solution was removed, and the wells washed with filtered water and covered with 50 $\mu$L containing $1 \times 10^6$ trypomastigotes in PBS. After 30 min incubation at room temperature (RT), parasites were fixed (2.5% glutaraldehyde in 0.1 M sodium cacodylate buffer), followed by 1 h incubation (RT). Samples were stored (4°C) prior to electron microscopy scanning at the Federal University of São Paulo facility (CEME, UNIFESP), as previously described [5].

*2.6. Nanoparticle Tracking Analysis (NTA).* The material released by the parasites was characterized by size and concentration using NTA (NanoSight, NS 300, Malvern, equipped with a CCD camera). Samples were either analyzed pure or diluted (1 : 10) in filtered PBS. Each capture was performed in triplicate always using the same threshold (24.7–24.9°C, 30 sec, camera level set to 10). Results were expressed in concentration (particles/mL), size, and distribution of EVs using NTA software (version 2.3 build 0017).

*2.7. EV Labeling and Reincorporation in the Parasite.* Purified EVs were concentrated by ultracentrifugation (18 h at $100{,}000 \times g$) and particles ($5 \times 10^8$/mL incubated with 2 $\mu$M PKH26 Red Fluorescent cell dye (MINI26, Sigma-Aldrich). After 30 min at 37°C (dark), the mixture was diluted 5x with PBS and ultracentrifuged (18 h, $100{,}000 \times g$). The pellet was resuspended with Diluent C, and the number of EVs determined by NTA. Different concentrations of labeled EVs were incubated with trypomastigotes ($1 \times 10^6$ /mL) in DMEM containing 5% glucose. Parasites were collected by centrifugation at different time points (5 min at $1{,}000 \times g$), washed once with PBS, and resuspended in PBS-0.5% p-formaldehyde. Samples were analyzed by flow cytometry (Fortessa, BD).

*2.8. Bone Marrow-Derived Macrophage (BMDM) Interaction with T. cruzi EVs.* Bone marrow cells obtained from 6- to 8-week-old female C57Bl/6 mice were submitted to differentiation in macrophages by culturing for 7 days in RPMI (Vitrocell Embriolife) culture medium containing 10% FBS, with the addition of L929 supernatant as previously described [12]. $1 \times 10^6$ macrophages were plated in 6-well plates. The cells were stimulated for 12 h with 50 ng/mL IFN-$\gamma$ and 500 ng/mL LPS (L2330, Sigma-Aldrich). These preactivated macrophages were then incubated for 24 h with $1 \times 10^8$ EVs released by *T. cruzi* from different conditions.

Table 1: Oligonucleotides used for amplification, sequence, and gene of each target gene.

| Oligonucleotide | Sequence | Gene |
|---|---|---|
| Arg1Fow | 5′-GAGACAGGGAAGTCTGAAGCAC | Arginase 1 |
| Arg1Rev | 5′-CATTGGCTTGCGAGACGTAGAC | Arginase 1 |
| iNOS Fow | 5′-ATGGACCAGTATAAGGCAAGC | iNOS |
| iNOS Rev | 5′-GCTCTGGATGAGCCTATATTG | iNOS |
| IL-23p19 Fow | 5′ AATAATGTGCCCCGTATCCAG | IL–23p19 |
| IL-23p19Rev | 5′ GCTCCCCTTTGAAGATGTCAG | IL–23p19 |
| IL-12p35 Rev | 5′-ACGAGAGTTGCCTGGCTACTA | IL-12p35 |
| IL-12p35Fow | 5′-CCTCATAGATGCTACCAAGGCAC | IL-12p35 |
| IL-12p40 Fow | 5′-TTGAACTGGCGTTGGAAGCACG | IL–12p40 |
| IL-12p40 Rev | 5′-CCACCTGTGAGTTCTTCAAAGGC | IL–12p40 |
| Ym2Fow | 5′-GTGACCCTACTGTTAGTGCTGG | YM2 |
| Ym2Rev | 5′CGGGAAGACAATAACTGCACCC | YM2 |
| IL-10 Fow | 5′GACTTTAAGGGTTACCTGGGTTG | IL-10 |
| IL-10 Rev | 5′TCACATGCGCCTTGATGTCTG | IL-10 |
| GAPDH forward | 5′AAATGGTGAAGGTCGGTGTG | GAPDH |
| GAPDH reverse | 5′TGAGGGGTCGTTGATGG | GAPDH |

The cell culture supernatant was stored at 4°C for analysis by NTA, and the cells were extracted for cytokine analysis.

*2.9. Gene Expression by qRT-PCR.* RNA was extracted from BMDM using RNeasy Plus Microkit (QIAGEN). All samples were also submitted to fluorometry analysis and DNAse treatment. Complementary DNA (cDNA) synthesis was performed using SuperScript II reverse transcriptase kit (Life Technologies), as previously described [13, 14]. Gene expression (qRT-PCR) used SYBR Green-based system detection (Applied Biosystems, Life Technologies). Each reaction was composed of 2 $\mu$M of forward and reverse oligonucleotides for each target gene (expression levels were normalized to those of the GAPDH control), 10 $\mu$L of the SYBR Green PCR master mix (Applied Biosystems), and 3 $\mu$L of cDNA 1 : 2.5 diluted cDNA. Cycling reactions were carried out in the Applied Biosystems 7500 System (Applied Biosystems) starting with one cycle of 50°C (2 min) and 95°C (1 min), followed by 45 cycles at 95°C (15 sec) and 60°C (1 min). Melting curves were determined with an additional cycle of 95°C (15 sec), 60°C (20 sec), and 95°C (15 sec), as previously described [13]. The reference genes using the $2^{(-\Delta\Delta Ct)}$ cycle threshold method, as previously described [13, 15, 16]. All qRT-PCR procedures were performed following the MIQE guidelines [16]. Each reaction was made in triplicate. The oligonucleotides used for amplification of each target gene are described in Table 1.

*2.10. Statistical Analysis.* Statistical analysis was performed using GraphPad Prism version 6 (GraphPad Software, La Jolla, CA, United States). Data were analyzed using one-way ANOVA test. $p$ values < 0.05 were considered significant.

## 3. Results

*3.1. Kinetics of EV Release under Different Conditions.* To follow the process of EV release by trypomastigotes derived from infected mammalian cells, their kinetics under different conditions were evaluated. EVs were collected after 30 minutes of parasite resuspension in the serum-free DMEM containing 5% glucose. The release was higher at 4°C (Figure 1(a)). At 37°C, EVs increased progressively in the supernatant and reached a maximal value at 120 minutes. The number of particles released by the parasites was significantly higher after incubation of trypomastigotes at 4°C compared to 26°C and 37°C (Figure 1(b)), without changes in size (Figure 1(c)). In all cases, the size of EVs was approximately 150 nm, as detected by NTA. SEM also showed a larger amount of material associated with the parasites at 4°C compared to those at 26°C and 37°C (Figures 1(d)–1(f)). No significant differences in the PrestoBlue signal activity, suggesting that the cell metabolic activity was not largely affected in trypomastigotes (Figure 1(g)) that were preincubated for 2 h from 4 to 37°C as shown underneath each image.

To evaluate parasites' ability to release/uptake EVs, they were labeled with PKH26 fluorescent probe, a dye that is incorporated into the glycocalyx of the membranes. Labeled EVs were incubated with trypomastigotes at 4°C or 37°C. A concentration-dependent increase not only in the internal fluorescence but also in the percentage of fluorescent parasites was detected (Figures 1(h) and 1(i)). This confirms that EVs in the medium can be reincorporated.

*3.2. EV Release Depends on Membrane Integrity.* To test the hypothesis that EV release could depend on membrane integrity [17], parasites were pretreated with $\beta$-methyl-

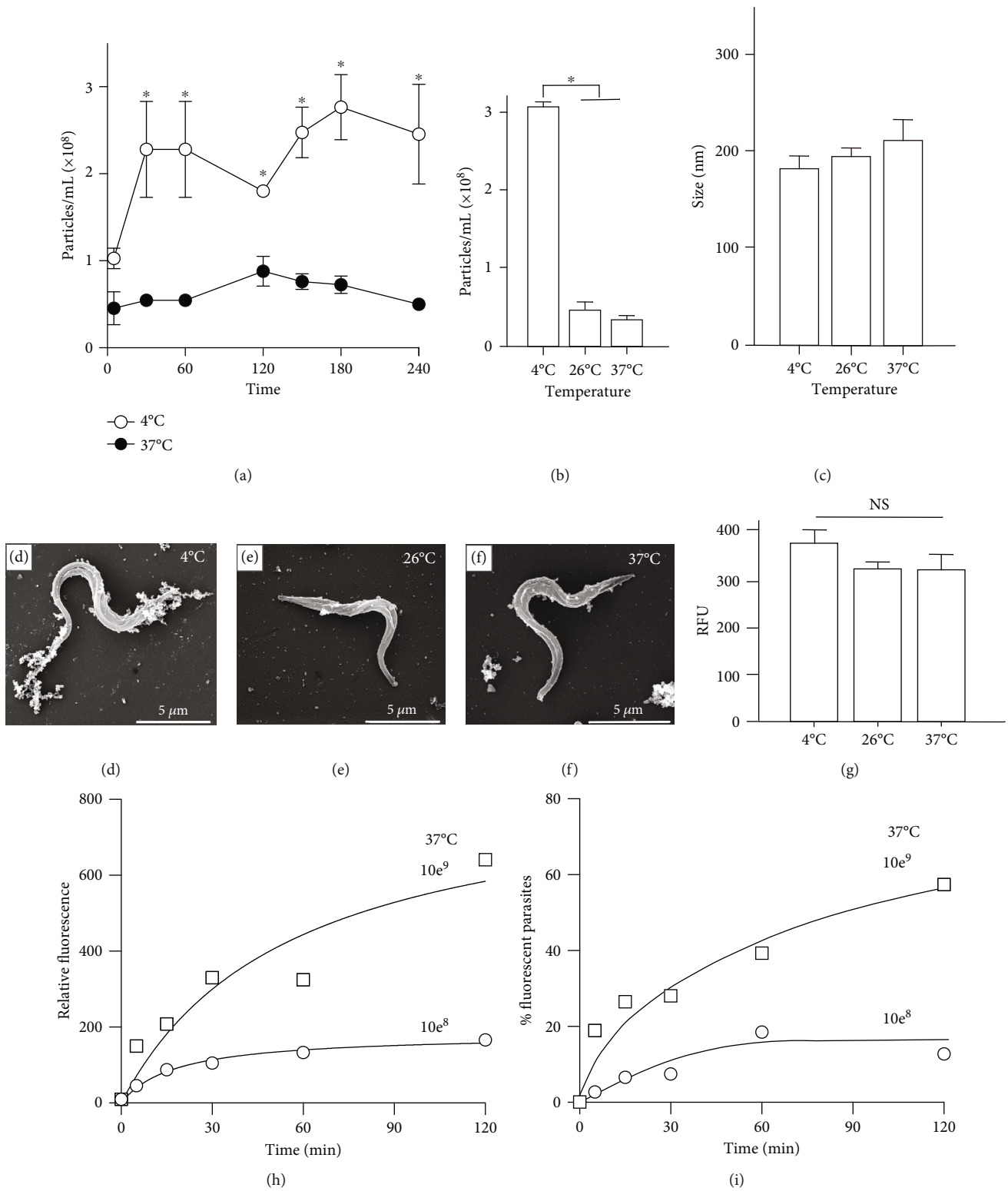


Figure 1: Kinetics of EV release by *T. cruzi* trypomastigote forms. $1 \times 10^7$ trypomastigotes were incubated in DMEM supplemented with 5% glucose at different temperatures. EV concentrations were determined at different time points by NTA (see Material and Methods). The panels show total EV concentration (a, b) and particle size (c) in the supernatants after 2 h of incubation at different temperatures ($^*<0.05$). SEM images of trypomastigotes incubated for 2 h at 4°C (d), 26°C (e), and 37°C ((f), size bars = 5 $\mu$m). Panel (g) indicates the correspondent relative fluorescence (RFU) of PrestoBlue viability reagent (mean and standard deviation, $n = 3$) showing no significant (NS) differences ($p > 0.05$). EVs labeled with PKH26 ($1 \times 10^8$/mL and $10^9$/mL) were incubated with $1 \times 10^7$ trypomastigotes/mL (37°C). The parasites were collected at different time points, and the median of fluorescence (h) or the percentage of labeled parasites (i) was evaluated by flow cytometry. Results are average values in triplicate measurements.

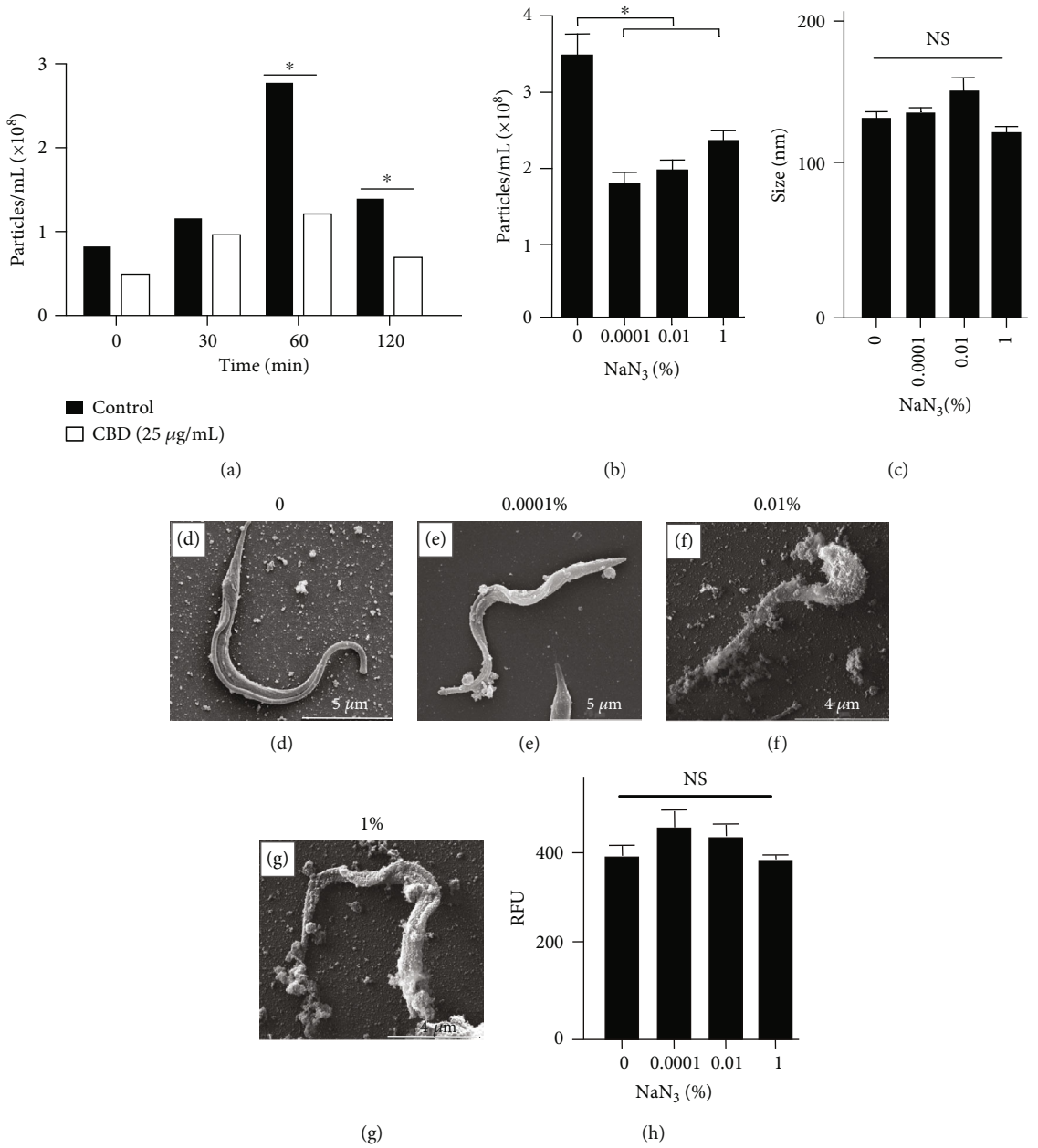


Figure 2: EV release (particles/mL), size (nm), and membrane integrity under chemical stress. *Trypanosoma cruzi* trypomastigotes were incubated in the absence or presence of methyl-beta-cyclodextrin (CBD) (25 $\mu$g/mL) or $NaN_3$ (0.0001 to 1%) for 2 h at 37°C. EVs in the supernatant were quantified by NTA in triplicate ($^*p < 0.05$). The panels show EV concentrations (a, b) and size (nm) (c) in the presence of chemical agents. SEM of trypomastigotes preincubated with the indicated concentrations of $NaN_3$ (d–g). Size bars are defined in each image. The relative fluorescence (RFU) of PrestoBlue viability reagent (mean ± standard deviation, $n = 3$) is shown in panel (h).

cyclodextrin (CBD), which affects trypomastigote structure by removing steroids from the membrane surface [18]. At lower concentrations of CBD (0.02 mM), parasites released less EVs than controls (Figure 2(a)). Furthermore, the inhibition was not reestablished up to two hours after treatment, when no morphological changes were detected in the parasites. This suggests that small membrane perturbations affect EV secretion.

*3.3. EV Discharge from the Parasite Is Dependent on Energy Sources.* Since EV release increased at low temperature, the effect of sodium azide, known to partially inhibit *T. cruzi* oxidative phosphorylation and interaction [19, 20], was evaluated. The reductive capacity towards resazurin (PrestoBlue) was detected only at 1% of $NaN_3$ (Figures 2(g) and 2(h)). This suggests that even in the presence of azide, *T. cruzi* is still able to perform oxidative phosphorylation through a modified electron transport chain [19]. Sodium azide decreased the number of EVs in the supernatant of the parasite in all concentrations (Figure 2(b)), but no changes in the size was noticed. SEM images, however, showed that the parasite membrane became more granulated at higher

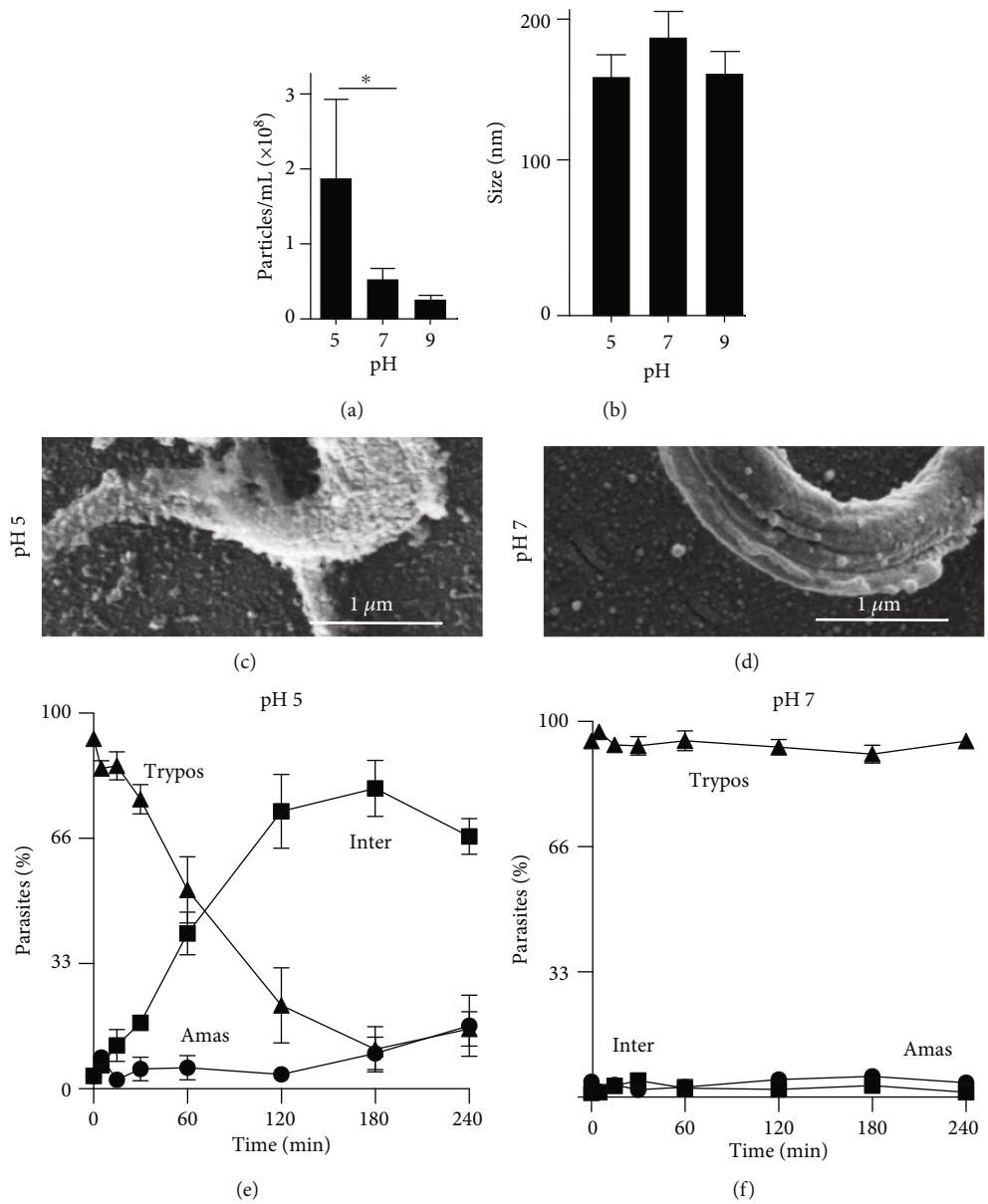


Figure 3: pH effect on EV release. Trypomastigote ($1 \times 10^7$/mL) forms incubated (2 h, 37°C) in culture medium containing 5% glucose previously adjusted to the indicated pH values. EV concentrations (a) and sizes (b) were analyzed by NTA ($^*p < 0.05$). After incubation at pH 5 (c) or pH 7 (d), parasites were analyzed by SEM. In parallel, parasites were incubated at pH 5 (e) or pH 7 (f), stained with Giemsa, and 300 parasites were evaluated according to their form: trypomastigotes (Trypos), intermediate (Inter), or amastigote (Amas). Their percentages were quantified in triplicate.

$NaN_3$ concentrations, and large blebs of parasite membrane are seen attached to the surface (Figures 2(d)–2(g)).

*3.4. Trypomastigote EV Release Is Boosted in Acidic Conditions.* After mammalian cell invasion, the parasite faces pH changes. Therefore, we examined the release of EVs after 2 h of incubation at pH 5, 7, and 9. The parasite did not have significant changes in cell metabolic activity at pH 5, a situation found inside cell lysosomes after cell invasion [21], while some decrease occurred at pH 9. The number of secreted EVs largely increased at pH 5 compared to pH 7 and pH 9 (Figure 3(a)), and there was no variation in the size of EVs (Figure 3(b)). This increased release can be seen by SEM images when trypomastigotes incubated under acidic conditions had more particles covering their surface compared to neutral conditions (Figures 3(c) and 3(d)). As already reported [22], at pH 5, trypomastigotes change shape and after 2 hours, they start to differentiate into amastigotes (Figure 3(e)). At pH 7, they remain unchanged (Figure 3(f)).

*3.5. Effect of Nitrosative Stress in the EV Release.* The major defense that eliminates *T. cruzi* in the mammalian host is nitrosative stress caused by nitric oxide (NO) [23]. We evaluated the effect of distinct $NaNO_2$ concentrations, from 0 to 100 $\mu$M, at pH 5.0 on EV production. At this pH, $NaNO_2$ is soluble and spontaneously produces NO [24–27]. We

observed a small effect in cell viability only at the concentration of 0.05 $\mu$M (Figure 4(a)). However, a major decrease in the size of EVs (Figure 4(b)) along with an increase in $NaNO_2$ was noticed (Figure 4(c)). SEM images showed that parasite integrity was conserved in all groups (Figure 4(d)).

The EV release induced by NO was confirmed by using S-nitrosoglutathione (SNOG), a NO generator that can be used at neutral pH. Trypomastigotes were incubated in DMEM with SNOG (100 $\mu$M), a toxic condition for cells. A decreased metabolic activity was detected (Figure 4(e)). In parallel, parasites released more EVs, reaching a maximum at 180 minutes without significant changes in size (Figures 4(f) and 4(g)) or morphology (Figure 4(h)). These results indicated that EV release by trypomastigotes is increased under nitrosative stress.

*3.6. Immunomodulatory Role of EVs Released under Different Stress Conditions in BMDM.* To investigate the immunomodulatory functions of EVs isolated under different stress conditions, IFN-$\gamma$-treated BMDM were exposed to them; differential gene expression was determined. In general, EVs activated BMDM in a similar manner of LPS, except for IL-12-p40 (Figure 5). No major differences were observed among the different types of EVs, suggesting that their functional cargo properties had a negligible effect under stress conditions.

## 4. Discussion

In nature, parasites deal with numerous environmental changes in vertebrate and invertebrate hosts, including variations in temperature, pH, and reactive oxygen and nitrogen species. In fact, these factors modulate signaling cascades that regulate parasite infection, proliferation, and survival [28]. Previous studies have already shown that different stages of *T. cruzi* release EVs under physiological conditions. They modulate NO and cytokine production by macrophages and delay parasite migration in the gut of vector [29, 30]. Here, several experiments evaluated the role of stress factors affecting EV release by *T. cruzi* trypomastigotes.

Studies on how temperature affects EV release in pathogens are very scarce. Early studies have already shown for *Leishmania mexicana* promastigotes, another trypanosomatid, that EV release increased at 37°C, but not at 4°C [31]. Interestingly, for *T. cruzi* trypomastigotes, we found that larger amounts of EVs accumulate at low temperature (4°C). Changes on the parasite surface organization, known to form patches containing different sets of components in the membrane, may be involved in this process in response to different environments [17]. Such distribution may change with temperature variations. For example, *Leishmania* promastigotes occur in the vector, where temperatures are around 25-26°C, whereas *T. cruzi* trypomastigotes are mainly found in the mammalian host (37°C). Most of the trypomastigote surface is composed of glycosylphosphatidylinositol- (GPI-) anchored proteins [32], and the lipid moieties are largely affected by decreasing the temperature. In fact, changes in temperature are largely sensed by *T. cruzi* triggering changes in gene expression [33]. It is also possible that the accumulation was due to diminished reincorporation at low temperatures. However, this possibility is unlikely as the difference in the release at 4°C was rapid, much faster than the kinetics of reincorporation at 37°C. Consistent with these observations, we observed that trypomastigote EVs are rapidly released and reincorporated. This may explain why after longer incubation periods, the amount of EVs in the supernatant reaches a saturation point. Uptake could be related to interparasite signaling as observed for *T. brucei* [34, 35]. It secretes EVs as nanotubes that are also released in knockouts of the Vps36. This protein is part of the endosomal sorting complexes required for transport (ESCRT) involved in exosome formation. In *T. cruzi* metacyclic trypomastigotes, a stage that corresponds to infective forms generated in the insect vector, EVs confer serum complement resistance in susceptible parasites [9], but in general, paracrine signaling is poorly related in *T. cruzi*. Therefore, more studies are required to evaluate whether EV reincorporation has a role for mammalian stages of *T. cruzi*. Since temperature affects EV secretion, our next step was to evaluate if chemical agents could also modulate this phenomenon in *T. cruzi* trypomastigotes.

Our results showed that methyl-$\beta$-cyclodextrin (CBD) inhibited EV secretion in a concentration that maintains parasite integrity. This supports the idea that the process depends on the membrane bilayer organization. CBD removes sterol, required for the assembly of lipid domains, from membranes [36]. These domains are observed in trypomastigotes, and the presence of lipid chains and cholesterol or ergosterol boundaries might be involved in EV release. In fact, two different EV populations enriched in mucins and members of TS family of glycoproteins are detected [18]. CBD prevents Ca2+-dependent release of EVs from platelets [37] and other cells [38]. Further experiments are required to evaluate whether divalent cations affect EV release and the dependency of the negative charges provided by parasite sialylation. Azide inhibits trypomastigote adhesion to mammalian cells, most likely by preventing lateral diffusion of membrane components [20]. Like CBD, sodium azide also decreased EV production, although no major changes in parasite's viability were detected. Interestingly, at higher concentrations, the parasite surface became more granular, covered with several larger vesicles that remained attached to the membrane. In the same manner, it inhibits EV release. In summary, CBD and azide affected EV release by trypomastigotes without a negligible effect in the size. At higher concentrations, visible effects were detected in the parasite surface morphology.

During their life cycle, trypomastigotes enter mammalian cells, differentiate into amastigotes in parasitophorous vacuole, and can be retained in the cell, which is consistent with both the data in the literature and our own [39]. This is also a common described phenomenon [22, 40] when parasites grow for longer periods in acidified culture medium. Interestingly, here, EV release was increased under acidic conditions and the surface became granular, suggesting significant alterations in membrane. However, like azide, no major changes in the size were detected. Consistent with the literature, at pH 5, trypomastigotes start to differentiate

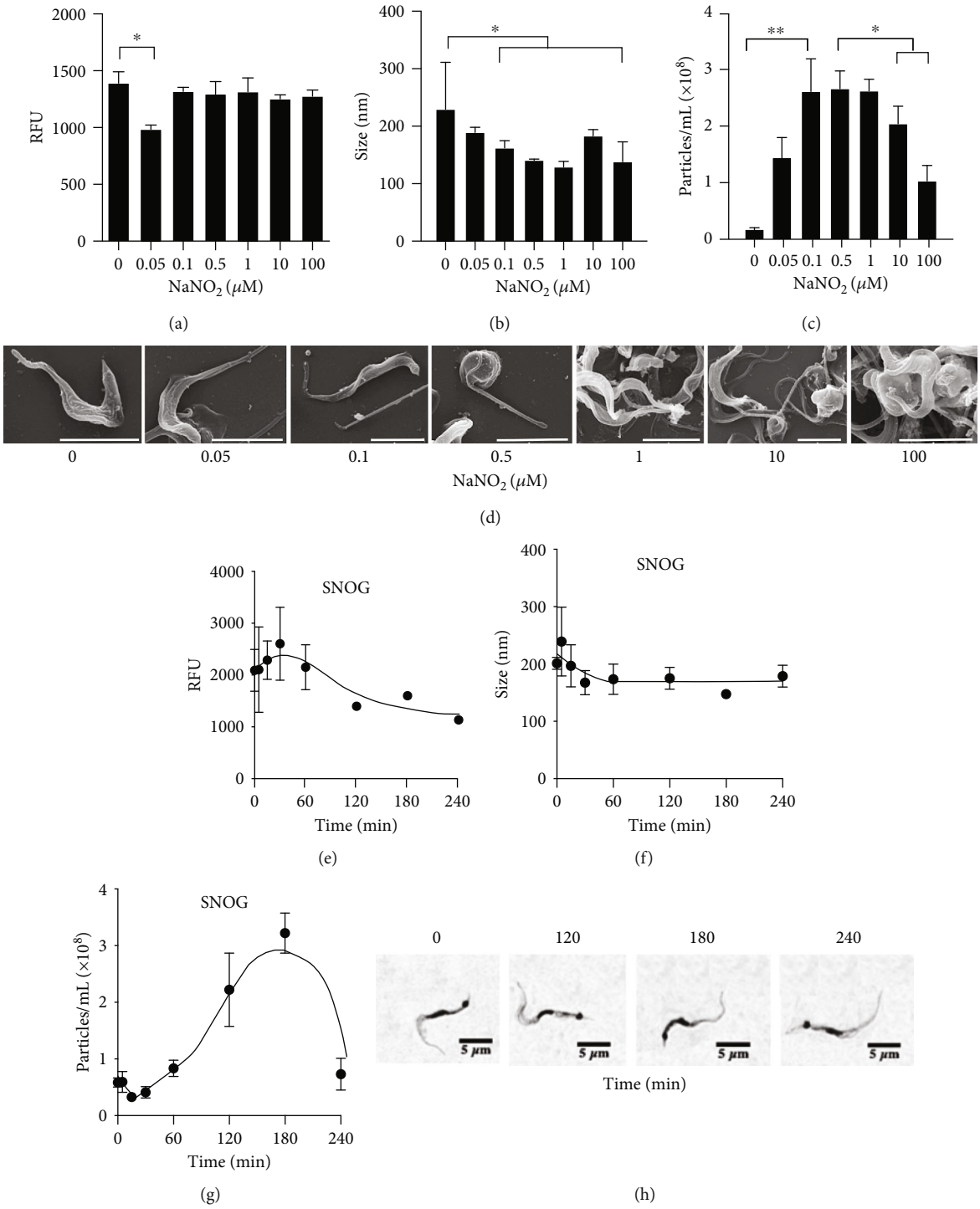


Figure 4: Effect of nitrosative stress on EV release by *T. cruzi* trypomastigotes. $1 \times 10^7$ trypomastigotes were incubated for 2 h at 37°C in culture medium adjusted to pH 5.0 with different concentrations of $NaNO_2$, including the control with the salt. After the incubation period, cell viability was evaluated by the PrestoBlue assay(a) and EV size (nm) (b) and EV concentration (particles/mL) (c) were measured by NTA ($^*p < 0.05$ and $^{**}p < 0.01$). SEM of trypomastigotes releasing EVs incubated under different $NaNO_2$ concentrations (d). Size bars = 5 μm. Alternatively, trypomastigotes were incubated at 37°C in DMEM supplemented with 5% glucose containing 100 μM SNOG. Parasite viability was evaluated at the indicated intervals by PrestoBlue assays (e), and the size (f) and concentration (g) of EVs in the supernatants were determined by NTA ($n = 3$). Panel (h) shows pictures of parasites stained by Giemsa after each incubation period.

into amastigote-like forms. Under acidic conditions, epimastigotes, the forms found in the vector, release membrane lipids [41]. *Trypanosoma cruzi* epimastigotes exhibit changes in morphology, especially in epimastigotes [42], which after 24 h induce large metabolic alterations [43]. However, it is still unclear how acidic conditions induce

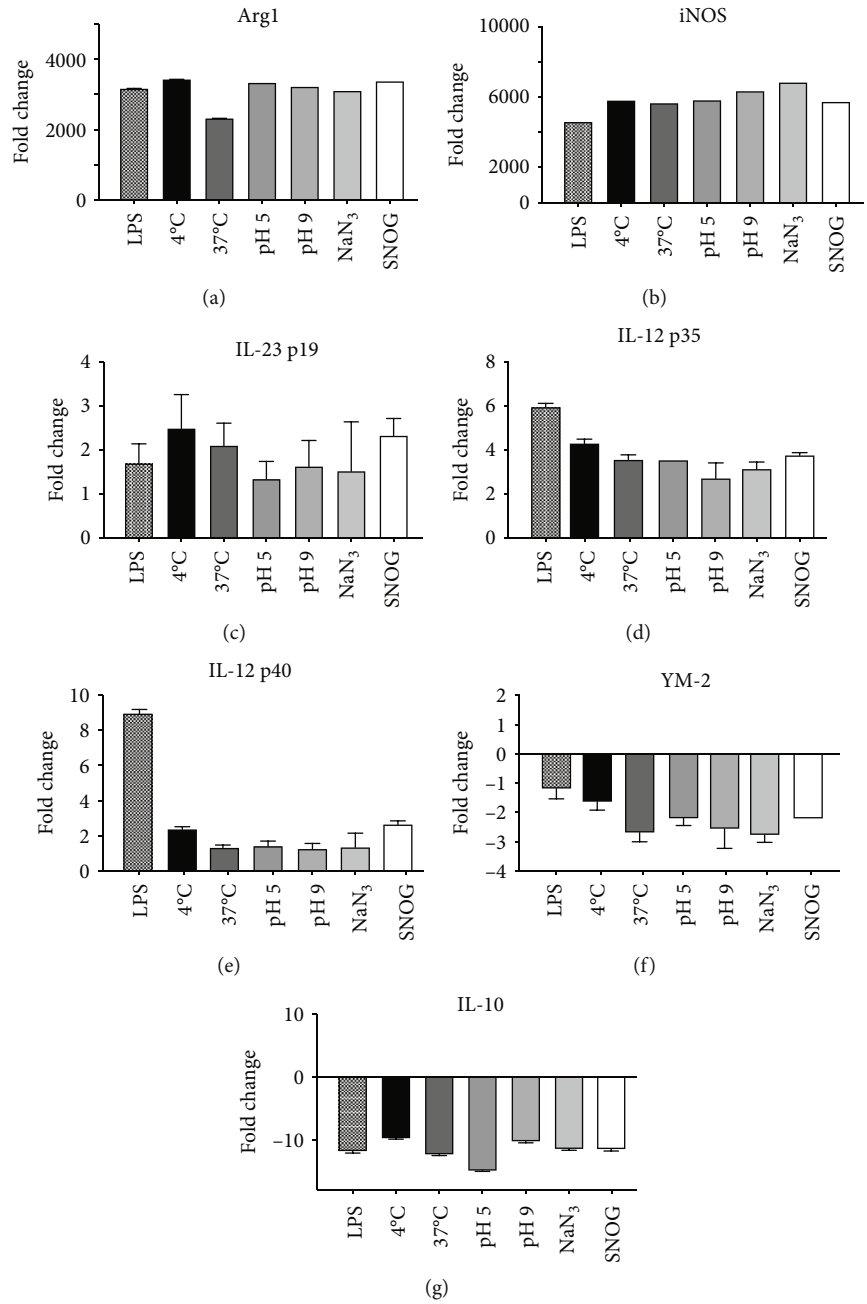


Figure 5: Immunomodulation of EVs obtained from *T. cruzi* submitted to different stress conditions. IFN-$\gamma$-primed macrophages (BMDM) were incubated (24 h, 37°C) with *T. cruzi* EVs. LPS from *E. coli* was used as positive control. qRT-PCR was performed to detect the expression of immune response genes: Arg 1 (a), iNOS (b), IL-23 p19 (c), IL-12 p35 (d), IL-12 p40 (e), YM-2 (f), and IL-10 (g) ($n = 3$, $^*p < 0.05$).

parasite changes over short periods. The EV release may be increased by alterations in the subpellicular cytoskeleton interaction with the membrane at pH 5 or through the activation of an acid-dependent and o-phenanthroline-insensitive GPI-phospholipase present in trypomastigotes [44]. Interestingly, vesicles released by epimastigotes are enriched in phospholipids compared to the cell, but no increase in lysophospholipids was observed [45]. In a preliminary analysis, in trypomastigote EVs, we detected the presence of phosphatidylethanolamine and phosphatidylserine, absent in epimastigotes, by thin-layer chromatography and gas chromatography followed by MALDI spectrometry analysis (in preparation).

Finally, we decided to focus on nitrosative stress, since this is also a common environment faced by the parasites inside the cells. We also noticed that the release of EVs increased with NO-produced $NaNO_2$ during medium acidification. A similar increase was observed at pH 7 by using SNOG as a NO source. These effects are relevant, because the interaction of trypomastigotes and macrophages triggers the activation of the innate host immune response, characterized by the production of proinflammatory cytokines,

activation of the NADPH oxidase complex, and the inducible nitric oxide synthase (iNOS) [46]. These enzymes produce radical superoxide ($O_2^-$) and NO, respectively [47]. These are responsible for the elimination of the parasite due to its trypanocide effect [48]. It is possible that the observed increase may be associated with the parasite's response to the stress suffered, a reflection of the mechanisms triggered by the protozoan to resist this stress, for example, via the trypanothione-dependent antioxidant system. Those events may be related to several factors, as a mechanism employed by the parasite to resist and survive nitrosative stress, involving intracellular signaling cascades that directly interfere with vesicular biogenesis. SNOG, as other NO donor molecules, is capable of inhibiting *T. cruzi* cruzipain (CZ), a cysteine protease, *L. infantum* cysteine proteinase, and *P. falciparum* falcipain by *S*-nitrosylation of the catalytic residue of the enzymes [49, 50]. These observations might, therefore, suggest a role for this major surface protease in the trypomastigotes in EV release.

*Trypanosoma cruzi* EVs display high proinflammatory profile depending on the strain [51]. Consistent with these observations, here, the EVs increased the expression of iNOS, IL-12, and IL-23 genes, typical of M1-like phenotype, as previously observed [29]. EVs from *T. cruzi* contain a wide range of pathogen-associated molecular patterns (PAMPs) that contribute to their ability to interact with the cellular milieu in the vertebrate hosts. Those include GPI-mucins, *trans*-sialidases, and cruzipains [3]. Here, regardless of the stress conditions applied to the trypomastigotes, the functional properties of EVs were not affected. This suggests that stress conditions are more likely to affect quantity rather than quality of the EVs.

## 5. Conclusion

In conclusion, the release of *T. cruzi* EVs is dependent on factors found in the variable environmental conditions faced by the parasite. As the EVs confer increased infectivity and virulence in a mammalian host [2], the stress-induced release is clearly a response to environmental changes. We can associate the release with a mechanism of surface budding dependent on the membrane organization. This is based on the variable size of EVs, their composition like the plasma membrane, and the rapid release upon stress. It is still unknown whether the release occurs in a similar way in host tissues or in the blood and what key molecular events are taking place during the vesiculation and release from the parasite surface. This work provides an initial support to answer these relevant questions, to get a better understanding of Chagas disease and help to deal with it.

## Data Availability

All data used to support the finding of this study are available from the corresponding authors upon request.

## Conflicts of Interest

No potential conflicts of interest were reported by the authors.

## Authors' Contributions

CIV, ACA, NS-M, JTM, WLB, PX, SS, and ACT conceived and designed the experiments. CIV, ACA, JTM, SS, WLB, and ACT performed most experiments. CIV, SS, RPS, and ACT wrote the manuscript. CIV, ACA, SS, PX, WLB, RPS, and ACT contributed to final manuscript revision.

## Acknowledgments

This work was financially supported by Fundação de Amparo à Pesquisa do Estado de São Paulo (2015/20031-0, 2019/15909-0, and 2020/07870-4, to SS; 2017/02416-0); Fundação de Amparo à Pesquisa do Estado de Minas Gerais (PPM-00202-18); CNPq (445655/2014-3, 424729/2018-0, and 302972/2019-6 and by the INCTVac-CNPq, to SS); and CAPES. We thank Claudio Rogerio for preparing the EVs, Nadjania Saraiva and Milena K Coló Brunialti for their help with flow cytometer analysis, and Lucas Barros for the help in some experiments.

## References

[1] O World Health, *Chagas Disease (Also Known as American Trypanosomiasis)*, 2021, https://www.who.int/news-room/fact-sheets/detail/chagas-disease-(american-trypanosomiasis).

[2] A. C. Torrecilhas, R. P. Soares, S. Schenkman, C. Fernandez-Prada, and M. Olivier, "Extracellular vesicles in trypanosomatids: host cell communication," *Frontiers in Cellular and Infection Microbiology*, vol. 10, p. 602502, 2020.

[3] O. Campetella, C. A. Buscaglia, J. Mucci, and M. S. Leguizamon, "Parasite-host glycan interactions during Trypanosoma cruzi infection: trans -sialidase rides the show," *Biochimica et Biophysica Acta. Molecular Basis of Diseases*, vol. 1866, no. 5, p. 165692, 2020.

[4] A. TROCOLITORRECILHAS, R. TONELLI, W. PAVANELLI et al., "Trypanosoma cruzi: parasite shed vesicles increase heart parasitism and generate an intense inflammatory response," *Microbes and Infection*, vol. 11, no. 1, pp. 29–39, 2009.

[5] K. S. Ribeiro, C. I. Vasconcellos, R. P. Soares et al., "Proteomic analysis reveals different composition of extracellular vesicles released by two Trypanosoma cruzi strains associated with their distinct interaction with host cells," *Journal of Extracellular Vesicles*, vol. 7, no. 1, p. 1463779, 2018.

[6] L. Retana Moreira, A. Prescilla-Ledezma, A. Cornet-Gomez et al., "Biophysical and biochemical comparison of extracellular vesicles produced by infective and non-infective stages of Trypanosoma cruzi," *International Journal of Molecular Sciences*, vol. 22, no. 10, p. 5183, 2021.

[7] L. Retana Moreira, F. Rodriguez Serrano, and A. Osuna, "Extracellular vesicles of Trypanosoma cruzi tissue-culture cell-derived trypomastigotes: induction of physiological changes in non-parasitized culture cells," *Plos Neglected and Tropical Diseases*, vol. 13, no. 2, article e0007163, 2019.

[8] L. M. de Pablos Torro, L. Retana Moreira, and A. Osuna, "Extracellular vesicles in Chagas disease: a new passenger for an old disease," *Frontiers in Microbiology*, vol. 9, p. 1190, 2018.

[9] M. P. Wyllie and M. I. Ramirez, "Microvesicles released during the interaction between Trypanosoma cruzi TcI and TcII strains and host blood cells inhibit complement system and

increase the infectivity of metacyclic forms of host cells in a strain-independent process," *Pathogen and Disease*, vol. 75, no. 7, 2017.

[10] I. V. Rossi, M. A. Ferreira Nunes, S. Vargas-Otalora, T. C. da Silva Ferreira, M. Cortez, and M. I. Ramirez, "Extracellular vesicles during TriTryps infection: complexity and future challenges," *Molecular Immunology*, vol. 132, pp. 172–183, 2021.

[11] C. Thery, K. W. Witwer, E. Aikawa et al., "Minimal information for studies of extracellular vesicles 2018 (MISEV2018): a position statement of the International Society for Extracellular Vesicles and update of the MISEV2014 guidelines," *J Extracell Vesicles*, vol. 7, no. 1, p. 1535750, 2018.

[12] D. S. Zamboni and M. Rabinovitch, "Nitric oxide partially controls Coxiella burnetii phase II infection in mouse primary macrophages," *Infection and Immunity*, vol. 71, no. 3, pp. 1225–1233, 2003.

[13] J. T. Maricato, M. N. Furtado, M. C. Takenaka et al., "Epigenetic modulations in activated cells early after HIV-1 infection and their possible functional consequences," *PLoS One*, vol. 10, no. 4, article e0119234, 2015.

[14] A. Cronemberger-Andrade, P. Xander, R. P. Soares et al., "Trypanosoma cruzi-infected human macrophages shed proinflammatory extracellular vesicles that enhance host-cell invasion via toll-like receptor 2," *Frontiers in Cellular and Infection Microbiology*, vol. 10, p. 99, 2020.

[15] T. D. Schmittgen and K. J. Livak, "Analyzing real-time PCR data by the comparative CT method," *Nature Protocols*, vol. 3, no. 6, pp. 1101–1108, 2008.

[16] S. A. Bustin, V. Benes, J. A. Garson et al., "The MIQE guidelines: minimum information for publication of quantitative real-time PCR experiments," *Clinical Chemistry*, vol. 55, no. 4, pp. 611–622, 2009.

[17] J. Mucci, A. B. Lantos, C. A. Buscaglia, M. S. Leguizamon, and O. Campetella, "The Trypanosoma cruzi surface, a nanoscale patchwork quilt," *Trends in Parasitology*, 2016.

[18] A. B. Lantos, G. Carlevaro, B. Araoz et al., "Sialic acid glycobiology unveils Trypanosoma cruzi trypomastigote membrane physiology," *PLoS Pathogens*, vol. 12, no. 4, article e1005559, 2016.

[19] A. O. M. Stoppani, R. Docampo, J. F. De Boiso, and A. C. C. Frasch, "Effect of inhibitors of electron transport and oxidative phosphorylation on Trypanosoma cruzi respiration and growth," *Molecular and Biochemical Parasitology*, vol. 2, no. 1, pp. 3–21, 1980.

[20] S. Schenkman, E. S. Robbins, and V. Nussenzweig, "Attachment of Trypanosoma cruzi to mammalian cells requires parasite energy, and invasion can be independent of the target cell cytoskeleton," *Infection and Immunity*, vol. 59, no. 2, pp. 645–654, 1991.

[21] G. A. Mott and B. A. Burleigh, "The role of host cell lysosomes in Trypanosoma cruzi invasion," *Sub-Cellular Biochemistry*, vol. 47, pp. 165–173, 2008.

[22] S. Tomlinson, F. Vandekerckhove, U. Frevert, and V. Nussenzweig, "The induction of Trypanosoma cruzi trypomastigote to amastigote transformation by low pH," *Parasitology*, vol. 110, no. 5, pp. 547–554, 1995.

[23] A. Santos-Miranda, J. V. Joviano-Santos, G. A. Ribeiro et al., "Reactive oxygen species and nitric oxide imbalances lead to in vivo and in vitro arrhythmogenic phenotype in acute phase of experimental Chagas disease," *PLoS Pathogens*, vol. 16, no. 3, article e1008379, 2020.

[24] J. Mauel, A. Ransijn, and Y. Buchmuller-Rouiller, "Killing of Leishmania parasites in activated murine macrophages is based on an L-arginine-dependent process that produces nitrogen derivatives," *Journal of Leukocyte Biology*, vol. 49, no. 1, pp. 73–82, 1991.

[25] T. Doi, M. Ando, T. Akaike, M. Suga, K. Sato, and H. Maeda, "Resistance to nitric oxide in Mycobacterium avium complex and its implication in pathogenesis," *Infection and Immunity*, vol. 61, no. 5, pp. 1980–1989, 1993.

[26] National Research Council (US), Committee on Nitrite, Alternative Curing Agents in Food, Assembly of Life Sciences (US), Committee on Nitrite, & Alternative Curing Agents in Food, *The Health Effects of Nitrate, Nitrite, and N-Nitroso Compounds: Part 1 of a 2-Part Study*, The National Academies Press, Washington, DC, 1981.

[27] S. M. Brown, R. Upadhya, J. D. Shoemaker, and J. K. Lodge, "Isocitrate dehydrogenase is important for nitrosative stress resistance in Cryptococcus neoformans, but oxidative stress resistance is not dependent on glucose-6-phosphate dehydrogenase," *Eukaryotic Cell*, vol. 9, no. 6, pp. 971–980, 2010.

[28] K. Caradonna, J. Engel, D. Jacobi, C.-H. Lee, and B. Burleigh, "Host metabolism regulates intracellular growth of Trypanosoma cruzi," *Cell Host & Microbe*, vol. 13, no. 1, pp. 108–117, 2013.

[29] P. M. Nogueira, K. Ribeiro, A. C. Silveira et al., "Vesicles from different Trypanosoma cruzi strains trigger differential innate and chronic immune responses," *Journal of Extracellular Vesicles*, vol. 4, no. 1, p. 28734, 2015.

[30] L. F. Paranaiba, A. A. Guarneri, A. C. Torrecilhas, M. N. Melo, and R. P. Soares, "Extracellular vesicles isolated from Trypanosoma cruzi affect early parasite migration in the gut of Rhodnius prolixus but not in Triatoma infestans," *Memórias do Instituto Oswaldo Cruz*, vol. 114, article ???, 2019.

[31] K. Hassani, E. Antoniak, A. Jardim, and M. Olivier, "Temperature-induced protein secretion by Leishmania mexicana modulates macrophage signalling and function," *PLoS One*, vol. 6, no. 5, article e18724, 2011.

[32] V. L. P. Chioccola, A. Acosta-Serrano, I. C. Almeida et al., "Mucin-like molecules form a negatively charged coat that protects Trypanosoma cruzi trypomastigotes from killing by human anti-alpha-galactosyl antibodies," *Journal of Cell Science*, vol. 113, no. 7, pp. 1299–1307, 2000.

[33] L. Cruz-Saavedra, M. Munoz, L. H. Patino, G. A. Vallejo, F. Guhl, and J. D. Ramirez, "Slight temperature changes cause rapid transcriptomic responses in Trypanosoma cruzi metacyclic trypomastigotes," *Parasites and Vectors*, vol. 13, no. 1, p. 255, 2020.

[34] D. Eliaz, S. Kannan, H. Shaked et al., "Exosome secretion affects social motility in Trypanosoma brucei," *PLoS Pathogens*, vol. 13, no. 3, article e1006245, 2017.

[35] A. J. Szempruch, L. Dennison, R. Kieft, J. M. Harrington, and S. L. Hajduk, "Sending a message: extracellular vesicles of pathogenic protozoan parasites," *Nature Reviews. Microbiology*, vol. 14, no. 11, pp. 669–675, 2016.

[36] R. Zidovetzki and I. Levitan, "Use of cyclodextrins to manipulate plasma membrane cholesterol content: evidence, misconceptions and control strategies," *Biochimica et Biophysica Acta*, vol. 1768, no. 6, pp. 1311–1324, 2007.

[37] H. Wei, J. M. Malcor, and M. T. Harper, "Lipid rafts are essential for release of phosphatidylserine-exposing extracellular vesicles from platelets," *Scientific Reports*, vol. 8, no. 1, p. 9987, 2018.

[38] E. Sezgin, I. Levental, S. Mayor, and C. Eggeling, "The mystery of membrane organization: composition, regulation and roles of lipid rafts," *Nature Reviews. Molecular Cell Biology*, vol. 18, no. 6, pp. 361–374, 2017.

[39] L. O. Andrade and N. W. Andrews, "The Trypanosoma cruzi -host-cell interplay: location, invasion, retention," *Nature Reviews. Microbiology*, vol. 3, no. 10, pp. 819–823, 2005.

[40] H. Kanbara, H. Uemura, S. Nakasawa, and T. Fukama, "Effect of low pH on transformation of Trypanosoma cruzi trypomastigote to amastigote," *Japanase Journal of Parasitology*, vol. 39, pp. 226–228, 1990.

[41] J. F. da Silveira, P. A. Abrahamsohn, and W. Colli, "Plasma membrane vesicles isolated from epimastigote forms of trypanosoma cruzi," *Biochimica et Biophysica Acta*, vol. 550, no. 2, pp. 222–232, 1979.

[42] D. Perez-Morales, K. D. Hernandez, I. Martinez, L. T. Agredano-Moreno, L. F. Jimenez-Garcia, and B. Espinoza, "Ultrastructural and physiological changes induced by different stress conditions on the human parasite Trypanosoma cruzi," *Cell Stress & Chaperones*, vol. 22, no. 1, pp. 15–27, 2017.

[43] Y. Pedra-Rezende, M. C. Fernandes, C. Mesquita-Rodrigues et al., "Starvation and pH stress conditions induced mitochondrial dysfunction, ROS production and autophagy in Trypanosoma cruzi epimastigotes," *Biochimica et Biophysica Acta. Molecular Basis of Diseases*, vol. 2021, no. 2, p. 166028, 2021.

[44] S. Schenkman, N. Yoshida, and M. L. Cardoso de Almeida, "Glycophosphatidylinositol-anchored proteins in metacyclic trypomastigotes of Trypanosoma cruzi," *Molecular and Biochemical Parasitology*, vol. 29, no. 2-3, pp. 141–151, 1988.

[45] J. F. Da Silveira and W. Colli, "Chemical composition of the plasma membrane from epimastigote forms of Trypanosoma cruzi," *Biochimica et Biophysica Acta*, vol. 644, no. 2, pp. 341–350, 1981.

[46] I. C. Almeida and R. T. Gazzinelli, "Proinflammatory activity of glycosylphosphatidylinositol anchors derived from Trypanosoma cruzi: structural and functional analyses," *Journal of Leukocyte Biology*, vol. 70, no. 4, pp. 467–477, 2001.

[47] L. Piacenza, M. N. Alvarez, G. Peluffo, and R. Radi, "Fighting the oxidative assault: the Trypanosoma cruzi journey to infection," *Current opinion in microbiology.*, vol. 12, no. 4, pp. 415–421, 2009.

[48] R. T. Gazzinelli, I. P. Oswald, S. Hieny, S. L. James, and A. Sher, "The microbicidal activity of interferon-$\gamma$-treated macrophages against Trypanosoma cruzi involves an L-arginine-dependent, nitrogen oxide-mediated mechanism inhibitable by interleukin-10 and transforming growth factor-$\beta$," *European Journal of Immunology*, vol. 22, no. 10, pp. 2501–2506, 1992.

[49] G. Venturini, L. Salvati, M. Muolo, M. Colasanti, L. Gradoni, and P. Ascenzi, "Nitric oxide inhibits cruzipain, the major papain-like cysteine proteinase from Trypanosoma cruzi," *Biochemical and Biophysical Research Communications*, vol. 270, no. 2, pp. 437–441, 2000.

[50] P. Ascenzi, A. Bocedi, M. Gentile, P. Visca, and L. Gradoni, "Inactivation of parasite cysteine proteinases by the NO-donor 4-(phenylsulfonyl)-3-((2-(dimethylamino)ethyl)thio)-furoxan oxalate," *Biochimica et Biophysica Acta*, vol. 1703, no. 1, pp. 69–77, 2004.

[51] N. P. Nogueira, F. M. Saraiva, P. E. Sultano et al., "Proliferation and differentiation of Trypanosoma cruzi inside its vector have a new trigger: redox status," *PLoS One*, vol. 10, no. 2, article e0116712, 2015.